

CHALLENGES IN THE PROCESSING OF PETROLEUM SUPPLEMENTS

By

George Richard Hill

College of Mines & Mineral Industries

University of Utah

Salt Lake City, Utah

Research and development work in the conversion of coal, of the kerogen in oil shale, and of the tar from bituminous sands to petroleum supplements has been a periodic phenomenon in the United States. During each period of intense effort major technical improvements have been made. Current research efforts have succeeded in bringing the cost of gasoline from these supplemental hydrocarbons much closer to the cost of gasoline from petroleum. One of the important factors which brings the cost closer is the increased cost of discovering and producing new petroleum reserves. Large scale commercial utilization of petroleum supplements will occur when the cost curves meet.

Historically, coal conversion research has been done largely by chemists and engineers employed in the coal industry, in government research laboratories or in research institutes. Only within the last few years has the petroleum industry seriously committed itself to studying production of liquids from coal, oil shale and bituminous sand. Earlier work in the petroleum research and development laboratories had been concentrated on petroleum feed stocks whose character is quite different from the liquids obtained from pyrolysis of other hydrocarbons.

Differences between the more familiar petroleum and the liquids produced from coal, oil shale and bituminous sands lie in the areas of; (1) oil composition, (2) the analytical techniques used in characterizing each material, (3) associated minerals, and (4) variations due to processing.

OIL COMPOSITION

Between the time of initial formation of petroleum and its migrating to and being trapped in the structure from which it is produced, any thermodynamically unstable molecules have undergone reaction or have been adsorbed or filtered from the bulk of the stable hydrocarbon constituting the final, presently produced petroleum. The liquids obtained from pyrolysis of coal, oil shale, and to a lesser degree, tar sands, on the other hand contain many very reactive hydrocarbons and heterocyclic compounds. The properties of the liquids produced during pyrolysis change appreciably over very short time periods due probably to condensation and polymerization reactions. This has been observed by many research groups who have noted that an initially light colored, very fluid, low pour point product from pyrolysis of oil shale or of coal darkens during the first few hours after distillation.

Both the pour point of the liquid and the viscosity increase noticeably after its production. Preliminary work in our laboratory indicates that the changes that occur are very sensitive to the presence of oxygen. They are apparently not photosensitive as had been earlier assumed. Nonetheless the changes are marked and will require either rapid subsequent processing of the liquid or a stabilization step to prevent the decrease in quality of the petroleum supplement.

ANALYTICAL TECHNIQUES

Another difference that petroleum refinery scientists and engineers must become aware of lies in the different types of analyses that have been developed for each of the potential petroleum substitutes.

Coal traditionally is characterized by "proximate analysis" and by "ultimate analysis". The proximate analysis comprises determinations of moisture, volatile matter, ash, and fixed carbon (the last by difference). With it is usually included a determination of sulfur and sometimes phosphorus. While the proximate analysis is the most widely used method for analyzing coals it is of little value in predicting convertibility of the coal to a petroleum supplement. Ultimate analyses are elemental analyses and take much longer to perform than the proximate analysis. Considerable technical skill is required and this analysis has not usually been done in coal plant operations.

Table 1. CHEMICAL COMPOSITION OF SOME COALS AND PETROLEUM

	Anthracite	Medium volatile bit.	High volatile A bit.	High volatile B bit.	Lignite	Petroleum Crude
C	93.7	88.4	84.5	80.3	72.7	83-87
H	2.4	5.0	5.6	5.5	4.2	11-14
O	2.4	4.1	7.0	11.1	21.3	
N	0.9	1.7	1.6	1.9	1.2	0.2
S	0.6	0.8	1.3	1.2	0.6	1.0
H/C atom ratio	0.31	0.67	0.79	0.82	0.69	1.76

Coal analysis on moisture and ash-free basis.
Ash content of coal 3 to 15%

G. Alex Mills, Industrial and Engineering Chemistry, vol. 61, No. 7,
July 1969.

Table 1 gives the ultimate analyses and hydrogen to carbon atom ratio of some coals and of petroleum. From the table we note that the hydrogen content of those coals most suitable for conversion into petroleum supplement by hydrogenation distillation, namely high volatile bituminous coals is in the range 5.5 percent. Petroleum on the other hand will contain from 11-14 percent hydrogen. Distillates from coal contain up to 9 percent hydrogen. Current technological methods for producing liquids from coal are based on the concept that the hydrogen rich components should be distilled from the coal and used as a petroleum supplement. The char or coke residue might better be used as a fuel rather than attempting the difficult task of converting the whole coal to hydrocarbons.

Table 2. HYDROGEN TO CARBON ATOM RATIO OF PETROLEUM AND SUPPLEMENTS

<u>Material</u>	<u>H/C Atom Ratio</u>
Texas Crude	1.55
Pennsylvania Crude	1.95
Bituminous Tar	1.75
Shale Oil	1.48
Coal Tar	1.32
Benzene	1.00
Toluene	1.14
Iso-octane	2.25

In Table 2 are listed the hydrogen to carbon ratios of typical petroleum supplements, of some pure hydrocarbons of value in gasoline, and of some Texas and Pennsylvania crude oils. Iso-octane has a hydrogen to carbon ratio of 2.25; a typical Pennsylvania crude oil high in paraffin content has a ratio of hydrogen to carbon of 1.95; a crude oil from Texas has a hydrogen to carbon ratio of 1.55, a typical bituminous tar has a ratio of 1.75, shale oil 1.48 and a straight coal tar distillate 1.32. The hydrogen to carbon atom ratio in a high volatile bituminous coal is 0.82. Included in the table are benzene and toluene, major components of coal oils, which have a hydrogen to carbon atomic ratio of 1.00 and 1.14.

There are two things of importance to note from these tables; first, the significantly higher hydrogen content of oil from coal compared to the original coal, and second, the hydrogen deficiencies compared to paraffinic crudes.

One compensating factor to be kept in mind is that relatively high percentages of the hydrocarbons in the coal liquid are aromatic. The final hydrogen to carbon ratio of a gasoline from coal could probably be in the range 1.4 to 1.5.

Table 3. ULTIMATE ANALYSES

	<u>Bituminous Tar</u>		<u>Shale Oil</u>		<u>Coal Tar</u>	
	<u>Wt.%</u>	<u>Atom%</u>	<u>Wt.%</u>	<u>Atom%</u>	<u>Wt.%</u>	<u>Atom%</u>
H	10.4	10.4	10.43	10.43	9.1	9.1
C	83.3	6.94	84.12	7.01	82.0	6.83
N	0.96	0.07	1.83	0.13	0.8	0.057
O	1.2	0.075	2.63	0.16	7.2	0.45
S	4.7	0.147	1.02	0.032	0.9	0.03

Table 3 gives the ultimate analysis of a bituminous tar, a shale oil, and a coal tar produced in University of Utah laboratories. In processing each liquid hydrogen will be required to remove the nitrogen, oxygen and sulfur from the liquids in addition to that required to increase the hydrogen content of the hydrocarbon components.

Table 4. HYDROGENATION-DISTILLATION LIQUID
FROM HIGH VOLATILE B BITUMINOUS COAL

Specific gravity, 20°C	0.9946°
Sulfur	0.3214 wt.%
Nitrogen	0.5820 wt.%
Tar acids	20.0 vol%
Distillation data	
I.B.P.	75°C
Up to 200°C	20.0 vol%
Up to 350°C	72.0 vol%
Hydrocarbon types in neutral oil	
Up to 350°C	
Saturates	46.0 vol%
Olefins	6.0 vol%
Aromatics	48.0 vol%

Table 4 gives a typical analysis of a liquid product from a partially hydrotreated coal distillate including the hydrocarbon type analysis in the liquid distilling below 350° centigrade. It is noted in this table that the bulk of the oxygen is present in tar acids which constitute 20% of the liquid distillate. Forty-eight percent of the

hydrocarbons in the neutral oil are aromatic.

The yield of liquid from coal or shale or tar sands depends very much upon the process used. This is also true of the quality of the distillate. Because of the different approaches to coal conversion, (1) straight carbonization pyrolysis, (2) hydrogenation-distillation and (3) solvent extractions, no single predictive method based on ASTM procedures is possible for determining the liquid product yield. For oil shale there has been developed the Fischer assay which gives the average yield of oil under a prescribed procedure of distillation⁽¹⁾. In the Fischer assay, the oil yield is that amount of distillate which results from the pyrolysis of the higher molecular weight organic insoluble kerogen. Some hydrocarbons and other organic type compounds remain in the shale after the distillation. Methods which differ from the Fischer assay technique produce oils of very different quality and somewhat different quantity than the usual shale oil (1,2,3).

Due to the afore-mentioned instability of shale oil and oil from coal the second distillation in a processing scheme generally leaves a much greater carbon residue than is true with distillation of petroleum feed stock. Ultimate product yield therefore cannot be determined except by direct experimental measurement.

As the processed oils are up-graded, the data are reported according to the methods used in the petroleum industry. For example, pour point, viscosity and API gravity are regularly determined. It is important to bear in mind that the numerical value of these three properties will depend upon how quickly they are determined after the preparation of the initial liquid distillate.

ASSOCIATED MINERALS

The initial instability and the presence of nitrogen, oxygen, and sulfur compounds in larger amounts than in petroleum renders the hydrogenation treatment of the liquid more difficult than the comparable treatment of a petroleum oil fraction. Some work is now being carried out and much more must be done of the development of catalysts which will be as effective for shale oil and coal oil upgrading as are the catalysts currently being used in the petroleum industry. In particular is this true in terms of sensitivity to poisons present in the ash from coal or shale oil conversion. This becomes evident if we compare the ash content of the raw material feed stocks.

A petroleum crude contains negligible ash. The ash content of coal will range from 3 to 15 percent. The ash content of oil shale ranges from 85-92 percent, the ash content of in situ bituminous sand will range upward from 50 percent. Unfortunately many current methods of producing liquid petroleum supplement from coal, oil shale or tar sands carry over into the "hydrocarbon" stream as much as a few percent of the mineral matter associated with the raw material. The primary liquid therefore contains many times as much material which will interfere with the operation of a catalytic conversion process as does a petroleum fraction. It is therefore important for the potential refiner to know of this mineral matter content and its constitution. Different combinations of minerals are found in the

finest carried overhead in the oil shale pyrolysis and in coal pyrolysis. In addition to vanadium compounds there will frequently be significant quantities of nickel, iron, and other transition metal compounds. The problems presented by the different kinds of contaminants are in no way insurmountable but must be taken into account by potential processors of the supplemental feed stocks.

A possible plus in the area of mineral constituents is the catalytic activity possessed by some components. This has been noted particularly in the University of Utah laboratory in the high liquid yields from Assam India Coal subjected to hydrogenation-distillation with only the naturally occurring minerals present as catalysts.

The vanadium, nickel and iron contents of petroleum supplements from different coals differs markedly and should be studied more intensively to determine enhanced catalytic activity as well as catalyst poisoning effects.

VARIATIONS DUE TO PROCESSING

The basic quality of the liquids produced from fossil fuels other than petroleum varies tremendously depending upon the process followed. The Bureau of Mines has given valuable input data on several approaches and has carried out demonstration projects. The Office of Coal Research has supported several coal conversion projects through the pilot plant stage. Carbonization processes like the COED process of FMC Corporation recovers the smallest volume of hydrocarbon type liquids of the three types of processes currently under investigation.

Solvent extraction processes like those of Consolidation Coal and some petroleum companies give much higher liquid yields by extraction with hydrogen donor solvents. Intermediate in liquid product yield are pressurized distillation processes in an hydrogen atmosphere. The HRI process and the method developed at the University of Utah use this approach. The quality of the liquid varies markedly depending on the process used.

Accompanying the higher yield of the solvent extraction processes is an increase in the quantity of high molecular weight aromatic ring clusters in the liquid product. New catalysts must be developed to convert this portion of the liquid to gasoline range hydrocarbons in good yield. Otherwise, the bulk of this portion ends up as carbon residue.

Dr. G. Alex Mills of the Bureau of Mines has written an excellent review paper on the conversion of coal to gasoline⁽⁴⁾ to which those interested in coal conversion processes and catalysts should refer.

Bituminous sand processing is very analogous in many regards to secondary recovery of heavy petroleum crudes. Various techniques are used to separate the bituminous material from the sand, clay and silt with which it is associated. The same possible processing difficulties encountered in processing shale oil and oil from coal will be anticipated unless a preliminary cleaning process is utilized.

That solid hydrocarbons can be converted into gasoline, diesel fuel and other salable products economically has been demonstrated during the past decade at the American Gilsonite Company oil refinery at Fruita, Colorado. The feed stock to this refinery has been the solid hydrocarbon, gilsonite, which is pipelined in a water slurry from Bonanza, Utah to Fruita, Colorado. After separation from the water the gilsonite is distilled in a primary coker. The liquid distillate is then hydrotreated and converted into the gasoline and diesel fuel used throughout the Grand Junction, Colorado market area. Problems of ash content in the feed stock and of the different metal compounds in the distillate have all been solved in the production of the gasoline which has been marketed at equal or lower cost than gasoline from conventional crude oils. There is no question about the ability of petroleum research, development, and production teams to utilize the supplemental feed stocks from other hydrocarbon sources as they become economic to use.

References

1. Hubbard, Arnold B., and Robinson, W. E., A Thermal Decomposition Study of Colorado Oil Shale, U. S. Bureau of Mines Report, Investigation #47441.
2. Hill, George Richard, Johnson, Duane J., Miller, Lowell and Dougan, J. L., Direct Product of a Low Pour Point High Gravity Shale Oil, I&EC Research Development, vol. 6, March 1967, pp. 52-59.
3. Hill, George Richard and Dougan, Paul, Characteristics of a Low Temperature In Situ Shale Oil, Quarterly of the Colorado School of Mines, vol. 62, no. 3, July 1967.
4. Mills, G. Alex, Conversion of Coal to Gasoline, Industrial and Engineering Chemistry, vol. 61, p. 8, July 1969.

A Synthetic Liquid Fuels Industry
Non-Technologic Factors

Harry Perry ^{1/}

U.S. Department of the Interior
18th and C Streets, N.W.
Washington, D.C. 20240

I. Introduction

Commercial production of synthetic liquid fuels from tar sands, oil shale and coal has been accomplished using each of these resources. Asphalt deposits occurring at the surface, which are a specialized type of tar sand, were used as early as biblical times in the Middle East countries. Based on tar sands, a plant with a capacity of 45,000 barrels of oil per day was dedicated in September of 1967 by Great Canadian Oil Sands Ltd. near Fort McMurray, Alberta, Canada, and is now in operation. The earliest reported commercial production of liquid fuels from oil shale was in France in 1839 but there were relatively large industries in Germany and Scotland during the 1800's. Commercial production is still reported in the U.S.S.R., Spain, Sweden, and China (mainland). Liquid products from coal first were produced as a by-product of coal carbonization and represented only 5% of the original coal substance. Production of liquid products such as "coal oil" for use as a fuel for lamps was commercially practiced as early as the latter part of the 19th century. Large scale production of liquid fuels by direct hydrogenation of coal started in 1926 in Germany. This was followed in 1933 by commercial production of liquid products from the catalytic reaction of carbon monoxide and hydrogen produced by gas manufactured from coal (the Fischer Tropsch process). Production in Germany continued on a large scale until the end of World War II when the plants were either destroyed or gradually converted to other uses. Relatively small scale plants for converting coal to liquid products were operated in a number of other countries during the period 1935 to 1960 but the only commercial synthetic liquid fuel from coal plant now in operation is a Fischer Tropsch plant in South Africa.

II. U.S. Interest in Synthetic Liquid Fuels

Interest in synthetic liquid fuels in the U.S. has varied greatly since the turn of the century. During and following World Wars I and II interest in alternatives to liquid fuel from petroleum was at its highest peak because of shortages that had occurred during the wars. The German commercial production from coal during World War II which assisted that country to wage war was pointed to as evidence for the need to establish a commercial industry in the U.S.

Throughout nearly all of this century, except for the period following the East and West Texas discoveries in the early 1920's and in 1930, there have been repeated predictions that the U.S. would shortly "run out of oil". These predictions have largely been based on the small inventory (approximately 11 to 20 years' supply) which the industry has traditionally maintained. A large inventory, however, would be difficult to justify economically and until the last several years the reserve to production ratio has remained relatively constant. However, after many years of remaining nearly constant, the reserve to consumption ratio of liquid hydrocarbons has declined sharply from 9.5 in 1965 to 7.5 in 1969. This has been in part an indirect effect of the increased imports of crude petroleum and residual fuel oil. Imports to the U.S. started shortly after World War II and in

^{1/} Mineral Resources Research Advisor, Assistant Secretary of Mineral Resources Office

spite of the oil import controls maintained on crude petroleum since 1959, for most of the U.S. the amount of imported liquid fuels now represents 23% of domestic liquid fuel consumption.

Projections of energy demand to the year 2000 have been made by a number of companies and organizations concerned with energy supply and demand. There is general agreement that by the year 2000 our energy requirement will about double. There is less uniformity in the projections about how much each of the energy sources (coal, oil, gas, uranium) will supply of this total. These projections, moreover, were made before the full impact of the new public policy of maintaining the quality of the environment could be factored into the projections. Low sulfur residual fuel oil has already made significant inroads into coal's electric utility markets on the east coast and it appears that residual will be used to replace higher sulfur coals in other marketing areas also. Even without this new consideration, liquid fuel demands were expected to increase by over 90% of 1969 consumption. The demand between 1970 and 1985 is expected to be greater than all the oil previously produced in the U.S.

Because of the declining reserve to consumption ratio and the projections for a very large demand in the future, industry has shown great interest in the past 3 years in synthetics produced from any source. The discovery of what appears to be a very large oil field in Alaska has apparently slowed research in synthetics as the oil companies reexamine the supply situation and their other investment needs. There remain major uncertainties with respect to the size of the Alaskan find as well as how and at what cost it can be brought to U.S. markets. However, unless the Alaskan discovery is much larger than even the most optimistic estimates that have been made, the onset of a synthetic industry would only be delayed a few years.

III. The Need for Synthetics

The highly competitive nature of the energy industries, because of the substitutability of energy sources at the point of use (for most purposes) and their convertibility from one form to another, requires that the entire energy spectrum be examined if we are to evaluate the potential role of synthetics in the energy economy. However, because liquid fuels are necessary under today's technologic conditions for certain energy uses, it is most important to examine the alternative sources for crude oil.

The question, "Is there a need for synthetics?" can be answered in many ways. If a shortage of liquid fuels develops, there are a variety of possible solutions. Among the more obvious are: direct substitution of other, more abundant energy sources for liquid fuels; increased imports; permitting the price of oil to rise; development of improved technology for finding, producing and utilizing existing and potential oil fields; increased exploration activity; and the production of synthetics from oil shale, tar sands or coal.

Selecting one or a combination of these alternatives requires considerable study and analysis. It is easy, however, to set the major criteria which would have to be met from a national viewpoint. These would include a secure, diversified supply of liquid fuels at the lowest cost consistent with other national goals.

With today's technology, transportation is the only end use for which liquid fuels are indispensable. Even for transportation, it is possible to foresee changes that would permit a high degree of substitution for liquid products. For example, autos or planes using natural gas or a car using electricity could be used if there was sufficient incentive. Widespread use of electric cars or electric trains would permit the primary energy source to be any fossil or nuclear fuel.

IV. Non-Technologic Factors

The technology for converting oil shale, tar sands and coal into an acceptable substitute for crude oil and its products has been demonstrated on a commercial scale and is currently being used in countries other than the U.S. A proven

technology at prices competitive with crude petroleum is a necessary but not sufficient prerequisite for the establishment of a synthetic liquid fuel industry. Many factors that influence both the price of crude petroleum and of synthetics will affect the timing and the rate at which an industry will develop.

1. Factors that affect competition from oil

Since synthetics would compete directly with crude oil, changes in any of the laws, regulations, or state and Federal practices that affect the domestic price of crude oil could have the greatest direct impact on a potential synthetics industry. The most important of the institutional factors influencing crude oil prices are the Oil Imports Program, the Federal depletion allowance, state prorationing practices, and Outer Continental Shelf and on-shore Federal leasing programs.

a. Oil Import Program

The Oil Import Program was created to promote a healthy domestic petroleum industry by limiting imports of low-cost foreign oil. The Program was designed to assure the Nation a secure petroleum supply and it has served to advance this purpose. However, the cost has been high: Domestic oil sells for between 75¢ and \$1.25 per barrel above world prices or from 30 percent to 60 percent higher than would otherwise prevail. The majority of the Cabinet Task Force on Oil Import Control recommended to the President in February 1970 that in place of the oil import quotas which had been in use, a tariff system be substituted with a three-year phase out of the quota system. The basis for the recommendations was that this would permit some liberalization of the Program but still be designed so that indicated reserves of North America would be sufficient to meet 1980 production estimates. Adjustments in the tariff levels would be made to insure that this goal was met. There was some support at the Cabinet level for a continuation of quotas in some form rather than the tariff approach. The final decision with respect to oil import controls is still to be made.

Any changes in the Oil Import Program would have a major impact on the development of synthetics. Increasing significantly the amount of imports would tend to decrease crude oil prices, which in turn would require a competitive drop in the price of synthetics, and this would reduce the return on plant investment. Since synthetics plants are capital-intensive, even minor changes in the competitive price of crude could have a major impact on their economics. Any reduction of domestic crude prices would delay the development of a synthetics industry with the present state of conversion technology and the potential for reduction in costs by methods that have been proposed to improve that technology.

If a quota system were continued, development of a commercial synthetics industry would raise a question as to how the oil when it is refined would be treated in determining the overall size of the oil import quota. If the oil were treated the same as domestic production of crude oil, a refinery would generate a quota for the synthetics processed, and for a small refiner, this could be worth as much as 11¢ per barrel.^{1/}

b. The depletion allowance

The depletion allowance for crude oil and gas is now 22 percent. Because of the high percentage of dry holes drilled in the search for oil, the allowance has been justified by industry on the basis that the resulting tax savings are needed to pay for exploration for new oil fields.

^{1/} The difference between the price of imported and domestic oil is about \$1.25 in the East and each barrel of domestic oil used in a refinery generates .090 barrels of oil import quota. Thus $\$1.25 \times .09 = 11¢/bbl$.

The oil industry has urged repeatedly that oil from shale receive the same tax treatment as crude oil, presumably because shale oil would be in direct competition with crude oil. Until this past year, the depletion allowance was 15 percent on the value of the mined rock. At this rate, the allowance is equivalent to about 18 cents per barrel of semirefined shale oil (before taxes). The 1969 Tax Act changed the depletion allowance to 15 percent on the shale oil and this would be equivalent to about 35 cents per barrel of shale oil at the retort. Depletion allowance on coal is 10 percent on the mined coal and this is estimated to be worth about 15 cents per barrel. Table 1 shows the effect on costs of various levels of depletion allowance when taken on the mined raw material and on the liquid, refined to two levels of quality.

c. State prorationing

State prorationing practices were developed to conserve oil, i.e., to prevent producing oil above the maximum efficient rate either for the purpose of recovering an investment quickly or preventing drainage of oil from a deposit by adjacent producers in the same field. Actually, however, prorationing practices have had the effect of maintaining a stable price for crude oil. Crude oil prices remained relatively constant for a 10-year period, but started to climb in 1968 with a 3 cents per barrel price rise followed by a 12 cents per barrel rise in 1969.

If prorationing were stopped, at least in the initial stage of development of synthetics, the synthetic industry might be adversely affected because crude prices would be expected to drop. This, in turn, would eliminate the high cost marginal wells, and as a result at some later time prices might tend to rise.

As long as the synthetic industry remained relatively small, the impact on those states practicing prorationing would be small, but as the productive capacity became significant some method would have to be developed to accommodate synthetics to the crude oil.

d. Federal leasing policies

If synthetics become competitive at present domestic prices of crude oil, interest in leasing of Federal oil and gas lands could be expected to decline. Since Outer Continental Shelf leasing is generally believed to offer more favorable opportunities for discovery, it would be affected less than on-shore leases. Nevertheless, the large amounts of capital required for synthetics plants might reduce interest in the Outer Continental Shelf and reduce the amounts of the bonus bids. If on the other hand, before the first synthetics plant was constructed a large number of favorable tracts on the Outer Continental Shelf were offered at frequent intervals, and if the drilling proved successful, the development of synthetics could be further delayed. There is already some evidence that the discovery of large petroleum resources in Northern Alaska has changed to some extent the planned timetable for synthetic fuels development by some oil companies.

2. Factors that affect conversion of oil shale to shale oil

a. Title clearance

Approximately 28 percent of the total oil shale acreage is in private ownership, but this contains only a little over 20 percent of the shale oil. Nearly 80 percent of the Federal lands have clouded title, consisting of 36,000 oil shale claims made before 1920 and 16,000 additional claims for various other materials filed since that date.

The pre-1920 claims, i.e., those made before passage of the Mineral Leasing Act, were made under conditions that permitted location and patenting of oil shale deposits. In 1964 several test cases were initiated to establish a set of legal principles for judging the validity of the pre-1920 claims. Hearings on these

issues before a hearing examiner of the Bureau of Land Management have been concluded. If a decision adverse to the claimant is issued, an appeal probably will be taken to the Secretary and then to the courts. At best, the issues cannot finally be resolved for several years.

The oil shale lands were withdrawn in 1930 and except for the three test leases recently offered, remain withdrawn. However, the passage of the Multiple Mineral Development Act of 1954 permitted the location of deposits of metalliferous minerals on oil shale lands. There were 5,200 claims filed on the oil shale lands in 1966, apparently in an attempt to obtain title by locating dawsonite on the oil shale lands. In January 1967, therefore, the lands were withdrawn from all mining location.

It is not possible to assess the validity of these more recent claims and nearly 3,000 of the 1966 claims are being contested by the U.S. Department of Interior.

b. The Mineral Leasing Act

Several provisions of the present Mineral Leasing Act, under which oil shale lands are leased, require modification if the lands are to be developed under optimum conditions. The limitation of one lease per person, association, or corporation, is unrealistic if an oil shale industry of any size is to come into existence. Moreover, the provision is a serious obstacle to building the first plant. This is because a pioneering plant might develop the technology at a loss and then be foreclosed from holding a second lease on which it could capture the benefits of that technology. These objections also can be raised with respect to the limitation of 5,120 acres per lease which is another provision of the present law. An acreage limitation has no real meaning since the ratio of the amount of shale oil represented per acre can range from as much as 100 to 1 depending on the thickness and quality of the reserve.

c. Bidding procedures

Under the terms of the Mineral Leasing Act any number of bidding methods is possible. The leasing can be competitive or non-competitive, and the bidding can be oral auction or sealed, profit sharing, bonus bidding, royalty bidding or a combination of these methods. In the test leases offered in December of 1968, competitive sealed bids with a combination bonus and royalty arrangement were used. Other methods might be tried in the future to attract stronger bids. The bidding procedures selected will have a marked effect on oil shale development since potential bidders may prefer one method over another and this could seriously affect the number and size of bids received.

d. Leasing procedures, terms and provisions

While various existing statutes require certain requirements to be stipulated in all leases--such as the non-discrimination clause--there is ample leeway for the lessor to include other provisions which can be designed either to encourage or discourage bidding, or, more important, to force the bidder to discount his bid so heavily that it will be rejected.

Such factors as the number of leases offered per sale, frequency of sales, size of tract offered and the quality of the resource could also be of critical importance to the rate and timing of oil shale development. The initial number of bidders will probably be small, so that the frequency of sales, at least in the beginning, should be low. The tract must contain sufficient shale oil so that a plant large enough to be economic can be supported and paid out with an adequate return in 20 years. At that time, renegotiation is required by the Mineral Leasing Act. In addition, there are great advantages when a resource is just reaching the

commercial stage to utilize the highest grade deposits, since if the best deposits are not offered, development would be delayed.

The conditions imposed by the leasing terms can also be critical. For example, a requirement that adequate conservation of the resource be assured can be so strictly interpreted that mining costs would be very high. The time allowed for the payment of royalties and bonuses may be either very short or generous. Conservation standards specified to protect other resource values and to prevent air and water pollution or serious damage to the land could be so strict that costs would skyrocket.

e. Availability of water

While there is sufficient water available in the States of Utah and Wyoming to establish a large oil shale industry without being limited by water availability, the richest known oil shale deposits in Colorado may have some problem with water availability. If the remaining uncommitted water is dedicated to the oil shale industry, and it is used prudently, an oil shale industry capable of at least one million barrels per day could be established (about 7 percent of U.S. consumption). Nevertheless, the only sources of water for the industry are from the Colorado River and its tributaries. These waters serve a very large geographic area and must provide water for both domestic use and a very diverse industrial and agricultural demand.

f. Location of the deposits

The rich oil shale deposits are concentrated in areas of Colorado, Utah, and Wyoming that are largely rural in nature. The establishment of any large new industry would require the development of a highly complex infrastructure that does not now exist and would mean either recruitment or training of various skilled labor and professionals which are not now found in the area. Adequate housing, schools, libraries, transportation and communication systems, water and power services and other community services would have to be provided. If a one million barrel a day oil shale industry were created it would require an additional 115,000 people in an area in which only 72,000 now reside. The orderly development of an infrastructure for such an expanded population would require careful physical and financial planning.

Another adverse effect of the location of the oil shale deposits is on the costs of transportation to refineries and large markets. There is not sufficient water in the area to refine the shale oil on site so it must be pipelined to refineries elsewhere that are located near markets where the finished products can be sold. Pipelining to suitable refineries would add a cost of about 50 cents a barrel to shale oil produced in the Colorado, Utah, and Wyoming area.

g. Environmental protection

Measures to protect the land from the potential adverse effects of mining are largely already fully developed. Air and water pollution as a result of the retorting and semi-refining of the shale oil can be controlled using existing technology. The handling of the spent oil shale, however, could present new environmental problems. With an average shale quality of 30 gallons per ton approximately 1.4 tons of spent oil shale must be handled for each barrel of semi-refined oil shale produced. If the spent shale is returned to the mine from which it was originally taken then this represents an added cost, and may be, on the average, 20 cents per barrel. All of the spent shale could not be replaced in any case since its volume is greater by virtue of the void space present in a mass of broken material as compared to a solid deposit. Thus provision will have to be made for some permanent surface storage of a portion of the spent shale. This will require methods for preventing leaching of the spent shale so that pollution by the leached salts of

ground water and streams can be avoided. Where fine shale is used for retorting, provision must be made to stabilize the spent shale to prevent air pollution by blowing fines when the pile is dry.

3. Factors that will affect conversion from coal to oil

Production of liquid fuels from coal will not be affected as much by Federal action or inaction as liquid fuels from oil shale. Unlike the high grade oil shale deposits, coal is found widely dispersed geographically with commercial type deposits reported in 34 states. This is shown in Figure 1. Although as much as 40 percent of these deposits may be on public lands--nearly all of this West of the Mississippi--this still leaves one trillion tons of recoverable reserves in private ownership. In addition, coals of all rank and susceptible to all types of mining systems are owned in abundance by individuals and large coal, oil and steel companies. Therefore, the questions that are crucial in oil shale development, such as title clearance, lease terms and provisions, should not be an important factor in the early stages of development of a commercial coal-to-oil industry.

a. Availability of water

The widespread geographic distribution of the coal deposits means that many of the deposits can be found in areas where the availability of water should create no great problems. All of the coal deposits East of the Mississippi are found in water abundant locations. Many of the large deposits of Wyoming, Montana, and North Dakota are in areas where enough water will be available for an industry. Moreover, competition in these areas for the water would be much smaller and there should be much fewer water rights problems than for the Colorado River and its tributaries. Some coal deposits are, however, found in water deficient areas, and for these locations there would be a choice of moving water to the coal or coal to the water. The selection of which would be done would depend upon other factors such as marketing conditions, the relative costs of transportation of coal, water or the finished oil, and other economic considerations.

b. Location of the deposits

As indicated under the discussion on oil shale, the location of the resource is important because of (1) the need for a well-developed infrastructure to serve the large scale plants that are required to achieve economies of scale, and (2) the importance of transportation costs in bringing the finished products to market. The very large wide-spread geographic distribution of coal, much of it near the centers of great population density and in well established communities where the infrastructure is well developed, and where skilled labor is available, should give coal a competitive advantage over oil shale or tar sands. Moreover, these same population centers would provide markets for the product at much reduced transportation costs.

c. Environmental protection

As in the case of oil shale, methods already exist for preventing adverse effects on the land from mining--either strip or underground. Technology also exists for preventing air or water pollution arising at the coal conversion processing plants. Unlike oil shale, however, solid waste disposal should present no significant problem nor will it involve the costs of disposal that are inherent when oil shale is retorted. Each ton of coal produces about 2.5 barrels of oil and only 200 pounds of ash so that only about 1/25th as much solid waste is generated per barrel of oil produced as when using oil shale. Disposal of the solid waste in the empty space left after the coal was mined would be one solution to the problem. Uses similar to those already developed for fly ash--a material which the waste from

conversion plants would resemble--might be found for the solid residue and thus turn a waste material into a useful product, although supply of spent shale could be expected to exceed demand for many years.

d. Other factors

Although conversion of coal appears to have far fewer non-technologic problems associated with its development than oil shale, processes for coal conversion may still not be developed before those for oil shale. At this time, there is considerably more pilot plant experience using various oil shale processes than there is experience with the more advanced coal-conversion processes that will be required for coal-conversion to be competitive with crude petroleum or shale oil. Moreover, coal is much more deficient in hydrogen than the crude shale oil, and the cost of producing the required hydrogen from coal is relatively high. Any breakthrough in hydrogen production costs would cause an important change in the relative attractiveness of coal and oil shale development.

4. Factors that affect tar sands development

Although information on tar sand reserves in the U.S. is limited, it appears that the total reserves of the high quality deposits of sufficient size for a large plant that would be needed for the initial development of an industry are limited. There may be individual deposits which are attractive, but the amount of production from these deposits can be expected to be small. As the need arises for other hydrocarbon sources to meet demand in the next century the lower grade deposits, of which there may be many, could be a useful source of hydrocarbon supply.

The Canadian tar sand reserves of good quality are large and concentrated geographically. The total is estimated at 85 billion barrels recoverable at today's costs. Presently, there is a 45,000 barrel-per-day commercial plant in operation with plans for a larger 80,000 barrel-per-day plant already drawn. Development of Canadian tar sands will be affected greatly by non-technologic factors--Canadian policy with respect to their development in competition with their own crude oil, with oil export policies of the Canadian government and with the joint U.S.-Canadian fuel policy that is now being developed.

5. Other factors common to all synthetics

a. State and local conditions

The actions that state and local governments take with respect to both property and personal taxes, zoning regulations, local conservation and environmental regulations, state water laws, and other related factors could have an important influence on synthetic development. Where deposits are located in remote areas, the actions of state and local government to provide the schools, transportation facilities, roads, libraries, and recreational facilities could have a significant impact on the rate at which an industry develops, since the ability to attract and keep the necessary labor force would be greatly influenced by these factors.

b. Capital requirements

With existing technology, capital requirements are very high, reaching as much as \$3,000-\$4,000 per daily barrel to produce a synthetic crude oil. This fact, combined with the need for the very large plants required to attain the economies of scale, dictates investments in the range of \$300 to \$400 million per plant. Few firms would be able to make investments of this size in single plants. Some of the major companies, either alone or in joint ventures, should be able to raise the necessary capital, although even for these very large companies the capital requirements present some obstacle. The high interest rates that are now common also

create a detriment to synthetic fuels industries because of the capital-intensive nature of synthetics plants.

c. Institutional practices of the oil industry

There is always a high degree of resistance by an industry to any radical change in raw material sources. There is a reluctance to give up a set of known problems which one has learned to manage, and to attack a completely new set of unknown ones. Coal, oil shale, and tar sands as resources differ from crude petroleum in that the approximate size and quality of the deposits can be ascertained with relative ease. However, they require new methods of processing, and a knowledge of mining technology--a technology generally unknown or unfamiliar to many oil companies. On the other hand, the vertical integration characteristic of much of the oil industry would appear to be useful, and possibly necessary, to a firm entering into a commercial synthetic industry. This suggests that there may be obstacles to the entry into synthetics by other than petroleum companies.

V. Summary

It is obvious that the many public policy issues that are associated with the complex, highly competitive and interrelated fuel resources will have an important impact on the development of a synthetic fuels industry. The demand for liquid fuels is expected to continue to rise in the future, but should a shortage develop, production of synthetics is only one of several ways that this energy requirement could be met. Whether synthetic production would be the preferred method would depend upon its attractiveness compared to that of the alternatives. This, in turn, would depend on both the state of technology, and the effect of non-technologic factors. The major non-technologic factors that are common to the development of any of the synthetics are related to those that affect the price of crude oil with which the synthetics would have to compete. These are (1) the rules governing the imports of crude oil or its products, (2) the depletion allowance, (3) state prorationing practice and (4) Federal leasing policies. Other non-technologic factors that would affect all of the synthetics are (1) state and local regulations, (2) very large capital requirements, and (3) institutional practices of the oil industry.

The non-technologic factors peculiar to oil shale are (1) title clearance problems with the land, (2) provisions of the Mineral Leasing Act, (3) uncertainties with respect to bidding procedures, (4) leasing procedures, terms and conditions, (5) in some areas the availability of water, (6) remote location of the deposits, and (7) extra problems associated with environmental protection.

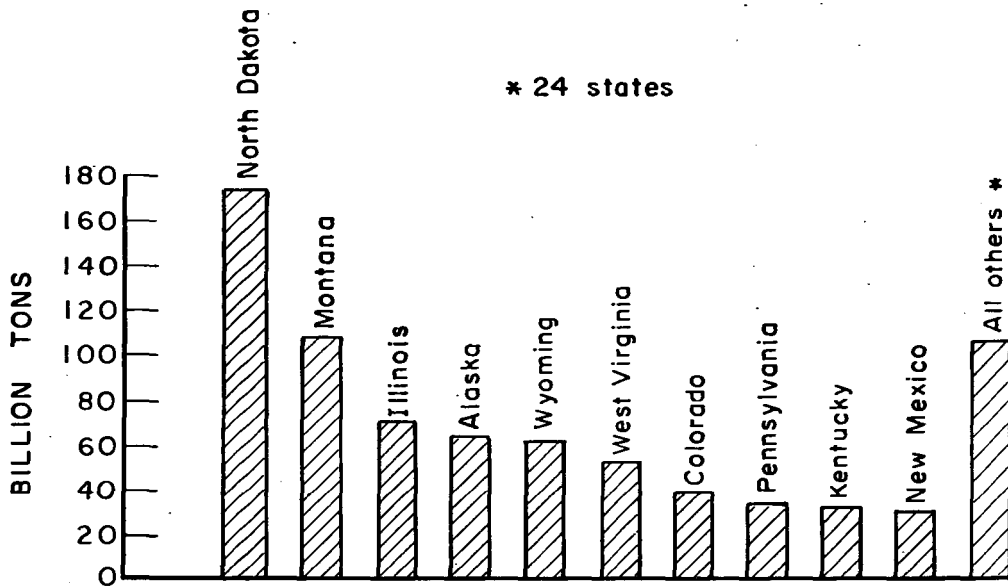
These seven non-technologic factors are of much less importance for coal than they are for oil shale. The favorable and extensive location of coal deposits and the large private holdings that permit an industry to develop with less government involvement sharply reduce the impact of non-technologic factors. Environmental factors should also be more favorable for coal but, in recent years, larger scale tests of oil shale processes have been made than have been made for coal. The major problem for coal is a technologic one--the high cost of producing hydrogen from coal with which to upgrade the coal to a liquid product.

Known U.S. deposits of tar sands are too small to have any great impact on total liquid fuel supplies. Development of the large reserves of Canadian tar sands, however, could be of no importance in the overall energy supply of North America. Their commercial production will be greatly influenced by non-technologic factors--namely Canadian policies with respect to how they will be developed in competition with Canada's crude oil deposits, Canadian export policies and the terms and conditions of the joint U.S.-Canadian fuel policy which is now under active consideration.

Table 1
Effect of Depletion Allowance on Cost of Synthetic Fuels

Percentage Depletion (percent)	Point where Depletion is Taken	Shale Oil					Coal				
		Cost of Oil Shale \$/ton	Cost of Oil at Retort \$/bbl	Depletion Before Taxes c/bbl	Cost of Semi-Refined Oil \$/bbl	Depletion Before Taxes c/bbl	Cost of Crude Synthetic \$/bbl	Depletion Before Taxes c/bbl	Cost of Hydro Refined Oil \$/bbl	Depletion Before Taxes c/bbl	
0	Oil Shale or Coal	1.43	2.68	0	3.93	0	2.81	0	6.46	0	
0	Shale Oil or Synthetic Crude	1.43	2.68	0	3.93	0	2.81	0	6.46	0	
10	Oil Shale or Coal	1.31	2.56	12	3.81	12	2.66	15	6.31	15	
10	Shale Oil or Synthetic Crude	1.43	2.44	24	3.57	36	2.55	26	5.87	59	
15	Oil Shale or Coal	1.25	2.50	18	3.75	18	2.59	22	6.25	21	
15	Shale Oil or Synthetic Crude	1.43	2.33	35	3.93	51	2.44	37	5.62	84	
22	Shale Oil or Synthetic Crude	1.43	2.20	48	3.22	71	2.30	51	5.30	116	
27½	Shale Oil or Synthetic Crude	1.43	2.10	58	3.08	85	2.20	61	5.07	139	

Figure 1
Recoverable reserves of
bituminous coal and lignite
by state 1967



Hydrogenation of Asphaltene From Coal Using Halide Catalysts

Walter Kawa, H. F. Feldmann, and R. W. Hiteshue

U.S. Bureau of Mines, 4800 Forbes Avenue
Pittsburgh, Pennsylvania 15213

INTRODUCTION

The Bureau of Mines has been investigating the use of high catalyst concentrations in the hydrogenation of coal to oil as a possible means of lowering hydrogenation costs. The objective has been to find or develop catalysts that would permit the use of milder conditions than were used in the conventional (Bergius-I.G. Farben) process, or catalysts that would cause an increase in oil yield, a decrease in hydrogen consumption, or other benefit.

Conditions used in commercial-scale operations of conventional plants depended on the reactivity of the coal being hydrogenated and on the catalyst used. Temperatures ranged from 450° to 490° C and pressures were 3,500 to 10,000 psi. Catalysts were used in suspended form in concentrations of from less than one-tenth percent to about three percent. These high temperatures and pressures were not needed for the initial coal liquefaction reactions but were needed to hydrocrack asphaltenes at reasonable rates. Asphaltene is a high-molecular weight nondistillable substance that is formed as a principal intermediate in the coal-to-oil reaction sequence. In a kinetics study made with bituminous coal at about 6,000 psi with a conventional catalyst (SnS plus NH₄Cl), Weller obtained specific reaction rate constants for coal hydrogenation to asphaltene and other liquid and gaseous products that were 25 times greater at 400° C and 10 times greater at 440° C than the specific reaction rate constants for asphaltene hydrogenation.^{1/} The reactions were first order with respect to coal or asphaltene concentration. It thus became evident that the hydrogenation of coal to oil at practical rates at mild conditions, e.g., 400° C and 1,500 psi, would require the use of catalysts that are highly effective for hydrogenating asphaltene.

The Bureau recently made a coal hydrogenation catalyst study in which a wide variety of materials were screened as potential catalysts. Equal weights of these materials and coal were used at one set of conditions. This paper presents results of screening experiments made with ten halide catalysts that were effective for producing high yields of oil with low asphaltene contents. Results are also presented for experiments in which the same catalysts were used in the hydrogenation of asphaltene produced by mild hydrogenation of the coal.

EXPERIMENTAL

Equipment and Materials

The reactor used was a 1.2-liter batch autoclave that was placed in a horizontal position and rotated during an experiment. A complete description of the vessel and accessory equipment has been published.^{2/} Charges were contained in a glass liner that fitted closely to the autoclave wall. Pressure was measured with a bourdon-tube type gage that was connected to and rotated with the autoclave. Temperature was measured with a thermocouple positioned axially in the autoclave in a thermowell.

Pittsburgh-seam high-volatile A bituminous coal from the Bureau's experimental mine at Bruceton, Pennsylvania and asphaltene produced by uncatalyzed hydrogenation of the same coal were used as feeds. The coal was pulverized to minus 60 mesh (U. S. Sieve) and dried in air at 70° C for about 20 hours. Asphaltene was produced by hydrogenating 200-gram charges of coal in the batch autoclave at 4,000 psi and 425° C for 2 hours. Asphaltene produced in 35 runs was combined and used as a feed material.

It is the fraction of product that is soluble in benzene and insoluble in n-pentane. The yield was about 35 percent by weight of moisture- and ash-free (maf) coal used. By laboratory analysis, it was found to contain 8.5 percent benzene insolubles, 83.6 percent asphaltene, and 7.9 percent n-pentane-soluble oil. Ultimate analyses of the feeds are shown in table 1.

Table 1.- Analyses of coal and asphaltene feeds

Material	Analysis, wt pct						
	Mois- ture	Ash	Elemental composition, maf basis				O (diff.)
			C	H	N	S	
Coal, hvab ^{1/} ...	0.4	7.5	83.7	5.4	1.6	1.2	8.1
Asphaltene ...	0.9	0.0	88.7	6.4	1.9	0.4	2.6

^{1/} High-volatile A bituminous coal, Pittsburgh seam.

Halide catalysts were either technical or reagent grade chemicals and were used in powdered form. Catalysts and coal or asphaltene were premixed in the glass liners before charging into an autoclave. Hydrogen was obtained from commercial cylinders.

Operating and Analytical Procedures

All experiments were made with 50-gram charges of coal or asphaltene. After purging air out of a charged and assembled autoclave, hydrogen was added to an initial pressure selected so that the desired pressure would be reached on heating to reaction temperature. Rotation was started, the autoclave was heated at about 7° C per minute to reaction temperature, temperature was maintained for a specified time, then the autoclave was cooled to room temperature. Rotation was continued until the temperature was 250° C or less. The cooling rate to 250° C was about 4° C per minute.

Gases were depressurized through a cold trap where light oil and water vapors were condensed and then through scrubbers that removed acid gases (CO₂, H₂S, and any hydrogen halide formed by catalyst reactions). The remaining gases were metered, collected in a holder, sampled, and analyzed by mass spectrometry. Light oil and water were then removed by vacuum distillation to about 110° C and 2 to 3 mm of Hg. These conditions are equivalent to an atmospheric distillation to about 290° C. Material remaining in the autoclave was washed out with benzene and then continuously extracted with benzene in a Soxhlet apparatus. The insoluble and soluble fractions were both water washed to remove the halide catalysts. An ash determination was made on the product insoluble in benzene and water. After water washing, the benzene solubles were separated into n-pentane insoluble (asphaltene) and n-pentane soluble (heavy oil) fractions.

The autoclave was weighed on a bullion balance before charging with hydrogen, after depressurizing, and after vacuum distillation. The weight of hydrogen charged was estimated from previous autoclave calibrations of hydrogen weight versus pressure. Bullion balance weighings permitted accurate determinations to be made of the weights of groups of products as follows: (1) Gases and vapors depressurized, (2) vacuum distillate, and (3) heavy liquids and solids. Actual recoveries were adjusted to correspond to values determined by bullion balance weighings by assuming that losses (or gains) in each group of products were distributed among the components of that group in the same proportions as actual recoveries.

Yields are expressed as weight-percent of maf charge. Organic benzene insolubles are defined as benzene and water insolubles minus ash; coal conversion on a percentage

basis is 100 minus the percent of organic benzene insolubles. Light oil includes oil recovered by vacuum distillation, oil condensed from gases during depressurization, and small amounts of pentanes in the scrubbed gases. Hydrocarbon gases consist of C₁ to C₄ hydrocarbons.

RESULTS AND DISCUSSION

Coal Hydrogenation Yields

Table 2 shows yields obtained in catalyst screening experiments made with equal

Table 2.- Distribution of products from the hydrogenation of Pittsburgh-seam coal
(50 grams of coal, 4,000 psi, 425° C, 1 hour)

Exp. No.	Catalyst	Catalyst-to-coal weight ratio ^{1/}	Yields, weight-percent of maf coal						Net water
			Organic benzene insols.	Asphaltene	Heavy oil	Light oil	Hydro-carbon gases	Acid gases and CO	
1	None	-	37	28	13	6	6	3	7
2	NiI ₂ .6H ₂ O	1.0	18	2	21	38	10	4	12
3	NiBr ₂	1.0	20	4	29	33	10	6	5
4	ZnI ₂	1.0	10	1	5	55	17	7	10
5	I ₂	1.0	23	1	8	48	15	3	11
6	ZnBr ₂	1.0	10	2	8	56	14	3	13
7	ZnCl ₂	1.0	12	2	16	45	14	4	11
8	SnCl ₂ .2H ₂ O	1.0	18	7	40	29	6	4	1
9	CdI ₂	1.0	17	3	24	37	13	1	12
10	FeI ₂ .4H ₂ O	1.0	20	9	13	41	10	2	5
11	SnI ₂	1.0	8	14	42	20	6	5	5
12	ZnCl ₂	0.01	33	26	18	8	8	4	7
13	SnCl ₂ .2H ₂ O	0.01	12	38	34	7	4	5	7
14	SnCl ₂ .2H ₂ O ^{2/}	0.01	7	7	36	18	26	1	9

^{1/} Does not include water of hydration.

^{2/} Thirty minutes at 480° C.

weights of halide catalysts and coal at 4,000 psi and 425° C for 1 hour. High coal conversions of 88 to 92 percent were obtained with 4 of the catalysts. Conversions were 77 to 83 percent with the remaining catalysts as compared to 63 percent without a catalyst. However, assuming that asphaltene was a principal intermediate product, all of the halides were very effective for asphalt hydrogenation. Asphaltene contents of the benzene-soluble oils (sum of asphaltene, heavy oil, and light oil) ranged from 1.6 percent with ZnI₂ to 18 percent with SnI₂.

The last three experiments listed in table 2 were made with a conventional catalyst concentration of 1.0 percent. ZnCl₂ at 1.0 percent was a very poor catalyst. Coal conversion was only 4 percent higher than without a catalyst, and asphaltene was the principal liquefaction product. SnCl₂ is one of the best of the conventional catalysts. With 1.0 percent SnCl₂ at 425° C, a high conversion of 88 percent was obtained, but the product oil was high in asphaltenes. The last experiment, which was made with SnCl₂ at 480° C, demonstrates that a high coal conversion and low asphaltene yield are obtained at conventional conditions. It also illustrates the advantage of

lower temperature hydrogenation from the standpoint of hydrocarbon gas production and consequent hydrogen consumption. The hydrocarbon gas yield at 480° C was 26 percent as compared to 14 to 17 percent at 425° C with the most effective of the halide catalysts.

Asphaltene Hydrogenation Yields

Experiments with coal and high concentrations of halide catalysts showed these catalysts to be effective for producing oils low in asphaltene when starting with coal. Experiments with a primary asphaltene and the same catalysts were made to determine whether the halide catalysts were equally effective when the starting material was asphaltene. Conditions used were 4,000 psi, 425° C, and 1 hour at temperature with a catalyst-to-asphaltene ratio of 1.0 by weight. Results are shown in table 3 along

Table 3.- Distribution of products from the hydrogenation of asphaltene^{1/}
(50 grams asphaltene, 50 grams catalyst, ^{2/}4,000 psi, 425° C, 1 hour)

Exp. No.	Catalyst	Yields, wt pct of moisture-free asphaltene charged.							Percent reduction of insol. plus asphaltene
		Organic benzene insols.	Asphaltene	Heavy oil	Light oil	Hydrocarbon gases	Acid gases and CO	Net water	
15	None	5	67	20	2	5	1	1	22
16	NiI ₂ .6H ₂ O	7	1	37	43	10	1	3	91
17	NiBr ₂	3	5	48	31	11	2	3	91
18	ZnI ₂	6	2	22	50	14	3	4	91
19	I ₂	4	5	25	58	13	2	2	90
20	ZnBr ₂	8	2	20	57	10	1	3	89
21	ZnCl ₂	4	7	31	37	14	1	4	88
22	SnCl ₂ .2H ₂ O	6	10	50	21	8	1	0	83
23	CdI ₂	4	14	63	18	7	<1	3	80
24	FeI ₂ .4H ₂ O	21	5	9	49	17	1	5	72
25	SnI ₂	5	23	48	19	6	1	3	70

^{1/} The asphaltene feed composition was 0.9 percent moisture, 7.6 percent organic benzene insolubles, 83.6 percent asphaltene, and 7.9 percent oil on a weight basis.

^{2/} Does not include water of hydration.

with results obtained without a catalyst. All of the catalysts were very effective for asphaltene reduction. However, a more significant measure of catalyst effectiveness is the extent of reduction of both the organic benzene insolubles and the asphaltene. As shown in table 3, reduction of these two components of the feed was 22 percent without a catalyst and 70 to 91 percent with catalysts. Lowest reductions were obtained with SnI₂ and FeI₂. In the experiment with FeI₂, the yield of asphaltene was low at 5 percent, but the yield of hydrocarbon gases was highest and an appreciable amount of insolubles was produced, presumably by condensation reactions. The formation of undesirable solids and gases is indicative of an imbalance in cracking and hydrogenation activities with FeI₂. Significant amounts of insolubles were not formed in any of the other experiments including the experiment without a catalyst.

The effects of reaction variables on asphaltene hydrogenation yields were investigated briefly. Using results obtained with equal weights of ZnCl₂ and asphaltene at

4,000 psi and 425° C for 1 hour as a basis for comparison, experiments were made at higher and lower pressures, temperatures, and catalyst concentrations and with longer and shorter times at temperature. Results are shown in table 4. In the first group

Table 4.- Asphaltene hydrogenation yields using ZnCl₂ catalyst.
Effects of pressure, temperature, time, and ZnCl₂ concentration.
(50 grams of asphaltene)

Exp. No.	ZnCl ₂ -to-asphal. weight ratio	Press., psi	Temp., ° C	Time, min.	Yields, wt pct of moisture-free asphaltene charged				Hydro-carbon gases	Percent reduct. of insol. plus asph.
					Organic benzene insols.	As-phal-tene	Heavy oil	Light oil		
26	1.0	2,000	425	60	5	9	29	39	13	83
21	1.0	4,000	425	60	4	7	31	37	14	88
27	1.0	8,000	425	60	2	3	45	34	15	95
28	1.0	4,000	400	60	4	9	43	36	12	86
29	1.0	4,000	450	60	6	1	23	45	19	92
30	1.0	4,000	425	15	5	8	37	30	10	86
31	1.0	4,000	425	30	4	6	39	34	11	89
32	1.0	4,000	425	120	3	4	42	38	16	92
15	0.0	4,000	425	60	5	67	20	2	5	22
33	0.01	4,000	425	60	2	41	44	7	6	53
34	0.5	4,000	425	60	4	7	52	26	11	88
35	2.0	4,000	425	60	7	2	14	48	28	90

of experiments which were made at 2,000, 4,000, and 8,000 psi, the pressure dependence of reactions involved in insolubles and asphaltene reduction was found to be small. Reductions were 83 percent at 2,000 psi and 95 percent at 8,000 psi. Light oil yields decreased with increasing pressure indicating an apparent pressure inhibition of the heavy oil-to-light oil conversion step. This group of experiments shows that with a high concentration of ZnCl₂ at 425° C asphaltene can be hydrogenated at a practical rate at 2,000 psi or possibly at lower pressures.

In the investigation of the effect of temperature, results at 400° C were very similar to those at 425° C. Raising the temperature to 450° C caused appreciable decreases in asphaltene and heavy oil yields and increases in light oil and hydrocarbon gas yields. The data indicate that asphaltene hydrogenation would be practical at 400° C and that this low temperature would be preferred because of the lower gas-to-oil ratio than at the higher temperatures.

Experiments made to investigate the effect of reaction time at 425° C showed that all of the reactions involved in molecular weight reduction were initially quite rapid, but the rates decreased considerably as time progressed. In 15 minutes, the reduction of insolubles and asphaltene was 86 percent and light oil production was 30 percent. With increasing time, the reduction of insolubles and asphaltene proceeded much more slowly, reaching a value of 92 percent in 2 hours. This amounts to a reduction of less than 50 percent of the insolubles plus asphaltene that remained after 15 minutes. During the same period, the light oil yield increased to only 38 percent. These decreases in hydrocracking rates are an indication of some loss of catalyst

activity. To some extent, it is also likely that as hydrogenation progressed the concentration of structural types more resistant to hydrogenation progressively increased in the solids and heavy liquids remaining.

The last group of experiments in table 4 shows the effect of increasing the catalyst-to-asphaltene ratio from 0.01 to 2.0. With a ratio of 0.01, reduction of insoluble plus asphaltene was appreciable at 53 percent. The reduction reached a value of 88 percent with a ratio of 0.5 and remained essentially constant with further increases to 1.0 and 2.0. However, the extent of heavy oil conversion to light oil continued to increase with increasing catalyst concentration. The data from this group of experiments show that although the depth of hydrogenation increased over the entire range of catalyst concentrations used, very high concentrations may not be necessary to obtain high conversions of asphaltene to heavy oil in relatively short reaction times.

Composition of Hydrogenation Products

Ultimate analyses of asphaltenes and heavy oils in the products of several asphaltene hydrogenation experiments are shown in table 5. The principal differences

Table 5.- Ultimate analyses of asphaltene and heavy oil products of asphaltene hydrogenation
(50 grams of asphaltene, 50 grams of catalyst, 4,000 psi, 425° C, 1 hour)

Exp. No.	Catalyst	Elemental composition, weight-percent				
		C	H	N	S	O (diff.)
<u>Asphaltene</u>						
20	ZnBr ₂	89.0	5.8	1.0	-	-
21	ZnCl ₂	91.2	6.0	0.6	0.2	2.0
22	SnCl ₂ ·2H ₂ O	89.9	6.7	0.9	0.1	2.4
<u>Heavy Oil</u>						
16	NiI ₂ ·6H ₂ O	89.1	10.9	0.0	0.05	0.0
20	ZnBr ₂	89.7	9.7	0.3	0.05	0.25
21	ZnCl ₂	90.3	8.5	0.3	0.1	0.8
22	SnCl ₂ ·2H ₂ O	88.1	8.8	0.05	0.1	2.95

between the compositions of the residual asphaltenes and the asphaltene feed was the lower nitrogen and sulfur contents of the unconverted asphaltenes. Heavy oils contained appreciably more hydrogen than the feed and much less nitrogen and sulfur. Percentages of oxygen varied considerably. As oxygen determinations were by difference, their values are not highly meaningful.

Ultimate and fluorescent indicator adsorption (FIA) analyses of light oils produced in several experiments with both coal and asphaltene are presented in table 6. All of the oils contained less than 0.1 percent each of nitrogen and sulfur. Considering the high aromaticity of the coal from which the oils were produced, their aromatics contents of about 17 to 36 percent by volume were surprisingly low. The aromatics and saturates fractions of the light oils produced in coal experiments with ZnBr₂ and ZnCl₂ were analyzed completely by gas-liquid chromatography. More than

Table 6.- Analyses of light oils from coal and asphaltene hydrogenation
(50 grams coal or asphaltene, 50 grams catalyst, 4,000 psi, 425° C, 1 hour)

Exp. No.	Catalyst	Feed	Elemental composition, wt pct					FIA analysis, vol pct		
			C	H	N	S	O (diff.)	Aro- matics and oxy- genates	Satur- ates	Ole- fins
2	NiI ₂ .6H ₂ O	Coal	86.7	13.2	0.0	<0.1	0.0	20.9	78.6	0.5
16	NiI ₂ .6H ₂ O	Asph.	86.5	13.3	0.0	<0.1	0.2	17.4	82.5	0.1
6	ZnBr ₂	Coal	87.2	12.7	<0.1	<0.1	0.0	30.9	68.6	0.5
20	ZnBr ₂	Asph.	86.5	12.7	0.0	<0.1	0.8	30.7	69.0	0.3
7	ZnCl ₂	Coal	87.1	12.7	<0.1	<0.1	0.1	32.8	66.8	0.4
21	ZnCl ₂	Asph.	86.6	12.2	<0.1	<0.1	1.1	35.6	64.0	0.4

90 percent of the oils consisted of compounds having boiling points under 200° C. The saturates were mainly paraffins, but the ratio of iso-to-normal paraffins was about 9 to 1 in both oils. Total cyclics (aromatics and naphthenes) amounted to about 47 percent. These analyses clearly indicate that the halide catalysts are highly active for nuclear hydrogenation and ring opening reactions.

Light oils produced from coal and from asphaltene using the same catalyst differed in composition by only small amounts. The differences are probably within the limits of the reproducibility of experiments and the analytical accuracy. This similarity of compositions provides additional evidence in support of the premise that asphaltene is a principal intermediate in the hydrogenation of coal to oil.

Elemental balances were made for the experiment with ZnCl₂ and asphaltene. The amounts of nitrogen, sulfur, and oxygen eliminated were found to be 90, 80, and 68 percent, respectively. Hydrogen consumption was 4.5 percent by weight of asphaltene charged.

Practical Utilization of High Concentrations of Halide Catalysts

Process advantages that apparently would be achieved by using high concentrations of halide catalysts include operation at lower pressure and temperature and production of less hydrocarbon gas with a resultant decrease in hydrogen consumption. Serious technical and economic problems that would be expected in commercial-scale coal hydrogenation are corrosion problems and problems associated with economic recovery and regeneration of the catalyst.

Of the ten halides used in this study, only NiI₂, NiBr₂, FeI₂, and ZnI₂ have melting points above 425° C and could be used as components of solid-phase catalysts. Iodine would be a vapor, while the remaining catalysts would be liquids. In a process, the use of gaseous or liquid catalysts would necessitate continuous feeding and withdrawal of such catalysts. In the presence of the amounts of hydrogen, hydrogen sulfide, and water that would be expected at coal hydrogenation conditions, reduction of the metal halide catalysts to the corresponding metals and conversions to oxides and sulfides are potential catalyst consuming reactions. Available free energy data for these reactions indicate that the metal halide is the thermodynamically favored form in each instance in the absence of an organic liquid phase. The halides may also react with ammonia to form complexes such as those formed with ZnCl₂ during coal extract hydrogenation,^{2/} or they may interact with and be retained in the product oil.^{2/} Some

of the catalyst reactions might possibly be avoided through the use of scavengers or by other controls of the partial pressures of gaseous reactants and products. The addition of a metal or oxide that preferentially reacts with hydrogen sulfide might prevent catalyst loss through sulfiding reactions, while reaction of a halide catalyst with hydrogen might be suppressed by adding a small amount of the corresponding hydrogen halide to the feed gas. The practicability of such measures is presently not known.

SUMMARY

Iodine and halides of Ni, Zn, Sn, Cd, and Fe, when used as catalysts in high concentration at 4,000 psi and 425° C, were found to be very effective for hydrogenating bituminous coal to oils containing only small amounts of asphaltene. When the feed material was an asphaltene produced by mild hydrogenation of the same coal, these catalysts were equally effective for converting the asphaltene to oil. Low-boiling oils produced from both coal and asphaltene were very similar in composition. These data show that the halides used are highly selective for hydrogenating asphaltene to oil. This is the slow and rate-controlling step when hydrogenating coal in the presence of conventional catalysts. A pressure of 3,500 psi or higher and a temperature of at least 450°C are required in conventional coal hydrogenation to reach low levels of asphaltene production in relatively short reaction times. With high concentrations of ZnCl₂, asphaltene hydrogenation to oil was readily accomplished in this study at 2,000 psi and 425° C and also at 4,000 psi and 400° C. Although halide catalysts in high concentration offer some process advantages, their practical utilization will require efficient and low-cost recovery and regeneration of the catalysts.

REFERENCES

1. Weller, Sol, M. G. Pelipetz, and Sam Friedman. Kinetics of Coal Hydrogenation. Conversion of Anthraxylon. *Ind. & Eng. Chem.*, 43, 1575 (1951).
2. Hawk, C. O., and R. W. Hiteshue. Hydrogenating Coal in the Batch Autoclave. *BuMines Bull.* 622, 1965, 42 pp.
3. Zielke, C. W., R. T. Struck, and Everett Gorin. Fluidized Combustion Process for Regeneration of Spent Zinc Chloride Catalysts. *Ind. & Eng. Chem. Process Des. & Dev.*, 8, 552 (1969).
4. Eddinger, R. T., and L. D. Friedman. Hydrogenation of Low-Temperature Coal Tars Using Iodine as Catalyst. *Fuel*, 47, 320 (1968).

Hydrogenation of Coal to Liquids on Fixed Beds
of Silica Promoted Cobalt Molybdate Catalyst

Sayed Akhtar, Sam Friedman, and R. W. Hiteshue

U.S. Bureau of Mines, 4800 Forbes Avenue
Pittsburgh, Pennsylvania 15213

INTRODUCTION

The essential steps in the conversion of coal to liquid fuels are coal liquefaction, ash removal, and processing of the de-ashed liquid for the removal of S, N, and O, conversion of asphaltenes to oil, addition of H, cracking, and if the objective is gasoline, octane improvement¹. In practice, the functions of the process steps may overlap. Thus, certain methods of coal liquefaction are accompanied by considerable conversion of asphaltenes to oil, cracking, and partial removal of the heteroatoms. The cost and complexities of processing the de-ashed liquid depend on its composition and, therefore, on the method of coal liquefaction. The present work describes the hydrogenation of slurries of coal in high-temperature tar to a liquid of low asphaltenes, S, N, and O content on fixed beds of pelleted cobalt molybdate catalyst in single pass experiments.

EXPERIMENTAL

Plant and Procedure

Figure 1 is a flow diagram of the hydrogenation plant. The combined stream of hydrogen and mixtures of coal and high-temperature tar passed through a preheater before entering the packed bed reactor which was an 11-foot long stainless steel tube of 3-inch id. The gases and liquids leaving the reactor were led through a receiver for liquid products which was fitted with a water-cooled condenser in its upper part. The heavy liquids and coal residues were collected in this vessel from where they were intermittently discharged into a secondary vessel at atmospheric pressure. The gases and vapors leaving the receiver for heavy liquids were passed through a second condenser to liquefy the lighter ends of the liquid products. The lighter liquid products were collected in a second receiver, and the gas stream was reduced to atmospheric pressure, metered, and flared.

As a precaution against runaway temperatures, the slurry was first introduced into the reactor at 350° C and the incipient hyperactivity of the catalyst was allowed to subside before the reactor was raised to higher temperatures. The heating rate was set at about 10° C per hour, and after the reactor had been heated to the desired temperature, the plant was operated for a nondata period of 2 hours to ensure steady conditions. Similarly, whenever any of the process variables was changed, the plant was allowed 2-3 hours of equilibration time.

The charge weight of catalyst was 31 pounds, and the paste feed rate was 10 lb/hr which is equivalent to a throughput of 20 lb/hr/cu ft of empty reactor. Hydrogen was introduced at a rate of 500 cu ft/hr. The liquid products were collected in batches of 50 pounds and analyzed by conventional methods. Gases were analyzed by gas-solid chromatography. The conversion of organic benzene insolubles to benzene solubles and gases was computed from the total organic benzene insolubles in the feed (maf coal + organic benzene insolubles from tar) and the organic benzene insolubles in the liquid products. To determine the conversion of maf coal, the conversion of organic benzene insolubles from tar under identical experimental conditions should be known separately. The latter information is available for only one set of temperature and pressure, namely 425° C and 4,000 psi².

Materials

Technical data for the commercial silica promoted cobalt molybdate catalyst employed in this work are presented in table 1, and the analyses for coals and high-temperature tars are given in tables 2 and 3 respectively. The three lots of coal differed chiefly in ash content: lot #1 coal had 4.7 percent ash compared to 7.0 percent ash in lot #2 coal, and 11.1 percent ash in lot #3 coal. The two lots of tar differed in ash content, oil distillable below 355° C, and viscosity. Hydrogen of better than 98.5 percent purity was prepared by catalytic reforming of natural gas.

RESULTS AND DISCUSSIONS

In view of the scale of the experiments, it was not practicable to investigate the influence of every change in each process variable with a fresh bed of catalyst. It was therefore decided to study the changes in one variable on one bed and to correct the results by empirically determined factors for catalyst de-activation before comparing them. Thus, the influence of changes in slurry composition was studied on one bed, that of changes in temperature on another bed, and the influence of changes in pressure on a third bed. The specifications for the three experiments were as follows:

1. Influence of slurry composition.

Temperature: 425° C
Pressure: 4,000 psi } constant

Slurry composition, wt pct: a. 20 coal - 80 tar
b. 30 coal - 70 tar
c. 40 coal - 60 tar

2. Influence of temperature.

Slurry composition, wt pct: 30 coal - 70 tar } constant
Pressure: 4,000 psi

Temperature: 450° C
460° C
470° C

3. Influence of pressure.

Slurry composition, wt pct: 30 coal - 70 tar } constant
Temperature: 425° C

Pressure: a. 4,000 psi
b. 3,000 psi
c. 2,000 psi
d. 1,000 psi

Catalyst De-activation

Batchwise analysis of the liquid products from these experiments revealed that under fixed experimental conditions the specific gravity of the liquid products and their composition in terms of organic benzene insolubles, asphaltenes, oil, H, N, and S were approximately constant over the duration of the experiment. The rate of catalyst de-activation vis-a-vis these properties of the liquid products thus appears to be negligible and the results from successive hydrogenations under different experimental conditions may be compared without any correction for catalyst de-activation. The data for a few selected parameters are plotted against time in figures 2-4.

Table 1.- Technical data^{1/} for silica promoted cobalt molybdate catalyst

Chemical composition, wt pct

CoO	3
MoO ₃	15
SiO ₂	5
Al ₂ O ₃	support

Physical properties

Bulk density, lb/cu ft	60
Surface area, m ² /g	200
Pore volume to 10,000 Å, cc/g	0.4
Pore diameter (average), Å	100
Size and form	1/8 inch x 1/8 inch tablets

^{1/} Supplied by the manufacturers.

Table 2.- Ultimate analysis of hvab Pittsburgh coal,^{1/} weight-percent

	<u>Lot #1</u>		<u>Lot #2</u>		<u>Lot #3</u>	
	<u>As recd.</u>	<u>maf</u>	<u>As recd.</u>	<u>maf</u>	<u>As recd.</u>	<u>maf</u>
Moisture	0.6		1.3		0.8	
Ash	4.7		7.0		11.1	
Carbon	79.8	84.3	77.2	84.2	73.5	83.4
Hydrogen	5.4	5.7	5.2	5.7	4.9	5.6
Nitrogen	1.6	1.7	1.5	1.6	1.4	1.6
Sulfur	1.2	1.3	1.6	1.7	1.3	1.5
Oxygen (by diff.)	6.7	7.0	6.2	6.8	7.0	7.9

^{1/} 70 percent through U.S. Standard sieve 200.

Table 3.- Inspection data for high-temperature tar

	<u>Lot 'A'</u>	<u>Lot 'B'</u>
<u>Solvent analysis, wt pct</u>		
Benzene insolubles	13.5	14.0
Asphaltenes	34.7	39.6
Oil	51.8	46.4
<u>Ultimate analysis, wt pct</u>		
Carbon	92.2	92.3
Hydrogen	5.1	4.9
Nitrogen	1.1	1.2
Sulfur	0.8	0.6
Oxygen (by difference) ..	0.8	1.0
<u>Ash, wt pct</u>	<0.1	0.7
<u>AWPA distillation, wt pct</u>		
325° C	2.9	0.0
325° - 355° C	11.1	0.1
<u>Viscosity, ssf at 180° F</u>		
(82° C)	389	500

The hours on stream for a batch plotted in these figures are computed for the point of time midway in the batch.

An additional check on the stability of the catalyst's activity was conducted while investigating the influence of pressure. After 150 hours of experiments at the series of pressures 4,000-1,000 psi, the plant pressure was restored to 4,000 psi and the hydrogenation continued for 29 hours. The batchwise inspection data of the liquid products from this period for organic benzene insolubles, asphaltenes, and specific gravity are given in figure 4, and the average analysis of the liquid products is compared with the average analysis of the liquid products from the earlier period of hydrogenation at 4,000 psi in table 4. The agreement in the results for the two periods is within experimental error. The experiment however revealed a measurable loss in the catalyst's activity with respect to the yield of oil boiling below 355° C: the average yield decreased from 53 percent by weight of the feed to 37 percent in 139.5 hours--the time interval between the midpoints of the two periods of experiment at 4,000 psi. To allow for catalyst de-activation, the actual yields in experiments at 425° C may therefore be corrected according to the following equation before comparison:

$$\text{Corrected yield} = \text{Actual yield} (1 + 0.0031 \times \text{hours on stream}).$$

Table 4.- Average analysis of liquid products
at 4,000 psi and 425° C

	<u>1st period</u>	<u>2nd period</u>
Hour on stream	0 - 50.5	150.5 - 179
<u>Solvent analysis, wt pct</u>		
Organic benzene insolubles	7.1	7.1
Asphaltenes	12.3	14.2
Oil	77.1	75.2
Ash	3.5	3.6
<u>Ultimate analysis, wt pct (ash-free basis)</u>		
Carbon	88.5	88.3
Hydrogen	8.3	8.1
Nitrogen	0.4	0.5
Sulfur	0.3	0.3
Oxygen (by difference)	2.5	2.9

Influence of Slurry Composition

The influence of slurry composition on the parameters of interest is shown in figure 5. At 425° C and 4,000 psi, approximately 74 percent of the combined organic benzene insolubles from coal and tar was converted to benzene solubles or gases, and the conversion was independent of slurry composition in the range 20-40 wt pct coal. This corresponds to an average conversion of about 81 percent maf coal. The concentration of residual organic benzene insolubles and asphaltenes in the liquid products increased linearly with increase of coal concentration in the feed and, correspondingly, the concentration of oil decreased. As the coal concentration increased from 20 to 40 percent in the feed, the concentration both of organic benzene insolubles and asphaltenes in the liquid products increased by about 50 percent, from 8.4 percent

to 12.7 percent and from 11.0 percent to 17.2 percent respectively. The oil concentration decreased from 80 to 68 percent.

Ultimate analysis of the liquid products revealed that the residual concentration of S, 0.2 percent, was only nominally affected by increase in coal concentration, but the concentration of N increased sharply from 0.3 to 0.7 percent as the coal concentration increased from 20 to 40 percent. For the same change in coal concentration, the H content of the liquid products decreased from 8.5 to 7.8 percent.

The yield of oil boiling below 355° C was highest at 30 percent coal concentration: the corrected yield amounted to 47 percent by weight of the feed compared to 37 percent at both 20 percent and 40 percent coal concentrations. The shape of the yield curve in figure 5 is of course arbitrary in-so-far as the precise location of the maxima is concerned.

The yield of total liquid products and gaseous hydrocarbons, 95 percent and about 1.5 percent of the paste feed respectively, were independent of slurry composition.

Influence of temperature

The influence of temperature on the hydrogenation of 30 weight-percent coal slurry at 4,000 psi is shown in figure 6. The results for 425° C are from the previous experiment. The conversion of organic benzene insolubles at 450° C was the same as at 425° C--about 75 percent--but decreased to 65 percent at 460° C and 55 percent at 470° C. The solvent and ultimate analyses of the liquid products showed a similar pattern of influence of temperature. The analyses of the products at 425° C and 450° C differed only marginally, but the analyses of the products at 460° C and 470° C were markedly different. The concentration of organic benzene insolubles, asphaltenes, S, and N increased rapidly with temperature above 450° C and the concentration of oil and H decreased. The yield of oil boiling below 355° C decreased from 38 percent by weight of the feed at 425° C to 29 percent at 470° C.

Another undesirable influence of increase in reaction temperature was an inordinate increase in the yield of gaseous hydrocarbons--from about 1.5 percent of the paste feed at 425° C to 9.2 percent at 450° C. Since the objective of this program calls for maximizing the yield of liquid products, the gaseous hydrocarbons represent a wasteful consumption of H₂. The yields of gaseous hydrocarbons at 460° C and 470° C were 7.8 and 5.7 percent of the paste feed respectively. Thus, in the range of temperature 425°-470° C, the yield of gaseous hydrocarbons appears to be maximum at 450° C.

The yield of total liquid products was 95 percent by weight of the feed at 425° C, 90 percent at 450° C, and 93 percent each at 460° C and 470° C.

Influence of Pressure

The influence of pressure on the hydrogenation of 30 wt pct coal slurry at 425° C in the range of 1,000-4,000 psi is shown in figure 7. The conversion of organic benzene insolubles even at the lowest pressure of 1,000 psi was 55 percent, and increased with pressure to 74 percent at 2,000 psi, and 79 percent at 3,000 psi. The conversion at 4,000 psi, 81 percent, was only nominally different from that at 3,000 psi. Thus, insofar as the conversion of organic benzene insolubles is concerned, the advantage in operating above 2,000 psi is nominal. However, the solvent and ultimate analyses of the liquid products and the figures for the yield of oil boiling below 355° C show substantial improvement in the quality of the liquid products between 2,000 and 4,000 psi.

the concentration of asphaltenes decreased from 24.9 percent at 2,000 psi to 12.3 percent at 4,000 psi, the concentration of N decreased from 0.8 percent to 0.4 percent, the H content of the liquid products increased from 6.9 percent to 8.3 percent, and the corrected yield of oil boiling below 355° C increased from 38 percent to 57 percent. Indeed, the H content of the liquid products and the yield of oil boiling below 355° C appear to be increasing at significant enough rates near the upper limit of our pressure range that some investigation at pressures higher than 4,000 psi may be profitable.

It may be noted that the removal of S is independent of pressure: the residual concentration of S in the liquid products was essentially constant at about 0.2-0.3 percent over the range of 1,000 to 4,000 psi. The removal of N, however, is pressure dependent. The residual concentration of N in the liquid products decreased linearly with increase in pressure, from 1.0 percent at 1,000 psi to 0.4 percent at 4,000 psi. The yields of total liquid products and gaseous hydrocarbons, 95-98 percent and about 3 percent of the paste feed respectively, were independent of pressure.

Throughout the series of experiments described in the present work, the material balance was 95-98 percent, and ash recovery was essentially quantitative.

Influence of Ash

In the course of the investigations described above, the hydrogenation of 30 wt pct coal slurry at 425° C and 4,000 psi was conducted twice: first during the investigation of the influence of slurry composition, and again during the investigation of the influence of pressure. We will call the former run A and the latter run B. A comparison of the results of the two runs--for convenience brought together in table 5-- shows that the conversion of organic benzene insolubles and the yield of oil boiling below 355° C was higher in run B than in run A. We believe this difference is due to the higher ash content of the coal and tar employed in run B compared to the ash content of the coal and tar employed in run A. In run B, the coal employed came from lot #3 which had 11.1 percent ash, and the tar came from lot B which had 0.7 percent ash. For run A, the coal had come from lot #1 which had 4.7 percent ash, and tar from lot A which had <0.1 percent ash. Ash from hvab Pittsburgh coal contains 10 percent or more Fe, a conventional catalyst for the conversion of coal to liquids. In addition, the ash has been reported to contain Sn, Mn, and other transition elements known to have catalytic activity in the hydrogenation of coal (3).

CONCLUSIONS

Slurries of coal in high-temperature tar can be hydrogenated on fixed beds of pelleted cobalt molybdate catalyst. The concentration of oil in the liquid products decreased as the concentration of coal in the feed increased from 20 to 40 percent. In the range of temperature 425° C-470° C and pressure 1,000-4,000 psi, hydrogenation of 30 wt pct coal slurry proceeded most favorably at 425° C and 4,000 psi. Under these conditions, 91 percent of maf coal was converted to liquids and gases, with the yield of liquid products amounting to 96 percent of the paste feed. Approximately 77 percent of the liquid products was oil, 7 percent organic benzene insolubles, 12 percent asphaltenes, and the balance ash. The liquid products contained 8.3 percent H, 0.4 percent N, and 0.3 percent S on an ash-free basis. The initial yield of oil boiling below 355° C was 53 percent by weight of the feed.

REFERENCES

1. Mills, G. Alexander. "Conversion of Coal to Gasoline," Ind. & Eng. Chem., v. 61, No. 7, 1969, pp. 6-17.
2. Akhtar, Sayeed, et al. Unpublished results.
3. Sol Weller and Michail G. Pelipetz. Catalysts in Liquid-Phase Coal Hydrogenation. Proceedings of the third World Petroleum Congress, 1951, Sec. 4, pp. 91-97.

Table 5.- Influence of ash on the hydrogenation of coal slurry in high-temperature tar

	Run A (low ash)	Run B (high ash)
Conversion of organic benzene	74	81
insolubles, wt pct	74	81
Conversion of maf coal, wt pct	81	91
<u>Solvent analysis of liquid products, wt pct</u>		
Organic benzene insolubles	10.2	7.1
Asphaltenes	13.6	12.3
Oil	74.7	77.1
<u>Ultimate analysis of liquid products, wt pct (ash-free basis)</u>		
Carbon	88.8	88.5
Hydrogen	8.1	8.3
Nitrogen	0.5	0.4
Sulfur	0.2	0.3
<u>Yield of oil boiling below 355° C, wt pct of feed (corrected for catalyst de-activation)</u>		
	46.9	56.6

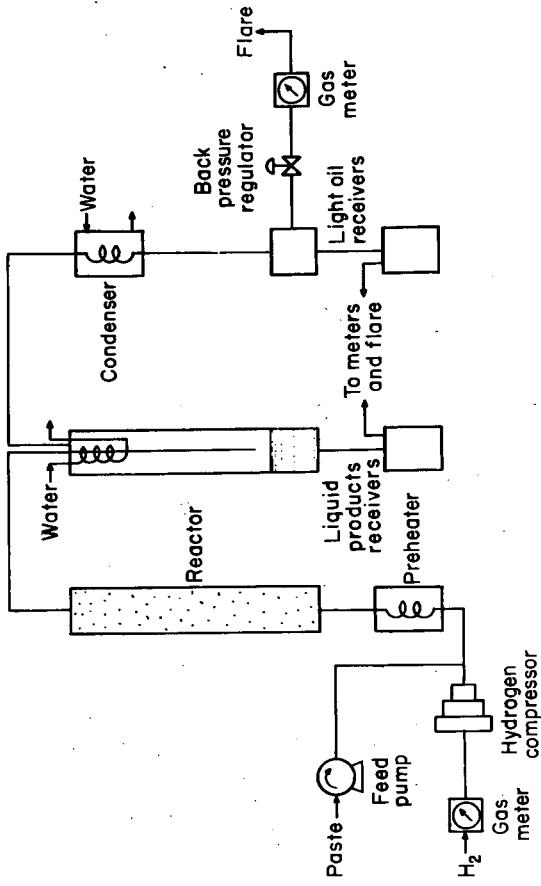


Figure 1—Hydrogenation plant.

L-11355

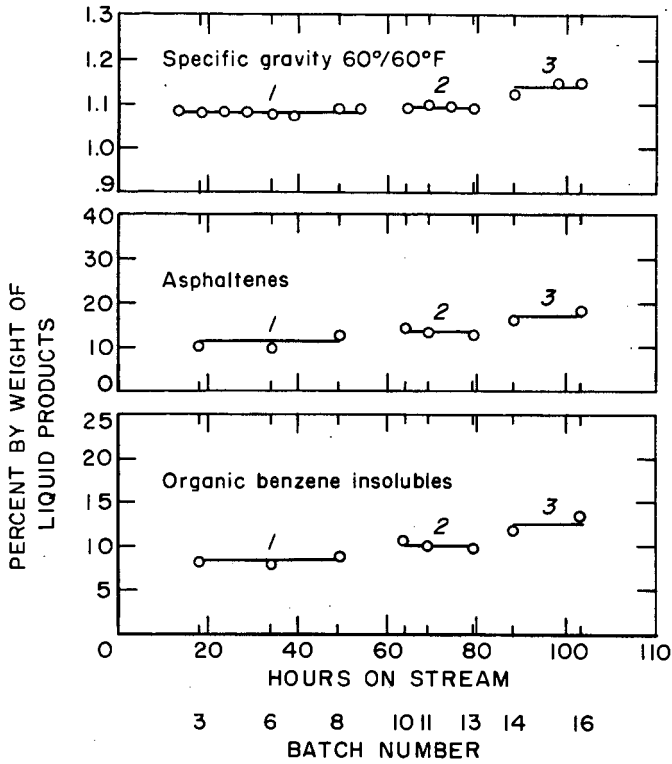


Figure 2 - Batchwise analysis of liquid products from the hydrogenation of coal slurries of different composition. 1. 20 coal-80 tar, 2. 30 coal-70 tar, 3. 40 coal-60 tar.

L-11631

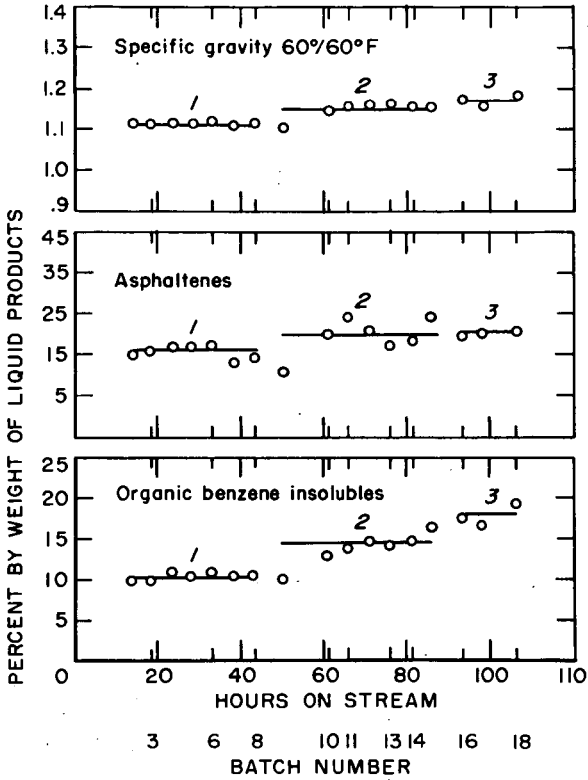


Figure 3-Batchwise analysis of liquid products from hydrogenation at different temperatures. 1. 450°C, 2. 460°C 3. 470°C

L-11632

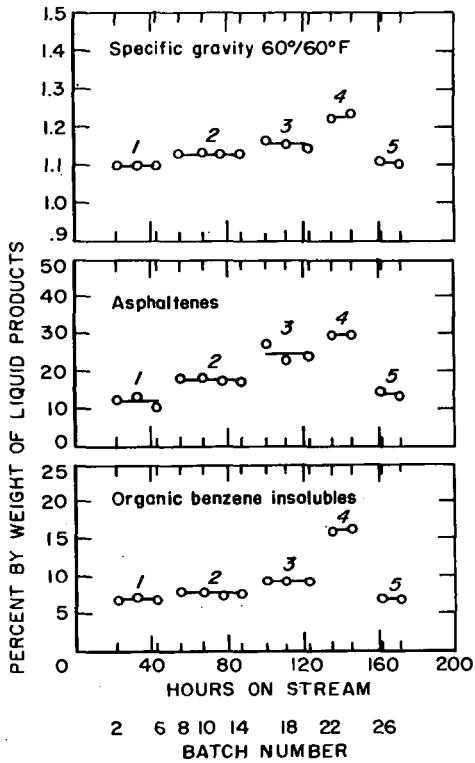


Figure 4- Batchwise analysis of liquid products from hydrogenation at different pressures.
1. 4,000 psi, 2. 3,000 psi
3. 2,000 psi, 4. 1,000 psi
5. 4,000 psi.

L-11633

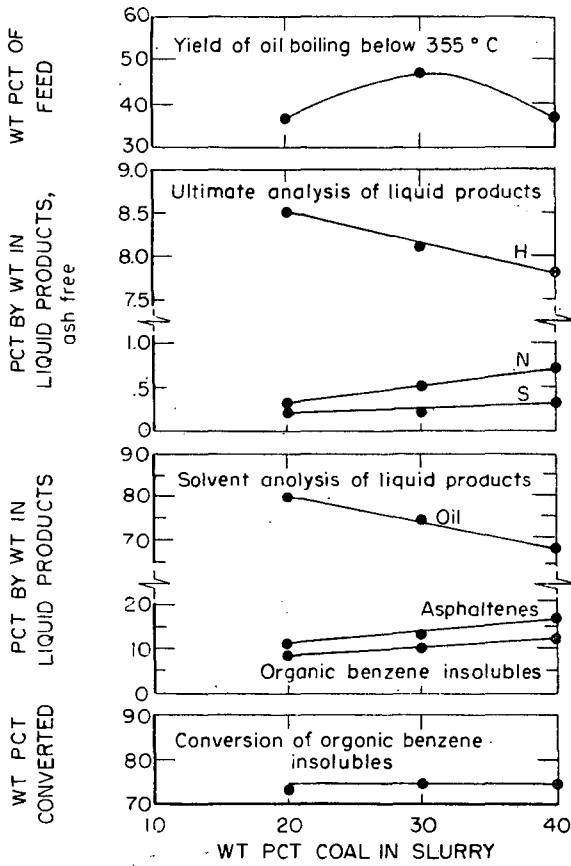


Figure 5—Influence of slurry composition on insols. conversion and composition of liquid products.

L-11634

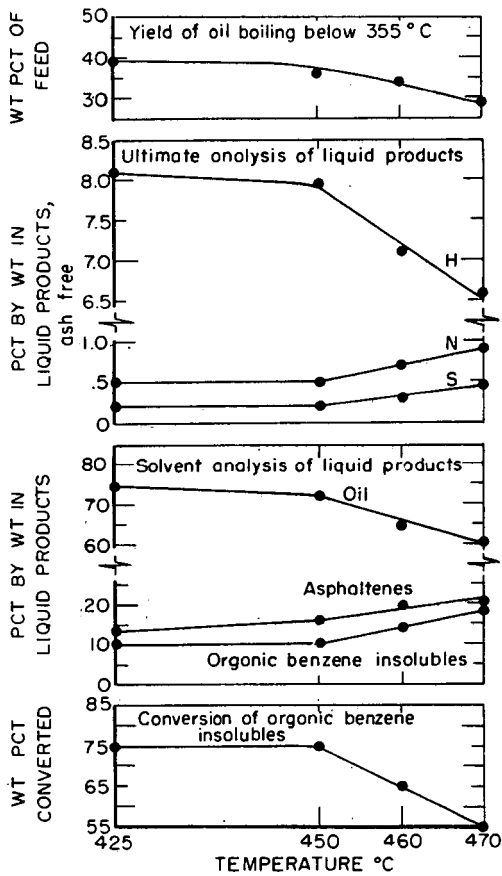


Figure 6—Influence of temperature on insols. conversion and composition of liquid products.

L-11635

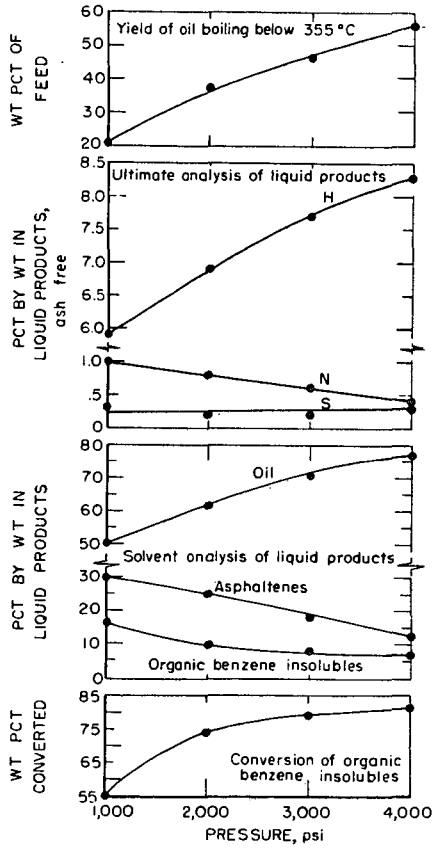


Figure 7—Influence of pressure on insols conversion and composition of liquid products.

L-11636

Hydrogenation of COED Coal Oils

Harry E. Jacobs

Atlantic Richfield Company, Harvey, Illinois

J. F. Jones and R. T. Eddinger

FMC Corporation, Princeton, New Jersey

Introduction

The Office of Coal Research, Department of the Interior, has sponsored several projects having as one of their objectives, the production of oil from coal. One of these, project COED, conducted by FMC Corporation, produces oil by low temperature pyrolysis of coal. The Atlantic Richfield Company, which had been conducting hydrogenation experiments on coal derived oils, was requested by the Office of Coal Research to hydrotreat some COED oils. Accordingly, the following work was carried out by ARCO in cooperation with FMC.

Raw oils from the COED process have a low hydrogen content and high concentrations of oxygen, nitrogen, and sulfur. Hence, hydrotreating is required before the oils can be used in present day petroleum refining processes. In the COED process, the oil product is taken from the reactors as a vapor, leaving the residual ash and char to be withdrawn separately as a fluidized solid. Any entrained solids in the oil vapor are removed by cyclones and by filters. Consequently the COED oil, being virtually solids free, can be hydrotreated in fixed bed reactors.

Hydrogenation Equipment

The equipment used by the ARCO laboratories is a typical bench scale high-temperature, high-pressure continuous unit of the type used in petroleum process research. The unit is shown schematically in Figure 1. The oil in a heated, gas blanketed charge tank is circulated by a low pressure, positive displacement pump. This serves to maintain a uniform mixture in the feed tank and to supply a positive pressure at the suction of the high pressure feed pump. The oil is combined with hydrogen and preheated before passing downflow through the 14 inch catalyst bed. The product is cooled and separated into gas and liquid fractions for sampling and analysis.

The double pumping system reduced the problem of interruption of flow. COED oil, being a pyrolysis product, can form polymers and coke at temperatures above 600°F. This is not a problem as long as liquid flow is maintained. However, if the flow is interrupted, the oil does not drain from the reactor fast enough to avoid coking.

The catalyst used is commercially available HDS-3A manufactured by American Cyanamid. It is a 1/16-inch extrudate containing 3% NiO and 15% MoO₃ on alumina.

Results of Hydrogenation

COED oils from three coals were charged. Their composition and gravity are shown in Table I.

Table I

PROPERTIES OF HYDROGENATION FEEDS

<u>Oil Source</u>	<u>% C</u>	<u>% H</u>	<u>% O</u>	<u>% N</u>	<u>% S</u>	<u>Density, °API</u>
Utah	83.3	8.5	6.8	1.1	.34	-3.5°
Illinois No. 6	80.1	7.2	9.1	1.1	2.50	-13.1°
Pittsburgh Seam	83.3	7.1	6.6	1.2	1.80	-12.3°

The Utah and Illinois No. 6 are high-volatile B bituminous coals. Pittsburgh seam is a high volatile A bituminous coal. The major differences between the oils are the lighter density, lower sulfur, and higher hydrogen content of the Utah oil. The Illinois No. 6 oil is highest in sulfur and oxygen.

All of the hydrogenation experiments discussed in this report, were conducted at 3000 psig. Hydrogen flow rates were generally between 8,000 and 12,000 SCF/Ebl. Variations in hydrogen rates did not have a significant effect on the hydrogenation reactions. The process variables were space velocity and temperature. The latter ranged from 650° to 850°F. and space velocities (WHSV) of 0.3 to 3.0 lbs./hr. of oil per lb. of catalyst were used.

Hydrogen consumption was between 1500 to 4500 SCF/Ebl. The exothermic reaction resulted in an uneven temperature profile in the catalyst bed. In a typical run the temperature rose 65° in the first 2 to 4 inches of the bed. The temperature then declined gradually in the remaining bed as the heat sink of the reactor and furnace removed heat from the system. The temperatures used for correlating the data are arithmetic averages of temperatures taken at one-inch intervals in the bed. This average temperature is about 20° less than the maximum temperature.

The data on removal of oxygen, nitrogen and sulfur were correlated by simple first-order kinetics. Figure 2 shows the removal of nitrogen from Illinois No. 6 oil. Nitrogen removal is plotted as a function of reciprocal space velocity and temperature. The temperature factor indicates an activation energy of 29,000 BTU per lb. mol. The temperature factor was obtained by first plotting the nitrogen removal vs. reciprocal space velocity. Deviations from a line through the data were plotted against temperature.

Figures 3 and 4 show similar correlation for oxygen removal and sulfur removal from Illinois No. 6 oil. Indicated activation energies are 15,000 BTU per lb. mol. for oxygen and 9,500 BTU per lb. mol. for sulfur removal. Qadar, Wiser and Hill(1) found that the activation energies for nitrogen and sulfur removal from a low temperature coal tar changed at about 750°F. The general scatter of the data and the method of determining average temperature in this work preclude the identification of different activation energies above and below 750°F.

Nitrogen is the most difficult of the heteroatoms to be removed. At 720°F. and 1 WHSV the removals from Illinois No. 6 oil are as follows: Nitrogen, 72%; Oxygen, 91%; and Sulfur, 98%.

The examination of the heteroatom removal from the other oils disclosed that the temperature trends found for the Illinois No. 6 oil also applied to all three. However, the reaction rates vary with the oils. Figure 5 shows that for nitrogen removal, the Utah oil requires only two-thirds the severity of the Illinois No. 6 oil. The Pittsburgh oil requires twice the severity of the Illinois No. 6 oil. Figure 6 shows oxygen removal. Pittsburgh oil requires 2½ times the severity of Illinois No. 6, and Utah oil needs 80% of the Illinois No. 6 severity. Sulfur removal shown in Figure 7 is slightly different. Pittsburgh oil needs 2.3 times the Illinois severity. Sulfur removal from Utah oil is indicated to be more difficult than from Illinois No. 6 oil. This difference may not be real. Because of

the low 0.3% sulfur content of the Utah oil feed, there is more scatter in the data on this feed than the other two.

The required space velocities for 80% oxygen, nitrogen and sulfur removal from the three oils are given in Table II.

Table II

SPACE VELOCITIES FOR 80% REMOVAL
CONDITIONS, 720°F. AND 3000 PSIG.

	80% Nitrogen Removal	80% Oxygen Removal	80% Sulfur Removal
	WHSV	WHSV	WHSV
Utah	1.2	1.8	1.8
Illinois No. 6	.8	1.5	2.6
Pittsburgh	.4	.6	1.1

Total hydrogen consumption was also correlated by pseudo first order kinetics. First the quantity of hydrogen required to convert the oil to cycloparaffins (C_nH_{2n}) and to remove all oxygen, nitrogen and sulfur as water, ammonia, and hydrogen sulfide was determined. This hydrogen saturation value assumes no cracking.

<u>Oil Source</u>	<u>Hydrogen for Total Saturation</u>
Utah	4600 SCF/Ebl.
Illinois No. 6	6200 SCF/Ebl.
Pittsburgh	6400 SCF/Ebl.

The observed hydrogen consumption, divided by the quantity needed for total saturation is reported as the percent hydrogen saturation. This value was then plotted as a function of reciprocal space velocity and temperature in the same manner as for heteroatom removal. As seen on Figure 8, when plotted in this manner, the data from Utah and Illinois No. 6 oils fall on a common line. The Pittsburgh oil requires $2\frac{1}{2}$ times as much severity to obtain a similar degree of saturation.

This method of correlating hydrogen consumption ignores any effect the approach to equilibrium may have on the rate of hydrogen usage. The fact that the data plots as well as it does indicates that the reactions are not equilibrium controlled.

The reasons for the differences in ease of hydrogenation and heteroatom removal for the three oils are not known, but they are probably related to the hydrogen-carbon ratio of the oils. The atomic ratios of the oils are as follows:

	<u>H/C Ratio</u>
Utah	1.22/1
Illinois No. 6	1.08/1
Pittsburgh	1.02/1

The last reaction examined is the production of gas by cracking. As seen in Figure 9, the gas yield climbs precipitously at temperatures above 780°F. The effect of temperature is so overwhelming that no trends with space velocity could be obtained. Cracking of all three oils fall on a common temperature line. This data indicates the necessity of keeping the catalyst bed temperature below 780°F. if oil is the desired product.

No catalyst life studies were made, but it is anticipated that catalyst life would be related inversely to the gas production.

Properties of the Hydrogenated Oils

The °API gravity of the products varies directly with the hydrogen consumption. However, as shown in Figure 10 the oils fall on three separate lines. For example, the production of a 25°API hydrogenated oil from Utah oil needs only 2700 SCF/Bbl. A similar product from Illinois No. 6 oil would need 4050 SCF/Bbl. and the Pittsburgh Seam oil would use 4550 SCF/Bbl.

Distillation curves of the three oil feeds and three products that were made with similar hydrogen consumption are shown in Figure 11. The consumption of 3600 SCF of hydrogen per barrel lowers the boiling range of each oil about 300°F. It should be noted that there is little, if any, residuum (material boiling above 1000°F.) left in these oils.

The properties of these three product oils are as follows:

Table III

PROPERTIES OF HYDROGENATED OIL PRODUCT

<u>Oil Source</u>	<u>Utah</u>	<u>Illinois No. 6</u>	<u>Pittsburgh</u>
<u>Conditions</u>			
Weight hourly space velocity	0.75	1.3	0.50
Temperature, °F.	748°	798°	742°
Pressure, PSIG	3000	3000	3000
<u>Hydrogen Consumption, SCF/Bbl</u>	3500	3600	3700
<u>C₄+ Liquid Product</u>			
°API	31.8°	22.5°	19.6°
Viscosity, SUS @ 180°F.	34.6	----	44.9
Pour Point, °F.	80°	30°	20°
Ramsbottom Carbon, Wt. %	0.44	----	3.85
% H	12.7	----	10.9
% O	0.13	----	0.7
% N	0.05	----	0.14
% S	< 50 ppm	----	0.03

The high pour point of the Utah oil product is caused by a larger paraffin content. A comparison of the reformer stock and middle distillate fractions from Utah and Pittsburgh oils shows this difference.

Table IV

PROPERTIES OF PRODUCT FRACTIONS

<u>Oil Source</u>	<u>Utah</u>	<u>Pittsburgh</u>
<u>Reformer Stock (C₆-400°F.)</u>		
Yield, Vol. %	12.5	9.6
°API	38.7°	37.6°
Paraffins, Vol. %	18	6
Cycloparaffins, Vol. %	65	74
Aromatics, Vol. %	17	20

Oxygen, Wt. %	.06	.47
Nitrogen, Wt. %	.10	.09
Sulfur	Trace	5 ppm
Middle Distillate (400-650°F.)		
Yield, Vol. %	68.2	38.9
°API	30.1°	22.5°
Paraffins, Vol. %	25	1
Cycloparaffins, Vol. %	39	55
Aromatics, Vol. %	36	44
Oxygen, Wt. %	.20	.48
Nitrogen, Wt. %	.06	.12
Sulfur	Trace	30 ppm

The two reformer stocks above are satisfactory reformer feeds after conventional pretreat steps to remove the residual oxygen and nitrogen. The high concentration of ring structures indicates that only a very mild reforming severity is needed to produce a high octane naphtha. The middle distillates can be used as heating oils, or after oxygen and nitrogen removal, by conventional pretreating, they can be charged to a hydrocracker for additional gasoline production.

The high cycloparaffin content of the hydrogenated COED oils would classify the syncrudes as the naphthenic type. Although the °API gravity of these oils may be lower than most crude oils, they contain much less residuum than typical crudes. These hydrogenated COED coal oil syncrudes can be processed in typical petroleum refinery units.

Conclusion

In summary, the removal of heteroatoms and the gross hydrogen consumption occurring during the hydrogenation of COED coal oils can be correlated by simple, first-order kinetics. The oil from Pittsburgh seam coal is more difficult to hydrogenate than the oils from Utah and Illinois No. 6 coals. The Utah oil requires less hydrogen consumption than the other two to produce a superior oil.

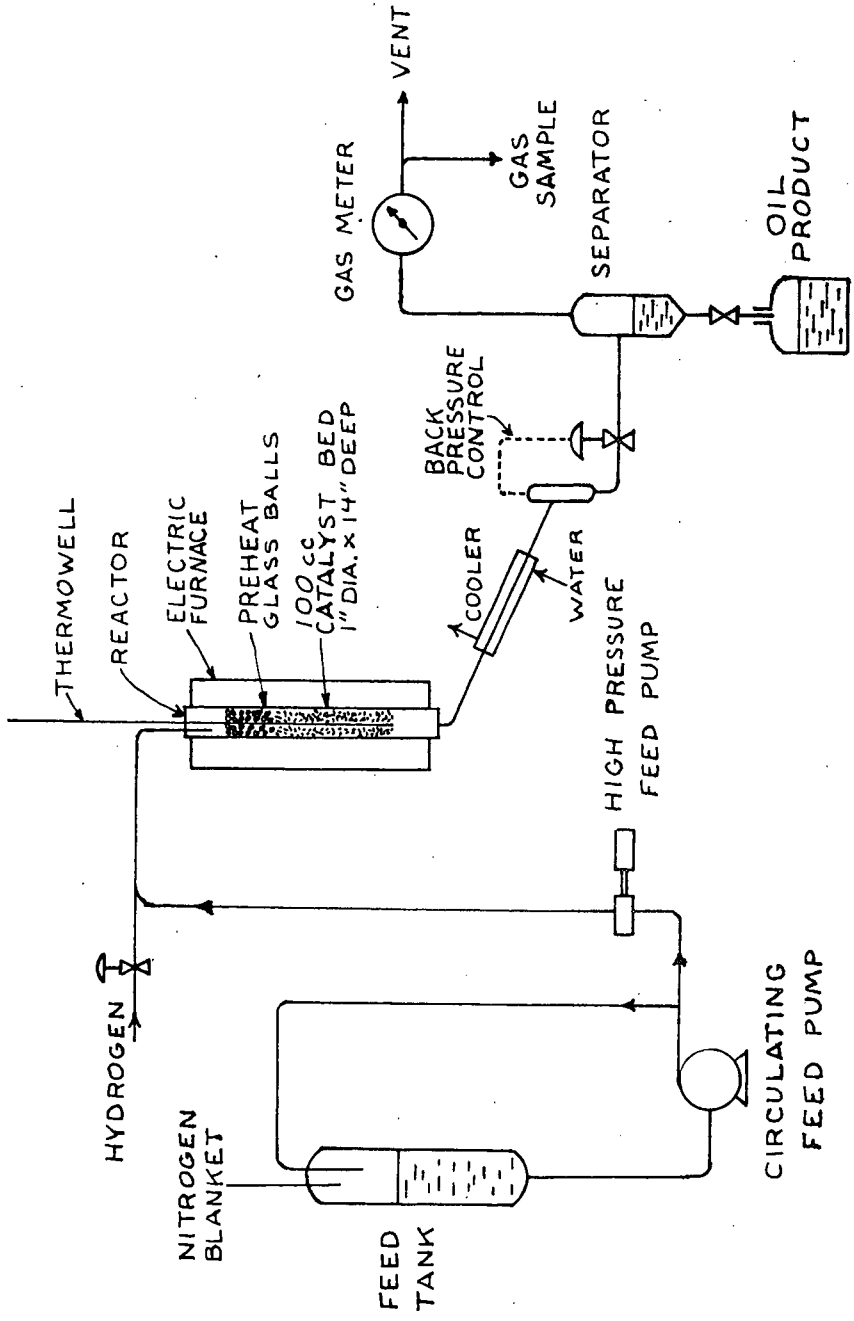
The product oils are naphthenic, containing high cycloparaffin concentrations. They contain little residuum and can be processed by conventional petroleum refining methods.

Bibliography

1. Qadar, Wiser and Hill, I and EC Process Design and Development, 7, No. 5, 390-397, July 1968.

FIG. 1

HYDROGENATION UNIT



HYDROGENATION OF COED ILLINOIS NO.6 COAL OIL

NITROGEN REMOVAL

FIG. 2

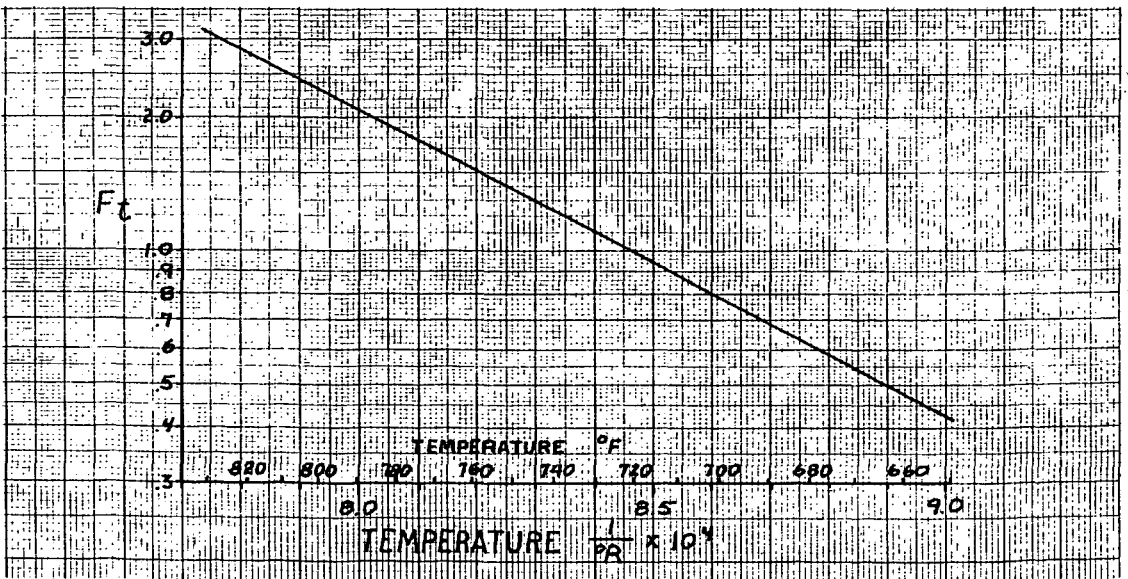
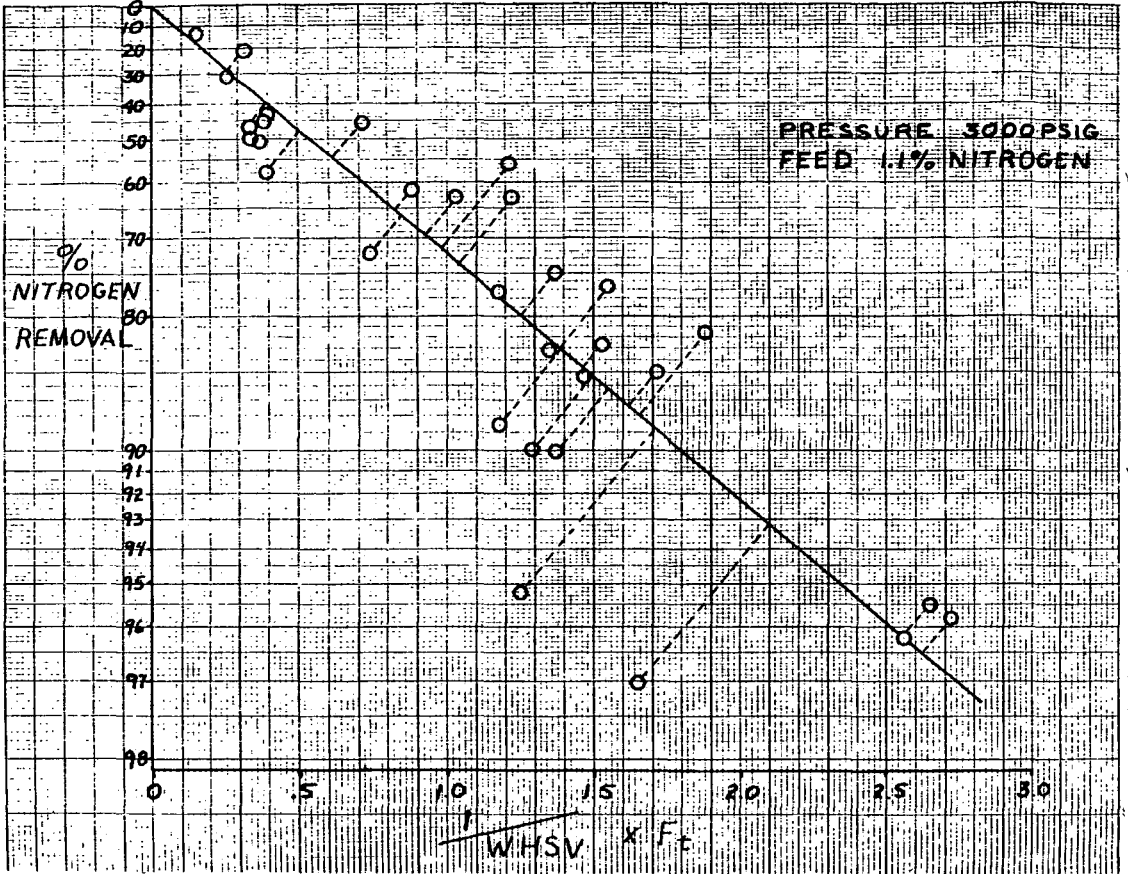
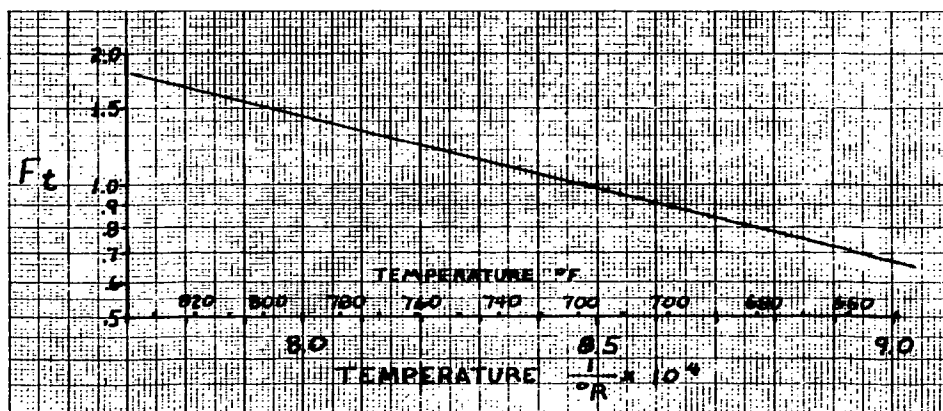
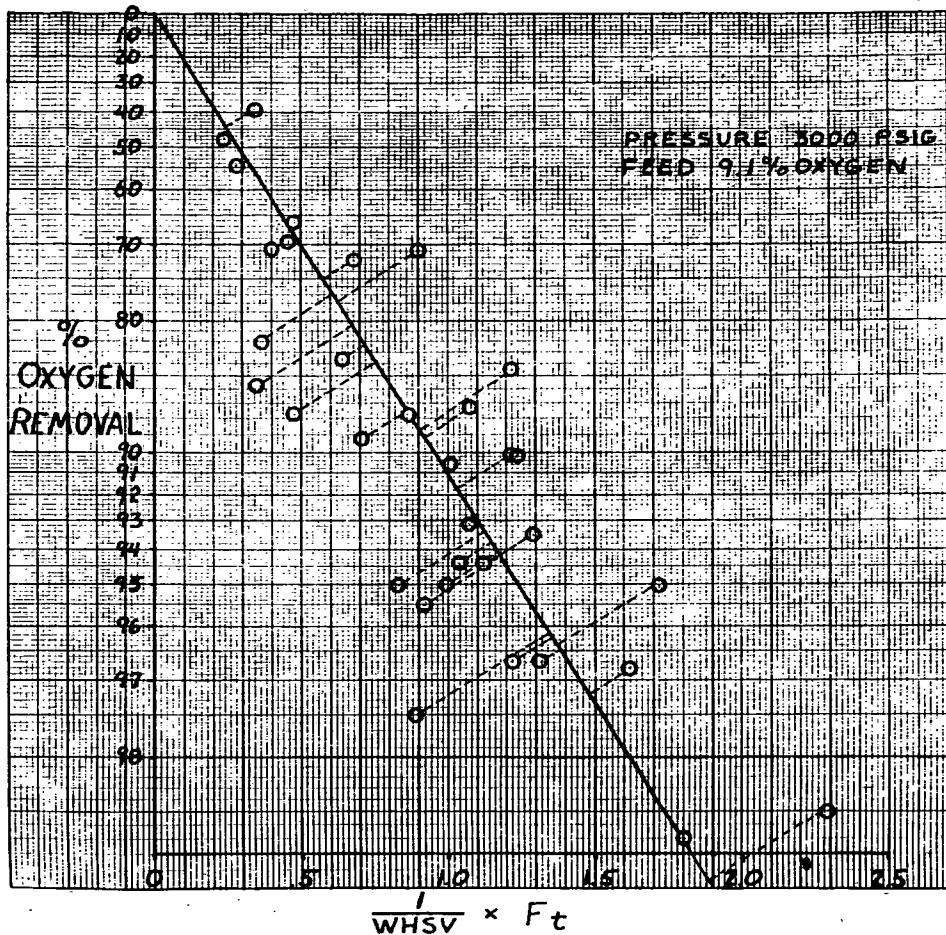


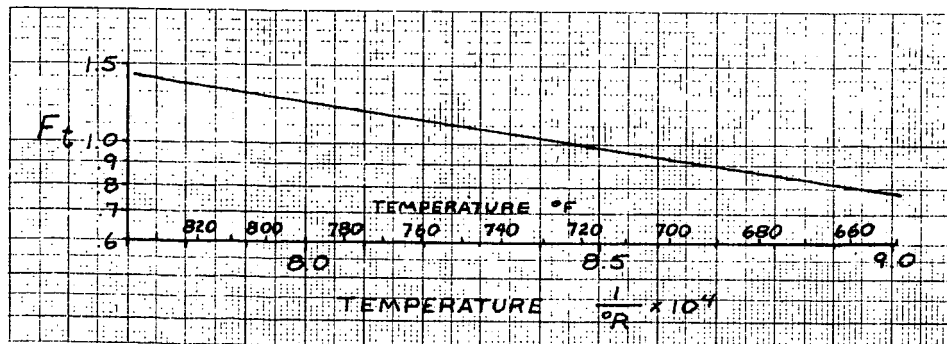
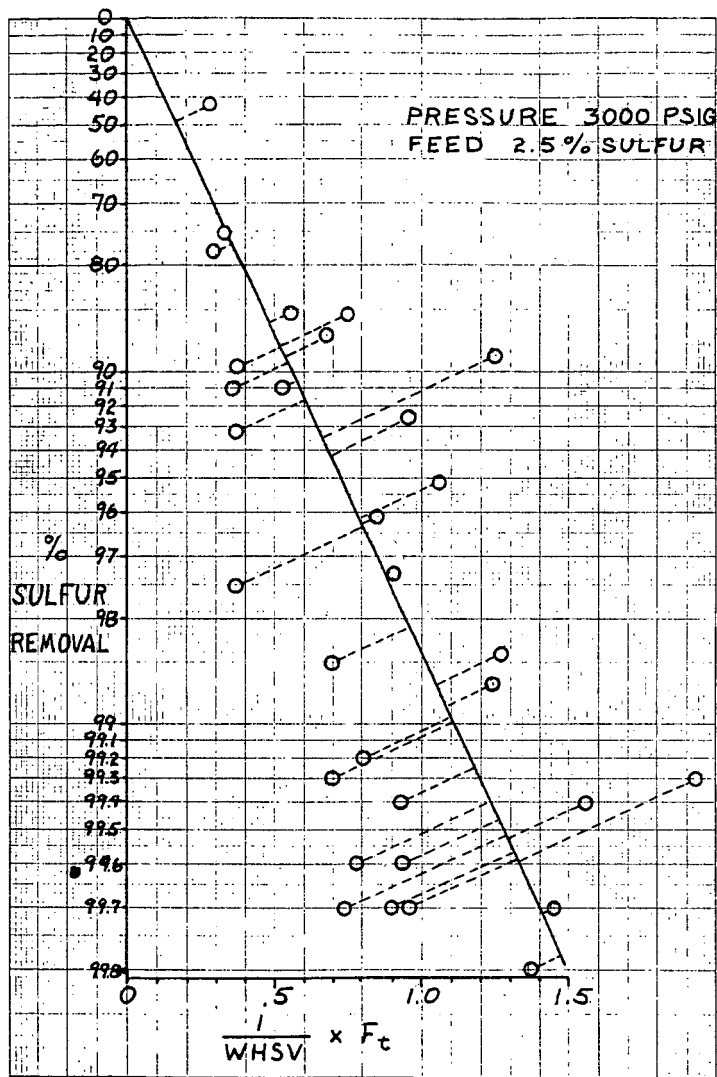
FIG. 3

OXYGEN REMOVAL



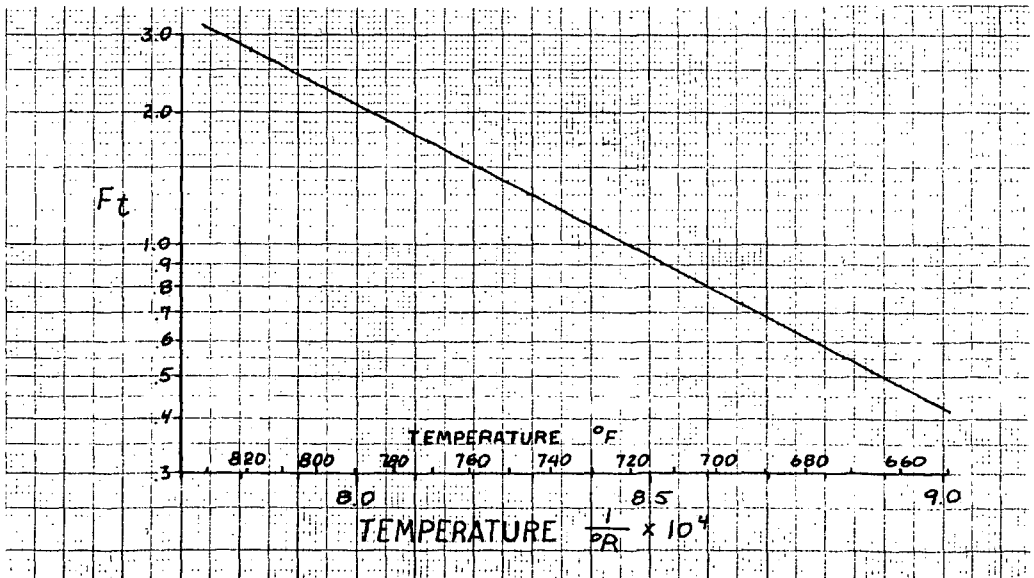
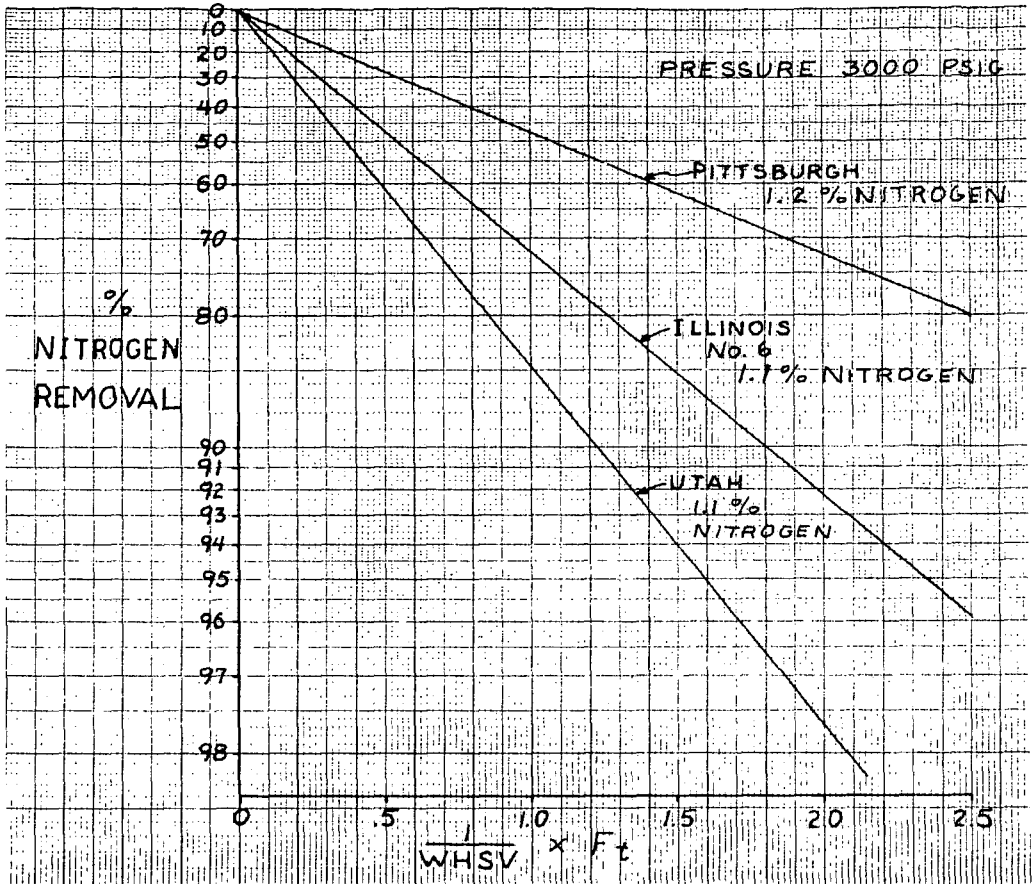
SULFUR REMOVAL

FIG. 4



- 51 -
 HYDROGENATION OF COED COAL OILS
 NITROGEN REMOVAL

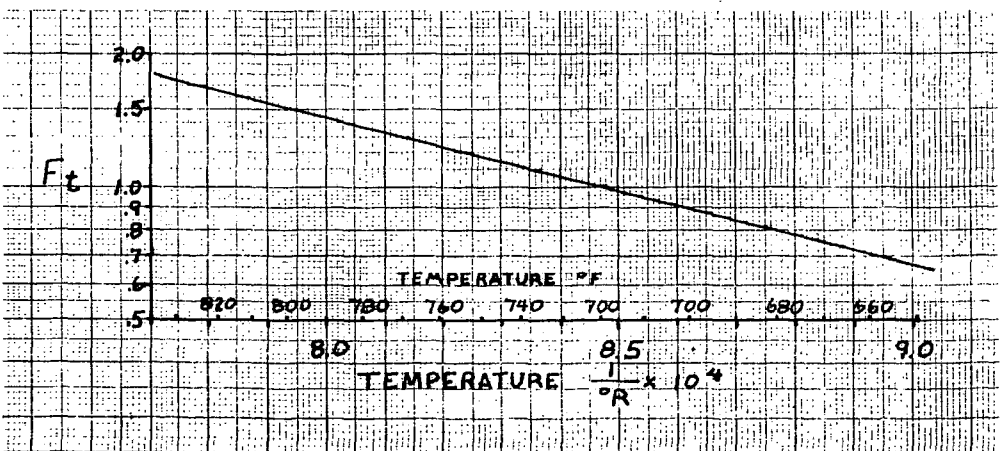
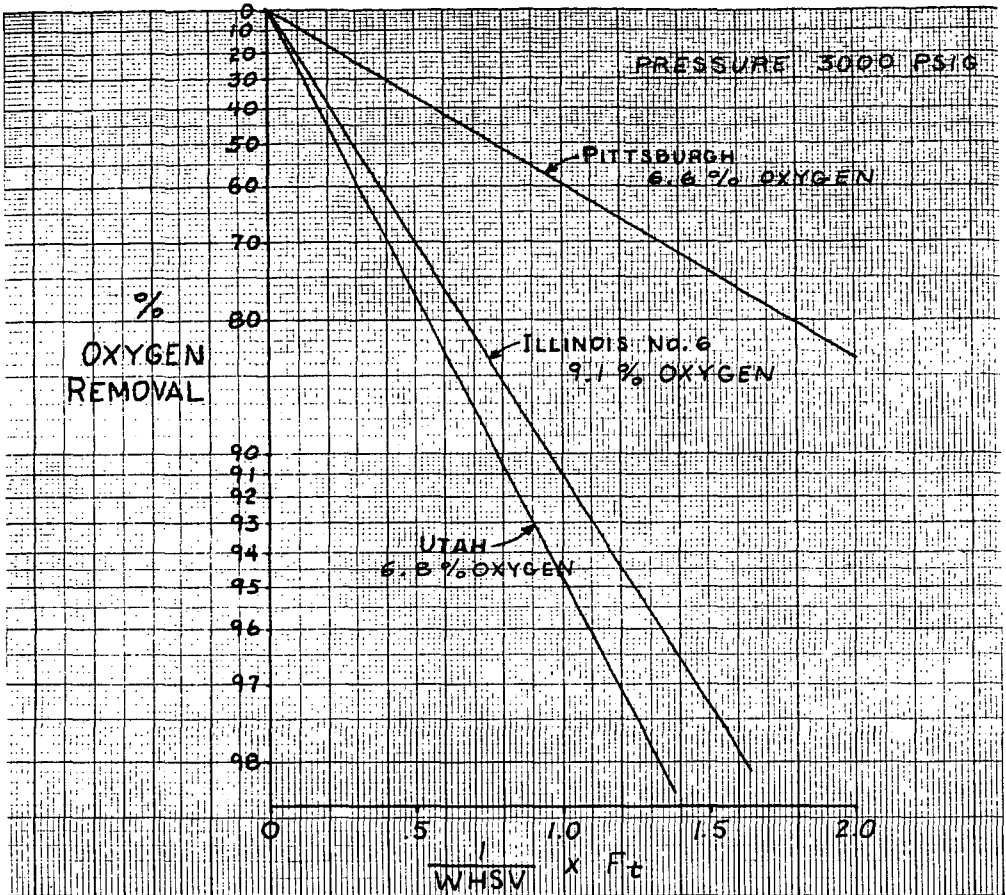
FIG. 5



HYDROGENATION OF COED COAL OILS

OXYGEN REMOVAL

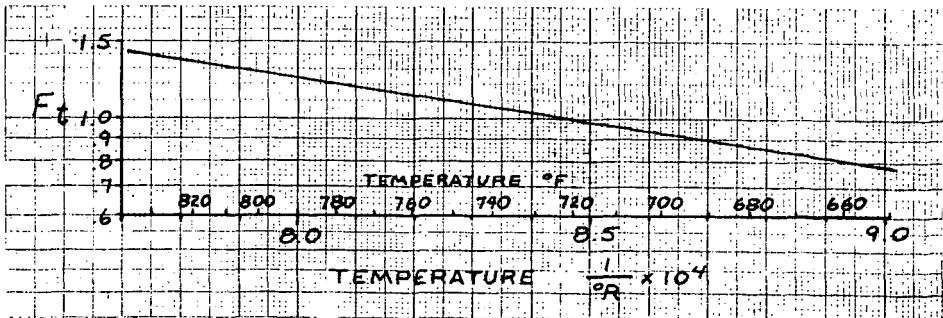
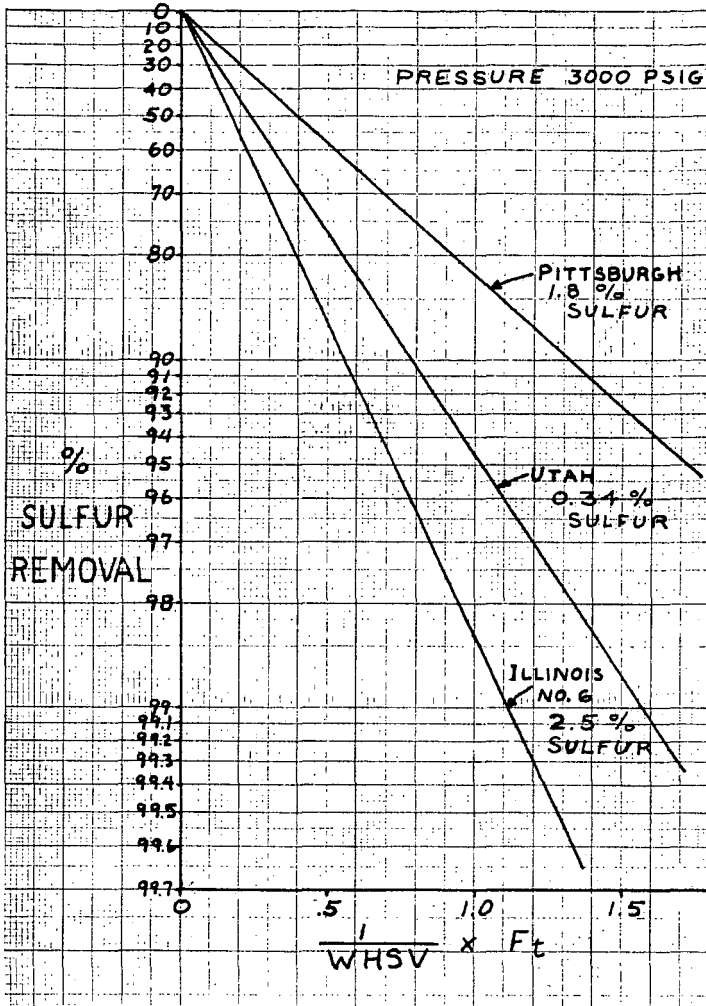
FIG. 6



HYDROGENATION OF COED COAL OILS

SULFUR REMOVAL

FIG. 7



HYDROGENATION OF COED COAL OILS PERCENT HYDROGEN SATURATION

FIG. 8

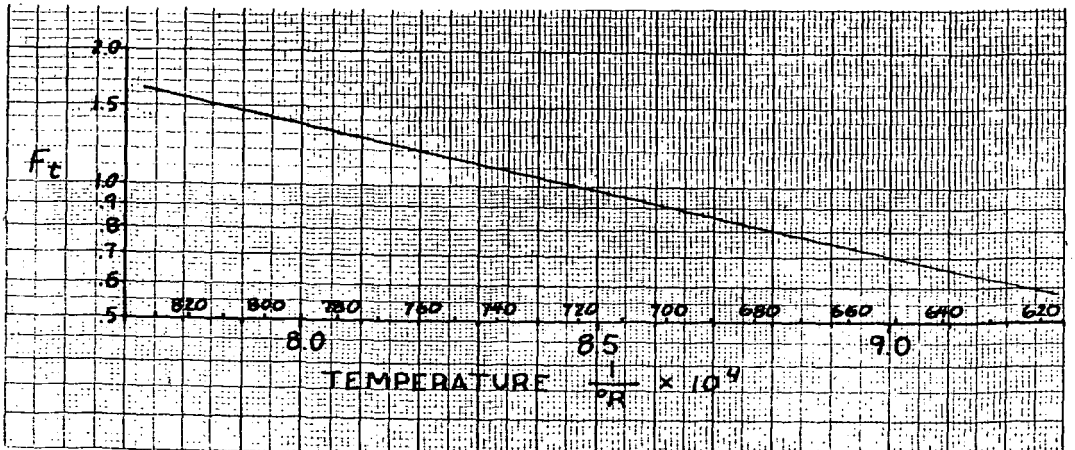
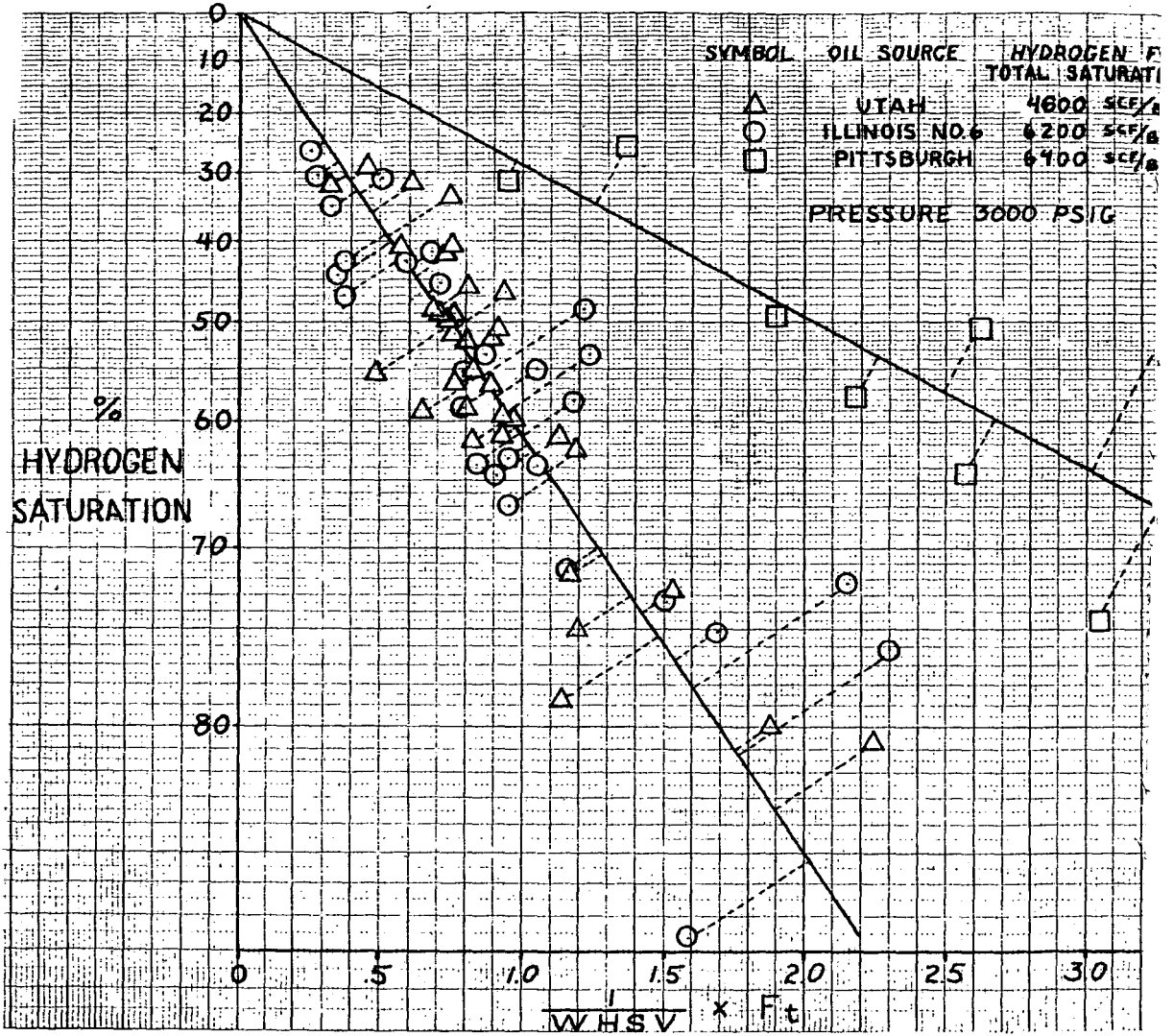


FIG. 9

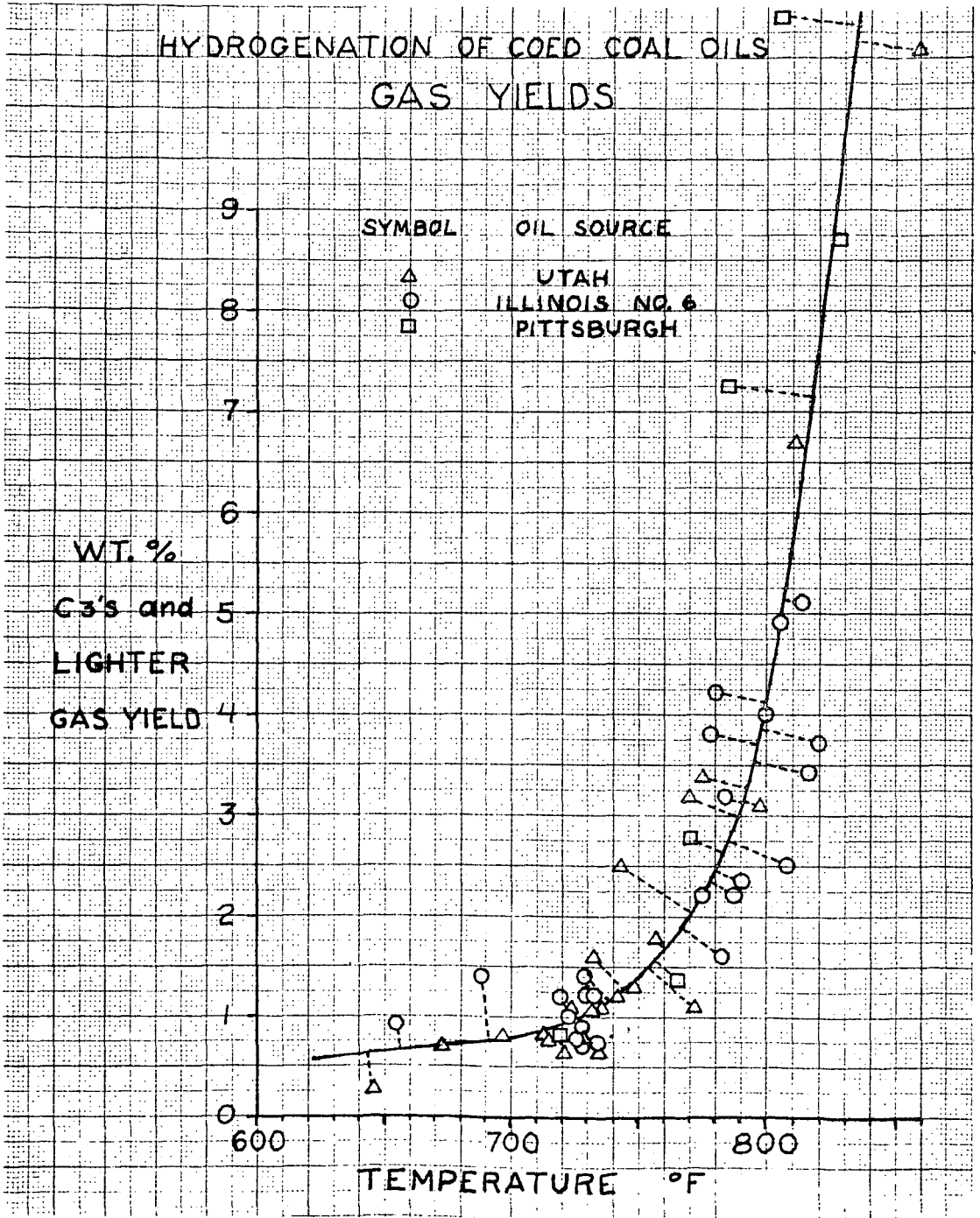


FIG. 10

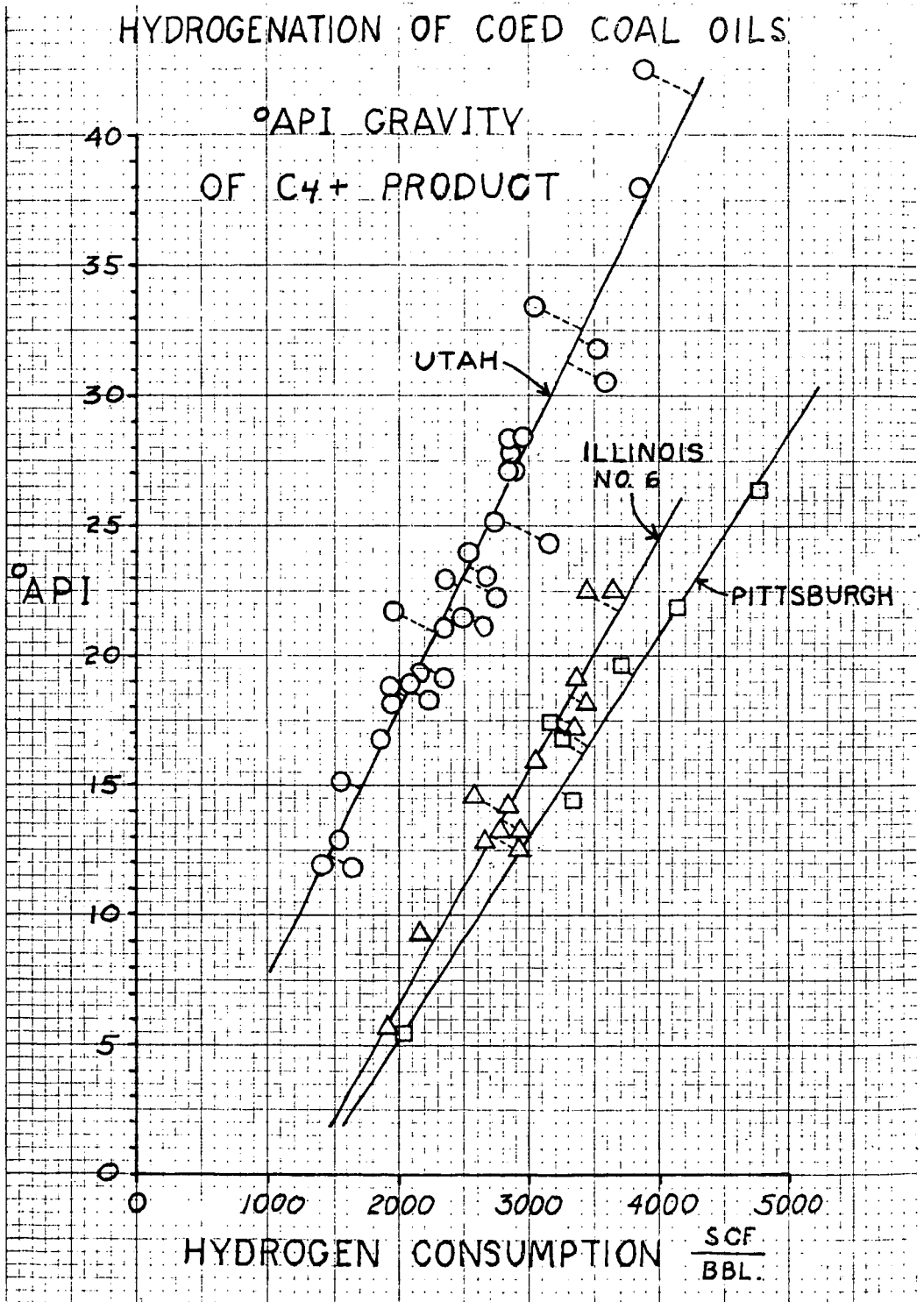
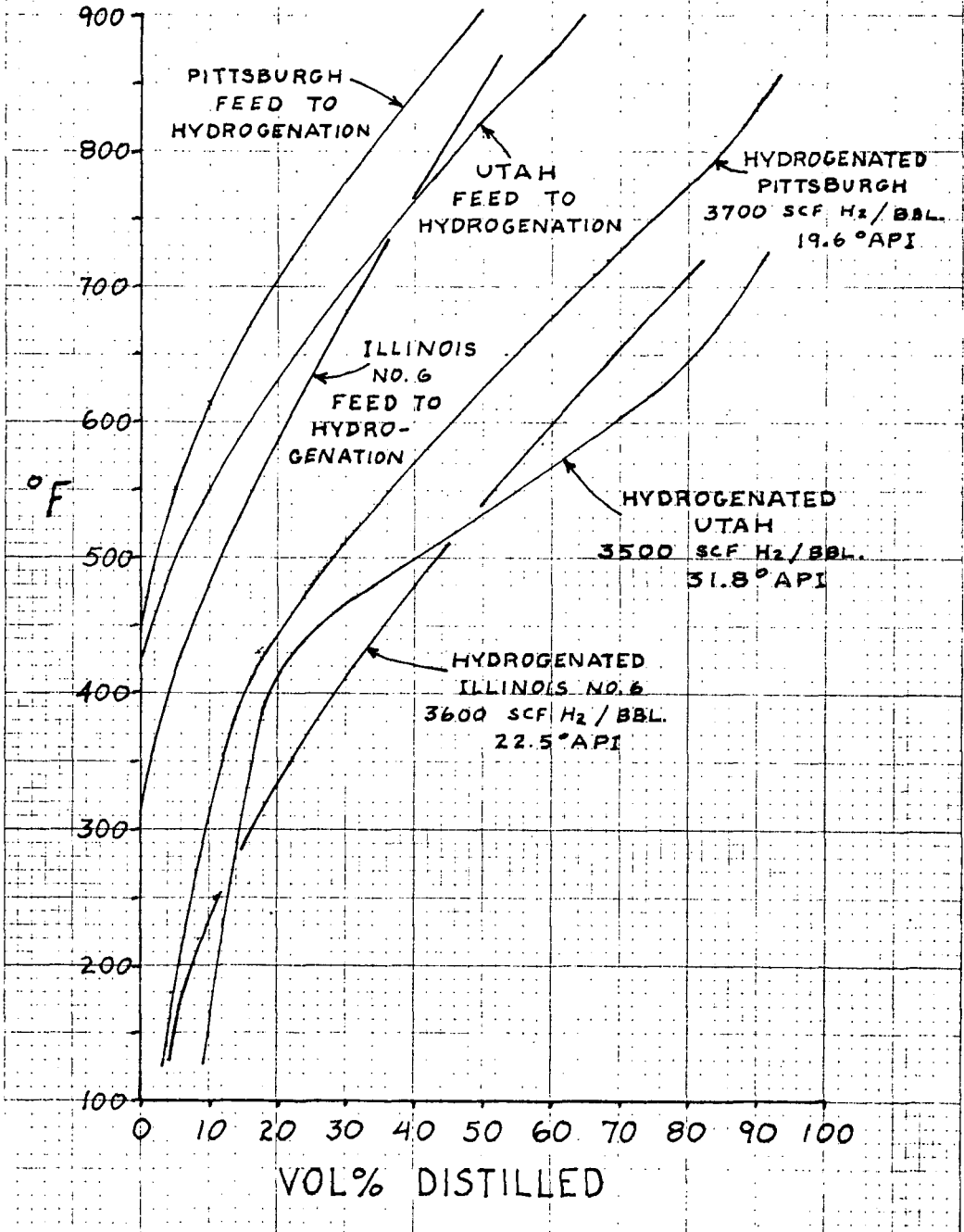


FIG. 11

HYDROGENATION OF COED COAL OILS DISTILLATION OF FEED AND PRODUCTS



LIQUID FUELS FROM TARS BY CARBONIZATION OF COALS IN HYDROGEN ATMOSPHERES

Clarence Karr, Jr., J. O. Mapstone, Jr., L. R. Little, Jr.,
R. E. Lynch, and J. R. Comberiat

U. S. Department of the Interior, Bureau of Mines,
Morgantown Energy Research Center, Morgantown, W. Va. 26505

The purpose of this investigation was to determine the feasibility of producing a gasoline boiling range product of satisfactory yield and quality by low-temperature (950° F) carbonization of coal in hydrogen atmospheres below 1,000 psig, with immediate catalytic hydrorefining of tar vapors and liquid tar issuing from the coal. Information on the effects of varying hydrogen pressure and catalyst temperature on the yields of individual compounds of interest in the gasoline boiling range product was also desired.

Very little previous work has been done along these particular lines. With respect to the processing of the uncondensed tar vapors, Flinn and Sachsel (1) conducted a low-temperature carbonization of a high-volatile bituminous coal at 445 psig hydrogen, passing the tar vapors through a cobalt-molybdenum on alumina catalyst at 800° F, obtaining in the vicinity of 100 lbs gasoline boiling range (up to 200° C) product per ton of coal. No information of any kind was reported on the individual constituents in this product.

With regard to the use of hydrogen pressures below 1,000 psig there is little information beyond that of Flinn and Sachsel. Qader, *et al* (2) have reported hydrorefining of previously condensed tar over a cobalt-molybdenum catalyst at 420° C and pressures as low as 1,500 psig. This tar was produced from a mixture of high volatile A bituminous coal and 15 wt-pct stannous chloride at 2,000 psig hydrogen and 515° C. With these two steps the yield of gasoline was 26 wt-pct of the tar. Without the catalyst the yield of tar was 20 wt-pct, and although this tar was not hydrorefined, if one assumes comparable results as with the tar from the coal-catalyst mixture, the yield of gasoline would have been about 100 lbs per ton of coal. No information of any kind was given on individual compounds in the gasoline.

EXPERIMENTAL

The experimental equipment is shown schematically in Figure 1. The reactor was a stainless-steel vessel 5-7/8-in. ID and 20-in. in depth, designed for operation at 1,000° F and 1,000 psig. The reactor was heated electrically with external strip heaters, the temperature being measured and controlled by a chromel-alumel thermocouple placed at the inside reactor wall.

Coal charge and catalyst were contained in wire-mesh baskets inserted into the reactor, the catalyst basket being at the bottom. Temperature of the coal bed was measured with a chromel-alumel thermocouple inserted in the bed center. Channeling of the gas stream around the thermowell, due to variable packing, settling, and shrinkage of the coal bed, led to variations in the recorded coal bed temperatures from the usual reactor temperature of about 950° F. The catalyst,

when in this same reactor, was probably in the vicinity of 950° F. This arrangement was used in the first 12 runs. For the last 9 runs a separate catalyst holder was installed, external to the carbonizing reactor, and with its own electrical heater to permit operating the catalyst bed at temperatures different from the reactor proper. The catalyst bed temperature was measured by a chromel-alumel thermocouple inserted into the bed. In these runs the coal bed had an annular configuration, as shown in Figure 1. The coal and catalyst bed temperatures for the 21 runs are shown in Table 1.

In operation, hydrogen, metered through an orifice meter at 8 to 10 SCFH (300 to 900 psig), was passed downward through coal and catalyst. Tar evolved during carbonization, both liquid and vapor, thus was carried down over the catalyst into an air cooled receiver, where heavier constituents were collected. Effluent vapors passed into a water-cooled condenser for further liquid collection, then through a regulating valve which controlled the system at desired operating pressure. Gases then passed into a silica gel trap to absorb uncondensed vapors and were metered through a wet test meter.

Coal used was Pittsburgh-seam high-volatile A bituminous, 40 to 60 mesh. The hydrodesulfurization catalyst was Girdler G-35B, a cobalt-molybdena on alumina in the form of 1/8-in. pellets. Analyses of the coal and char were made using standard ASTM methods.

Total liquid product was obtained by combining the contents of the air-cooled and water-cooled receivers. Any vapors trapped in the silica gel were counted as product but were not recovered. The liquid was distilled on a small glass Vigreux column taking an overhead weight of water and light oils (b. p. <200° C) and discarding the water. A second distillation cut was made between 200° - 400° C and designated heavy oils. Any liquid product boiling above 400° C was reported as distillation residue. The light oils were analyzed by gas-liquid chromatography with the results shown in Table 2.

Gas samples were taken at intervals from the line before the wet-test meter. These were analyzed by gas-solid chromatography.

RESULTS AND DISCUSSION

As shown in Table 1, the lowest total oil yield, 56 lbs, was obtained when nitrogen was substituted for hydrogen in the runs with the catalyst. In the absence of the catalyst, as the hydrogen pressure increased from 300 to 600 to 900 psig the yield of total oil progressively decreased from 190 to 110 lbs.

The majority of the runs were made with 10 wt-pct catalyst, based on the coal. The yields of total oils and light oils produced from the tar vapors and liquid tar passing through this catalyst are shown in pounds per ton of dry ash-free coal versus hydrogen pressures from 0 to 900 psig at catalyst temperatures of 650°, 750°, and 950° F in Figures 2, 3, and 4, respectively. At all temperatures the yield of total oils declined with increasing pressure to a value of about 150 lbs, with increased formation of gas and water. However, the light oils, or material boiling up to 200° C, in these total oils increased, most dramatically at 750° F, rising from 10 lbs at 0 psig (1 atm hydrogen) to a maximum of about 100 lbs around 600 psig, or a ten-fold increase. The 650° runs also showed a maximum light oil yield at 600 psig.

The quality of this gasoline boiling range light oil at maximum yields was good. It was a completely clear, water-white liquid with a sweet, clean odor. Analyses demonstrated that it was olefin-free, and, as shown later, rich in BTX, that is, about 70 wt-pct benzene, toluene, and xylenes. The gas was likewise olefin-free and rich in methane, about 50 volume-pct. The presence of ammonia and hydrogen sulfide in obviously much larger amounts than experienced during ordinary low-temperature carbonizations of the same coal indicated that substantial denitrogenation and desulfurization occurred. Elemental analyses demonstrated that there were little or no nitrogen and sulfur compounds in the light oils obtained under the better operating conditions, as shown in Table 3. The oxygen values were determined by difference, and found to fluctuate around zero for those light oils with low nitrogen and sulfur contents.

From Figures 2, 3, and 4 it is evident that the operating conditions for maximum yield of gasoline boiling range product were a catalyst temperature of 750° F and a hydrogen pressure of 600 psig. Based on many studies, the recommended temperature at low hydrogen pressures for cobalt-molybdenum on alumina catalysts is in the vicinity of 750° F. At much higher temperatures, substantial cracking to gas is experienced. The impossibility of obtaining good light oil yields at temperatures as high as 950° F was demonstrated by the fact that at 900 psig hydrogen the same yield, 40 lbs, was obtained with no catalyst, with 10 wt-pct catalyst; and with 25 wt-pct catalyst.

The yields of desired individual compounds, in particular benzene and toluene, were as high, or higher, at 600 psig than at 900 psig, demonstrating that hydrogen pressures well below 1000 psig were practical. Figure 5 shows that the yields of benzene and toluene at 750° F rose from 1.4 and 3.6 lbs, respectively, at 0 psig to a maximum of about 29 lbs each at 600 psig. The yields of benzene and toluene at 0 psig were close to the yields typical in ordinary low-temperature carbonization of this same Pittsburgh-seam coal, with no treatment of the evolved tars (3, 4).

Figures 6 and 7 show the variations at 300 and 900 psig, respectively, in the yields of benzene, toluene, total xylenes, and total aliphatics in the light oils obtained at the various catalyst bed temperatures from 650° to 950° F. The curves for benzene are similar at these pressures up to 750° F, showing yields of about 13 lbs at this temperature. However, the 300 psig curve for benzene has its maximum at 750° F whereas the 900 psig curve rises a little to about 15 lbs at 950° F. The 750° F maximum for toluene is increased from about 19 lbs at 300 psig to about 25 lbs at 900 psig. As previously noted, the 750° F maximum for both benzene and toluene is about 29 lbs each at the intermediate pressure of 600 psig, which is the optimum pressure.

The xylenes curves in Figures 6 and 7 apparently have similar shapes, but the maximum yield of about 16 or 17 lbs is displaced from about 750° F at 900 psig to about 600° F at 300 psig. The 600 psig trend for xylenes is similar to that for 300 psig, with a maximum of 15 or 16 lbs at about 600° F. Apparently at the higher pressure of 900 psig the temperature must be increased about 150° F to obtain the same amount of degradation of the xylenes. Presumably the higher pressure inhibits the cracking of the xylenes.

At 300 and 600 psig the total aliphatics declined with increasing temperature, as might be expected on the assumption that the aliphatics in the tar would be increasingly cracked to gas with increasing temperature. However, as shown in Figure 7, at 900 psig the aliphatics rose from the value of about 5 lbs at 650° F, held in common with the 300 psig run at this temperature, to a value of about 7 lbs at 750° through 950° F, a 40 pct increase. About 2 to 5 lbs aliphatics was typical for the light oil from this same coal in ordinary low-temperature carbonizations (3, 4). Presumably at the higher pressure of 900 psig, cracking of the light oil boiling range aliphatics to gas was suppressed, whereas the higher molecular weight aliphatics in the tar were broken down to increase the yield of light oil aliphatics with increase in temperature. This was demonstrated by conducting urea extractions on the 900 psig oil products boiling above 200° C. The amounts of n-aliphatics decreased to the point that none could be extracted.

CONCLUSIONS

1. The optimum operating conditions for conversion of the combined tar vapors and liquid low-temperature tar immediately upon being produced from an hvab coal were a hydrogen pressure of 600 psig and a hydrodesulfurization catalyst temperature of 750° F.
2. Under these conditions about 100 lbs or 14 gallons of gasoline boiling range light oil could be obtained per ton of dry ash-free coal. Previous investigations indicate that this is probably a typical yield for low-pressure hydrogenation with fixed-bed carbonization of hvab coal. Yields would be higher with fluidized-bed or entrained-bed carbonization.
3. This colorless, sweet smelling, olefin-free product, which contained about 70 wt-pct BTX and little or no sulfur, nitrogen, and oxygen might be suitable for blending in the production of nonleaded gasoline.
4. The unusually low optimum hydrogen pressure of only 600 psig for this particular process would allow substantial reduction in plant cost compared with other processes in which pressures of 1500 psig, or higher, are required.

REFERENCES

1. Flinn, James E., Sachsel, George F. Ind. Eng. Chem., Process Design Develop. 1968, 7 (1), 143-9.
2. Qader, S. A., Haddadin, R. A., Anderson, L. L., Hill, G. R. Hydrocarbon Process. 1969, 48, (9), 147-52.
3. Karr, Clarence, Jr., Comberiat, Joseph R., Estep, Patricia A., Mapstone, Jesse O., Jr. J. Inst. Fuel, 1967, 40 (12), 561-3.
4. Comberiat, Joseph R., Karr, Clarence, Jr., Childers, Edward E., Mapstone, Jesse O., Jr., Estep, Patricia A. Amer. Chem. Soc., Div. Fuel Chem., Prepr. 1969, 13 (4), 160-78.

TABLE 1. - Operating conditions and material balances

Run no.	Bed temp., °F	Catalyst temp., °F	Hydrogen pressure, psig	Coal charged, g	Catalyst: coal ratio	Material balance on wt-pct coal as charged ^a			
						Char	Water	Total oils	Gas and loss
1	1,050	ND ^b	600	1,816	0.25	68.2	---	15.5	16.3
2	1,000	ND	300	1,816	0.25	71.2	8.8	5.6	14.4
3 ^c	1,000	ND	900	1,816	0.25	64.3	9.7	4.6	21.4
4 ^d	860	ND	300	1,816	0.25	82.7	3.9	2.6	10.8
5	920	ND	300	1,816	-----e	75.6	4.3	8.8	11.3
6	810	ND	600	1,816	-----e	79.6	3.8	5.5	11.0
7	930	ND	900	1,816	-----e	74.6	4.6	5.1	15.7
8 ^f	830	ND	900	1,816	0.25	73.6	8.1	5.7	12.5
9	850	ND	300	1,816	0.10	73.2	6.6	6.4	13.8
10 ^g	720	ND	300	1,247.3	-----e	89.1	2.1	3.0	5.9
11 ^h	960	ND	900	1,816	0.10	70.2	5.1	6.7	18.0
12	875	ND	0	1,816	0.10	72.1	5.3	12.7	10.0
13	865	750 ⁱ	0	1,816	0.10	67.9	4.6	9.2	18.3
14	890	755 ⁱ	300	1,816	0.10	69.1	6.7	8.3	16.0
15	980	745 ⁱ	900	1,816	0.10	69.3	6.2	5.8	18.5
16 ^j	925-940	745 ⁱ	300	1,816	0.10	77.1	8.1	6.3	8.5
17	850	725 ⁱ	900	1,816	0.10	71.5	8.4	6.6	13.5
18 ^j	885	645 ⁱ	300	1,816	0.10	78.1	7.7	7.5	6.7
19	950	640 ⁱ	900	1,823.6	0.10	76.8	7.2	6.1	9.9
20	950	745 ⁱ	600	1,816	0.10	69.2	8.3	7.6	14.8
21	950	650 ⁱ	600	1,816	0.10	75.8	7.6	6.1	10.4

a Determined by difference.

b Not determined; assumed to be about equal to bed temperature.

c Exothermic gasification; bed temperature over 1,200° F for 25 minutes.

d Blank run using nitrogen.

e Uncatalyzed.

f Rerun of No. 3.

g Rerun of char from No. 5.

h Possible leakage.

i Using separately heated catalyst reactor.

j Composite data of two runs.

TABLE 2. - Analysis of dewatered liquid products^a

Run no.	Distillation of total oil			GLC analysis of light oil				
	Total oil ^b	Light oil ^c	Heavy oil ^d	Residue ^e	Total aliphatics	Benzene	Toluene	Total xylenes
1	ND ^f	ND	ND	ND	ND	ND	ND	ND
2	130	38	6	14	0.0	13.8	15.8	4.2
3	100	32	4	4	0.0	23.2	5.0	1.0
4	56	20	8	8	0.0	3.6	9.2	4.2
5	190	34	62	60	4.0	5.4	9.6	6.6
6	120	34	42	18	2.4	4.4	11.8	8.0
7	110	44	32	14	0.6	19.8	13.6	5.2
8	90	40	16	20	2.0	16.8	14.8	3.8
9	140	28	58	22	2.0	9.4	15.4	1.4
10	ND	ND	ND	ND	ND	ND	ND	ND
11	144	40	66	66	6.8	14.8	16.8	1.2
12	276	28	62	116	6.2	0.8	7.4	7.8
13	200	10	66	64	1.4	1.4	3.6	1.6
14	180	56	74	28	4.2	16.8	19.2	8.4
15	128	72	12	26	4.0	23.6	24.8	10.6
16	146	66	16	32	0.4	13.2	29.0	15.8
17	156	84	0	50	7.0	12.6	30.4	16.4
18	172	66	34	36	5.6	5.6	17.6	17.0
19	140	66	30	14	9.4	5.0	20.6	14.2
20	176	96	36	16	6.4	29.0	28.6	12.6
21	144	76	38	10	8.4	5.8	16.0	14.8

a All data in lbs/ton dry ash-free coal.

b Includes oils trapped on silica gel but not recovered for distillation.

c lbp to 200° C.

d 200° to 400° C.

e > 400° C.

f Not determined.

TABLE 3. - Elemental analysis of light oils

Run No.	Weight-percent			
	C	H	N	S
1	Not determined			
2	91.9	8.0	0.08	0.1
3	91.9	8.0	0.08	0.08
4	89.3	8.8	0.2	0.3
5	87.7	9.8	0.3	0.4
6	87.6	9.3	0.2	0.3
7	89.0	8.9	0.4	0.2
8	90.7	8.9	0.05	0.1
9	90.8	9.3	0.02	0.03
10	Insufficient sample for analysis			
11	90.4	9.6	0.0	0.05
12	86.5	11.2	0.2	0.5
13	87.3	11.1	0.1	0.4
14	89.1	9.8	0.2	0.05
15	90.4	9.6	0.02	0.06
16	90.9	8.8	0.01	0.04
17	89.8	10.2	0.0	0.04
18	88.9	10.6	0.2	0.04
19	88.2	10.8	0.2	0.02
20	89.7	10.0	0.08	0.03
21	88.3	11.0	0.08	0.04

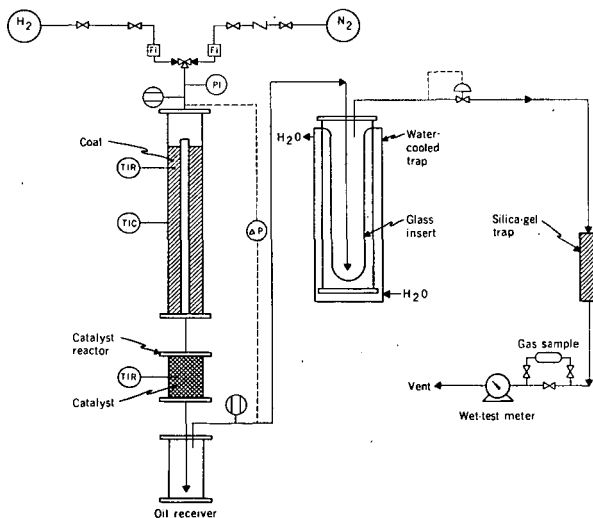


FIGURE 1. - Flow Plan of Hydrocarbonization Equipment for Catalytic Treatment of Tar Vapors and Liquids.

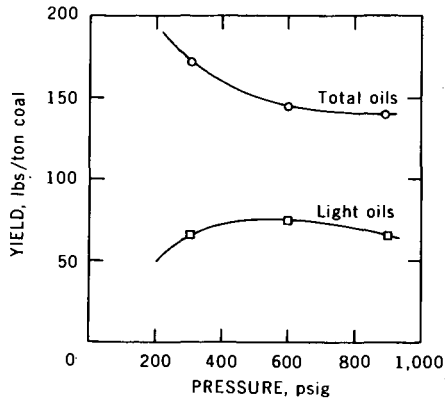


FIGURE 2. - Effect of Pressure on Yields of Total and Light Oils with 10 wt-pct Catalyst at 650° F.

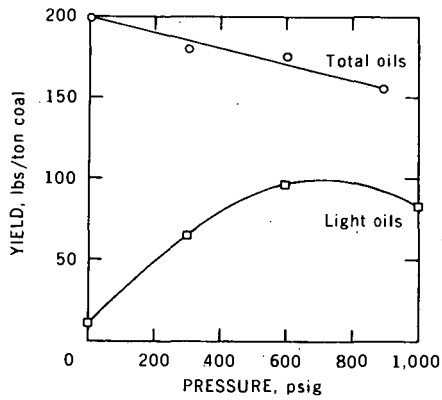


FIGURE 3. - Effect of Pressure on Yields of Total and Light Oils with 10 wt-pct Catalyst at 750° F.

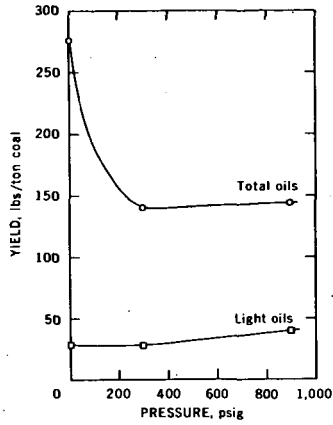


FIGURE 4. - Effect of Pressure on Yields of Total and Light Oils with 10 wt-pct Catalyst at 950° F.

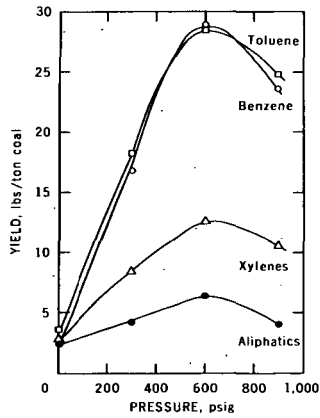


FIGURE 5. - Effect of Pressure on Yields of Major Light Oil Components with 10 wt-pct Catalyst at 750° F.

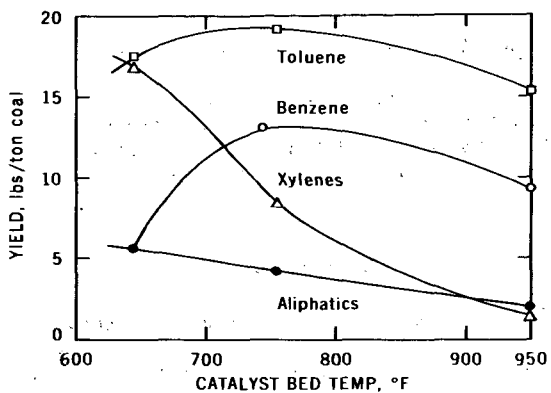


FIGURE 6. - Effect of Catalyst Bed Temperature on Yields of Major Light Oil Components at 300 psig.

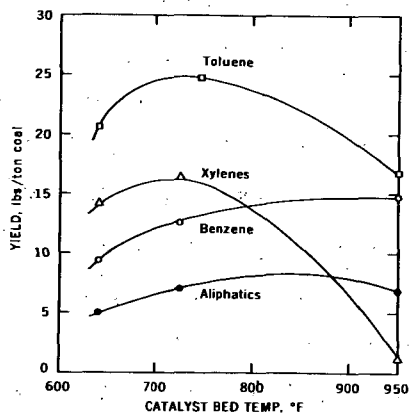


FIGURE 7. - Effect of Catalyst Bed Temperature on Yields of Major Light Oil Components at 900 psig.

CATALYTIC HYDROCRACKING OF COAL LIQUIDS

William T. House
Synthetic Fuels Research Laboratory
Esso Research and Engineering Company
Baytown, Texas

Introduction

The conversion of coal to gasoline involves removal of mineral matter, sulfur, nitrogen and oxygen. This is well illustrated in Table I which compares the composition of a coal and gasoline. In addition the hydrogen-to-carbon atomic ratio in gasoline is approximately double that in the coal so that large amounts of hydrogen must be added. Coal is a solid from which very little volatile material is obtained until cracking temperatures are reached, whereas gasoline boils in a relatively low temperature range. Thus, the large, complex coal molecules must be broken down into smaller volatile compounds.

The coal-to-gasoline process consists broadly of two essential steps as illustrated in Table II. The first step is to convert at least a portion of the coal to liquid product. The processes suggested for this range from simple pyrolysis to non-catalytic hydrogenation to catalytic hydrogenation, all with and without a liquid vehicle. A small amount of gasoline range material may be produced in this step, but the liquid product is usually largely higher boiling. Some of these heavy liquids may be recycled to the liquefaction step, but the remainder must be upgraded to the gasoline range by a subsequent refining step such as hydrocracking, which may or may not be followed by reforming. In this paper the results of catalytic hydrocracking (with and without previous hydrofining) of a 400-700°F fraction of liquid obtained through the non-catalytic hydrogenation of coal are discussed. Much work has been done on hydrocracking of various coal

liquids^{1-14,16,17} and it should be borne in mind that the results are highly dependent on the coal used initially and the method of liquefaction as well as the catalyst used and the conditions employed. An excellent review of hydrogenation of coal and tar was issued by the Bureau of Mines in 1968.¹⁸

Experimental

A simplified schematic diagram of the hydrocracking unit is shown in Figure 1. The hydrogen treat gas rate was maintained at approximately 8000 SCF per barrel of feed. The hydrofined feedstock was spiked back up to its original nitrogen and sulfur levels with suitable nitrogen and sulfur containing compounds which react quickly at the conditions employed to give ammonia and hydrogen sulfide. This was done in order to simulate commercial conditions of some hydrocracking units wherein the liquid and gas product from the hydrofiner may be fed directly to the hydrocracker without previous scrubbing.

The properties of the two feedstocks are listed in Table III. The aromatics contents of the 400°F+ material are considerably higher than those of typical petroleum hydrocracking feedstocks¹⁵ and also higher than those reported for some of the coal liquids¹⁴. In addition to the reduction of the organic nitrogen content a good deal of hydrogen addition was accomplished by the hydrofining. A large part of the indicated conversions of 400°F+ material to 400°F- was probably due to hydrogenation of aromatic compounds boiling slightly above 400°F to hydroaromatic and naphthenic compounds boiling slightly below 400°F.

Results and Discussion

It was found that, over the range of conversions studied, the results for both the raw (unhydrofined) feedstock and the hydrofined feedstock could be correlated with first order kinetics, i.e.,

$$\frac{-d(400^{\circ}\text{F}+)}{dt} = k(400^{\circ}\text{F}+) \quad (1)$$

This is illustrated in Figure 2 where the holding time was taken as the reciprocal of the liquid hourly space velocity in weights of liquid per weight of catalyst per hour. Since the raw feedstock was more resistant to hydrocracking, the kinetic data were obtained at a different temperature for each feedstock. It should be borne in mind that we do not have simple pure compounds here, but complex mixtures; thus, the correlations with first order kinetics are probably fortuitous. At least inference of a mechanism from this correlation is probably unwarranted.

Mass spectral data, however, made it possible to follow the changes in concentration of specific molecular weights. Figure 3 shows a first-order plot for $C_{14}H_{10}$, which consists of anthracene and phenanthrene and which was the highest molecular weight present in the feed in any appreciable concentration. In all probability no hydrocracking of anthracene or phenanthrene occurs as a first step and the kinetics here represent the rate of the first hydrogenation step.

Table IV shows that prior hydrofining has a beneficial effect on the hydrocracking rate. As mentioned before, the hydrofined feed was spiked back up to the original nitrogen and sulfur level of the raw feed.

Experiments have shown that even the hydrofined coal liquid fraction is considerably more resistant to hydrocracking than are petroleum feedstocks. This is probably due in part to the higher total nitrogen content. This view is somewhat reinforced by the results shown in Table V. This table compares the conversions obtained on the respiked hydrofined feed with those obtained on the unspiked 400°F+ material recovered from the product. The higher activity with the latter feed is probably also partially due to its higher hydrogen content.

The beneficial effects of the prior hydrofining are further illustrated in Figure 4 which shows the Arrhenius temperature dependence of the first order rate constants for hydrocracking both feeds. At 650°F the rates for the two feeds are approximately the same, but too low to be of interest. The hydrofined

feed has a higher apparent energy of activation so that, as the temperature is increased, the benefit of hydrofining increases. As mentioned earlier, some boiling point conversion was obtained in the hydrofining operations, but this was probably largely due to hydrogenation of aromatic compounds boiling slightly above 400°F to hydroaromatic and naphthenic compounds boiling slightly below 400°F. In the case of the raw feed some conversion of this type also occurs in the hydrocracking operation.

Increasing hydrocracking pressure also has a greater effect on the rate constant with hydrofined feed than with the raw feed. This is shown in Table VI. Increasing the pressure from 1500 psig to 3000 psig approximately tripled the rate with the hydrofined feed whereas the rate with the raw feed was approximately doubled.

Figure 5 shows the change in concentration of certain specific molecular weights and carbon numbers as compared to boiling point conversion and holding time for both the raw feed and the hydrofined feed. For the hydrofined feed the boiling point conversion which is plotted is the sum of that obtained in hydrofining and hydrocracking although the holding times are only those for hydrocracking. The completely aromatic compounds such as naphthalene, $C_{10}H_8$, and anthracene and/or phenanthrene, $C_{14}H_{10}$, were completely converted to saturated and partially saturated compounds in the hydrofining operation. The total concentration of C_{10} compounds remains relatively constant over a wide range of holding time and conversion, indicating that C_{10} compounds are being formed from higher molecular weight compounds at approximately the same rate that they are consumed to form lower molecular weight compounds. Some of the specific molecular weights have maxima in their concentration vs. holding time curves, indicating that they are initially produced faster than they are consumed. Benzene is produced in much higher-than-equilibrium concentrations, indicating that a considerable amount of cracking of higher molecular weight compounds occurs before they are completely saturated.

Table VII shows analyses of some fractions of the naphtha from a hydrocracking product from the hydrofined feed. The paraffin content is very low except for the lowest boiling cut which is itself only a small fraction of the naphtha. The high naphthene content should make this naphtha an excellent feed for catalytic reforming.

These studies have shown that higher boiling liquids obtained in coal liquefaction can be catalytically hydrocracked to the gasoline boiling range under reasonable conditions although more severe than those required for petroleum stocks. Prior hydrofining is beneficial and the advantage increases with increasing hydrocracking temperature and pressure. The higher resistance to hydrocracking of coal liquids is probably largely due to higher nitrogen content. Mass spectral data indicate that a fair amount of cracking of higher molecular weight compounds occurs before they are completely saturated. The naphtha products should be excellent feedstocks for reforming.

References

1. Albert, S. P., Johanson, E. S., Schuman, S. C., Chem. Eng. Progr. 60, No. 6, 35 (1964).
2. Archibald, R. C., Greensfelder, B. S. Holzman, G., Rowf, D. W., Ind. Eng. Chem. 52, 745 (1960).
3. Carpenter, H. C., Cottingham, P. L., Frost, C. M., Fowkes, W. W., Bur. Mines Rept Invest. 6237 (1963).
4. Craig, R. G., Forster, H. A. Oil Gas J. 45, 159(1966).
5. Duir, J. H., Hydrocarbon Processing Petrol Refiner 46, 127(1967).
6. Flinn, R. A., Larson, O. A., Benthler, H., Ind. Eng. Chem. 52, 152 (1960).
7. Gordon, K., J. Inst. Fuel 9, 69(1935); 20, 42(1946); 21, 53(1947).
8. Greensfelder, B. S., Voge, H. H., Good, G. M., Ind. Eng. Chem. 41, 2573 (1949).
9. Kuelemans, A. I. M., Voge, H. H., J. Phys. Chem. 63, 476(1959).
10. Krönig, W., Ind. Eng. Chem. 41, 870(1949).
11. Larson, O. A., Maciver, D. S., Tobin, H. H., Flinn, R. A., Ind. Eng. Chem. Proc. Res. Develop. 1, 300(1962).
12. Myers, C. G., Garwood, W. E., Rope, B. W., Wadlinger, R. L., Hawthorne, W. P., J. Chem. Eng. Data 1, 257(1962)
13. Pier, M., Z. Electrochem. 53, No. 5, 291 (1949).
14. Quader, S. A., Hill, G. R., Ind. Eng. Chem. Proc. Design Develop. 8, 450, 456, 462(1969).
15. Reichle, A.D., and Weller, N. O., Oil Gas J. 66, No. 26, 79(1968)
16. Weisz, P. B., Prater, C. D., Advan. Catalysis 9, 575(1957)
17. Zielke, C. W., Struck, R. T., Evans, J. M. Costanza, C. P., Gavin, E., Ind. Eng. Chem. Proc. Design Develop. 5, 151, 1958 (1966).
18. Wu, W. R. K., and Storch, H. H., Bur. Mines Bull. 633(1968)

Table I
Comparison of Coal and Gasoline

	<u>Coal</u>	<u>Gasoline (From Coal)</u>
Mineral Matter, Wt. %	~13	0
Sulfur, Wt. %*	3.4	Trace
Nitrogen, Wt. %*	1.3	Trace
Oxygen, Wt. %*	10.6	Trace
Hydrogen, Wt. %*	5.6	12-13
Carbon, Wt. %*	79.1	87-88
H to C Atomic Ratio	0.85	1.6-1.8
Boiling Range, °F	N.A.	160-400

* Dry, Mineral Free

Table II

Process Steps

1. Conversion of a portion of the coal to liquid product. Some gasoline range material but most heavy liquid.
 - Pyrolysis
 - Hydrogenation
2. Upgrading of heavy liquids to gasoline range.
 - Hydrocracking
 - Catalytic reforming

Table III
Feed Stock Properties

	<u>Unhydrofined</u>	<u>Hydrofined</u>
Carbon, Wt. %	89.84	89.30
Hydrogen, Wt. %	8.33	10.45
Sulfur, ppm	520	-
Nitrogen, ppm	3400	5
Specific Gravity 400°F-, Wt. %	1.0060	0.9402
	6.0	18.6
Sulfur, ppm	280	-
Nitrogen, ppm	2800	-
Paraffins, Vol. %	0.0	2.4
Naphthenes, Vol. %	26.5	50.1
Aromatics, Vol. %	73.0	47.5
400°F+, Wt. %	94.0	81.4
Sulfur, ppm	460	-
Nitrogen, ppm	3500	-
Saturates, Vol. %	2.7	22.8
Aromatics, Vol. %	97.3	77.2

Table IV

Effect of Hydrofining

750° F

	<u>Raw Feed</u>	<u>Hydrofined Feed</u>
Total Nitrogen, ppm	3400	3400
Organic Nitrogen, ppm	3400	5
First Order Rate Constant, Hr ⁻¹	0.25	0.46

Table V

Effect of Total Nitrogen Content

675°F

	<u>Hydrofined Feed</u>	<u>400°F+ Material Recovered from Hydrocrackate</u>
Total Nitrogen, ppm	3400	6
Organic Nitrogen, ppm	5	6
Hydrogen, Wt. %	10.45	11.00
400°F+ Conversion, Wt. %	14	85

Table VI

Effect of Pressure

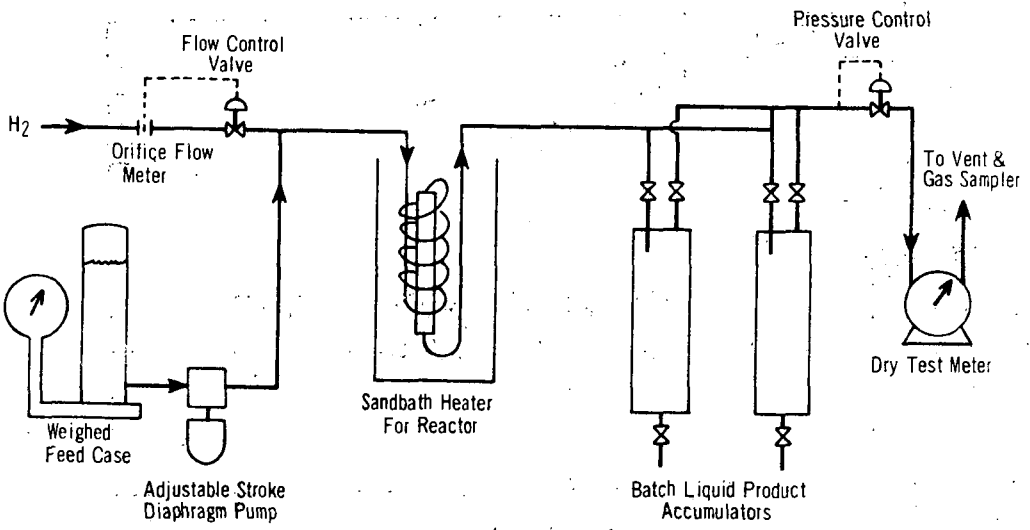
	<u>Raw Feed</u>	<u>Hydrofined Feed</u>
Temperature, °F	700	650
First Order Rate Constant, Hr ⁻¹		
at 1500 psig	0.13	0.041
at 3000 psig	0.24	0.12

Table VII

Analyses of Naphtha Cuts

Hydrofined Feed, 30% Total Conversion

Boiling Range, °F	<u>IBP-160</u>	<u>160-300</u>	<u>300-350</u>	<u>350-400</u>
Wt. % of Naphtha	3.9	31.0	14.3	50.8
Benzene	23.1	10.3	0.4	
Toluene		8.0	1.5	
C ₈ Benzene		9.3	6.0	
C ₉ Benzene		1.6	10.7	
C ₁₀ Benzene			3.1	
C ₁₁ Benzene			0	
Indan		0.1	15.8	
Naphthenes	61.9	68.9	35.0	
Paraffins	15.0	0.9	0	
Condensed Naphthenes		0.9	27.5	
Naphthalenes			0	
	100.0	100.0	100.0	



SIMPLIFIED FLOW DIAGRAM OF BENCH UNIT

FIGURE 1

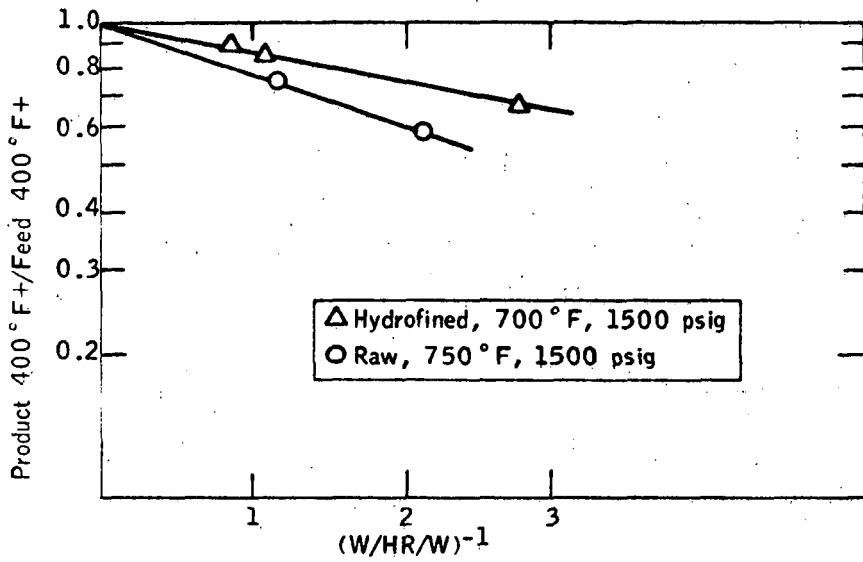


Fig. 2

HYDROCRACKING OF 400-700°F CUT

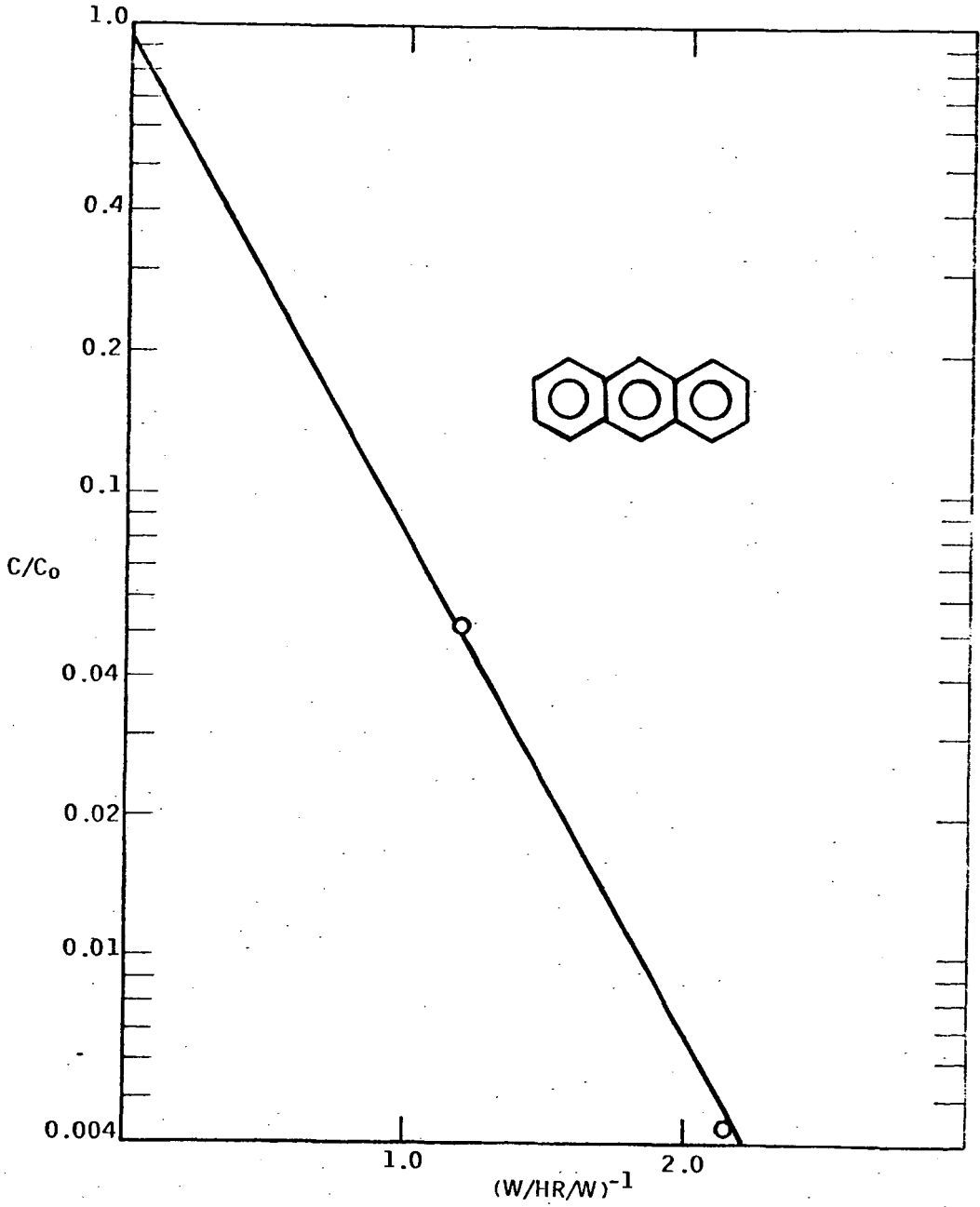


Figure 3

ANTHRACENE IN HYDROCRACKING RAW 400-700°F
750°F, 1500 psig

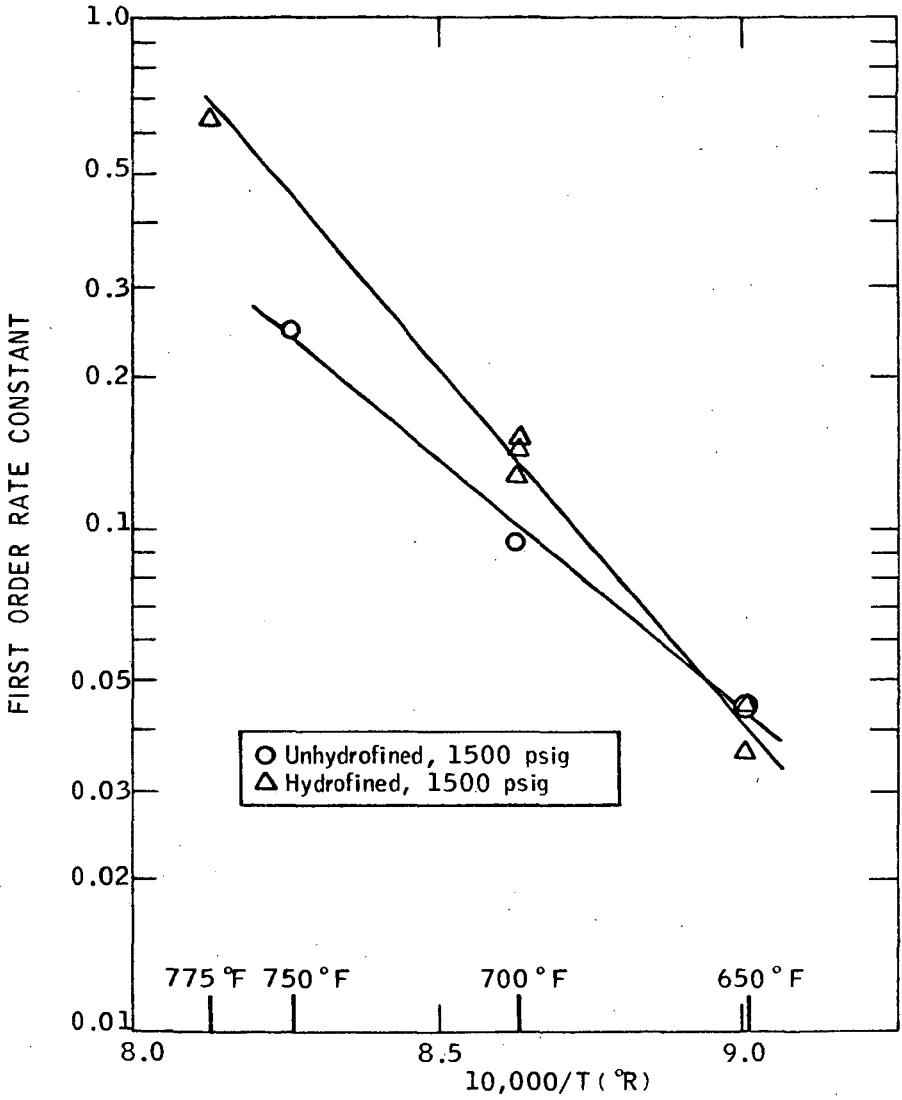


Fig. 4
HYDROCRACKING OF 400-700 °F DISTILLATE

Raw Feed, 750 °F

Hydrofined Feed, 700 °F

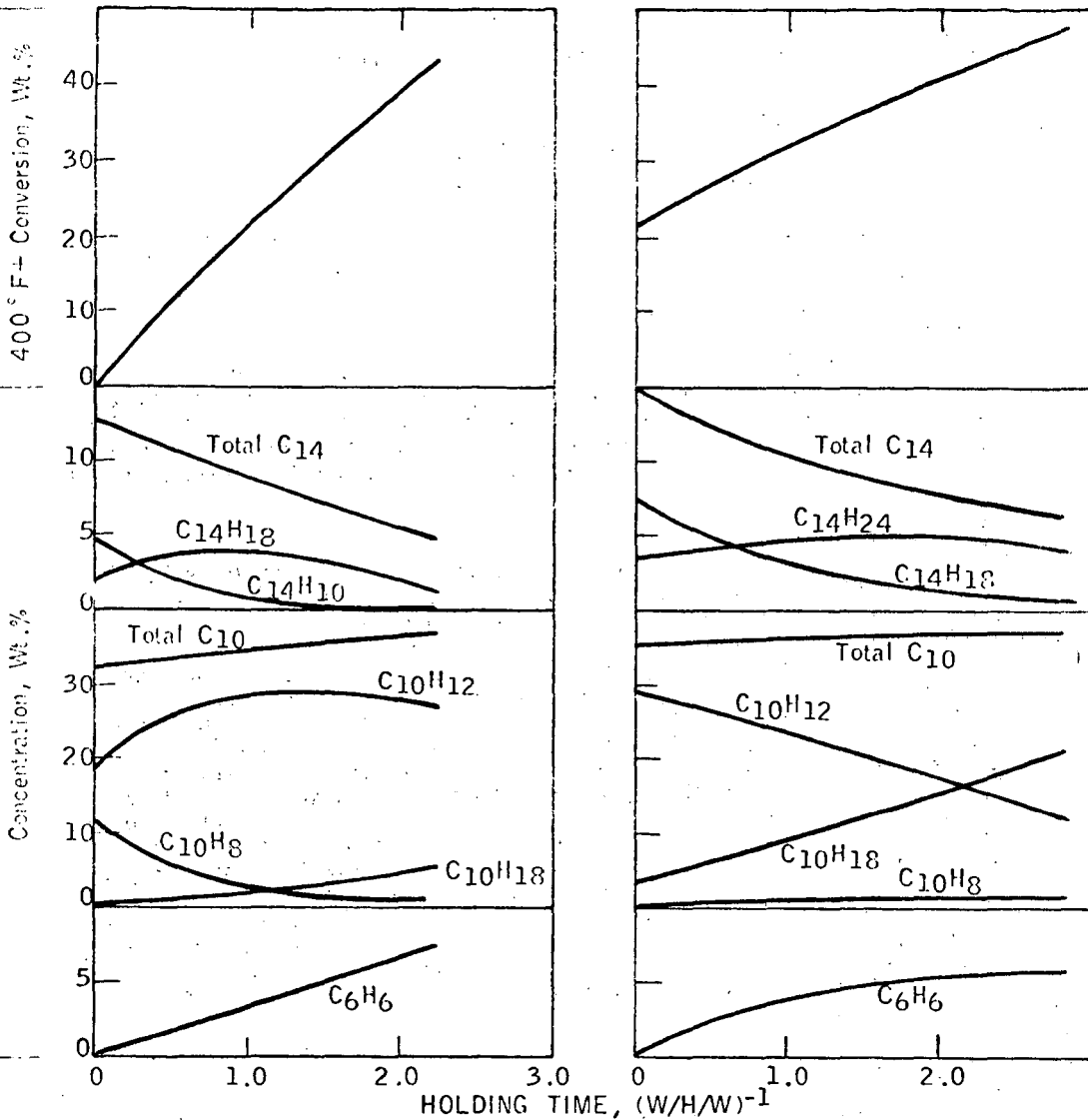


Fig. 5

HYDROCRACKING OF 400-700 °F CUT

HYDROCRACKING OF AROMATIC COMPOUNDS

S. A. Qader and G. R. Hill
Mineral Engineering Department
University of Utah
Salt Lake City, Utah

Abstract

Dualfunctional catalysts based on Cobalt, Molybdenum and Nickel were used for the hydrocracking of different types of hydrocarbons and heterocyclic compounds. The interfering effect of heterocyclic compounds on the hydrocracking of hydrocarbons was studied. The deactivation of the dualfunctional catalysts by some of the heterocyclic compounds was investigated.

Introduction

Hydrocracking over dualfunctional catalysts is a versatile method for converting polynuclear aromatic hydrocarbons and heterocompounds to lower boiling compounds. Though hydrocracking has been widely employed for the processing of petroleum and synthetic oils¹⁻³, the published data on the hydrocracking of pure aromatic hydrocarbons and heterocompounds are very meager. Flinn et. al.⁴ studied the hydrocracking of n-butylbenzene and tetralin over a nickel sulfide on silica-alumina catalyst and found that the principal reactions occurring were ring opening, dealkylation and dehydrogenation. Sullivan et. al.^{5,6} investigated the hydrocracking of different types of aromatic hydrocarbons over a nickel sulfide on silica-alumina catalyst and reported the occurrence of the 'paring reaction' which involves the removal of methyl groups attached to aromatic nuclei and their elimination as light isoparaffins with no loss of aromatic rings. They also reported the isomerization and cyclization of side chains to varying degrees forming indane type of structures. In this communication, the data on the hydrocracking of different types of polynuclear aromatic hydrocarbons over several dualfunctional catalysts are presented. The effect of the presence of sulfur, nitrogen and oxygen compounds on the conversion of aromatic hydrocarbons is reported.

Experimental

Pure grade hydrocarbons and heterocompounds were used for hydrocracking. The catalysts contained 20% by weight of oxides of molybdenum, cobalt and nickel on silica-alumina. The quantity of the catalyst used was 25% by weight of the reactants unless otherwise mentioned.

Equipment: The hydrocracking work was done in a batch autoclave of 300 c.c. provided with all controlling and recording devices.

Hydrocracking procedure: Experiments were carried out with 10 gm of the hydrocarbon and heterocompound mixture with varying amounts of the catalyst at 475°C. The hydrogen to hydrocarbon mole ratio was maintained

at 15.51 and 21.57 in case of naphthalene and anthracene respectively. The starting (cold) pressure was kept constant at 1000 p.s.i. and the final pressure varied between 1700-1800 p.s.i.

Results and Discussion

Synthetic crude oils produced from coal contain large quantities of aromatic hydrocarbons and heterocyclic compounds. The processing of these crudes mainly involves the conversion of aromatic hydrocarbons in admixture with aliphatic hydrocarbons and heterocompounds. A better understanding of the conversion of polynuclear aromatic hydrocarbons alone and in admixture with heterocyclic compounds to lighter products will be very useful in the development of efficient processes for the processing of synthetic crudes. The conversion of polynuclear aromatic hydrocarbons to lower boiling products can best be done by hydrocracking over dualfunctional catalysts. The aromatics have to be either partially or completely hydrogenated before they can crack to lighter products. Therefore, the temperature, hydrogen pressure or concentration and the activity and selectivity of the catalyst control the product distribution of the hydrocracking reaction. The data in Table I shows that the conversion of naphthalene increased with reaction time up to 2 hours. The yields of gas and coke and hydrogen consumption increased with naphthalene conversion. Alkylation of naphthalene took place during hydrocracking to a significant extent. The low concentration of decalins and saturated C₅-C₆ hydrocarbons in the liquid product indicates that naphthalene was mainly hydrogenated to tetralin but only to a small extent to decalin.

The activity and selectivity of the dualfunctional catalyst depend upon the relative amounts of the hydrogenation and cracking components. The data in Table II shows that a MoO₃ content of 20 to 25% is optimum to get maximum hydrogenation and cracking functions. The total conversion also depends upon the hydrocarbon to catalyst ratio as shown by the data in Table III. Maximum hydrogenation activity was obtained at 25% of catalyst whereas cracking reached a maximum at 15%. Hydrogen concentration also plays an important part in the hydrogenation-cracking system as shown in Table IV. Both the hydrogenation and cracking increased with hydrogen concentration. The gas yield increased while the coke yield decreased slightly. Higher hydrogen concentration also increased the formation of decalin from naphthalene as can be seen from the higher concentrations of decalins and saturated C₅-C₆ hydrocarbons in the liquid product.

As mentioned earlier, synthetic crudes contain large quantities of oxygen, sulfur and nitrogen containing compounds and it is of interest to know the effect of their concentration on hydrocarbon conversion. The effect of phenol on the conversion of naphthalene is shown by the data in Table V. The conversion of naphthalene increased with the phenol content up to 20%. However, the cracking activity was not affected even at 30% phenol though the hydrogenation activity decreased to some extent. The yields of gas and coke decreased and the yield of liquid product increased. The data indicates that the presence of phenol up to about 30% improves the hydrocarbon conversion. On the contrary, the presence of carbazole and

quinoline reduced naphthalene conversion (Tables VI and VII) to a significant extent. The effect was more pronounced at higher nitrogen contents. However, the yields of gas and coke decreased at higher nitrogen concentrations. The effect of the presence of dibenzothiophene on naphthalene conversion is shown by the data in Table VIII. 1% sulfur improved naphthalene conversion but a sulfur content of 2% and above, decreased the conversion significantly. The gas yield decreased while the coke yield increased. Like dibenzothiophene, n-hexyl mercaptan and diethyl sulfide also improved naphthalene conversion (Table IX) when they were present to the extent of 1% sulfur.

Anthracene was hydrocracked under similar conditions as naphthalene and the effect of reaction time on conversion is shown by data in Table X. Hydrogenation of anthracene reached a maximum of 95% at one hour while the cracking increased with reaction time up to 3 hours. In contrast to naphthalene hydrocracking, anthracene cracking produced more coke but less gas. The main products were the partially hydrogenated anthracenes and naphthalenes. Small amounts of tetralins and decalins present in the product indicate that either more hydrogenation activity is necessary for converting anthracene to monoring compounds as compared to naphthalene or anthracene hydrocracking has to be carried out in several stages.

The hydrocracking product distribution depends upon the type of catalyst used. Naphthalene and anthracene were hydrocracked over catalysts containing oxides of cobalt, molybdenum and nickel and the data are given in Tables XI and XII. In case of naphthalene hydrocracking, all the three catalysts affected similar naphthalene conversions of about 74 to 75%. However, cobalt and nickel exhibited slightly more hydrogenation and cracking activities and yielded more gas. The coke yield was more in case of molybdenum. Almost similar results were obtained with anthracene except cobalt exhibited more hydrogenation and cracking activity when compared to molybdenum and nickel, the latter exhibiting similar activities. Molybdenum yielded more coke.

Acknowledgment

Research work was supported by the Office of Coal Research and the University of Utah.

References

1. Qader, S. A., Hill, G. R., Ind. Eng. Chem., Process Design and Develop., 8, 98 (1969).
2. Qader, S. A., Hill, G. R., Ind. Eng. Chem., Process Design and Develop., 8, 462 (1969).
3. Myers, C. G., Garwood, W. E., Rope, B. W., Wadlinger, R. L., Hawthorne, W. P., J. Chem. Eng. Data, 7, 257 (1962).
4. Flinn, R. A., Larson, O. A., Beuther, H., Ind. Eng. Chem., 52, 153 (1960).
5. Sullivan, R. F., Egan, C. J., Langlois, G. E., Sieg, R. P., J. Am. Chem. Soc., 83, 1156 (1961).
6. Sullivan, R. F., Egan, C. J., Langlois, G. E., J. Catalysis, 3, 183 (1964).

TABLE I
EFFECT OF REACTION TIME ON NAPHTHALENE CONVERSION

Catalyst: MoO₃ on Silica-alumina

<u>Reaction Time, Minutes</u>	<u>30</u>	<u>60</u>	<u>120</u>
Product Distribution, wt, %			
Gas	6.1	10.4	12.9
Coke	3.8	5.8	7.6
Naphthalene	49.6	16.7	15.5
Alkyl naphthalenes	6.3	16.7	10.3
Tetralin	11.7	9.6	7.8
Alkyl tetralins	8.1	5.1	4.2
Decalins	Traces	1.3	1.3
Saturated hydrocarbons (C ₅ -C ₆)	1.4	6.1	1.7
Alkyl benzenes	13.0	28.3	38.7
Hydrogen Consumption	3.1	4.1	4.5
Naphthalene Conversion	44.1	66.6	74.2
Hydrogenation	44.1	66.6	74.2
Hydrocracking	24.3	50.6	60.9

TABLE II
EFFECT OF MoO₃ CONTENT ON NAPHTHALENE CONVERSION

Catalyst: 10% by Weight of Naphthalene

Reaction Time: 120 Minutes

MoO ₃ Content, Wt. %	15	20	25	35
Product Distribution, Wt. %				
Gas	10.0	11.0	11.7	10.5
Coke	5.1	5.2	5.0	4.9
Naphthalene	21.6	21.2	20.9	20.7
Alkyl naphthalenes	10.8	10.5	8.9	12.0
Tetralin	12.1	11.7	13.5	10.7
Alkyl tetralins	1.0	1.1	1.4	2.6
Decalins	0.5	1.0	1.3	0.5
Saturated Hydrocarbons (C ₅ -C ₆)	1.0	1.2	1.3	1.0
Alkylbenzenes	37.9	37.1	36.0	37.1
Hydrogen Consumption	4.1	4.0	4.2	4.1
Naphthalene Conversion	67.6	68.3	70.2	67.3
Hydrogenation	67.6	68.3	70.2	67.3
Hydrocracking	54.0	54.5	54.0	53.5

TABLE III
EFFECT OF CATALYST CONCENTRATION ON NAPHTHALENE CONVERSION

Reaction Time: 120 Minutes

Catalyst: MoO₃ on Silica-alumina

<u>Catalyst Wt. % of Naphthalene</u>	<u>10</u>	<u>15</u>	<u>20</u>	<u>25</u>
Product Distribution, Wt. %				
Gas	10.5	13.0	12.8	12.9
Coke	5.2	5.7	5.9	7.6
Naphthalene	21.2	19.2	16.1	15.5
Alkyl naphthalenes	11.0	8.5	11.4	10.3
Tetralin	11.7	9.6	8.7	7.8
Alkyl tetralins	1.1	1.4	2.0	4.2
Decalins	1.0	1.1	0.7	1.3
Saturated Hydrocarbons (C ₅ -C ₆)	1.2	0.8	1.8	1.7
Alkylbenzenes	37.1	40.7	40.6	38.7
Hydrogen Consumption	4.1	4.2	4.3	4.5
Naphthalene Conversion	67.8	72.3	72.5	74.2
Hydrogenation	67.8	72.3	72.5	74.2
Hydrocracking	54.0	60.2	61.1	60.9

TABLE IV
EFFECT OF HYDROGEN CONCENTRATION ON NAPHTHALENE CONVERSION

Catalyst: MoO₃ on Silica-alumina

<u>Hydrogen/Naphthalene Mole Ratio</u>	<u>15.51</u>	<u>20.68</u>
Product Distribution, Wt. %		
Gas	12.8	15.0
Coke	5.9	4.8
Naphthalene	16.1	15.2
Alkyl naphthalenes	11.4	5.7
Tetralin	8.7	8.2
Alkyl tetralins	2.0	0.8
Decalins	0.7	1.5
Saturated Hydrocarbons (C ₅ -C ₆)	1.8	3.1
Alkyl benzenes	40.6	45.7
Hydrogen Consumption	4.3	4.6
Naphthalene Conversion	72.5	79.1
Hydrogenation	72.5	79.1
Hydrocracking	61.1	69.6

TABLE V
EFFECT OF PHENOL ON NAPHTHALENE CONVERSION

Reaction Time: 60 Minutes

Catalyst: MoO_3 on Silica-Alumina

<u>Phenol Content, Wt. %</u>	<u>0.0</u>	<u>10.0</u>	<u>20.0</u>	<u>30.0</u>
Product Distribution, Wt. %				
Gas	10.4	9.0	8.5	7.6
Coke	5.8	4.2	4.0	4.0
Naphthalene	16.7	16.6	15.6	14.3
Alkyl naphthalenes	16.7	13.6	9.5	14.3
Tetralin	9.6	9.5	9.9	10.2
Alkyl tetralins	5.1	3.0	5.8	2.6
Decalins	1.3	1.1	1.8	0.9
Saturated Hydrocarbons ($\text{C}_5\text{-C}_6$)	0.7	4.0	5.4	6.6
Alkylbenzenes	33.7	39.0	39.5	39.5
Naphthalene Conversion	66.6	69.8	74.9	71.4
Hydrogenation	66.6	69.8	74.9	71.4
Hydrocracking	50.6	56.2	57.4	57.7

TABLE VI
EFFECT OF CARBAZOLE ON NAPHTHALENE CONVERSION

Catalyst: MnO_3 on Silica-alumina

<u>Nitrogen Content, Wt. % Naphthalene</u>	<u>0.0</u>	<u>1.0</u>	<u>2.0</u>
Product Distribution, Wt. %			
Gas	10.4	7.1	5.1
Coke	5.8	3.0	2.6
Naphthalene	16.7	38.2	41.6
Alkyl naphthalenes	16.7	7.2	5.9
Tetralin	9.6	26.9	28.7
Alkyl tetralins	5.1	0.4	0.2
Decalins	1.3	Traces	0.1
Saturated Hydrocarbons (C_5-C_6)	0.7	1.0	0.3
Alkyl benzenes	33.7	16.2	15.5
Naphthalene Conversion	66.6	54.6	52.5
Hydrogenation	66.6	54.6	52.5
Hydrocracking	50.6	27.3	23.5

TABLE VII
EFFECT OF QUINOLINE ON NAPHTHALENE CONVERSION

Catalyst: MoO₃ on Silica-alumina

<u>Nitrogen Content, Wt. % of Naphthalene</u>	<u>0.0</u>	<u>1.0</u>	<u>2.0</u>
Product Distribution, Wt. %			
Gas	10.4	8.8	7.4
Coke	5.8	2.7	2.6
Naphthalene	16.7	33.4	36.0
Alkyl naphthalenes	16.7	7.3	20.0
Tetralin	9.6	20.0	15.9
Alkyl tetralins	5.1	2.1	0.9
Decalins	1.3	Traces	0.5
Saturated Hydrocarbons (C ₅ -C ₆)	0.7	1.7	1.0
Alkyl benzenes	33.7	24.0	15.7
Naphthalene Conversion	66.6	59.3	44.0
Hydrogenation	66.6	59.3	44.0
Hydrocracking	50.6	37.2	26.7

TABLE VIII
EFFECT OF DIBENZOTHIOPHENE ON NAPHTHALENE CONVERSION

Reaction Time: 60 Minutes

Catalyst: MoO_3 on Silica-Alumina

Sulfur Content: Wt. % of Naphthalene	<u>0.0</u>	<u>1.0</u>	<u>2.0</u>	<u>3.0</u>
Product Distribution, Wt. %				
Gas	10.4	9.0	8.9	8.2
Coke	5.8	6.1	6.4	6.2
Naphthalene	16.7	14.8	17.4	15.0
Alkyl naphthalenes	16.7	16.6	16.6	24.4
Tetralin	9.6	11.5	11.4	11.1
Alkyl tetralins	5.1	2.9	3.8	2.7
Decalins	1.3	1.5	1.0	0.7
Saturated Hydrocarbons ($\text{C}_5\text{-C}_6$)	0.7	1.9	1.2	1.2
Alkyl benzenes	33.7	35.7	33.3	30.5
Naphthalene Conversion	66.6	68.6	66.0	60.6
Hydrogenation	66.6	68.6	66.0	60.6
Hydrocracking	50.6	52.7	49.8	46.1

TABLE IX
EFFECT OF DIFFERENT SULFUR COMPOUNDS ON NAPHTHALENE CONVERSION

Sulfur Content: 1.0% by Weight of Naphthalene

Catalyst: MoO₃ on Silica-alumina

<u>Sulfur Compound</u>	<u>Dibenzo- thiophene</u>	<u>n-Hexyl mercaptan</u>	<u>Diethyl Sulfide</u>
Product Distribution, Wt. %			
Gas	9.0	9.8	10.5
Coke	6.1	4.2	5.0
Naphthalene	14.8	16.4	16.3
Alkyl naphthalenes	16.6	14.0	12.6
Tetralin	11.5	10.6	11.9
Alkyl tetralins	2.9	3.4	6.0
Decalins	1.5	1.7	1.2
Saturated Hydrocarbons (C ₅ -C ₆)	1.9	1.7	1.0
Alkyl benzenes	35.7	38.2	35.5
Naphthalene Conversion	68.6	69.6	71.1
Hydrogenation	68.6	69.6	71.1
Hydrocracking	52.7	53.9	52.0

TABLE X
EFFECT OF REACTION TIME ON ANTHRACENE CONVERSION

Catalyst: MoO₃ on Silica-alumina

<u>Reaction Time, Minutes</u>	<u>60</u>	<u>120</u>	<u>180</u>
Product Distribution, Wt. %			
Gas	5.1	5.8	6.8
Coke	13.5	14.1	15.2
Anthracene	4.9	5.5	5.4
Hydroanthracenes	34.8	30.2	23.6
Naphthalenes	31.1	30.5	30.6
Tetralins and Decalins	2.2	3.1	5.3
Alkylbenzenes	8.4	10.8	13.1
Anthracene Conversion	95.1	94.5	94.6
Hydrogenation	95.1	94.5	94.6
Hydrocracking	60.3	64.3	71.0

TABLE XI
NAPHTHALENE CONVERSION WITH DIFFERENT CATALYSTS

Reaction Time, 120 Minutes

<u>Catalyst</u>	<u>Cobalt Oxide (CoO)</u>	<u>Molybdenum Oxide (MoO₃)</u>	<u>Nickel Oxide (NiO)</u>
Product Distribution, Wt. %			
Gas	16.2	12.9	15.4
Coke	5.6	7.6	7.0
Naphthalene	13.5	15.5	13.1
Alkyl-naphthalenes	11.3	10.3	11.5
Tetralin	4.9	7.8	6.6
Alkyltetralins	2.0	4.2	1.7
Decalins	4.9	1.3	3.3
Saturated Hydrocarbons (C ₅ -C ₆)	3.0	1.7	2.0
Alkylbenzenes	38.6	38.7	39.4
Naphthalene Conversion	75.2	74.2	75.4
Hydrogenation	75.2	74.2	75.4
Hydrocracking	63.4	60.9	63.8

TABLE XII

ANTHRACENE CONVERSION ON DIFFERENT CATALYSTS

Reaction Time: 120 Minutes

<u>Catalyst</u>	<u>Cobalt Oxide</u>	<u>Molybdenum Oxide</u>	<u>Nickel Oxide</u>
Product Distribution, Wt. %			
Gas	7.2	5.8	6.2
Coke	11.0	14.1	12.2
Anthracene	4.8	5.5	4.7
Hydroanthracenes	26.0	30.2	30.9
Naphthalenes	32.1	30.5	32.3
Tetralins and Decalins	4.0	3.1	2.8
Alkylbenzenes	14.9	10.8	10.9
Anthracene Conversion	95.2	94.5	95.3
Hydrogenation	95.2	94.5	95.3
Hydrocracking	69.2	64.3	64.4

A PROCESS FOR DRY HYDROGENATION OF LOW RANK COALS WITH HIGH YIELDS OF PHENOLICS

Charles W. Albright and Hubert G. Davis

Union Carbide Corporation
Research and Development Department
Chemicals and Plastics
P.O. Box 8361
South Charleston, West Virginia 25303

INTRODUCTION

The available methods for converting coal into gaseous or liquid fuels or chemicals are generally forms or combinations of three basic processes. These are pyrolysis or carbonization, hydrogenation, and CO-H₂ synthesis gas production with further conversion of the synthesis gas if desired. The doubtful economics and precarious existence of the forms which these basic processes have taken stem from several factors. Low-temperature carbonization produces a crude tar product in low yield and must be coordinated with a power-plant requiring the residual coke or char. High-pressure hydrogenation, as in the commercialized German Bergius process, is technologically difficult, requires heavy investment per barrel of crude product, and consumes large amounts of expensive hydrogen from synthesis gas. The handling of the pulverized coal as a slurry in heavy recycle "pasting" oil is a complicating feature. The various CO-H₂ syntheses, such as the Fischer-Tropsch process, require high investment in both synthesis gas production and the synthesis step itself.

In seeking a more economically attractive route to products from coal, we have studied the pyrolysis of coals under mildly hydrogenating conditions in the absence of a liquid vehicle; i. e., in a fluidized bed of solid particles of coal and reacted char. We looked for coals that gave attractive yields of tar by carbonization, we investigated regions of low hydrogen consumption to minimize the cost and we accepted an incomplete conversion of coal substance to gas and liquid product with the char by-product treated as the basic fuel for plant operation. As a chemical company we were seeking chemical rather than energy products and were particularly interested in the potentially high phenolic yields obtainable from low-rank coals.

Dry hydrogenation of coal was investigated briefly and apparently abortively in Germany during World War II⁽¹⁾. The U.S. Bureau of Mines⁽²⁾ followed up this work immediately after the war and coined the term hydrocarbonization which we use in this report. The Bureau describes their effort to develop a process by hydrocarbonization as an alternate to the Bergius process for the production of liquid fuels from coal. However, there seems to have been no major effort at exploitation of this work at any later time.

The work reported here is primarily based on a bench-scale experimental effort (about one pound of coal per hour) carried out several years ago mainly with a Wyoming, subbituminous C coal from Lake de Smet. Two scale-ups were also successfully operated, at about 10 and about 1500 pounds per hour. Each of these scale-ups produced its own operating problems. But in each case these were surmounted and operability and yields equivalent to those from the bench-scale operation were achieved. Several other coal feeds were studied. Wyoming (subbituminous C) from Wyodak, Texas Lignite, and North Dakota Lignite were essentially equivalent to Lake de Smet coal. Elkol and Brilliant Wyoming coals and weathered Pittsburgh No. 8 were less satisfactory but could be handled.

EXPERIMENTAL

Apparatus (Bench-Scale Unit)

The bench-scale hydrocarbonization unit as it finally evolved is shown in Figure 1. Its nominal capacity is 1.0 lb/hr of 40-100 mesh coal.

The system consists of the following major items:

Coal Feed Hopper - sized to hold about 3500 grams of coal, enough for 6-10 hours operation. Constructed from schedule 80, 3-inch carbon-steel pipe, 4 feet high.

Calibrated Thermal-Feed Rate Device - a miniature heat exchanger to indicate a rough coal feed rate.

Calibrated Vibratory Coal Feeder - based on a chicken-feeder principle for gas flow to pick up a controlled amount of coal.

Fluidized Reactor - stainless steel, 1-inch I. D., 1/4-inch wall thickness, 9 inches high with expanded head 18 inches high made of 2-inch schedule 80 pipe. Char overflow line and vapor outlet made from 1-inch schedule 80 pipe. A 1/4-inch thermowell is installed in the center of the reactor. Thermocouples are located one inch, four inches, seven inches and twelve inches from the bottom of the reactor. The lower three thermocouples are in the fluidized carbonization bed while the upper one is in the vapor space above the bed. The reactor is equipped with four independent electrical heating circuits, one each for the reactor, the expanded head, the vapor outlet line, and the char overflow line.

Char Receiver - a duplicate of the coal feed hopper.

Steam-Cooled Primary Condenser - stainless steel, 1-1/2-inch, schedule 80, 22 inches long with a 2-inch steam jacket.

Water-Cooled Condenser - carbon steel, 1-inch, schedule 40, 44 inches high with a 1-1/2-inch jacket.

Ice-Water-Cooled Condenser - duplicate of water-cooled condenser.

Operating, Sampling, and Analytical Procedures

The feed coal was removed from a vacuum drier at ambient temperature and a weighed sample was charged to the feed hopper. Meanwhile, fine adjustments of the current to the electrical heating elements brought the various parts of the unit to the target temperatures. The unit was pressurized and gas flows at target conditions were established. The run was then started by opening the shut-off valve in the line separating the feed hopper from the coal feeder and starting the Syntron vibrator which was attached to the coal feeder body. Prior to starting the coal-feed, the current to the electrical heating element on the thermal feed-rate device had been adjusted to a level such that the thermocouple indicated a temperature of 140°C. After establishing coal flow, the cold coal flowing through the tube from the hopper to the feeder conducted heat away from the metal core of the feed-rate device and the thermocouple temperature lined out at a lower level. Calibration of the feeder, prior to experimental runs, showed that a temperature level of about 100°C. would result in a coal feed rate of about one pound per hour, the desired rate for the majority of the experiments. The amplitude of vibration to the feeder was, therefore, varied to adjust the temperature to the 100°C. level. The feeder device works on the principle of a "chicken feeder"; i. e., the gas flowing across the supply of coal in the enlarged part of the body below the cut-off tubing eats away the coal which is continuously replaced by coal from the hopper. The function of the vibrator is to ruffle the coal interface so that more coal will be picked up as the amplitude of vibration is increased.

The vibrations also insure that the down-tube from the coal hopper remains full. Minor feed-rate adjustments of about 50 grams on a base of 450 grams per hour could be achieved by changing the amplitude of vibration. During the run, the quality of fluidization was monitored by the temperature spread in the bed as indicated by a spread, top to bottom, of about 10°C. It was desirable to have good fluidization with the minimum of fluidizing gas in order to minimize char carryover. Therefore, the gas flow to the unit was generally reduced to a point where a slight temperature spread in the bed developed, then the flow was increased in small increments until the spread disappeared. To achieve equilibrium at target operating conditions required about 10 minutes.

A composite gas sample was collected at a constant rate by liquid displacement throughout the run. Spot gas samples were also taken.

Normally, with minor adjustments, the runs proceeded until the coal feed-hopper was empty. This point was rapidly indicated by a sudden increase in the temperature of the thermal feed-rate device. With the termination of the experiment, the unit was closed in at pressure, gas flows stopped, electric circuits turned off and the unit was allowed to cool overnight.

The char receiver was drained and the char weighed to determine the char yield. It was found that the char ignited spontaneously at room temperature in an open container. It was therefore stored in a drum pressurized with nitrogen.

The condensers were drained into a common receiver jar and a net liquid gross product weight was determined. The entire liquid product was then filtered and charged to a 1-inch I. D. by 20-inch-high glass distillation column packed with 1/4-inch protruded packing. The char filter cake weight was determined after it was dry and this weight, between 15 and 30 grams, was added to the char yield.

The product was then stripped of water by distilling at atmospheric pressure and on total make to a kettle temperature of 200°C. Some oil azeotroped with the water and was subsequently separated by decantation and returned to the kettle after it cooled. The tar was then cut into four fractions as follows:

- (1) IBP to 130°C. at atmospheric pressure and a 3 to 1 reflux ratio.
- (2) 130-260°C. light oil, at 50 mm and a 6 to 1 reflux ratio.
- (3) 260-340°C. middle oil, at 10 mm and a 3 to 1 reflux ratio, and
- (4) Residue, boiling >340°C. and consisting of the heavy oil and pitch. In some runs the heavy oil (340-350°C. at 10 mm) and pitch fractions were determined by a Vigreux distillation.

The analyses performed on the various samples, for the most part, are standard or well-known and it is not necessary to document them here. However, there was one special analytical development during the course of the experiments, i. e., the determination of the concentration of various tar acids boiling through the xylenols, without separation from the neutral oil, by a gas chromatographic technique. This method of determining at least a partial distribution of phenolics in raw light oils from coal carbonization, etc., can be extremely useful in following effects of changes in processing. With a column packed with Chromosorb coated with Apiezon N stopcock grease, or with similar neutral columns, the order of elution is: Phenol; o-cresol; m-p-cresols; o-ethylphenol; 2,5-xylenol; 2,4-xylenol; 2,3-xylenol, m-p-ethylphenol; 3,5-xylenol; and 3,4-xylenol. 2,6-Xylenol is eluted somewhere between m-p-cresol and o-ethylphenol, and m-p-ethylphenol about the same time as 2,3-xylenol. M- and p-cresol are unresolved, and the nine ethylphenols and xylenols give at most six incompletely resolved peaks,

some of which may also contain small amounts of C₃-phenols. Nevertheless, considerable information concerning a sample may be obtained by this simple form of chromatography, certainly enough to follow substantial changes in distribution. Interference from hydrocarbons present is corrected for by a comparison with the chromatograph of a typical neutral oil, prepared by extraction of product oil with caustic.

Protection of Coal from Oxidation

In the preliminary experiments with Lake de Smet coal, an important lesson on handling the coal was learned. It was found that extreme care was necessary in order to prevent oxidation and obtain truly representative yields from this low-rank coal. The precautions decided upon as a result of the preliminary work were used in succeeding experiments with Lake de Smet coal.

A sample of Lake de Smet coal was obtained by core-drilling south of the lake on property of the Northern Wyoming Land Company. The sample of coal was carefully protected for shipment by placing the wet cores in polyethylene bags and surrounding the bags with wet core-cuttings in a wooden packing box. On arrival at the research laboratory, an aliquot sample of the cores was taken, partially dried at ambient temperature in a vacuum desiccator, ground and analyzed. The remaining core samples were placed in a commercial vacuum drying oven and dried overnight at 50°C. The cores were then ground to yield sufficient 40-100 mesh coal for two experimental runs.

The analysis of the aliquot sample, the sample prepared for experimental use and an analysis reported by the United States Bureau of Mines, Denver, Colorado, are shown in Table I. The operating conditions and the product yields are shown in Table II.

The yield of tar from the experimental supply of Lake de Smet coal was only 5.9% MAF coal when carbonized in an inert atmosphere as shown in Column 1, Table II. This compares with a 10.9% yield reported by the U.S.B.M., shown in Column 4. The respective char yields were 76.6% and 68.4%. Furthermore, Column 2 shows that in a hydrogen atmosphere, at a hydrogen partial pressure of 320 psi, the tar yield increased to only 8.9%. We had anticipated a tar yield of about 17% as shown in Column 3. The respective char yields were 68.9 and 57.0%. Turning to the ultimate analyses given in Table I, it is apparent that the experimental supply of coal lost hydrogen, down from 5.3 to 4.3% and gained oxygen, up from 19.1 to 20.3% during the drying and grinding operations. The adverse effect of oxidation on the tar yields from these preliminary experiments shows that extreme care is required in handling the coal in order to obtain truly representative yields.

After this experience the following procedure was used to prevent oxidation of the feed coal. The Lake de Smet coal was received from Wyoming in drums with the coal completely submerged in water. As needed for a series of experiments, lumps of coal were removed from the water and placed in the vacuum dryer. The coal was dried initially to a moisture level between 20 and 25%, the drying-time required being determined by trial and error. (The coal as mined has a 30% moisture content). The vessel and the partly dried coal were then allowed to cool to ambient temperature prior to breaking the vacuum and removing the coal. The partly-dried coal was ground and screened to obtain a maximum yield of coal in the range of 40-100 mesh. This was the size of coal used throughout the experiments. The minus 100 mesh was rejected in order to minimize char carryover with the vapors from the fluid bed into the condensers. Between runs, the partly dried ground coal was stored in sealed drums under positive pressure supplied by high-purity nitrogen cylinders.

The day before a run was to be made, sufficient coal for making the run (about 4000 grams) was removed from the nitrogen-pressurized drum and charged to the vacuum oven for final drying at 50°C. About 6 hours were required to reduce the moisture content from 20-25% to about 1-3%. The oven was allowed to cool before the coal was removed.

EXPERIMENTAL RESULTS

The experimental results presented in this paper are all based upon Lake de Smet, Wyoming, coal. This unusual coal formation exists in the form of a lens of coal lying near the surface and with thickness up to 200 feet. At some time in the past the coal has partially burned out, forming a basin now filled with water and known as Lake de Smet. The coal is of subbituminous C rank, with a heating value of about 7,000 B.t.u. per pound as mined. Because the thickness of the seam and the relatively modest overburden make for low-cost mining, the deposit is a potential cheap source of raw material.

A typical analysis of Lake de Smet coal is:

Ultimate Analysis, Wt. % on Moisture-free and Ash-free Basis

C	72.0
H	5.5
N	1.4
S	1.1
O (by difference)	20.0
Ash, dry basis	17.0

North Dakota and Texas lignites, and Wyodak, another Wyoming subbituminous C coal, have similar analyses and give almost identical results.

Comparison of Hydrocarbonization with Carbonization

It is clear from the data presented, and the comparison given with carbonization in nitrogen, that hydrocarbonization differs substantially and quantitatively from carbonization. There is considerable reaction with hydrogen, the yield of tar is roughly doubled, the proportions of light oil and of -230°C . phenols in the tar are increased. The following short table summarizes the main differences. Before any experimentation on Lake de Smet coal, yields of tar from hydrocarbonization were predicted from the Bureau of Mines carbonization data with factors estimated from German and Bureau work on dry coal hydrogenation. At 1000 psi, 525°C . and 8 minutes coal residence time a tar yield of about 25% was predicted. Coal residence time is defined as the time required to fill the reactor with fresh coal feed.

<u>Yields as Wt. % MAF Coal</u>	<u>Carbonization in N_2 This Work</u>	<u>Carbonization By Parry Process USBM Data⁽³⁾</u>	<u>Hydrocarbonization This Work 1.6% H_2 Reacted</u>
Char	67	67	49
Tar	12	12	25
Gas	9	8	14
Water	12	13	14
< 260°C ., Light Oil	4	3	10
< 230°C ., Phenols	2	1.5	5.2
Phenol	0.5	0.5	1.9

A decided advantage of hydrocarbonization is the possibility of recycling products, especially phenolics, to the reactor and reducing their molecular weight to the range desired - to phenol if necessary. Even in a straight carbonization plant enough facility and hydrogen would probably have to be supplied to carry out this hydrocracking step.

Effects of Operating Variables

Effect of Temperature

Operating temperatures of 478 to 567°C . were studied with hydrogen

partial pressure and coal residence time held approximately constant at 900 psia and 9 minutes, respectively. Figure 2 shows the dependence of hydrogen consumption on the temperature variable and Figure 3 shows the yields. Figure 4 shows that at temperatures much above 520°C. rapid increase in hydrogen consumption does not result in significant increases in tar yield. Actually the curve drawn in Figure 3 indicates a maximum tar yield at about 540°C.

Effect of Hydrogen Partial Pressure

The partial pressure of hydrogen was varied in the range 0 to 940 psia with temperature and coal residence time held at about 540°C. and 8 minutes, respectively. Figure 5 indicates a roughly linear dependence of hydrogen consumption on partial pressure. Figure 6 shows that tar rises proportionately. A single experiment at 1500 psi indicated that the yield of tar is still an increasing function of pressure above 1000 psi.

Effect of Coal Residence Time

Figure 7 shows the effect of coal residence time at constant temperature and hydrogen partial pressure (about 900 psia). The shape of the curves we have drawn, at low residence times, is roughly that of a typical first-order reaction. Rate constants can be estimated by assuming each curve approaches some maximum hydrogen consumption. This is shown for 540°C. where 3.5% hydrogen consumed is arbitrarily called "complete reaction." Figure 8 shows product yields at 540°C. as a function of residence time. At this temperature there is little or no gain in tar yield after about 8 minutes, although hydrogen consumption continues to rise.

Effect of Ash and Water

Batches of Lake de Smet coal from two sections of the area had quite different ash contents. The results plotted in Figure 9 show that the low ash sample was slightly less reactive, perhaps indicating some catalytic activity in the ash.

Batches of Lake de Smet coal dried to various water contents were also studied, but no differences noted.

Composition of Gas, Tar, and Char Products

Gas: Table III shows typical gas product analyses under mild and severe hydrocarbonization conditions. In both cases the B. t. u. content is high and there are potential chemical values.

Tar: Table III also gives typical analyses for tars from the same experiments. Our particular interest is in the phenolics content and distribution. The tar acid distribution seems to be fairly insensitive to the severity of hydrogenation and there is a surprisingly high content of phenol itself.

Char: The ultimate analyses of the chars for the runs are given in Table III. There is still some oxygen in the char at the higher severity, although other experiments have shown this to approach zero at slightly higher temperatures or longer residence times. There is about 4% hydrogen in both chars. In general we have found the hydrogen content to be relatively independent of operating conditions.

Hydrocarbonization Under Mild Conditions

Studies under very mild hydrocarbonization conditions showed that a high percentage of the tar and phenolic value could be recovered with very low hydrogen consumption at a hydrogen partial pressure of about 300 psi. For example a 5.1% light oil tar acid yield was obtained with only 1.4% hydrogen consumption. The yield of phenol was 1.8%. This compares to a light oil tar acid yield, at 900 psi hydrogen partial pressure, of 5.7% of MAF coal. However, the hydrogen consumption was 2.2% and the phenol yield was 1.6% MAF coal. Since a major cost factor in the process is the consumption of hydrogen per unit of phenolics produced, a mild condition of hydrocarbonization is probably economically desirable.

TABLE I
PROPERTIES OF LAKE DE SMET COAL

<u>Proximate Analysis, Wt. %</u>	<u>Aliquot Sample as Received</u>	<u>Experimental Sample</u>	<u>Denver Station, USBM, Run 146</u>
Volatile Matter	33.8	38.2	28.2
Fixed Carbon	35.8	45.9	30.9
Moisture	19.3	1.5	24.8
Ash	11.1	14.4	16.1
<u>Ultimate Analysis, Wt. % MAF Coal</u>			
C	72.4	72.2	70.2
H	5.3	4.3	5.5
N	1.6	1.5	1.5
S	1.6	1.7	0.7
O (by difference)	19.1	20.3	22.1

TABLE II
CARBONIZATION AND HYDROCARBONIZATION
OF LAKE DE SMET COAL

	<u>Operating Conditions</u>			<u>U.S.B.M. Denver Station, Run 146</u>
			<u>Estimate*</u>	
Fluidization Gas	Nitrogen	Hydrogen	Hydrogen	Nitrogen
Pressure, psig	200	400	400	Atmospheric
Temperature, °C.	515	515	515	500
Hydrogen Partial Pressure, psi	nil	320	320	nil
	<u>Yield, Weight % MAF Coal</u>			
Char	76.6	68.9	57.0	68.4
Tar	5.9	8.9	17.0	10.9
Gas	9.0	11.6	15.0	8.4
Water	8.5	11.5	12.0	12.3
Hydrogen	-	<u>-0.9</u>	<u>-1.0</u>	-
	100.0	100.0	100.0	100.0

* Estimated by interpolation of German and USBM data on low-rank coals.

TABLE III
COMPOSITION OF GAS, TAR, AND CHAR

<u>Operating Conditions</u>		
<u>Hydrocarbonization</u>	<u>Mild</u>	<u>Severe</u>
Temperature, °C.	560	567
Hydrogen Partial Pressure, psi	310	940
Residence Time, Minutes	8.2	10.2
<u>Yields, Weight % MAF Coal</u>		
Char	50.4	38.4
Tar	21.3	29.0
Water	13.2	19.2
Gas	16.0	16.2
Hydrogen	-1.4	-3.5
Unaccounted for	0.5	0.7
	100.0	100.0

Gas Composition, Volume %, H₂ Free

<u>Component</u>		
Methane	46.3	63.1
Ethane	9.1	13.7
Propylene	1.8	0.3
Propane	4.7	4.5
Butenes	1.1	0.6
n-Butane	0.4	0.5
i-Butane	0.7	0.4
C ₅ 's	0.2	0.1
CO	28.2	14.1
CO ₂	7.5	2.5
H ₂ S	0.2	0.2
Molecular Weight	25.5	22.36
Wt. % Hydrogen in Gas	12.1	17.34

Tar Composition

Distillation, Weight % of Tar

<u>Fraction, From-to, °C.</u>		
IBP-260°C.	37.0	44.5
260-340°C.	12.0	7.0
340°C.	51.0	48.5

Tar Acids, Weight % MAF Coal

IBP-260°C.	5.1	7.6
260-340°C.	1.5	0.8

Yield of Basic Aromatics, Lb/Ton MAF Coal

Benzene	0.1	0.4
Toluene	0.2	0.2
Naphthalene	0.3	0.6

TABLE III, CONTINUED
COMPOSITION OF GAS, TAR, AND CHAR

Tar Composition, Continued

<u>Hydrocarbonization</u>	<u>Mild</u>	<u>Severe</u>
<u>Light Oil (130-260°C.) Tar Acid Distribution, Wt. %</u>		
Phenol	34.5	33.4
o-Cresol	8.7	7.8
m, p-Cresol	27.2	24.5
Ethylphenols and Xylenols	17.1	18.9
Higher Phenols by Difference	12.5	15.4

Phenol Yield, Weight % MAF Coal

	1.8	2.2
--	-----	-----

Char Composition

C	90.1	93.0
H	3.9	3.8
N	1.2	1.3
S	1.0	0.6
O (by difference)	3.8	1.3

Oil Recycle Experiments

The hydrocarbonization of Lake de Smet coal produces considerable tar boiling above 230°C. As a general rule, about 50% or more of the tar falls in this category. Tar acid content of the +230°C. tar is roughly 50 weight %. Experiments on both bench- and pilot-plant scales have shown that this oil can be recycled to extinction in the reactor, thus converting the heavy tars to oils boiling below 230°C.

The bench-scale unit was modified by the addition of a heated pump, so that the hydrocarbonization tar boiling above 230°C. could be fed into a fluidized bed of char produced from previous hydrocarbonization experiments. The results of these experiments show that the conversion of +230°C. tar acids to -230°C. phenolics was about 40% by weight. Thus the yield from recycling +230°C. tar is 40% of 50% or about 20 weight % of the total +230°C. tar cycled. The consumption of hydrogen per pound of -230°C. phenolics produced is about half that for phenolics from raw Lake de Smet coal. Therefore, it should be feasible and economical to recycle these higher-boiling tars to the basic hydrocarbonization process.

DISCUSSIONS AND CONCLUSIONS

Chemistry

Coals of lignitic or subbituminous rank are statistically polymers of fairly small aromatic "nuclei" averaging perhaps 10 aromatic carbon atoms per nucleus. These are substituted with paraffin side-chains, probably largely methyl, saturated rings, hydroxyl and other groups and are linked and perhaps cross-linked through hetero-atoms or by direct C-C bonding. The pyrolytic break-down of these crude polymers produces fragments averaging much higher hydrogen content than the coal. Thus, a large amount of a material of low hydrogen content, char or coke, must be produced. When molecular hydrogen is present this can intervene to supply some of the H requirement of the hydrogen-rich fragments, thus reducing the amount of char formed and increasing tar and gas yields.

We would expect the hydrogen action to be roughly first-order in unreacted coal substance (if such a thing is definable) and, by analogy to the well-known thermal dealkylation reaction, half-order in H_2 . The activation energy of the reaction should correspond to that of hydrodealkylation or of thermal cracking and be in the 50-60 kcal/mol range.

In practice this very simplistic view of the kinetics of the process is helpful in rationalizing the results but is hardly very satisfactory quantitatively. If we pick a suitable percentage of hydrogen as complete reaction (say 3.5 lbs H_2 /100 lbs MAF coal), we can roughly reproduce the general shape of the plots of hydrogen reacted vs coal residence time as a first-order plot (see Figure 7). However, the rate of hydrogen conversion depends upon the first or even higher power of the hydrogen partial pressure (see Figure 5) and the temperature coefficient is low (we estimate the energy of activation to be about 33 kcal/mole).

If we think of degree of reaction strictly in terms of hydrogen consumption per 100 pounds of coal, we can deduce a convenient rule of thumb from the collected data. Doubling the coal residence time is equivalent to doubling the hydrogen partial pressure and either is equivalent to a 25°C. increase in reaction temperature.

The relative rate of desirable and undesirable competitive reactions is extremely important in setting the reactor design and operating conditions. The vapor residence time must be such as to allow a high degree of conversion of the recycled high-boiling tars without serious destruction of the valuable 180-230°C. phenolics. Methanation of carbon monoxide, and other reactions which use up hydrogen non-productively should be minimized, while conditions favoring supplemental production of hydrogen by the shift reaction are desirable. These problems of setting optimum conditions were among those studied on the pilot-plant scale and it is believed that reasonable solutions are found.

It is of interest to follow the oxygen balance from coal substance to products. Under optimum mild hydrogenation conditions the following is typical.

<u>Oxygen in Product Named, lbs/100 lbs MAF Coal</u>	
180-230°C. Phenolics	0.7
+230°C. Tar	1.1
Char	2.0
Gas (Carbon Oxides)	3.2
Water	<u>14.0</u>
Total in Coal Feed	21.0

Clearly, most of the coal oxygen is converted to water and the percentage convertible to useful phenolics is small. Direct determination of OH in subbituminous and lignite coals shows as much as 8% phenolic oxygen, but evidently most of this is unstable to pyrolysis or hydrogenation. Nevertheless, the 0.7 pound of oxygen in the 180-230°C. phenolics represents about 90 pounds of phenolics per ton of MAF coal with perhaps another 50 or 60 pounds obtainable by recycle of the +230°C. tars. Our data indicate a total hydrogen consumption of less than two pounds per hundred pounds of MAF coal to achieve this yield.

Economics

The economics of any coal conversion process is so strongly tied to the cost of mining, transportation, cooling water, etc., and to the marketing problems that it is futile to generalize. The authors believe that the dry hydrogenation process worked out by Union Carbide will, at corresponding scales and under particular, realistically possible, raw material and marketing conditions, look economically good in comparison with any of the known variations of the conversion reactions -- to chemicals or fuels -- discussed in the introduction.

LITERATURE CITED

- (1) Donath and Rotter, Pressure Hydrogenation of Dry Coal, Tech. Oil Mission Translation Number T-323 (1947).
- (2) Report of Investigations 4456, Part I, Oil from Coal - Synthetic Liquid Fuels - 1948 Annual Report of the Secretary of the Interior (1949).
- (3) Landers, W. S., Parry, V. F., Gomez, M., Wagner, E.O., Goodman, J. B., and Nelson, C. R., Carbonizing Properties of Wyoming Coals, U. S. Bureau of Mines, Report of Investigations 5731, (1961).

HYDROCARBONIZATION UNIT

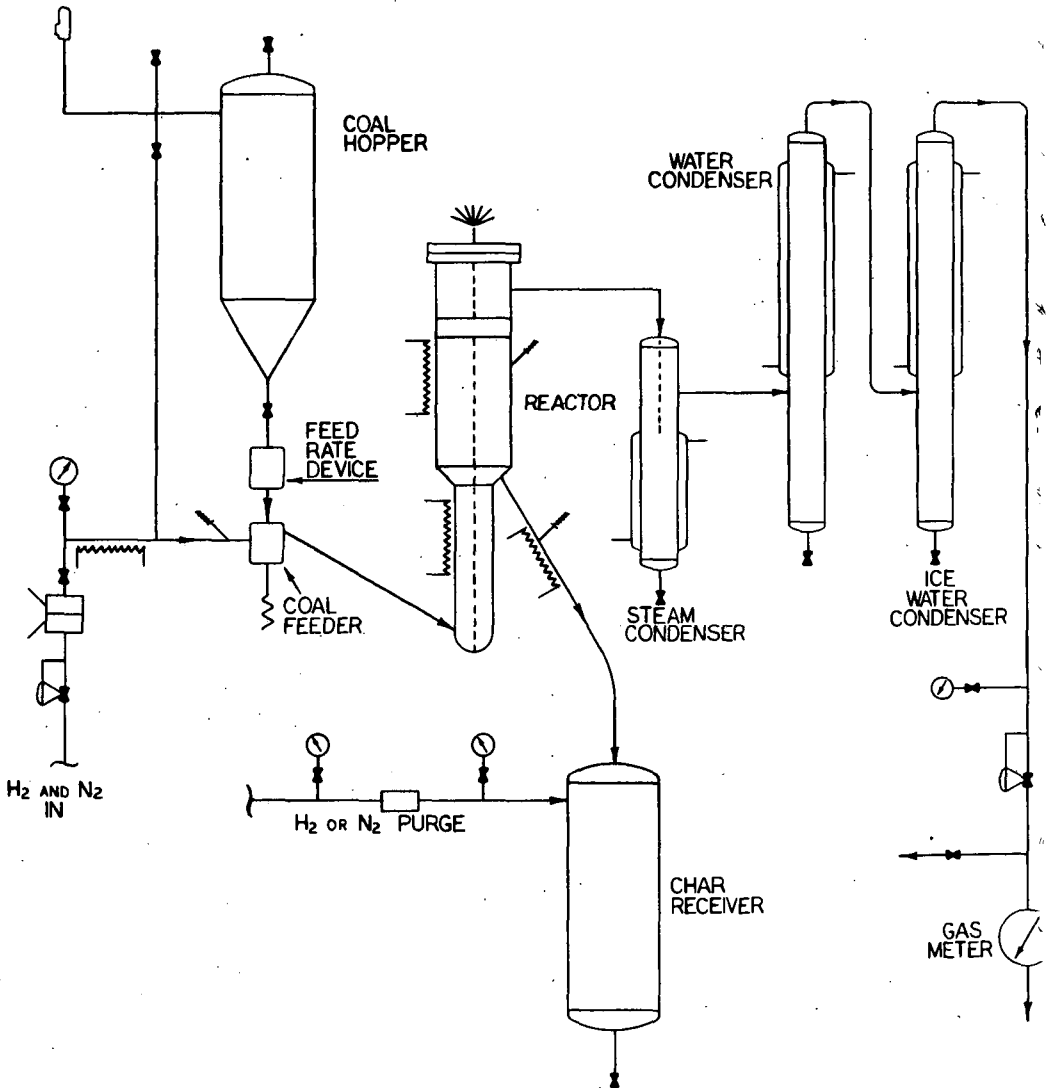


FIG. 1

HYDROGEN CONSUMED AS A FUNCTION OF TEMPERATURE

COAL RESIDENCE TIME ABOUT NINE MINUTES
HYDROGEN PARTIAL PRESSURE ABOUT 950 psi

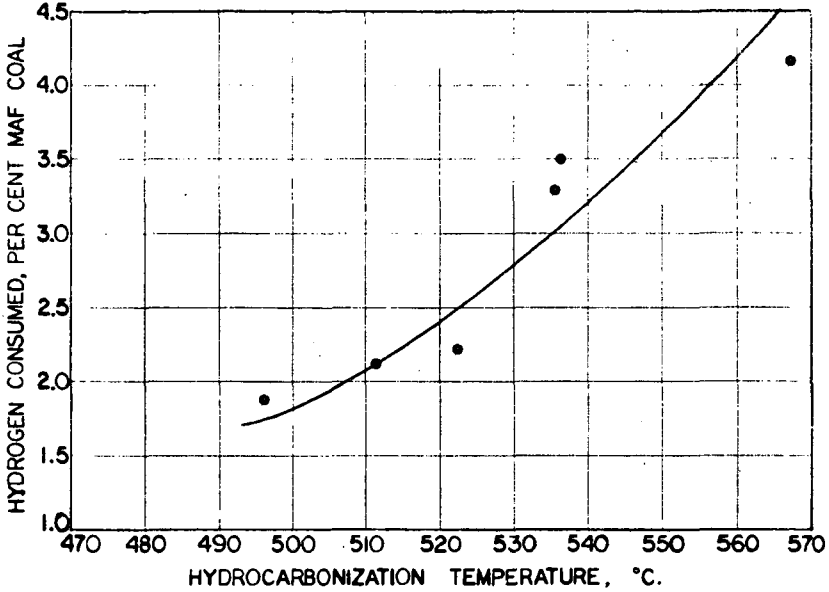


FIG. 2

PRODUCT YIELDS AS A FUNCTION OF TEMPERATURE

COAL RESIDENCE TIME ABOUT NINE MINUTES
HYDROGEN PARTIAL PRESSURE ABOUT 950 psi

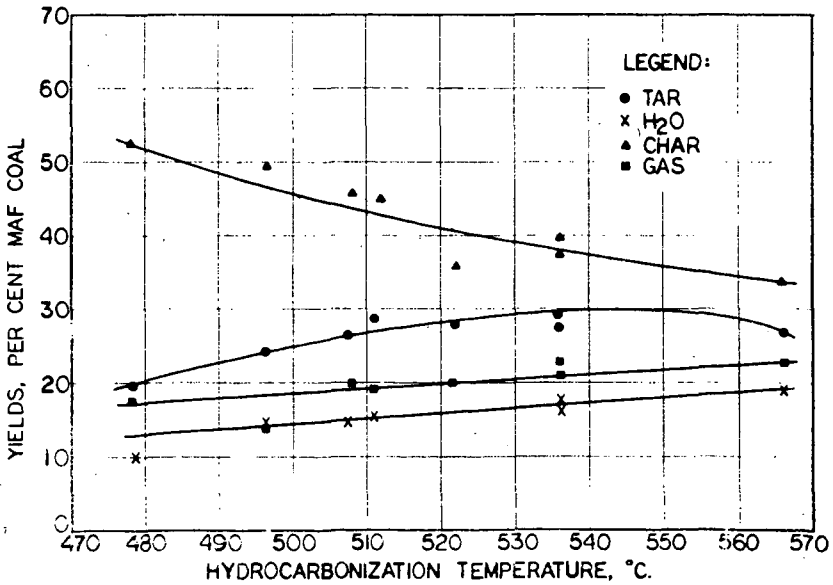


FIG. 3

POUNDS OF TAR PER POUND OF HYDROGEN AS A FUNCTION OF TEMPERATURE

COAL RESIDENCE TIME ABOUT NINE MINUTES
HYDROGEN PARTIAL PRESSURE ABOUT 950 PSI

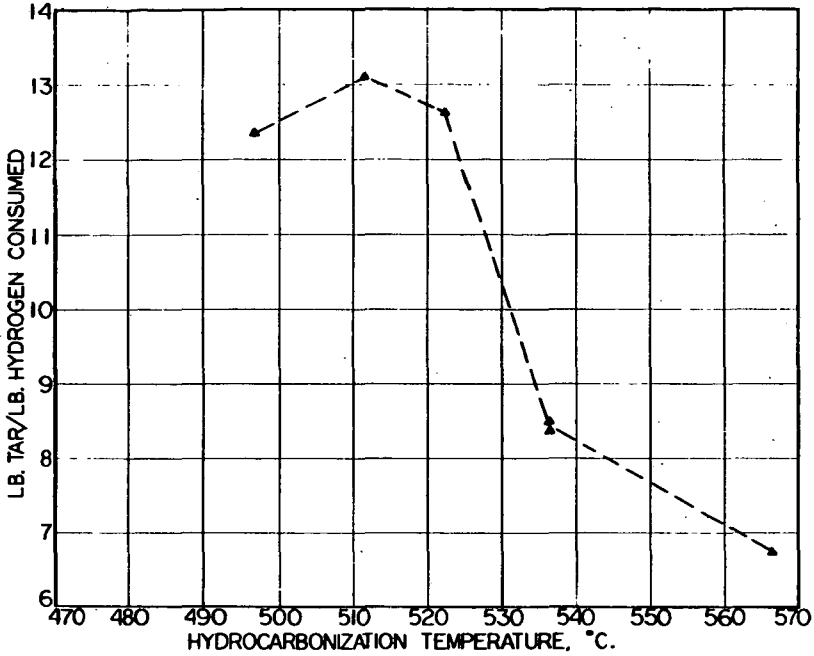


FIG. 4

HYDROGEN CONSUMED AS A FUNCTION OF HYDROGEN PARTIAL PRESSURE

COAL RESIDENCE TIME ABOUT NINE MINUTES
TEMPERATURE ABOUT 540 °C

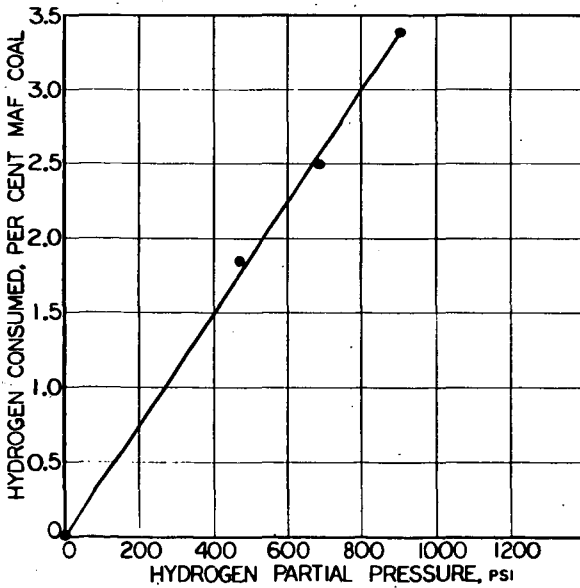


FIG. 5

PRODUCT YIELDS AS A FUNCTION OF HYDROGEN PARTIAL PRESSURE

COAL RESIDENCE TIME ABOUT NINE MINUTES
TEMPERATURE ABOUT 540 °C

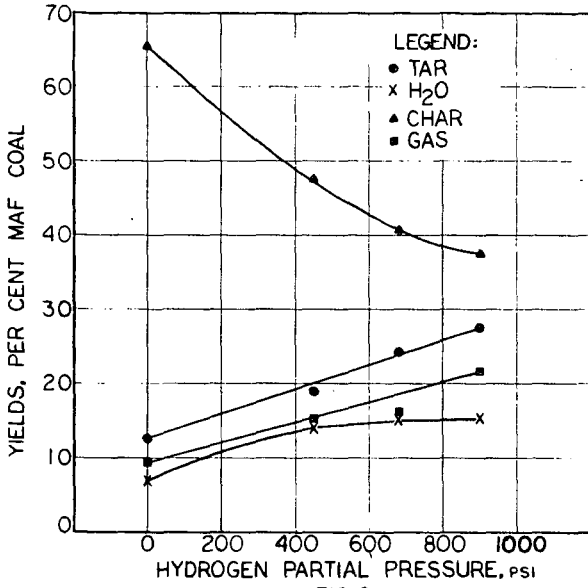


FIG. 6

HYDROGEN CONSUMED AS A FUNCTION OF COAL RESIDENCE TIME AND TEMPERATURE

HYDROGEN PARTIAL PRESSURE ABOUT 950 PSI

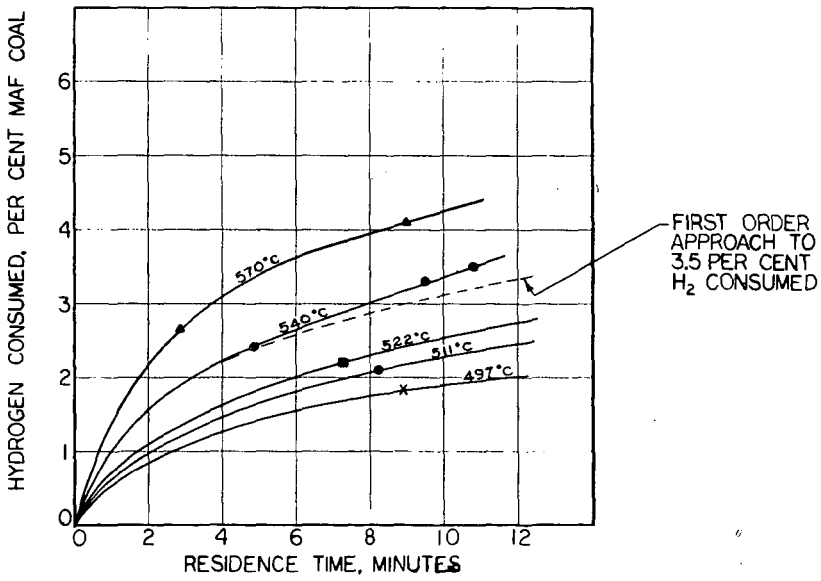
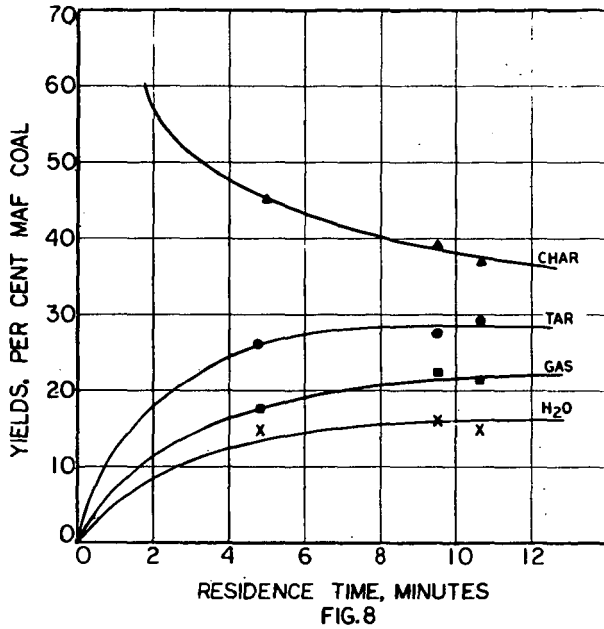


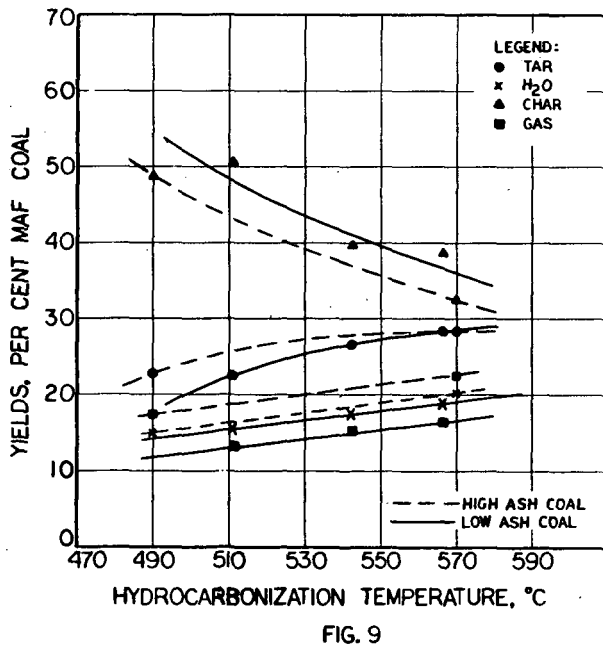
FIG. 7

PRODUCT YIELDS AS A FUNCTION OF COAL RESIDENCE TIME AT 540 °C
HYDROGEN PARTIAL PRESSURE ABOUT 950 PSI



PRODUCT YIELDS OF LOW ASH VERSUS HIGH ASH COAL

COAL RESIDENCE TIME ABOUT NINE MINUTES
HYDROGEN PARTIAL PRESSURE ABOUT 950 PSI



THERMAL CRACKING OF SHALE GAS OIL UNDER A HYDROGEN ATMOSPHERE

G. E. Lessley and H. F. Silver

Department of Chemical Engineering
University of Wyoming, Laramie, Wyoming 82070

H. B. Jensen

U.S. Department of the Interior, Bureau of Mines
Laramie Petroleum Research Center, Laramie, Wyoming 82070

INTRODUCTION

Reserves of shale oil in the Green River Formation of Colorado, Utah, and Wyoming in deposits 10 or more feet thick that average 10 or more gallons of shale oil per ton are estimated to be in excess of two trillion barrels.¹ This oil represents a vast, untapped source of energy. Although there is no commercial shale-oil industry in the United States today, it is generally felt that shale oil will be a valuable supplement to petroleum reserves in the future. Shale oil is produced from the solid organic matter occurring in oil shale by heating the shale to about 900° F or higher in a retort.² Crude shale oils prepared from the Green River shale by many retorting methods are heavy, hydrogen-deficient oils and contain very little material boiling in a gasoline range.³ Therefore, some sort of cracking process is necessary to convert the higher boiling portions of crude shale oil to gasoline.

An investigation of the thermal cracking of shale gas oil under a hydrogen atmosphere has been undertaken in a batch reactor as part of a program designed to study the effect of reaction variables on high pressure hydrogenation of shale oil. Kinetic parameters obtained in this investigation suggest that the initial phases of the cracking reaction involve the more reactive, straight-chain structures, whereas later stages involve aromatic structures. There also appears to be a change in the reaction mechanism as the reaction proceeds.

Other reaction parameters--including hydrogen consumption, hydrocarbon gas and naphtha yields, and nitrogen and sulfur concentration in the unconverted gas oil--have been correlated as functions of cracking conversion.

EQUIPMENT AND EXPERIMENTAL PROCEDURES

The experimental thermal cracking studies of shale gas oil have been carried out in a 2.7-liter Aminco rocking reactor. Details of the experimental equipment and procedure have been reported.⁴

The first step in the experimental procedure was to add 500 grams of shale gas oil to the reactor. Hydrogen was added to the reactor until all air had been flushed from the reactor and the pressure in the system reached 1,000 psi. The reactor was then heated by an electric heating mantle to the desired run temperature and held at this temperature for a predetermined period. At the end of this period the reactor was allowed to cool to room temperature.

The gases produced during a run were analyzed using an Orsat apparatus and a Beckman GC-2A gas chromatograph, and their molecular weights were measured using glass density balloons. The

liquid product was removed from the reactor and water washed to remove low-boiling nitrogen, oxygen, and sulfur compounds. The oil was diluted with toluene and distilled in a Dean-Stark apparatus using the procedure outlined in ASTM D 95-62 in order to eliminate any water remaining in the sample after the water wash.⁵ The toluene added to the liquid shale-oil product during the Dean-Stark distillation and the naphtha boiling below 410° F were removed from the mixture by atmospheric distillation. That portion of the shale-oil product that boiled below 555° F was then separated from the unconverted shale gas oil by a vacuum distillation. The nitrogen concentration in the unconverted gas oil was determined using a Kjeldahl nitrogen analysis procedure, and the sulfur concentration was determined using the procedure outlined in ASTM D 129-58.^{5,6}

RAW MATERIALS

The shale gas oils used in this study were derived from a Green River (Colorado) shale in a gas combustion retort at Rifle, Colorado. Properties of the shale gas oils are presented in table 1.

TABLE 1. - Properties of shale gas oil feed stocks

Property	Feed stock No.	
	1	2
Gravity, °API	23.0	23.0
Nitrogen, wt pct	1.78	1.83
Sulfur, wt pct	.62	.70
Distillation, I.B.P., °F	420	405
10 vol pct, °F	567	580
50 vol pct, °F	700	720
95 vol pct, °F ^a	800	800
Boiling above 555° F, wt pct	91.7	95.2

^a Estimated from simulated distillation by GLC.

EXPERIMENTAL RESULTS AND CALCULATIONS

The extent to which shale gas oil was thermally cracked under a hydrogen atmosphere has been correlated with time and temperature using a parameter called cracking conversion, X_c . Cracking conversion is defined by the relationship:

$$X_c = \frac{W_F - W_P}{W_F} \quad (1)$$

where W_F = grams of shale gas oil that boil above 555° F in the gas oil charged to the reactor, and W_P = grams of shale gas oil that boil above 555° F in the reactor product.

If it is assumed that the cracking reaction is first order with respect to the unconverted gas oil ($1 - X_c$), the integrated rate expression takes the form:

$$\ln(1 - X_c) = -kt, \quad (2)$$

where $(1 - X_c)$ = the unreacted gas oil boiling above 555° F,
 k = reaction rate coefficient, and
 t = reaction time.

The experimental data obtained in this study have been plotted in the form suggested by equation 2 in figure 1 for reaction temperatures from 600° to 825° F. The times shown in figure 1 are uncorrected for heat-up and cool-down times. The curvature shown in these plots was expected because others have reported this same effect in studies of the cracking of petroleum gas oils. Weekman,⁷ for example, suggests that a similar curvature, which he obtained in a plot of catalytic-cracking results, may be due to the multiplicity of reactant molecular types in the original petroleum charge as well as to catalyst deactivation.

The variation of the reaction rate coefficient (k) with temperature (T) can be described by the Arrhenius equation:

$$k = A \exp(-E_a/Rt). \quad (3)$$

However, this equation does not account for the observed effect of cracking conversion on the reaction rate coefficients. In order to introduce this effect, it has been necessary to compare reaction rate coefficients at the same cracking conversion level but at different reaction temperatures. The results of these comparisons at selected conversion levels have been used to calculate Arrhenius activation energies (E_a) and Arrhenius frequency factors (A) as functions of shale-gas-oil cracking conversion. The relationship that provided the best, least-squares fit between the experimental activation energy and conversion was

$$E_a(\text{kcal/mole}) = 29.4 + 135.5 X_c. \quad (4)$$

Thus the Arrhenius activation energy increases linearly from 29.4 kcal/mole at the onset of cracking to 124.3 kcal/mole at a conversion of 0.70 for X_c , a fourfold increase. This increase in activation energy could indicate that the cracking reaction changes from one involving straight-chain structures to one involving aromatic structures as conversion increases.

The relationship that provided the best fit between the experimental frequency factor and conversion was

$$A(\text{min}^{-1}) = \exp(16.71 + 91.45 X_c). \quad (5)$$

Figure 2 shows the dependency of the 750° F reaction rate coefficient, calculated using equations 3, 4, and 5 upon conversion values. Thus we see a decrease of three orders of magnitude in the coefficient as conversion increases from zero to 0.70. The calculated values at these two conversion levels are $4.9 \times 10^{-3} \text{ min}^{-1}$ at zero conversion and $4.5 \times 10^{-6} \text{ min}^{-1}$ at a conversion of 0.70.

The agreement between the conversions predicted by using the Arrhenius equation, modified to account for the effect of conversion, and the experimentally measured conversion is shown in table 2. The corrected times listed in this table take into account the fact that the cracking reaction proceeds to a certain extent during the time that the reactor is being heated to and cooled from the nominal reaction temperature.

Although the literature on thermal cracking of petroleum does not report data relating the dependency of E_a and of A upon conversion, Nelson⁸ has reported their values at conversions between 0.20 and 0.25 for a petroleum gas oil. He reported an activation energy of about 55 kcal/mole and the value for shale gas oil as calculated by equation 4 is 56.5 kcal/mole. Table 3 compares the specific rate coefficients as reported by Nelson for a petroleum gas oil with those calculated using equations 3, 4, and 5 for shale gas oil. These results suggest that at a conversion of 0.20 shale gas oil may be somewhat more refractory than petroleum gas oil. However, at zero conversion, distillation data suggest that petroleum gas oil is more refractory than shale gas oil. For

TABLE 2. - Comparison of experimental and calculated conversions

Run temperature, °F	Corrected time, ^a hours	Conversion, X _c	
		Experimental	Calculated
600	0.90	0.031	0.011
	3.32	.011	.031
	6.29	.037	.045
	8.35	.029	.053
700	.42	.004	.036
	.81	.009	.059
	3.32	.089	.126
	6.37	.131	.164
	8.29	.123	.179
750	.38	.032	.074
	.92	.210	.128
	3.32	.264	.226
	6.34	.308	.279
	8.29	.315	.302
	8.51	.369	.305
825	.1.20	.508	.394
	3.39	.642	.563
	6.41	.707	.665
	8.41	.699	.706
	8.55	.706	.709

^a Corrected for the amount of reaction taking place during the time the reactor is being heated to and cooled from nominal reaction temperature.

TABLE 3. - Comparison of reaction rate coefficients at a conversion of 0.20 for shale gas oil and petroleum gas oil

Temperature, °F	Reaction rate coefficient, min ⁻¹	
	Shale gas oil	Petroleum gas oil ^a
700	1.1 × 10 ⁻⁴	1.8 × 10 ⁻⁴
750	6.8 × 10 ⁻⁴	1.0 × 10 ⁻³
825	8.0 × 10 ⁻³	1.5 × 10 ⁻²

^a See reference 8.

example, in the Bureau of Mines routine distillation⁹ used in crude petroleum analysis, the atmospheric distillation is carried to a temperature of 527° F; whereas, to avoid cracking in the analysis of crude shale oil, the atmospheric distillation is carried to a temperature of only 392° F. One is led to conclude, then, that shale oil contains materials that crack very readily as well as materials that crack with extreme difficulty.

The exponential relationship best relating conversion to frequency factor (equation 5) is suggestive of the exponential relationship between the theoretical frequency factor from the theory of the activated complex and the entropy of activation.¹⁰ Because of this similarity, entropies of activation were calculated for the shale-gas-oil cracking reaction at 825° F. These entropies of activation ranged from a -32 e.u. at low conversion to +89 e.u. at high conversion. This range in entropies of activation may be compared with values obtained by Wiser,¹¹ who observed values ranging from -63 e.u. at low conversion to -12 e.u. at high conversion during coal pyrolysis. Entropy of activation values of about -30 e.u. have been reported for polymerization reactions.¹² Condensation reactions might also be taking place. Thus the assumed polymerization and condensation products of the early part of the reaction would add to the multiplicity of the aromatic structures in the original charge oil. These proposed, additional aromatics would have their influence in the latter stages of the cracking reaction.

Other reaction parameters obtained in this study have been correlated as functions of cracking conversion. The amount of hydrogen consumed in the reaction is correlated as a function of cracking conversion in figure 3. Figure 4 shows the weight percent of the charge that was converted to gasoline and to hydrocarbon gases. The results in figure 3 suggest that there was a net production of hydrogen below a conversion of about 0.2, and that only above this conversion was the rate of consumption of hydrogen greater than the rate of production. This consumption of hydrogen at higher conversion levels undoubtedly resulted from the hydrogenation of low-molecular-weight fragments to form the quantities of hydrocarbon gas and gasoline shown in figure 4. For example, at a conversion of 0.70, the combined quantities of hydrocarbon gases and gasoline amount to 70 weight-percent of the original oil.

The weight-percents of nitrogen and sulfur in the unreacted gas oils are shown in figures 5 and 6 as functions of conversion. Because the nitrogen in shale gas oil is primarily in heterocyclic aromatic structures,¹³ the increase in nitrogen in the unreacted gas oil can be explained by postulating that the nitrogen heterocyclics do not react to form lower boiling materials as rapidly as does the nonaromatic portion of the gas oil. This lack of any thermal denitrification of shale gas oil under hydrogen pressure was also observed by Koros.¹⁴

On the other hand it appears from the results shown in figure 6 that up to conversion levels of 0.30, the sulfur-containing molecules are more easily cracked to lower boiling compounds than are the nonsulfur compounds. It also appears that at conversion levels greater than 0.30, the sulfur-containing compounds crack at about the same rate as does the bulk of the remaining shale gas oil.

SUMMARY

The results obtained in this work show that the rate at which shale gas oil cracks at constant temperature under hydrogen pressure decreases as the extent of cracking conversion increases. The values for the reaction rate coefficient for the 750° F cracking reaction decrease from $4.9 \times 10^{-3} \text{ min}^{-1}$ at zero conversion to $4.5 \times 10^{-6} \text{ min}^{-1}$ at a conversion of 0.70. Calculated Arrhenius activation energies range from 29.4 kcal/mole at the onset of conversion to 124.3 kcal/mole at a conversion of 0.70. These variations could indicate a change in reacting species as the reaction proceeds. For example, initial phases of the shale-gas-oil cracking reaction could involve

long, straight-chain structures, whereas later phases of the reaction involve aromatic structures. Entropies of activation, calculated for the reaction at 825° F, ranged from -32 e.u. at low conversions to +89 e.u. at high conversions. The results could indicate a shift in reaction mechanism from polymerization reactions at low conversions to decomposition reactions at high conversions. Hydrogen-consumption data, product-yield data, and the rates of denitrification and desulfurization also suggest changes in the reacting species as well as in the reaction mechanism.

ACKNOWLEDGMENTS

This work was undertaken as partial fulfillment of the requirements for the Master of Science degree in Chemical Engineering at the University of Wyoming by G. E. Lessley. Mr. L. C. Huang assisted in the preparation of this paper. The work was carried out under Research Grant PET-2 from the U.S. Department of the Interior, Bureau of Mines.

Reference to a company or product name does not imply approval or recommendation of the product by the U.S. Bureau of Mines to the exclusion of others that may be suitable.

LITERATURE CITED

1. Dinneen, G. U., K. E. Stanfield, G. L. Cook, and H. W. Sohns. Developments in Oil Shale Technology. Chem. Eng. Prog. Symp. Ser., v. 64, No. 85, 15 (1968).
2. Dinneen, G. U. Shale Oil--What Is It? Pet. Ref., v. 33, No. 2, 113 (1954).
3. Frost, C. M., H. C. Carpenter, C. G. Hopkins, Jr., S. S. Tihen, and P. L. Cottingham. Hydrogenating Shale Oil and Catalytic Cracking of Hydrogenated Stocks. BuMines Rept. of Inv. 5574 (1960), 17 pp.
4. Lessley, G. E. Kinetic Study of the Non-Catalytic Hydrogenation of Shale Gas Oil. Master's Thesis, University of Wyoming, Laramie (1968). Available through interlibrary loan.
5. American Society for Testing and Materials. ASTM Standards on Petroleum Products and Lubricants, Philadelphia (1959).
6. Lake, G. R., P. McCutchan, R. A. Van Meter, and J. C. Neel. Effects of Digestion Temperature on Kjeldahl Analysis. Anal. Chem., v. 23, No. 11, 1634 (1951).
7. Weekman, V. W. A Model of Catalytic Cracking Conversion in Fixed, Moving, and Fluid-Bed Reactors. Ind. Eng. Chem. Proc. Des. and Dev., v. 7, No. 1, 90 (1960).
8. Nelson, W. L. Petroleum Refinery Engineering. McGraw-Hill, New York (1958).
9. Stevens, R. F., G. U. Dinneen, and J. S. Ball. Analysis of Crude Shale Oil. BuMines Rept. of Inv. 4898 (1952), 20 pp.
10. Glasstone, S., K. J. Laidler, and H. Eyring. The Theory of Rate Processes. McGraw-Hill, New York (1941).
11. Wisler, W. H., G. R. Hill, and N. J. Kertmaus. Kinetic Study of the Pyrolysis of High Volatile Bituminous Coke. Ind. Eng. Chem. Proc. Des. and Dev., v. 6, No. 1, 133 (1967).

12. Frost, A. A., and R. G. Parson. Kinetics and Mechanism. Wiley, New York, 2nd ed. (1961).
13. Dinneen, G. U., G. L. Cook, and H. B. Jensen. Estimation of Types of Nitrogen Compounds in Shale-Oil Gas Oil. Anal. Chem., v. 30, 2026 (1958).
14. Koros, R. M., S. Bank, J. E. Hofman, and M. I. Kay. Hydrodenitrogenation of Shale Oil. Am. Chem. Soc., Div. of Pet. Chem. Preprints, v. 12, No. 4, B-165 (1967).

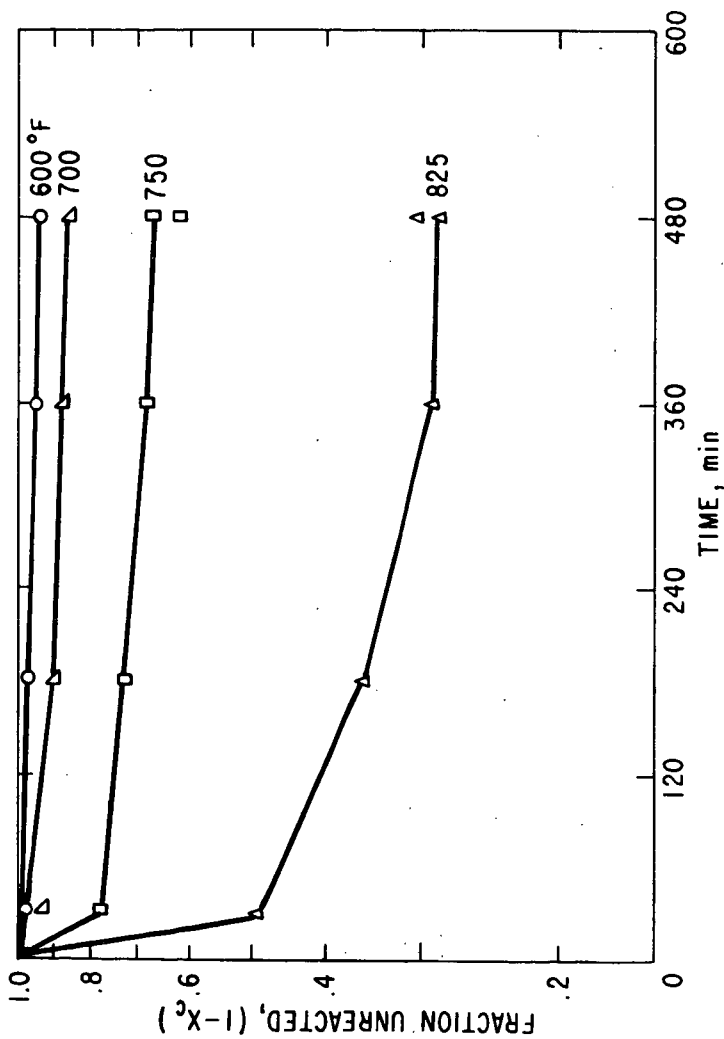


FIGURE 1.-First-Order Plot for Shale Gas Oil Cracking.

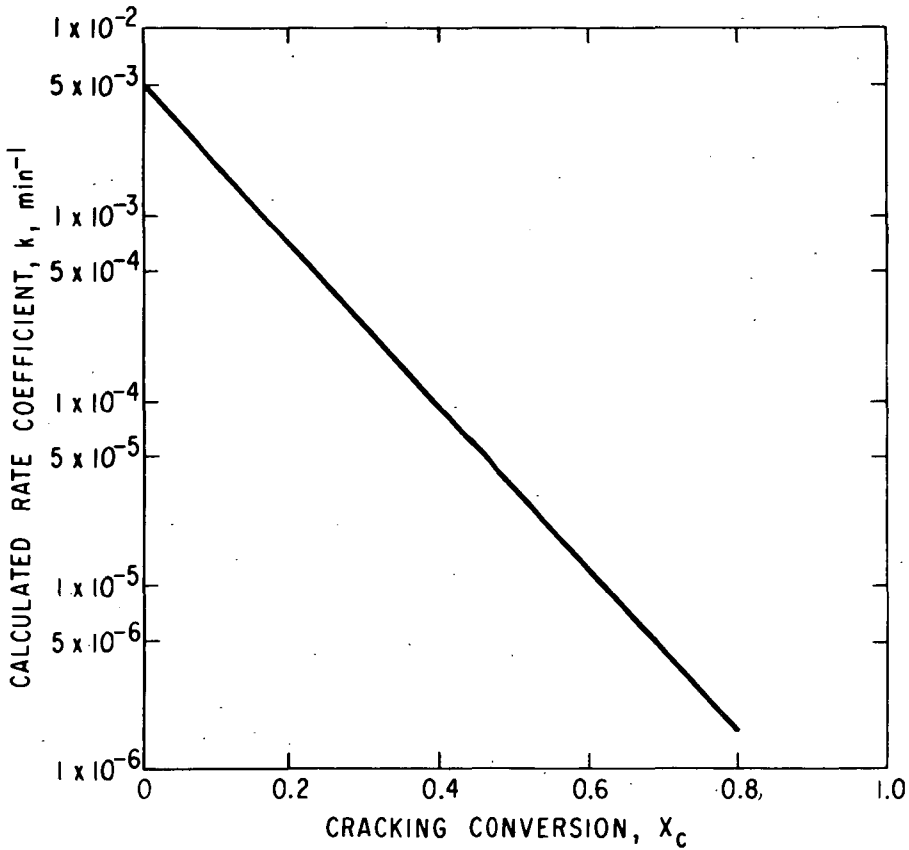


FIGURE 2.—Effect of Conversion on Shale Gas Oil Cracking Reaction Rate Coefficients at 750° F Cracking Temperature.

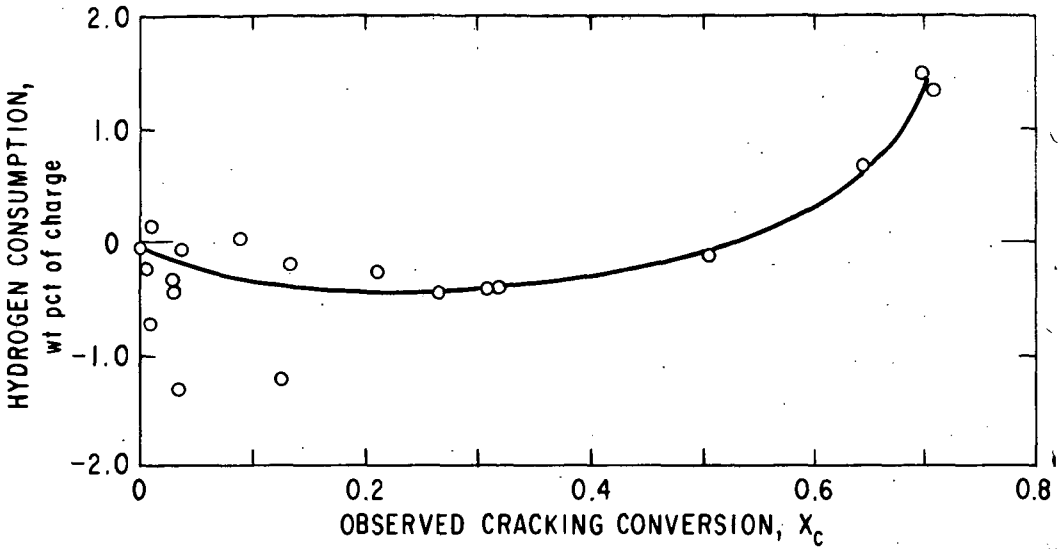


FIGURE 3.-Hydrogen Consumption.

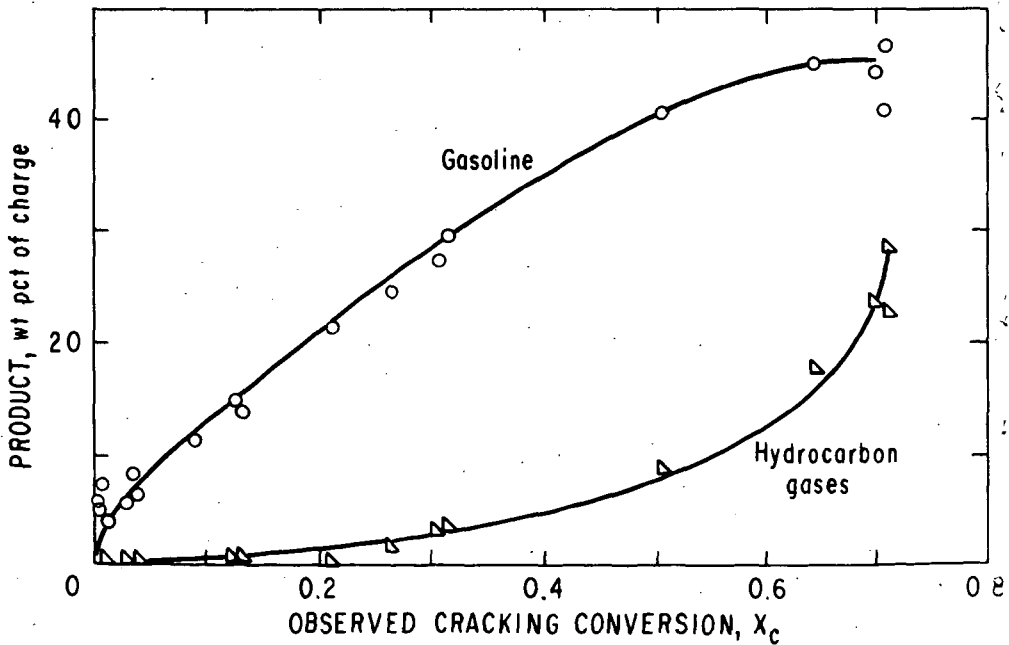


FIGURE 4.-Hydrocarbon Gases and Gasoline Production.

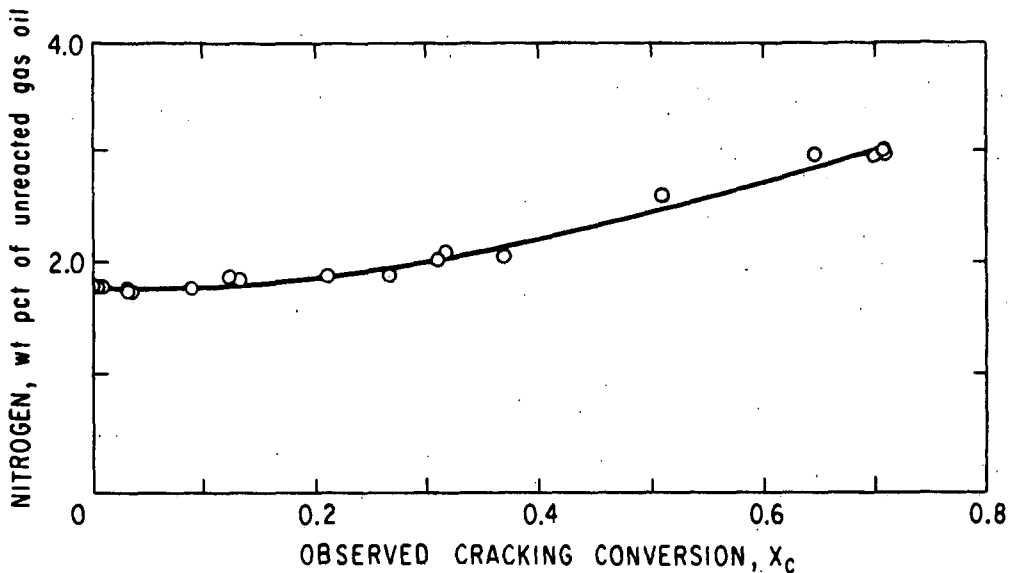


FIGURE 5.—Nitrogen Concentration in Unreacted Shale Gas Oil.

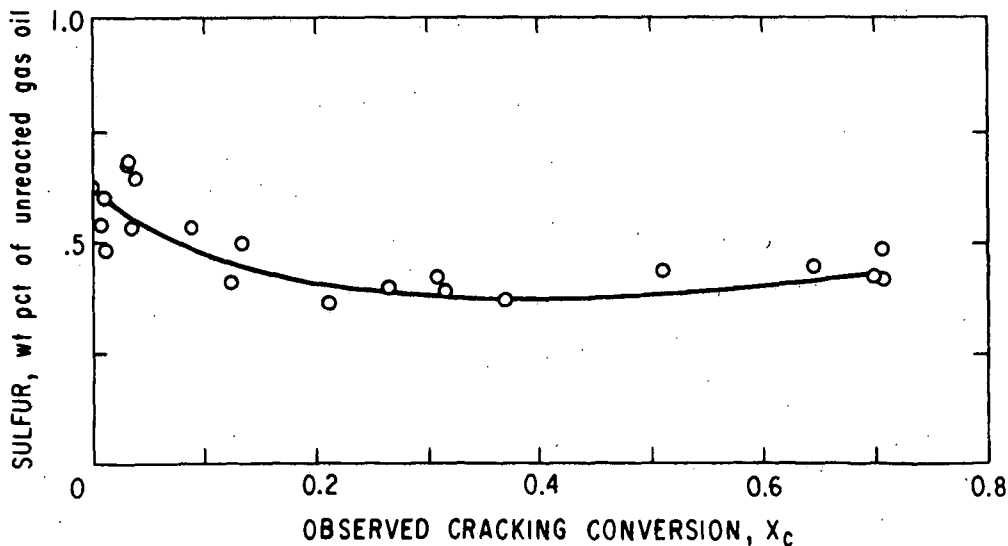


FIGURE 6.—Sulfur Concentration in Unreacted Shale Gas Oil.

METHANATION FOR COAL HYDROGASIFICATION

A. L. Lee, H. L. Feldkirchner and D. G. Tajbl*

Institute of Gas Technology
Chicago, Illinois 60616

INTRODUCTION

The goals of this study are as follows:

- Test commercial methanation catalysts to determine the most suitable one for the methanation step of the IGT HYGAS Process for producing pipeline gas from coal.
- Perform a life study on the chosen catalyst.
- Obtain pilot plant design data for anticipated gas compositions from the hydrogasification reactor.
- Develop a kinetic equation for the methanation catalyst selected under actual operating conditions.

Dirksen and Linden⁴ did extensive work on synthesis-gas methanation and gave detailed discussions of their work. Tajbl et al.¹⁰ presented the results of the commercial catalyst selection for the HYGAS Process and described the experimental apparatus. Earlier we obtained a rate expression⁶ for the design of the pilot plant reactor and developed a practical reactor operating scheme.

This paper presents the results of the catalyst life study, a reactor stability study, and a kinetic study. In addition to the references cited in the text, we have also presented a literature survey. For a more complete review of literature prior to 1963, refer to the bulletin by Dirksen and Linden.⁴

KINETIC STUDY

The apparatus used for this study was described in detail previously.¹¹ A schematic diagram of the modified system is presented in Figure 1. The modifications are the benzene saturator, high-pressure sampling, and a better gas chromatograph. The purpose of a benzene saturator is to study the effect of traces of benzene in the feed gas on the rate of methanation and the long-term activity of the catalyst. Benzene is produced in the HYGAS Process for use in the slurry feeding of coal to the gasifier. Thus, traces of benzene will be present in the methanator feed stream.

To obtain pilot plant design data, three feed gases covering the range of anticipated methanation feed compositions were used (Table I). The results were presented elsewhere.¹¹ To summarize these findings, we found that a rate expression⁶ (Equation 1) represents the data:

$$r = k p_{\text{CO}}^{0.62} \quad (1)$$

* Now with Mobil Oil Corporation, Paulsboro, New Jersey.

Table 1. COMPOSITIONS OF FEED GASES

Feed	High CO	Intermediate CO	Low CO
	mole %		
Carbon Monoxide	10.0	7.0	2.4
Carbon Dioxide	2.1	2.1	2.0
Hydrogen	34.5	26.1	13.5
Methane	53.4	64.8	82.1
Total	100.0	100.0	100.0

Using the same data, Wen et al.¹³ found a rate equation:

$$r = k p_{\text{CO}}^{0.7} p_{\text{H}_2}^{0.3} \quad (2)$$

Both equations of the form of 1 and 2 can fit the data reasonably well, as Weller¹¹ has shown.

To improve the above rate expressions for the IGT methanation process, the reaction-rate study was extended, mainly in tests on 1/4-inch catalyst pellets that will be used in our plant. Feed gases containing only H₂ and CO were used to determine the CO order; feed gases containing H₂, CO, and He were used to determine the H₂ order and the effect of an inert on the methanation rate; feed gases containing H₂, CO, and CH₄ were used to determine the effect of a large CH₄ concentration in the feed on the rate of methanation and hence on the CH₄ order; feed gases containing H₂, CO, CH₄, and C₆H₆ were used to determine the effect of benzene; and feed gases of H₂, CO, CH₄, and C₆H₆ with traces of mercaptan (0.3 ppm) and thiophene (0.8 ppm) were used to determine the effect of organic sulfur on the activity of the catalyst. These data are presented in Table 2.

We found that the H₂ order is about 0.5, with and without CH₄ in the feed gas, as illustrated in Figure 2; the effect of CH₄ is noticeable only at near-equilibrium conditions (Figure 2); the order of CO is about 1 (Figure 3); the effect of He is nil; the effect of C₆H₆ (up to 1% in feed) is nil; and the effect of organic sulfur in the gas on the rate of the methanation reaction is nil at the low concentration levels studied (mercaptans and thiophene up to 1.1 ppm).

The rate expression:

$$r = k p_{\text{CO}} p_{\text{H}_2}^{0.5} \quad (3)$$

correlates most of the experimental data except when excess H₂ and/or CH₄ are present. To cover the entire range of gas compositions, Equation 3 was modified to the following form:

$$r = \frac{k p_{\text{CO}} p_{\text{H}_2}^{0.5}}{1 + K_2 p_{\text{H}_2} + K_3 p_{\text{CH}_4}} \quad (4)$$

The results are presented in Table 2 and Figure 4.

There are numerous rate expressions proposed for methanation in the literature. Some of those that are related to this study are presented in Table 3. Most of the work in the literature was done with feed gases containing H₂ and CO or H₂, CO, and CO₂ only and at relatively low pressures. Table 3 is presented to give a quick over-all view of the various methanation rate equations proposed.

Table 3. RATE EQUATIONS FOR METHANATION PROPOSED BY VARIOUS INVESTIGATORS

Author(s)	Rate Equation	Temperature, Pressure	Remarks
Nicola et al. ⁸	$r = k \frac{P_{CO}^{0.7} P_{H_2}^{0.3}}{P_{CO}}$	250-300°C, 0.1-1.0 atm	This work is concentrated on CO ₂ hydrogenation on a nickel catalyst. Very little work is done on CO methanation.
Akers and White ¹	$r = \frac{K_1 P_{CO} P_{H_2}}{K_2 + P_{CO} + P_{CO_2} + P_{CH_4}}$	300-350°C, 1 atm	A reduced nickel catalyst was used. The water-gas shift reaction was also studied and a rate equation for the formation of CO ₂ was discussed.
Purley et al. ⁹	$r = \frac{1.1 P_{CO} P_{H_2}^{0.5}}{1 + 1.5 P_{H_2}}$	500-700°F, 14.7-400 psia	A nickel catalyst was used to study the initial rate of the CO-H ₂ reaction. This equation was derived by using sulfur-free mixtures of CO and H ₂ containing less than 30 mole % CO.
McKee ⁷	$r = k \frac{P_{CO}^{0.5} P_{H_2}^{0.5}}{P_{CO}}$	220°C, 21.4 atm	Platinum group metals were used as catalysts for the reaction: ZCO + 2H ₂ ⇌ CH ₄ + CO ₂ .
Barkley et al. ²	$r = \frac{k P_{CO} P_{H_2} - \frac{P_{CO} P_{H_2} O}{K}}{1 + K_1 P_{CO} + K_2 P_{CO_2}}$	1000°F	A study of the gas-phase reaction CO ₂ + H ₂ ⇌ CO + H ₂ O over an iron-copper catalyst. A mechanism for this reaction was postulated.
Bunder and White ³	$r = \frac{C_1 \left(\frac{P_{CO_2} P_{H_2} - P_{CO} P_{H_2} O}{K_1 P_{H_2}} \right)}{P_{H_2}^{0.5} + C_2 P_{CO} + C_3}$	500-750°F, 1 atm	A reduced nickel catalyst was used.
and	$r = \frac{C_1 \left(\frac{P_{CO_2} P_{H_2} - \frac{P_{CO} P_{H_2} O}{K_1}}{P_{H_2}^{0.5} + C_2 P_{CO_2} + C_3} \right)}{P_{H_2}^{0.5} + C_2 P_{CO_2} + C_3}$		
Weller ¹²	$r = k P_{CO} P_{H_2}^{0.5}$		
Schoubye ¹⁰	$r = \frac{Z_1 \exp \left[-\frac{E_1}{RT} \right] P_{H_2}^n}{1 + Z_2 \exp \left[\frac{16650}{RT} \right] \left(\frac{P_{CO}}{P_{H_2}} \right)^{0.75}}$	200-300°C, 2-15 atm	Used Akers and White's data ¹ and arrived at this simpler rate expression which correlates rate data with about the same accuracy. Excellent discussion on the analysis of data. Nickel catalysts were used. Order of CO was found to be from 0 to -0.5.
Wan et al. ¹¹	$r = k \frac{P_{CO}^{0.5} P_{H_2}^{0.5}}{P_{CO}}$	550-850°F, 14.7-1000 psia	IGT data were used in this analysis.
Tajiri ¹¹	$r = 7.85 \times 10^5 \exp \left[-\frac{17200}{RT} \right] \times CO$	550-600°F, 69 atm	Initial analysis of effluent gas mixture from hydrosulfur.
Lee ⁵	$r = k P_{CO} P_{H_2}^{0.5}$	550-850°F, 14.7-1000 psia	Analysis of feed gas mixtures of H ₂ -CO; H ₂ -CO-H ₂ ; H ₂ -CO-CH ₄ ; and H ₂ -CO-CH ₄ -CO ₂ -C ₂ H ₆ .
This study	$r = \frac{k_1 P_{CO} P_{H_2}^{0.5}}{1 + k_2 P_{H_2} + k_3 P_{CH_4}}$	550-850°F, 14.7-1000 psia	

CATALYST LIFE TESTS

When this program was begun, no successful work had been reported on fixed-bed methanation of high carbon monoxide, high-methane-content gases with typical commercial nickel catalysts. Thermodynamic calculations indicated that the gases that would have to be methanated would be capable of depositing carbon in the range of temperatures and pressures expected. Further, in packed-bed reactors, the high heat of reaction was expected to cause catalyst deactivation through hot spots and carbon deposition. These problems had been encountered by others.

We, therefore, set up a small laboratory test unit to test commercial catalysts in a fixed-bed reactor under the expected operating conditions. A schematic diagram of the unit is given in Figure 5. Synthetic gas mixtures were prepared having the following typical composition ranges.

<u>Component</u>	<u>Composition, mole %</u>
CO	3.5-12.7
CO ₂	0.6-3.2
H ₂	18.8-57.5
CH ₄	24.3-72.6
C ₂ H ₆	0.1-1.3
N ₂	1.2-4.0

Sulfur was removed from the feed gas to less than 0.1 ppm by beds of activated carbon and zinc oxide.

The unit was designed for around-the-clock operation with a minimum of operator attention. The feed gas rate, the reactor and guard chamber temperatures, and the unit pressure were controlled and recorded. The condensed product water was drained from the unit automatically by a liquid-level controller. The product-gas CO content was monitored by an MSA Lira model infrared analyzer and recorded continuously. Exit-gas volumes were recorded manually at regular intervals, and samples of feed and exit gases were taken throughout the test periods for analysis by gas chromatography.

A diagram of the reactor and electric heater and furnace is given in Figure 6. The 4-inch-deep catalyst bed was held between two packed beds of glass beads. The upper part of the reactor was enclosed in an electric furnace and the lower part was wrapped by an electric resistance heater. Bed temperatures were recorded at the four points indicated.

Initial tests were with a commercial nickel-on-alumina catalyst. The catalyst, supplied as 1/4-inch pellets, was crushed to -12+18 USS. Feed gases contained 4 mole percent CO in some tests and 13 mole percent in others. In all tests with this catalyst there was considerable carbon deposition. Higher temperatures were required to obtain sufficient catalyst activity for the desired reduction of carbon monoxide to 0.1 mole percent, which may have accelerated carbon deposition rates.

Tests with 1/8-inch pellets of nickel-on-kieselguhr catalyst were successful. One run lasted 1420 hours, during which time conditions were varied considerably (Table 4). Space velocities of over 9000 SCF/CF cat.-hr were used. The run was terminated voluntarily with the CO content of the exit gas still at only 0.1 mole percent. The CO₂ conversion showed no consistent trend with variations in operating conditions. Ethane hydrogenolysis was nearly complete for the entire run.

Table 4. LIFE TEST RESULTS

Run No.	Catalyst		LT-11		Nickel on Kieselguhr		0.00352		1250		1320		1391		1420	
	19	80	217	288	421	464	558	653	771	820	820	1006	1006	1000	1000	1010
1000	1005	1003	1000	1006	1006	1000	1000	1003	998	1014	1005	1006	1006	1000	1000	1010
655	640	630	625	605	605	435	545	465	490	480	450	565	470	535	515	515
710	700	695	685	665	600	600	600	535	515	545	510	625	540	600	595	595
855	880	875	870	890	840	840	840	840	790	810	740	900	730	855	795	795
635	635	630	620	605	580	545	580	485	485	425	610	650	770	645	825	825
585	580	575	570	550	490	445	425	425	425	480	470	515	540	525	600	600
4.3	4.0	3.5	3.5	4.0	4.0	4.0	4.0	3.7	3.7	3.8	4.2	3.7	3.7	3.7	3.7	3.7
1.5	1.4	1.0	1.0	0.8	0.8	0.8	0.8	0.7	0.7	0.6	0.6	0.8	0.8	0.8	1.0	1.0
18.8	19.4	18.8	18.8	20.1	20.1	20.1	20.1	21.3	21.3	19.8	20.0	18.9	18.9	18.9	19.6	19.6
70.1	69.3	70.0	70.0	69.0	69.0	69.0	69.0	68.0	68.0	71.9	72.2	72.6	72.6	72.6	71.7	71.7
2.7	2.7	3.4	3.4	3.7	3.7	3.7	3.7	3.7	3.7	1.2	1.1	0.9	0.9	0.9	0.9	0.9
2.6	3.2	3.3	3.3	2.4	2.4	2.4	2.4	6.0	6.0	2.7	1.9	3.1	3.1	3.1	3.1	3.1
100.0	100.0	100.0	100.0	100.0	100.0	100.0	100.0	100.0	100.0	100.0	100.0	100.0	100.0	100.0	100.0	100.0
2539	2590	2599	2596	2619	2619	2551	4798	2619	2619	4803	5284	4832	6852	6852	4193	8664
8.99	9.12	9.15	9.14	9.22	16.56	8.34	16.89	9.24	9.24	16.91	18.60	17.01	24.12	24.12	14.76	30.50
0.2	0.1	0.2	0.1	0.1	0.0	0.1	0.1	0.1	0.1	0.1	0.1	0.1	0.1	0.1	0.1	0.1
0.9	1.0	1.0	0.8	0.6	0.1	0.2	0.1	0.1	0.1	0.0	0.0	0.1	0.1	0.1	0.3	0.5
1.8	1.8	1.7	1.4	1.5	1.6	1.5	2.1	3.3	3.3	2.8	4.2	3.0	3.3	3.3	2.9	4.0
93.6	93.5	93.6	94.4	94.2	94.9	95.0	94.3	92.9	93.9	93.9	92.5	93.3	92.9	93.4	92.6	93.3
0.2	0.1	0.2	0.2	0.2	0.1	0.1	0.1	0.4	0.4	0.0	0.0	0.0	0.0	0.1	0.0	0.0
3.3	3.5	3.3	3.1	3.4	3.3	3.1	3.3	3.1	3.2	3.2	3.2	3.6	3.6	3.7	3.7	4.0
100.0	100.0	100.0	100.0	100.0	100.0	100.0	100.0	100.0	100.0	100.0	100.0	100.0	100.0	100.0	100.0	100.0
0.77	0.77	0.77	0.78	0.78	0.82	0.64	0.80	0.88	0.88	0.86	0.84	0.82	0.82	0.82	0.80	0.80
942	940	941	948	950	955	957	947	949	949	952	940	949	944	941	932	938
91	92	93	93	92	96	77	97	104	103	103	99	98	98	99	96	100
91	92	91	92	91	96	82	94	103	102	102	98	97	97	97	94	94
95	98	102	91	110	101	106	106	115	106	106	79	85	91	67	82	65
92	92	92	91	94	97	77	98	104	103	103	99	97	97	97	95	94
10.40	9.88	10.37	7.26	10.24	19.62	8.34	19.00	11.15	18.96	16.80	15.98	23.69	11.67	26.89	10.97	29.47
96	98	96	98	98	100	98	98	98	98	97	98	100	98	98	98	98
53	44	44	37	41	90	84	89	87	100	100	100	90	90	90	81	60
94	97	94	95	96	98	98	98	98	90	100	100	100	100	100	100	100

Feed Gas Composition (Dry), mole %

CO

CO₂

H₂

CH₄

C₂H₆

N₂

Total

Space Velocity, SCF/cu ft-hr

Feed Rate, SCF/hr

Product Gas Composition (Dry), mole %

CO

CO₂

H₂

CH₄

C₂H₆

N₂

Total

Product, SCF/SCF feed

Heating Value, Btu/SCF

Carbon Recovery, %

Hydrogen Recovery, %

Oxygen Recovery, %

Total Material Recovery, %

Water Collected by Condensate Measurement, g/hr

CO Conversion, %

CO₂ Conversion, %

C₂H₆ Conversion, %

Although the nickel-on-kieselguhr catalyst is less strong than the nickel-on-alumina one, its superior performance makes it the preferred catalyst for the HYGAS Process.

REACTOR STABILITY

Because the methanation reaction is highly exothermic, it is conceivable that the catalyst-bed temperature could exceed the calculated adiabatic equilibrium temperature at some operating conditions and in some reactor configurations. Preliminary calculations indicated possible instability in the packed-bed methanation reactors for the HYGAS pilot plant and large-scale plants being designed. Therefore, a more detailed study of reactor stability was undertaken.

The first approach was an attempt to test for stability without requiring the solution of the several partial differential equations involved. One can reason that in an adiabatic steady-state system with the single-path catalytic reaction presumed here, the temperature of the gas phase must lie between the initial and final equilibrium temperatures. The difference between the catalyst and gas-phase temperature is proportional to the reaction rate if the gas-particle heat transfer coefficient is assumed constant. Therefore, if the catalyst temperature is not excessive at the known inlet conditions, a sufficient condition for the system to be stable is that the reaction rate decreases with distance through the reactor; that is, a sufficient condition for stability is -

$$\frac{dr}{dz} < 0 \quad (5)$$

But in this system the reactant CO decreases with distance so that the condition is equivalent to:

$$\frac{dr}{d(X_{CO})_g} > 0 \quad (6)$$

where the reaction rate is a function of the catalyst temperature, and the concentration of CO near the surface is in turn dependent on the CO concentration in the gas phase. Equation 7 follows directly from Equation 6:

$$\left(\frac{\partial r}{\partial (X_{CO})_s} \right)_{T_s} \frac{d(X_{CO})_s}{d(X_{CO})_g} + \left(\frac{\partial r}{\partial T_s} \right) (X_{CO})_s \frac{dT_s}{d(X_{CO})_g} = \frac{dr}{d(X_{CO})_g} > 0 \quad (7)$$

From steady-state considerations and neglecting the second-order effects of variation in physical properties with temperature and composition, one can show that -

$$T_s = \frac{r \cdot \Delta H}{h_t} + \left[\frac{(X_{CO})_o - (X_{CO})_g}{c_g} \right] (\Delta H + T_o) \quad (8)$$

$$(X_{CO})_s = (X_{CO})_g - \frac{r}{\rho_g h_m} \quad (9)$$

Operating on these equations leads to:

$$\frac{dr}{d(X_{CO})_g} = \frac{\left[\partial r / \partial (X_{CO})_s \right] - \Delta H / c_g \left[\partial r / \partial T_s \right]}{1 + \left[1 / h_m \rho_g \right] \left[\partial r / \partial (X_{CO})_s \right] - \Delta H / h_t \left[\partial r / \partial T_s \right]} \quad (10)$$

The right-hand side of Equation 10 requires the kinetics of the reaction in terms of the catalyst conditions. This is the case at hand. Noting that this quantity is greater than zero if the reaction rate is temperature-independent, one can conclude that for the kinetics proposed by Wen¹³ the system is always stable. Wen's interpretation of IGT data is that there is no temperature effect above 600 °F. However, our kinetic data retain a significant temperature dependence at high temperatures, which leads to negative values for the expression in Equation 10 with h_t and h_m appropriate to the expected flow regime.

A positive value of Equation 10 is sufficient for stability but not necessary. Consequently, negative values leave us in an indeterminate position. But we can, and did, calculate the values of T_s for the possible range of values of $\{X_{CO}\}_g$ from Equations 8 and 9. At the expected levels of transfer rates, with our kinetics, the computed catalyst temperature never exceeds the final temperature.

In Figure 7 the estimated catalyst temperatures are shown as a function of degree of conversion at the expected transfer rates (30,000 Btu/hr-sq ft per cu ft of void volume) for a 540 °F feed gas containing 4 mole percent CO in excess H_2 . Figure 7 also shows results for transfer rates that are reduced 30-fold (the heat and mass transfer coefficients proportionately) — an effect corresponding to a meaningless 900-fold decrease in velocity. The higher temperature levels only exceed the final temperature by 25 °F. Therefore, even spots in the reactor where the velocity is unusually low still would not become excessively hot.

The kinetics and the mass and heat transfer rates collected by IGT were used to estimate the required space velocities for the methanation process. In Figure 8, the results are given for a 4 mole percent CO feed gas at a 550 °F feed temperature in a steady-state system, with a feed rate of 126 lb-mole/hr-sq ft of reactor cross section. For a product gas with 0.1 mole percent CO, the space velocity is computed to be 47,000 SCF/CF-hr. A ninefold change in velocity affects the required space velocity by only 8%.

As a check, the system was calculated using kinetics proposed by Wen,¹³ which, because of the assumption of temperature independence above 600 °F, do not predict as high a reaction rate at the higher temperature as do our kinetics. The results are also given in Figure 8. Wen's kinetics lead to an estimate of space velocity to produce 0.1 mole percent CO at 550 °F with a space velocity of 27,000 SCF/CF-hr. Since it is quite probable that Wen interprets a diffusion limitation in the original experiments as a slow reaction rate, the 27,000 represents a lower bound on estimates of space velocities based on our original data. Our pilot plant methanation reactors were designed using a space velocity of less than 5000 SCF/CF-hr. It is possible that we can methanate the entire pilot plant output in two methanation stages.

ACKNOWLEDGMENT

This work is sponsored by the American Gas Association, Research and Development, and the U. S. Department of the Interior, Office of Coal Research. Their support is gratefully acknowledged. The advice and contributions of F. C. Schora, B. S. Lee, S. A. Weil, R. Noresco, and A. Talwalker are appreciated.

NOMENCLATURE

A	= surface equilibrium constant ¹
B	= surface equilibrium constant ¹
c	= heat capacity
C ₁	= reaction rate constant ³
C ₂	= surface equilibrium constant ³
C ₃	= surface equilibrium constant ³
C ₁ '	= reaction rate constant ³
C ₂ '	= surface equilibrium constant ³
C ₃ '	= surface equilibrium constant ³
D	= surface equilibrium constant ¹
E	= surface equilibrium constant ¹
E ₁	= activation energy ¹⁰
h _t	= heat transfer coefficient
h _m	= mass transfer coefficient
ΔH	= heat released per unit reaction
k	= reaction rate constant
K	= surface equilibrium constant
n	= order of reaction
p	= partial pressure
r	= reaction rate
r ₀	= initial reaction rate
R	= gas constant
T	= temperature
X	= mole fraction
Z	= distance through reactor
Z ₁	= Arrhenius constant ¹⁰
Z ₂	= constant ¹⁰

Greek Letter

ρ = density

Subscripts

g = gas

o = initial

s = surface

REFERENCES CITED

1. Akers, W. W. and White, R. R., "Kinetics of Methane Synthesis," Chem. Eng. Progr. 44, 553-66 (1948).
2. Barkley, L. W. et al., "Catalytic Reverse Shift Reaction," I&EC 44, 1066-71 (1952).
3. Binder, G. G. and White, R. R., "Synthesis of Methane From Carbon Dioxide and Hydrogen," Chem. Eng. Progr. 46, 563-74 (1950).
4. Dirksen, H. A. and Linden, H. R., "Pipeline Gas From Coal by Methanation of Synthesis Gas," IGT Res. Bull. No. 31. Chicago, July 1963.
5. Institute of Gas Technology, "Pipeline Gas From Coal - Hydrogenation," A.G.A. Project IU-4-1 and OCR Contract No. 14-01-0001-381 (1). Chicago, November 1969.
6. Institute of Gas Technology, "Pipeline Gas From Coal - Hydrogenation," A.G.A. Project IU-4-1 and OCR Contract No. 14-01-0001-381 (1). Chicago, September 1968.
7. McKee, D. W., "Interaction of H₂ and CO on Platinum Group Metals," J. Catal. 8, 240-49 (1967).
8. Nicolai, J., D'hont, M. and Jungers, J. C., "The Synthesis of Methane From Carbon Monoxide and Hydrogen on Nickel," Bull. Soc. Chim. Belgium 55, 160-76 (1946).
9. Pursley, J. A., White, R. R. and Sliepcevich, C., "The Rate of Formation of Methane From CO and H₂ With a Nickel Catalyst at Elevated Pressures," Chem. Eng. Progr. Sym. Ser. 4, 51-58 (1952).
10. Schoubye, P., "Methanation of CO on Some Ni Catalysts," J. Catal. 14, 238-46 (1969).
11. Tajbl, D. G., Feldkirchner, H. L. and Lee, A. L., "Cleanup Methanation for the Hydrogasification Process," ACS Div. Fuel Chem. Prepr. No. 4, 235-45 (1966) September; also in Advances in Chemistry Series No. 69, 166-79. Washington, D.C.: American Chemical Society, 1967.
12. Weller, S., "Analysis of Kinetic Data for Heterogeneous Reactions," A.I.Ch.E. J. 2, 59-62 (1956).
13. Wen, C. Y. et al., "Optimization of Fixed Bed Methanation Processes." Paper presented at the ACS Meeting, Atlantic City, New Jersey, September 1968.

LITERATURE SURVEY

1. Andrew, S.P.S., "Catalysts and Catalytic Processes in the Steam Reforming of Naphtha," I&EC Prod. Res. Develop. 8, 321-24 (1969).
2. Bienstock, D. et al., "Synthesis of High Btu Gas From CO and H₂ Using a Hot Gas Recycle Reactor," Paper No. CEP-60-14 in Proceedings of American Gas Association Operating Section. New York, 1960.
3. Boudart, M., "Kinetics on Ideal and Real Surfaces," A.I.Ch.E. J. 2, 62-64 (1956).
4. Carberry, J. J., "Designing Laboratory Catalytic Reactors," I&EC 56, 39-46 (1966).
5. Carberry, J. J., "Transport Phenomena and Heterogeneous Catalysis," Chem. Process Eng. 306-15 (1963) June.
6. Demeter, J. J., Haynes, W. P. and Youngblood, A. J., "Experiments With a Self-Generated Carbon-Expanded Iron Catalyst for Synthesis of Methane," Report No. 6425. Washington, D.C.: U.S. Dept. Interior, Bureau of Mines, 1963.
7. Dent, F. J. and Hebben, D., "The Catalytic Synthesis of Methane as a Method of Enrichment in Town Gas Manufacture," Gas Research Board Communication GRB 51. London, 1949.
8. Dent, F. J. et al., "An Investigation Into the Catalytic Synthesis of Methane for Town Gas Manufacture," Gas Research Board Communication GRB 20. London, 1945.
9. Feldkirchner, H. L. and Kniebes, D. V., "Effect of Nuclear Irradiation on the Activity of Iron Methanation Catalysts." Paper presented at ACS Meeting, Washington, D.C., March 20-24, 1962.
10. Field, J. H. et al., "Development of Catalysts and Reactor Systems for Methanation," I&EC Prod. Res. Develop. 3, 150-53 (1964).
11. Goldberger, W. M. and Othmer, D. F., "The Kinetics of Nickel Carbonyl Formation," I&EC Process Design Develop. 2, 202-09 (1963).
12. Greyson, M., "Methanation," in Catalysis, Vol. IV, Emmet, P. H., Ed., 473-511. New York: Reinhold, 1956.
13. Greyson, M. et al., "Synthesis of Methane," Report No. 5137. Washington, D.C.: U.S. Dept. Interior, Bureau of Mines, 1955.
14. Linden, H. R., "Conversion of Solid Fossil Fuels to High-Btu Pipeline Gas." Paper presented at A.I.Ch.E. Meeting, Denver, August 26-29, 1962.
15. Meller, A., "Catalytic Hydrogenation of CO - Methane Synthesis From Water Gas," Aust. Chem. Inst. J. Proc. 10, 100-14, 123-29 (1943).
16. Schlesinger, M. D., Demeter, J. J. and Greyson, M., "Catalyst for Producing Methane From H₂ and CO," I&EC Prod. Process Develop. 48, 68-70 (1956).
17. Schuster, V. F., Panning, G. and Bulow, H., "Methanation in Gas Mixtures Containing Carbon Monoxide and Carbon Dioxide With Various Nickel Catalysts," Brennst. Chem. 14, 306-07 (1935).
18. Strickland-Constable, R. F., "The Synthesis of Methane From Carbon Monoxide and Hydrogen on a Nickel Catalyst," Gas Research Board Communication GRB 46 London, 1949.

19. Vlasenko, V. M., Yuzefovich, G. E. and Rusov, M. T., "Hydrogenation of CO and CO₂ on Nickel Catalyst," Kinet. Kataliz 6, 938-41 (1965).
20. Vlasenko, V. M., Yuzefovich, G. E. and Rusov, M. T., "Kinetics of CO₂ Hydrogenation on a Nickel Catalyst," Kinet. Kataliz 2, 525-28 (1961).
21. Wainwright, H. W., Egleston, G. C. and Brock, C. M., "Laboratory-Scale Investigation of Catalytic Conversion of Synthesis Gas to Methane," Report No. 5046. Washington, D.C.: U.S. Dept. Interior, Bureau of Mines, 1954.
22. Yang, K. H. and Hougen, O. A., "Determination of Mechanism of Catalyzed Gaseous Reactions," Chem. Eng. Progr. 46, 146-57 (1950).

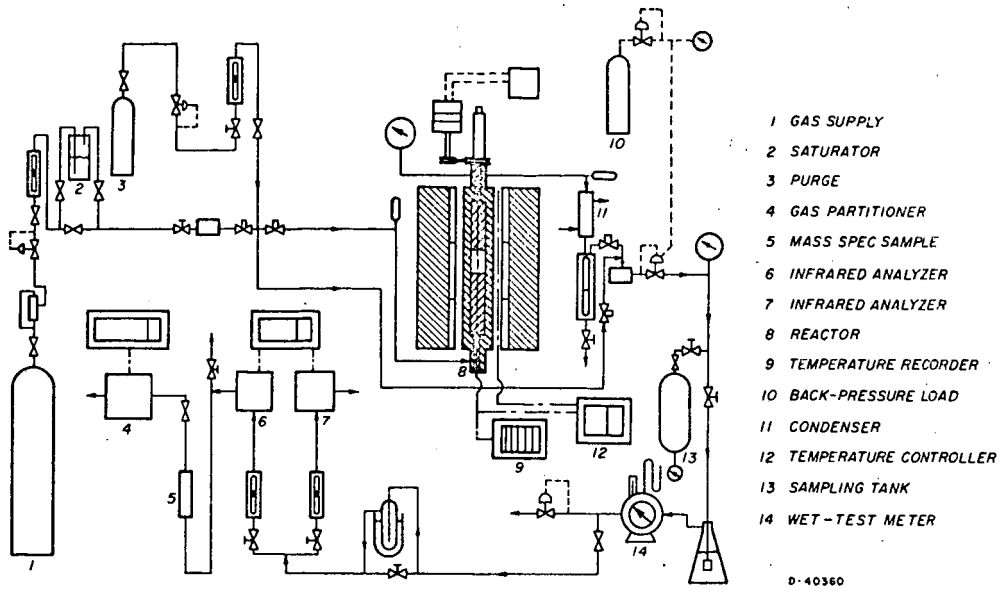


Figure 1. SCHEMATIC DIAGRAM OF METHANATION APPARATUS

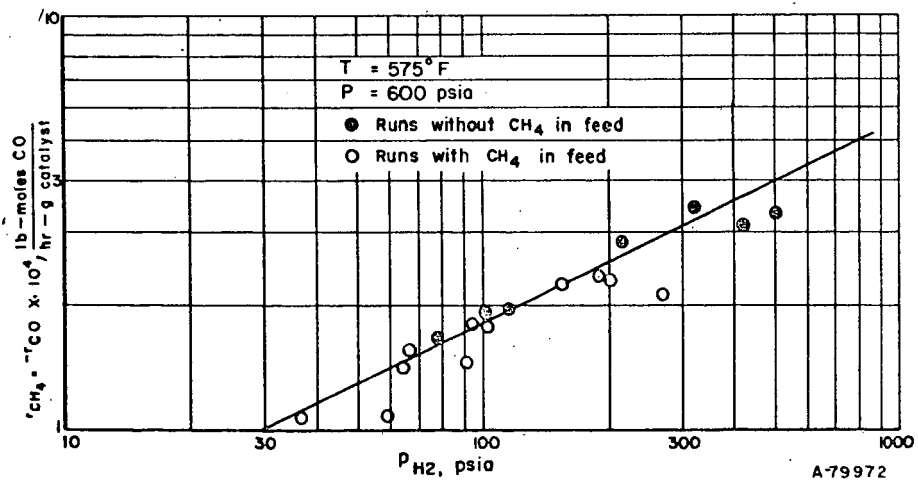


Figure 2. ORDER OF METHANATION REACTION WITH RESPECT TO HYDROGEN IS 1/2

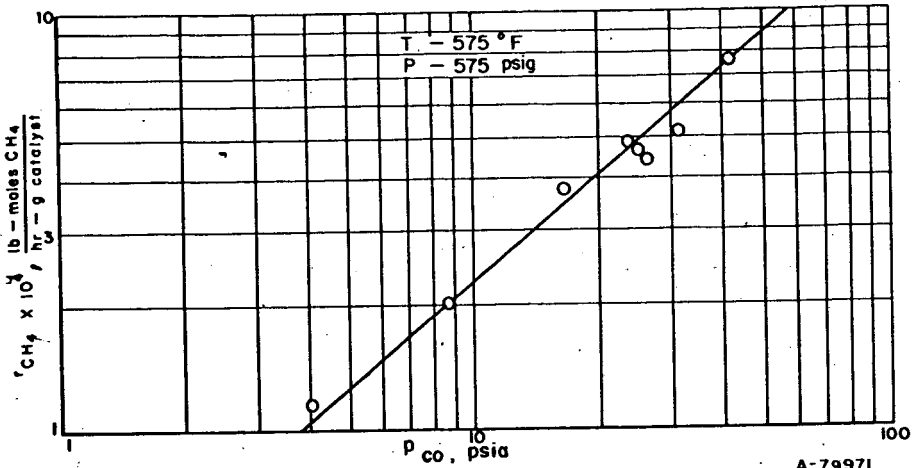


Figure 3. ORDER OF METHANATION REACTION WITH RESPECT TO CARBON IS 1

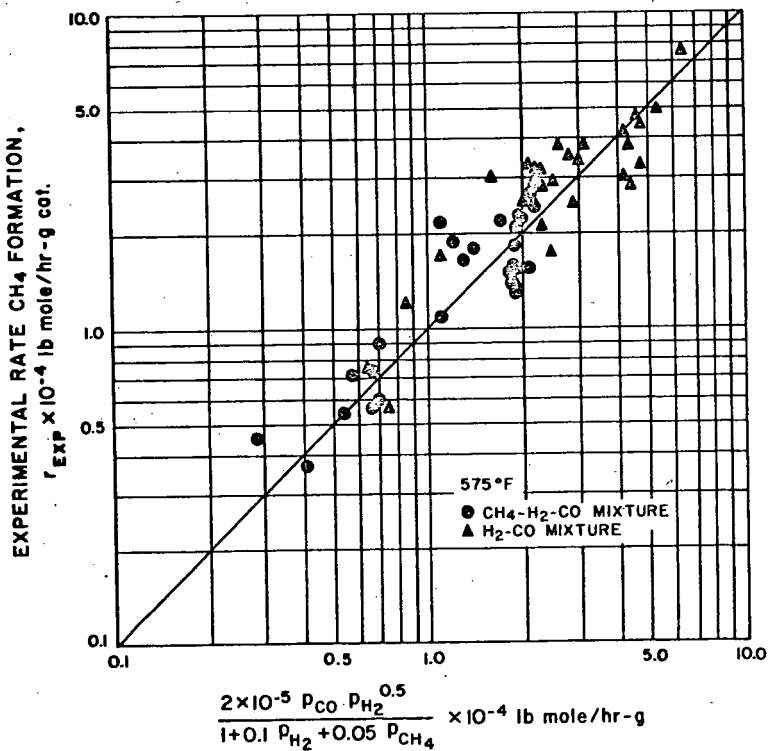


Figure 4. ANALYSIS OF METHANATION DATA

- LEGEND**
- A FEED-GAS STORAGE
 - B N₂ PURGE-GAS STORAGE
 - C FILTER
 - D PRESSURE GAGE
 - E PRESSURE REGULATOR
 - F ELECTRIC HEATER
 - G SULFUR REMOVAL
 - H ORIFICE
 - I DIFFERENTIAL PRESSURE TRANSMITTER
 - J FLOW RECORDING CONTROLLER
 - K SAFETY SHUTOFF
 - L DIFFERENTIAL PRESSURE GAGE
 - M ELECTRIC FURNACE
 - N METHANATION REACTOR
 - O CONDENSER
 - P DRAIN POT
 - Q STRIP CHART RECORDER
 - 1. TEMPERATURE
 - 2. COMPOSITION
 - R LEVEL CONTROLLER
 - S TEMPERATURE CONTROLLER
 - T ROTAMETER
 - U GAS DRIER
 - V INFRARED CO ANALYZER
 - W ZERO GAS
 - X CALIBRATION GAS
 - Y SATURATOR
 - Z WET-TEST METER

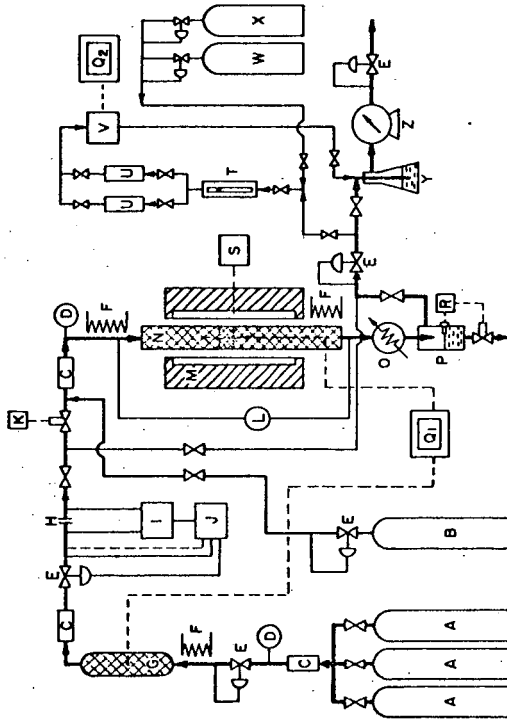


Figure 5. METHANATION LIFE-TEST UNIT

B-40334

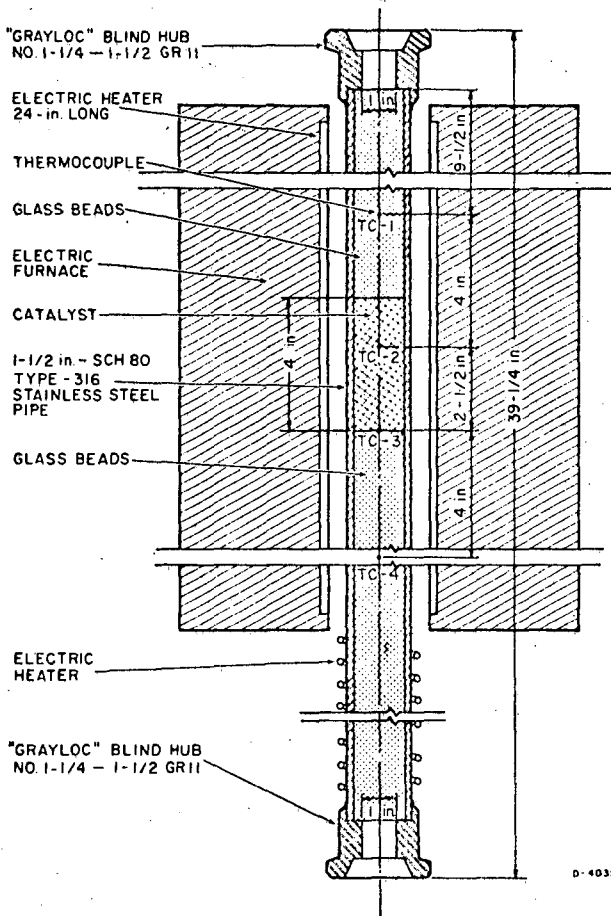


Figure 6. LABORATORY FIXED-BED REACTOR

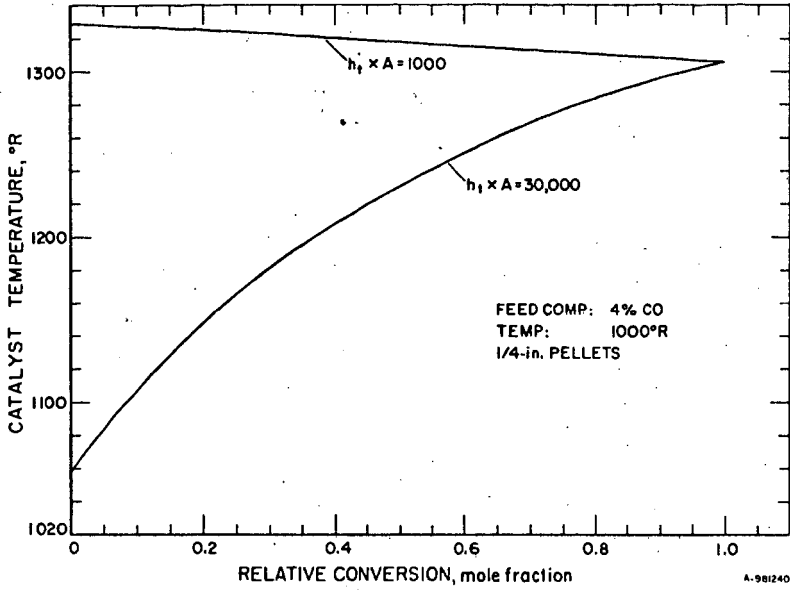


Figure 7. ESTIMATED STEADY-STATE TEMPERATURES IN METHANATION REACTOR

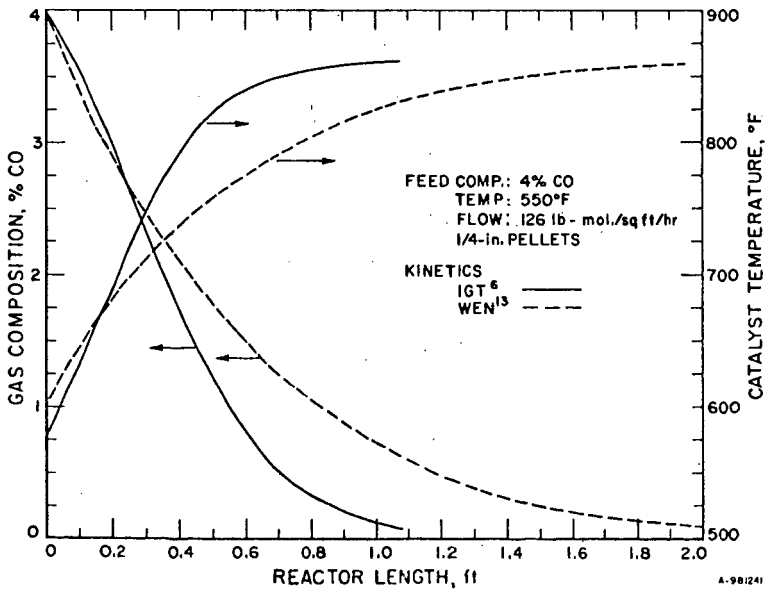


Figure 8. CALCULATED METHANATION REACTOR PERFORMANCE

Reaction Model for Bituminous Coal Hydrogasification
in a Dilute Phase

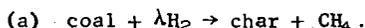
H. F. Feldmann, W. H. Simons,^{1/} J. A. Mima, and R. W. Hiteshue

U.S. Bureau of Mines, 4800 Forbes Avenue
Pittsburgh, Pennsylvania 15213

INTRODUCTION

Increasing demands and decreasing reserves of natural gas^{1,2/} have intensified research and development efforts directed towards the production of supplementary pipeline gas. Several processes are currently being developed^{2/} which will utilize our abundant fossil fuel reserves to meet the anticipated need for supplementary gas. One of these processes under investigation at the U.S. Bureau of Mines is the hydrogasification of raw bituminous coal to produce a pipeline quality gas consisting primarily of methane. There are certain features involved in the hydrogasification of raw bituminous coal which are economically and technically attractive: First, as shown by this study, the external hydrogen consumption required per unit of methane produced is low because of the efficient utilization of the hydrogen already in the coal; secondly, direct production of a high-Btu gas and use of a dilute-phase concurrent reactor (which minimizes agglomeration problems) are both possible because of the high reactivity which raw coal has for methane formation; and thirdly, process costs associated with pretreatment, inherent in other coal conversion processes based on bituminous coal feed stocks, are eliminated.

In this paper we describe a kinetic model for the overall reaction occurring in the hydrogasification reactor; that is



This model is being used in other studies to evaluate and optimize various types of hydrogasifier schemes as well as to predict by computer simulation temperature profiles in commercial sized reactors.

Most of our experimental data on the hydrogasification of coal comes from a reactor using concurrent gas-solids flow with the solids freely falling through the reactor. Although the primary reason for using this contacting system is to avoid agglomeration problems,^{3/} this dilute-phase operation may also offer some advantages in temperature control because of the reduced heat generation per unit volume of reactor compared to moving bed or fluidized systems.

EXPERIMENTAL

Equipment and Procedure

The basic elements of the hydrogasification system are shown in figure 1. Hydrogen from a gasholder at atmospheric pressure is metered and compressed to reaction pressure in a 5-stage reciprocating compressor and is heated in tubing coiled around the reactor before being injected into the top of the reactor. Heat is supplied to the reactor and gas preheat coils with banks of individually controlled electric-resistance furnaces. Coal is fed to the reactor at system pressure using a 4-vaned feeder connected to a variable-speed motor; it passes by gravity flow through a nozzle of 5/16-inch diameter before entering the reactor. This nozzle is water-cooled to keep the coal below its softening temperature and is insulated to minimize heat losses. The coal is dispersed into the reactor where it contacts and reacts with the hydrogen. The reactor is of 3-inch inner diameter and the heated section below coal entry point has been varied from 3 to 6 feet in length. The coal must be heated very rapidly

^{1/} Mathematician, Department of Mathematics, West Virginia University, Morgantown, West Va. 26506.

through its plastic temperature (350°-480° C for hvab coal, Pittsburgh seam) in order to produce a dry char, free of agglomerates. Residence time of volatile products varies with system pressure and gas rate but for most experiments made at 3,000 psig, this residence time runs about 5 minutes. Two types of reactors have been used for these experiments. For experiments made at 725°-750°C (EHR series), thick-walled stainless steel reactor with a 6-inch od x 3-inch id was used. For experiments at 900° C (IHR series), an internally-heated reactor was designed in which the reactor proper consists of 3-inch schedule 10 stainless steel pipe. The IHR reactor and heating elements are enclosed in a 10-inch pressure vessel and are insulated so that wall temperatures on this vessel do not exceed 150° C at reaction temperatures of 900° C. Equalized pressure is maintained across the wall of the 3-inch reactor.

Char is collected in an air-cooled receiver located below the reactor. Product gas passes through a water-cooled vessel in which water, traces of oil, and some volatile salts are condensed and collected. The gas is then expanded to atmospheric pressure through a regulator, metered, and flared. A separate sample stream, taken from a point near the bottom of the reaction zone, passes through a continuous analyzer that determines the concentration of hydrogen in the stream. Periodic samples are taken for complete analysis by chromatography. The char from the receiver is weighed and ultimate and proximate analyses made.

Experiments were made with hvab coal from the Pittsburgh seam having a free-swelling index of 8 and a volatile content of 39-41 percent, moisture-ash-free basis. Ultimate and proximate analyses are given in table 1. The feed was sized to 50 x 100 mesh sieve fraction, U.S. Standard.

Table 1.- Analyses of high-volatile A bituminous coal

	As received, percent	Maf, percent
Ultimate		
Carbon	78.5	84.0
Hydrogen	5.4	5.7
Nitrogen	1.6	1.7
Sulfur	1.4	1.5
Oxygen ^{1/}	7.2	7.1
Ash	5.9	-
	100.0	
Proximate		
Moisture	0.7	-
Volatile matter	38.2	40.9
Fixed carbon	55.2	59.1
Ash	5.9	-

^{1/} By difference.

Development of Reaction Model

Ordinary methods of treating integral reactor data are not applicable to our data because, judging from product gas analyses, the system never reached steady state in the time allowed by the coal capacity of the pressurized hopper. The gas concentration versus operating time curves indicate substantial backmixing was occurring in the reactor and this backmixing was responsible for the delay in reaching steady state. A tracer experiment was conducted under controlled conditions and without the complications of chemical reactions to observe the precise behavior of the IHR reactor as a

mixer. In this experiment the hopper was charged with an inert solid (anthracite) and the same operating procedure was followed as in a run except that shortly after the start of feeding the anthracite, the hydrogen flow was turned off and inert gas fed in its place. The dimensionless concentration of nitrogen in the sample gas is shown in figure 2 as a function of time. These results indicate that based upon the so-called dispersion model,⁴ the reactor may be treated as if the gas phase were perfectly mixed.

Because the reactor is backmixed and the residence time of the free-fall particles is short compared to the time over which a significant change in gas composition occurs, each particle entering the reactor sees an essentially constant gas composition while passing through the reaction zone. Of course, particles falling through the reactor at different operating times see different gas compositions so the char collected at the end of an experiment is a nonhomogeneous material composed of particles all of which experienced different reaction conditions. Thus, in the formulation of the hydrogasification model two time scales are necessary. The physical interpretation of these two time scales is illustrated by the following rate equation which was found to best fit the experimental data,

$$(1) \quad \partial z^*(t, \theta) / \partial \theta = k p_{H_2}(t) (1 - z^*),$$

where z^* is the carbon conversion at particle residence time θ and at operating time t , k is the reaction rate constant, and $p_{H_2}(t)$ is the hydrogen partial pressure at operating time t . Since the measured carbon conversion, \bar{z} , is based on the total char collected, it is an average conversion and therefore may be assumed to be related to the instantaneous conversion by

$$(2) \quad \bar{z} t_R = \int_0^{t_R} z(t) dt,$$

where t_R is the duration of the run, $z(t) = z^*(t, \theta_0)$ and θ_0 is the particle residence time.

Because the change in gas composition is negligible over a time span equal to the particle residence time θ_0 , equation (1) may be integrated with respect to θ with t held constant. This yields

$$(3) \quad \int_E^{z(t)} dz^*(t, \theta) / (1 - z^*) = k p_{H_2}(t) \theta_0,$$

where the physical interpretation of E is the fraction of carbon that is immediately vaporized. From equation (3) and the definition $\theta_0 = L/U_T$, the carbon conversion of coal falling through the reactor at operating time t is given by

$$(4) \quad z(t) = 1 - (1 - E) \exp(-k p_{H_2}(t) L / U_T).$$

As previously mentioned, the solid carbon conversion measured is an average conversion so substitution of equation (4) into equation (2) gives

$$(5) \quad \bar{z} = 1 - (1 - E) / t_R \int_0^{t_R} \exp(-k p_{H_2}(t) L / U_T) dt$$

as the expression for the average solid carbon conversion over the run time t_R .

We have experimental values for \bar{z} , t_R , L , $p_{H_2}(t)$ as a discrete function of operating time t , and a rough estimate for U_T of 32,400 ft/hr at 205 atm. Equation (5) was used to correlate the hydrogasification data by the following steps:

1. Select a value for E
2. For each experiment, with this E solve equation (5) for k by numerical methods.

3. Calculate the average k value for those experiments all performed at the same temperature, and using this k value in (5), calculate a \bar{z} for each of these experiments.

4. Determine the value of E that minimizes

$$\sum |\bar{z}_{\text{measured}} - \bar{z}_{\text{calculated}}|,$$

where the summation is taken over the experiments of step (3).

Results of experiments at the two temperature levels studied are shown with the feed conditions in table 2. For each temperature, the results presented in table 2

Table 2. - Tabulated reaction rate constants and reactor conditions

IHR Run Series, T = 900° C, E = 0.14							
Run	Reactor pressure, atm.	Solids feed rate, lb/hr	Average solid carbon conversion, %	Gas feed rate, lb-mole/hr	Hydrogen in feed gas, vol%	Reactor length, ft	Reaction ^{2/} rate constant k, atm ⁻¹ hr ⁻¹
36	205	6.4	31.0	0.447	1/48	5	23.7
37	205	13.6	27.1	0.550	1/50	5	21.4
38	205	13.0	22.0	0.434	1/45	5	13.4
39	205	13.2	28.1	0.695	1/45	5	21.0
61	205	13.4	26.0	0.663	1/50	5	19.4
96	205	4.3	47.6	0.329	98	5	19.2
101	205	6.1	49.6	0.347	96	5	23.4
104	205	6.9	42.7	0.363	99	5	16.7
107	205	8.8	53.0	0.480	99	5	25.4
108	205	7.2	49.8	0.450	98	5	24.0
109	205	8.1	47.8	0.480	98	5	23.1
110	205	8.2	41.6	0.468	99	3	27.5
111	205	7.9	39.8	0.463	99	3	25.2
113	205	8.3	43.0	0.405	99	3	21.7
129	205	8.4	40.0	0.423	100	5	19.5
130	205	8.1	40.2	0.437	97	5	18.8
131	205	8.4	42.0	0.408	96	5	21.2
132	205	8.8	37.7	0.432	99	5	14.3
133	205	8.2	40.5	0.348	99	5	15.7
136	205	7.8	39.9	0.447	99	5	17.8
125	69	8.1	36.8	0.516	97	5	39
128	69	8.2	37.8	0.368	93	5	43
					Average k ^{3/} = 21 atm ⁻¹ hr ⁻¹		

1/ Except for about 2 vol pct the remainder of the gas is methane.

2/ Based on estimated average particle velocity of 32,400 ft/hr with char produced at 205 atm.

3/ Runs at 69 atm corrected for particle residence time for inclusion in average k.

(Table 2 continued on next page.)

Table 2-continued-

EHR Run Series, T = 725° C, E = 0.22							
Run	Reactor pressure, atm	Solids feed rate, lb/hr	Average solid carbon conversion, %	Gas feed rate, lb-mole/hr	Hydrogen in feed gas, vol%	Reactor length, ft	Reaction ^{2/} rate constant k, atm ⁻¹ hr ⁻¹
346	205	6.4	22.8	0.458	1/58	6	5.89
347	205	6.3	25.2	0.458	1/52	6	2.87
349	205	6.6	25.6	0.466	1/51	6	3.13
352	205	5.3	23.4	0.458	1/49	6	12.38
377	205	6.0	39.4	0.478	98	6	7.08
394	205	6.2	23.8	0.416	1/29	6	3.00
399	205	6.4	24.0	0.548	1/27	6	3.29
Average k at 205 atm = 5.4 atm ⁻¹ hr ⁻¹							
369	103	6.3	29.6	0.461	1/55	6	12.00
370	103	6.7	27.0	0.461	1/56	6	7.03
373	103	5.9	27.7	0.455	1/57	6	8.63
374	103	7.6	25.1	0.463	1/54	6	4.81
375	103	6.0	31.0	0.455	96	6	7.64
397	103	6.5	24.8	0.422	1/23	6	11.11
398	103	6.7	25.9	0.548	1/24	6	13.98
404	103	6.5	29.8	0.950	1/46	6	12.48
Average k at 103 atm = 9.7 atm ⁻¹ hr ⁻¹							
Average k at 725° C corrected for residence time effects = 6 atm ⁻¹ hr ⁻¹							

1/ Except for about 2 vol pct the remainder of the gas is methane.

2/ Based on estimated average particle velocity of 32,400 ft/hr with char produced at 205 atm.

are those calculated using the value of E in step (4). These results indicate an effect of pressure on k; however, this is merely a residence time effect due to the dependency of the char density on the system pressure. This dependency is shown in figure 3 where the bulk density of the char is plotted as a function of the reactor pressure. Apparently, the hollow spheres of which most of the char consists are smaller when formed under higher pressure. Photographs of char in figure 4 show this bulk density difference. Correction for the change in bulk density and the corresponding particle residence time gives k values that are independent of pressure, and these are the average values reported in table 2.

There is considerably more spread in the calculated k values at 725° C than at 900° C for the following reasons: Extensive carbon conversion at 725° C is due to devolatilization because of relatively low k values, the short residence time (<1 sec) in free-fall, and the low hydrogen partial pressure due to the higher methane concentrations in the feed gas. Thus, in equation (3) z(t) is close to E, and therefore, small errors in z(t) and E generate large errors in k. In view of this inherent instability, the calculational scheme described above was carried out under the additional constraint that E be less than the lowest measured carbon conversion. A comparison of the measured values of carbon conversion with those predicted by the model using the average k is shown in figure 5.

An apparent activation energy is calculated by plotting $\ln k$ versus $1/T$ for the two temperature levels studied in figure 6. Also shown in figure 6 is a k value reported by Wen and Huebler^{5/} using a coal-char and a k value calculated from data reported by Moseley and Paterson^{6/} also on char hydrogasification. The apparent activation energy calculated from figure 5 is about 16 k cal/gram-mole carbon reacted. This is in basic agreement with a hydrogasification activation energy of 15 k cal reported by Zahradnik and Glenn.^{2/}

Physical Interpretation of the Reaction Model

In this section we establish a physical basis for our reaction model, not only to gain confidence in the model but also to ascertain the limits of its applicability. In order to provide this physical basis we must rely on intuition and the experimental work of others even though the bulk of the latter was generated with coal-char as a feed material rather than coal.

We have already compared in figure 6 the temperature dependency of the rate constants calculated in this study with those reported or calculated from references 5, 6, and 7. This comparison is encouraging in the sense that it tells us what we intuitively would suspect; that is, the activation energies for the hydrogasification of coal and char are not greatly different. Another encouraging factor is the variety of reactor configurations and solid-gas contacting schemes employed in the studies used to calculate activation energies. For example, Moseley and Paterson^{6/} used an entrained reactor for their studies, Wen and Huebler^{5/} treated data generated in both a semiflow (fixed coal charge and flowing hydrogen) and continuous countercurrent tubular reactor. Moseley and Paterson's char data also indicate that the hydrogasification reaction rate constant decreases with increasing char preparation temperature and would thereby be expected to be highest for raw coal, as our data confirm.

Since Moseley and Paterson conducted their entrained reactor studies with excess hydrogen, the hydrogen partial pressure remains essentially constant; therefore, it is possible to calculate reaction rates in their entrained reactor because mixing patterns need not be considered. In figure 7, using a k value calculated from their data, the rates predicted by our model are compared with their experimentally measured rates at the various hydrogen partial pressures used in their studies. The goodness of the fit is a further indication that this reaction model can be used under a rather wide range of contacting schemes and reactor conditions.

Since, in this model, the hydrogasification rate is a function of temperature, hydrogen partial pressure, and carbon conversion level, we should establish a range for these variables over which the model applies. A very conservative estimate is obtained by simply restricting the variables to the range covered by the present experimental study. From a process viewpoint, the range of variables in this study, as shown in table 2, is sufficiently wide to cover most practical process situations. Thus, the model can be used to design most reactor systems without extrapolating beyond the range of experimental conditions.

Equation (1), which describes the rate of hydrogasification, has the simple physical interpretation that the coal particle consists of a number of reaction sites all equally accessible to hydrogen. The porous nature of coal-chars formed during hydrogasification (as shown by a cross sectional view of some typical char particles in figure 8), indicates that this interpretation is reasonable. The rate of reaction under these circumstances is given by

$$-\frac{1}{N_{s0}} \frac{dN_s}{d\theta} = k_{pH_2} \frac{N_s}{N_{s0}}$$

which can be directly written in terms of conversion as

$$dz/d\theta = k_{pH_2}(1-z).$$

Hitashue and co-workers conducted semiflow experiments^{8/} at the rapid heating rates typical of continuous operation. Their results indicate that the number of so-called reaction sites N_{SO} capable of being converted in the relatively short residence times of free-fall operation are not equal to the number of carbon atoms in the coal. Data from reference 8 are plotted in figure 9 to show how the fraction of total carbon available for reaction at short residence times is increased by increases in temperature and hydrogen partial pressure. The increase in the amount of more highly reactive carbon with increasing temperature was also pointed out by Wen and Huebler.^{9/} A fairly reasonable physical interpretation of this phenomena is that the carbon containing molecules in the coal are unstable at the hydrogasification temperatures and can either form molecules amenable to further hydrogenation by the addition of hydrogen to the solid phase or form more highly aromatic, and hence unreactive, structures by polymerization. This basic explanation of hydrogasification has also been postulated by both Moseley and Paterson^{6/} and Zahradnik and Glenn.^{2/} The material remaining after the highly reactive carbon is hydrogasified also hydrogasifies, but at a much lower rate. The kinetics of hydrogasification of this more unreactive carbon are currently being analyzed using the data in reference 8. Though the kinetic analysis of the hydrogasification of the more unreactive fraction of carbon is incomplete, it also seems to follow the basic rate law

$$\frac{dz}{d\theta} = k p_{H_2}^a (1-z),$$

where a is the yet undetermined order of the reaction with respect to hydrogen partial pressure.

Thus, hydrogasification of raw coal can be explained by assuming the existence of the following three types of carbon:

Type 1. The highly reactive solid carbon contained in side chains which is extremely easy to split off from the solid molecule. This is the fraction of carbon denoted by E in this report.

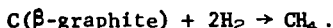
Type 2. The highly reactive solid carbon which readily hydrogasifies but at a lower rate than the carbon denoted by E . This is the fraction of carbon whose hydrogasification rate is described in this paper. As shown in figure 8, the fraction of reactive carbon depends on both the temperature and hydrogen partial pressure in the reactor.

Type 3. The low-reactivity residual carbon which seems to react according to the same rate law as type 2 but with a much lower value of k .

Alternate models based on char containing carbon of two different reactivities have been proposed by Wen and Huebler and Blackwood and McCarthy.^{7/}

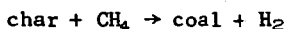
Our attention has thus far been focused on the solid carbon phase, and we should now consider the important role of the gaseous products on the hydrogasification reaction. One major effect of these gaseous products is, of course, the lowering of hydrogen partial pressure. Also, since the objective of these studies is to produce high-Btu gas, the maximum concentration of methane that can be produced and how it depends on the contacting scheme and reactor conditions should be determined. Our system is not a particularly good one for determining the maximum methane concentrations attainable because of the short solids residence time and the non-optimum solid-gas contacting system. In spite of these drawbacks, it is possible to produce a high-Btu gas after methanating the low concentrations of carbon monoxide to bring the gas into compliance with pipeline standards. For example, results of some experiments with hydrogen-methane feed gas at 900° C are presented in table 3. The feed gas composition used in these experiments comes from an experimental study^{10/} which established the feasibility of a two-stage hydrogasification system in which the raw coal is contacted while in free-fall with the product gas coming from a moving-bed char hydrogasifier. Details of this system are given in reference 10 and reference 3.

Two important facts may be observed from the results in table 3. First, since the same hydrogasification rate expression applies to systems containing up to 80 mole-percent methane, the only effect of high methane concentrations is to reduce the partial pressure of hydrogen. (Zielke and Gorin¹¹ also report that in differential bed studies with methane-hydrogen gas mixtures and a Disco char, the only effect of methane is to reduce the hydrogen partial pressure.) Secondly, the experimentally measured group $(Y_{CH_4}/Y_{H_2}P)$ is much higher than the equilibrium constant for the reaction



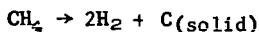
This is very important to process design because the relation between the partial pressures of methane and hydrogen and the solid carbon containing phase has been explained on thermodynamic grounds^{5,9,12,13} as if there exists an equilibrium between a solid of changing activity level and the reacting species in the gas phase. This explanation leads to the experimentally unjustified conclusion that low temperatures (1,300° to 1,500° F)¹² are necessary to achieve the direct production of a high-Btu gas in continuous systems. Indeed, this thermodynamic analogy is causing concern regarding the feasibility of direct hydrogasification because it implies the necessity of removing heat from hydrogasification systems to maintain temperatures at the levels predicted by thermodynamic considerations to yield high-Btu gas. That these heat removal concerns are, at least at the present, unjustified is shown not only by the work reported here where 80 percent methane gas has been produced at temperatures of 900° C (1,652° F), but also by work reported by Birch and co-workers¹⁴ on the hydrogasification of brown coal in a fluidized bed where large increases in both gasification rate and methane yield are obtained by increasing temperatures from 750° C to 950° C (1,742° F). So, based on presently available data, it appears that high-Btu gases can be produced at temperatures at least as high as 1,650° F. Kinetic studies at higher temperature are needed to determine whether heat removal from large reactors will be necessary or if it will simply suffice to provide wall cooling to protect materials of construction.

The danger in applying thermodynamic considerations (especially for extrapolational purposes) to hydrogasification systems becomes clear when one considers that the reactions involved in the production of methane from coal or char are not in any sense reversible and reversibility is a fundamental condition a system must satisfy to give the concept of equilibrium meaning. For example, the reaction



has never been known to occur. Therefore the behavior of hydrogasification systems must be considered to be dictated, at least to a large degree, by the kinetics of the above reaction.

A qualitative kinetic explanation for the behavior of hydrogasification systems is not difficult. For example, the generation of methane from raw coal or char can be represented by the rate equation developed in this paper which shows that the rate of methane formation increases exponentially with temperature up to the highest temperature studied (900° C). Figure 9 as well as data in reference 8 indicates that this increase in hydrogasification rate with temperature extends to 1,200° C. We have already seen that at 900° C methane/hydrogen ratios greatly exceed the ratio required for the formation of β -graphite and that the only effect of methane on hydrogasification rate even at these high methane levels is the reduction in hydrogen partial pressure. This simply means that the carbon deposition reaction



is slow compared to the formation rate of methane in spite of a thermodynamic driving force for the carbon deposition reaction. This could be due to a number of factors such as the lack of catalytic surfaces for deposition to occur on or their rapid poisoning by sulfur and/or nitrogen compounds in the coal.

Table 3.- Final product gas methane concentrations/ from the hydrogasification of raw coal with hydrogen-methane mixtures at 900° C

IHR Run	36		37		38		39		61	
	Feed	Product	Feed	Product	Feed	Product	Feed	Product	Feed	Product
H ₂	48.4	23.0	50.3	15.2	44.6	12.9	44.7	17.3	50.4	18.5
CH ₄ ...	47.7	73.0	46.0	78.7	51.6	81.1	52.1	77.9	45.3	75.5
CO		0.6		2.7		1.8		1.6		1.5
CO ₂				0.2		0.7				
N ₂	3.8	3.3	3.6	2.9	3.8	3.3	3.2	2.9	4.2	4.3
C ₂ H ₆		0.1		0.2		0.2		0.2		0.2
Total ₂ /	99.9	99.9	99.9	99.9	100.0	100.0	100.0	99.9	99.9	100.0

1/ These are experimental values and not the calculated steady state values.

2/ The difference between the total reported and 100 is due to a small amount of oxygen contamination of the samples.

Based on these kinetics, one suspects that the carbon deposition reaction would be most predominant at high carbon conversions, because of the low methane formation rates due to the influence of the $(1-z)$ term, and at long gas phase residence times which give the methane formed time to crack. Both of these conditions can be minimized in continuous systems where carbon conversion levels will probably be on the order of 45 percent and the vapor phase residence time can be kept short. Thus, the continuous system may be able to operate at substantially higher temperatures and methane concentrations than batch systems without encountering appreciable carbon deposition.

Behavior of Experimental Reactor Using Model

Basically, what we have thus far developed is a model that allows the rate of conversion of carbon to be calculated when the environment of the char particles is known. In order to use this model to simulate reactor behavior, we must be able to establish the particle environment as a function of controllable reaction parameters. In the laboratory reactor described we can control feed gas rate G_0 , coal feed rate W_{SO} , temperature T (in a larger adiabatic reactor the temperature would be a function of input variables rather than independently controllable), total pressure P , the composition of the inlet gas, and the length of the reactor (within certain limits). Since we have already established that the flow regime in our reactor is backmixed, the unsteady state methane flux in the reactor is described at operating time t by

$$(6) \quad G_0 y_{m0} - G y_m(t) + W_{SO} f_{CO} z(t) = \alpha V_R dy(t)/dt,$$

where G_0 = feed gas rate, y_{m0} = concentration of methane in the feed gas, G = exit gas rate, $y_m(t)$ = concentration of methane in the exit gas at time t , W_{SO} = coal rate, f_{CO} = molar concentration of carbon in the coal, $z(t)$ = coal carbon conversion level, α = effective gas capacity of the reactor, and V_R = effective reactor volume. Substituting equation (4) into (6) and using the approximate empirical relation

$$y_{H_2}(t) = 0.98 - y_m(t),$$

for the methane-hydrogen mixtures used in these tests give

(7) $G_0 y_{m0} - G y_m(t) + W_{SO} f_{CO} (1 - (1-E) \exp(-kP(0.98 - y_m(t))L/UT)) = \alpha V_R dy_m(t)/dt$, which may be used to simulate unsteady state reactor behavior when G and α are determined. The relation between G and G_0 in terms of λ , W_{SO} , f_{CO} , and z is

$$(8) \quad G = G_0 - (\lambda - 1) W_{SO} f_{CO} z.$$

Figure 10 shows λ , as defined by equation (8), as a function of solid carbon conversion for the raw coal calculated two different ways. The curve determined by the experimental points is based on measured solid carbon conversion and the ratio of inlet/exit gas rates. Average residue and raw coal analyses were used to compute curves (a) and (b). Curve (a) assumes all the coal oxygen consumes hydrogen to form water; curve (b) assumes no hydrogen is consumed by the oxygen in the coal. Also shown are points based on data presented by Pyrcioch and Linden (15) as well as a few points from reference (5) both of which are based on the hydrogasification of pretreated coal. The difference between the curves for raw coal and pretreated coal is of primary economic importance because it reflects the difference in hydrogen consumption required to produce methane from the two feed stocks. The primary reasons for the difference in hydrogen consumption are the H/C atom ratio of the raw coal is about 0.83 while it is only about 0.52 for the pretreated coal and the oxygen content of the raw coal is lower.

As figure 10 indicates, for a raw coal feed at $z < .45$ $\lambda = 1$ so under these conditions $G = G_0$. Equations (7) and (8) together with an estimate of α may be used to simulate the behavior of the experimental reactor. Because of the internal construction of the IHR reactor used to test the simulation model, it is difficult to determine the effective volume for gas mixing and it was therefore necessary to find the value of α from experimental data rather than calculating it from reactor volume, temperature, and pressure. The use of this technique to simulate a typical unsteady state performance of the experimental reactor with hydrogen feed is illustrated in figure 11 by comparing the predicted methane concentration with that measured. Figure 12 shows the simulation of the unsteady state period of some runs using a hydrogen-methane feed gas. Results in figures 11 and 12 indicate that the reactor approaches steady state quicker with hydrogen-methane mixtures than with hydrogen alone. The reason for the lowering of α with increasing methane concentration, which is also indicated in figure 11, is not known but might be due to either the increased density of the gas, causing less transfer of hydrogen-rich hopper gas into the sample system, or due to the lower diffusivity of the mixture which would also result in less transfer between the reactor and insulating shell. Thus, average values of α may be calculated from experimental data and the average α together with equations (7) and (8) can be used to simulate unsteady state behavior of the reactor. However, while simulation of the unsteady-state behavior of the reactor is useful in that it lends credibility to the model, establishes the operating time necessary to approach steady state, and allows experiments to be simulated at conditions not experimentally attainable, it is the steady state behavior of the reactor that is most important. Calculation of steady-state operating parameters is accomplished by simply setting $dy_m(t)/dt = 0$ in equation (7). Steady state behavior in terms of input parameters is then summarized by

$$(9) \quad G_0 y_{m0} - y_{ms} (G_0 - (\lambda - 1) W_{so} f_{CO} z_s) + W_{so} f_{CO} (1 - (1 - E) \exp(-kP(0.98 - y_{ms})L/UT)) = 0,$$

and

$$(10) \quad z_s = 1 - (1 - E) \exp(-kP(0.98 - y_{ms})L/UT),$$

where the subscript s refers to steady state conditions.

CONCLUSIONS

A reaction model for the hydrogasification of raw bituminous coal has been developed. This model is shown to be physically reasonable and to allow for the correlation of char hydrogasification data as well as the data for raw coal. The hydrogasification data indicates that the solid carbon reacts with hydrogen in three definite modes each of which has a different reactivity than the preceding.

The hydrogasification of raw coal is found to have two processing advantages over coal-chars in addition to the savings in pretreatment cost. These are a considerably higher hydrogasification rate than coal-chars and a much lower hydrogen consumption to produce a unit of methane.

Finally, the thermodynamic analogue, which has been widely used to predict desirable conditions for high methane concentrations in hydrogasification processes, is questioned and an alternate approach via kinetics is suggested as a means of determining the relationships between concentrations of gas phase species and the solid phase.

SUMMARY OF NOTATION AND UNITS

θ = the particle residence time at any point in the reactor, hr.

θ_0 = the particle residence time at the reactor exit, hr.

t = the operating time defined as $t = 0$ when the coal feed starts and $t = t_R$ when the coal feed is terminated, hr.

z^* = the instantaneous solid carbon conversion at any point in the reactor, $z^* = z^*(t, \theta)$.

$z(t)$ = the instantaneous carbon conversion at the reactor exit, $z(t) = z^*(t, \theta_0)$.

\bar{z} = the integrated average solid carbon conversion over the run time t .
 z_s = the steady state solid carbon conversion level.
 k = the reaction rate constant, $\text{atm}^{-1}\text{hr}^{-1}$.
 $p_{\text{H}_2}(t)$ = the hydrogen partial pressure in the reactor at time t , atm.
 P = total reactor pressure, atm.
 L = reactor length, ft.
 U_T = particle terminal velocity, ft/hr.
 E = fraction of carbon in coal that is immediately devolatilized.
 N_s = number of carbon atoms in coal, $N_s = f(t, \theta)$.
 N_{s0} = initial number of carbon atoms in coal.
 $y_m(t)$ = mole fraction of methane in exit gas at operating time t .
 y_{m0} = mole fraction of methane in feed gas.
 y_{ms} = mole fraction of methane in exit gas at steady state.
 $y_{\text{H}_2}(t)$ = mole fraction of hydrogen in feed gas at operating time t .
 G_0 = gas feed rate, lb-mole/hr.
 G = exit gas rate, lb-mole/hr.
 W_{s0} = coal feed rate, lb/hr.
 f_{CO} = carbon content of coal feed, lb-mole/lb-coal.
 V_R = effective volume of reactor, cu ft.
 α = effective reactor gas capacity, lb-mole/cu ft reactor.
 λ = a stoichiometric coefficient.

REFERENCES

1. Liversidge, A. Not Enough Gas in the Pipelines. *Fortune*, November 1969; pp. 120-122, 189-190.
2. A Staff Report on National Gas Supply and Demand. Federal Power Commission, Bureau of Natural Gas, Washington, D.C., September 1969.
3. Hiteshue, R. W. The Hydrogasification of Raw Bituminous Coal. Proceedings of the Synthetic Pipeline Gas Symposium, Pittsburgh, Pa., Nov. 15, 1966, pp. 13-23.
4. Levenspiel, O. Chemical Reaction Engineering. John Wiley and Sons, New York, 1962, pp. 261-264.
5. Wen, C. Y. and J. Huebler. Kinetic Study of Coal-Char Hydrogasification - Rapid Initial Reaction. I. & E.C. Process Design and Development, v. 4, No. 2, April 1965, pp. 142-147.
6. Moseley, F. and D. Paterson. The Rapid High-Temperature Hydrogenation of Coal-Chars Part 2: Hydrogen Pressures up to 1,000 Atmospheres. *J. Inst. of Fuel*, Sept. 1965, pp. 378-391.
7. Zahradnik, R. L. and R. A. Glenn. The Direct Methanation of Coal. Fuel Division preprints of the 158th National A.C.S. Meeting, New York, N.Y., Sept. 7-12, 1969, pp. 52-70.
8. Hiteshue, R. W., S. Friedman, and R. Madden. Hydrogasification of High-Volatile A Bituminous Coal, BuMines Rept. of Inv. 6376, 1964.
9. Blackwood, J. D. and D. J. McCarthy. The mechanism of Hydrogenation of Coal to Methane, *Australian Journal of Chemistry*, 1966, 19, 797-813.
10. Lewis, P. S., S. Friedman, and R. W. Hiteshue. High-Btu Gas by Direct Conversion of Coal. Fuel Gasification, Advances in Chemistry 69, A.C.S. Publications, 1967.

11. Zielke, C. W. and E. Gorin. Kinetics of Carbon Gasification. I. & E. C., v. 47, No. 4, April 1955, pp. 820-825.
12. Feldkirchner, H. L. and J. Huebler. Reaction of Coal With Steam-Hydrogen Mixtures at High Temperatures and Pressures. I. & E. C., Process Design and Development, v. 4, No. 2, April 1965, pp. 134-142.
13. Dent, F. J. The Hydrogenation of Coal to Gaseous Hydrocarbons. International Conference on Complete Gasification of Mined Coal, Liege Belgium, May 3-5, 1954.
14. Birch, T. J., K. R. Hall and R. W. Urie. Gasification of Brown Coal With Hydrogen in a Continuous Fluidized-Bed Reactor. J. Inst. Fuel, Sept. 1960, pp. 422-435.
15. Pyrcioch, E. J. and H. R. Linden. Pipeline Gas by High-Pressure Fluid-Bed Hydrogasification of Char. I. & E. C., v. 52, No. 7, July 1960, pp. 590-594.

ACKNOWLEDGMENT

The authors express their appreciation to Miss Cynthia Deitz of West Virginia University for her help in the preparation of the computer programs which were used in this paper.

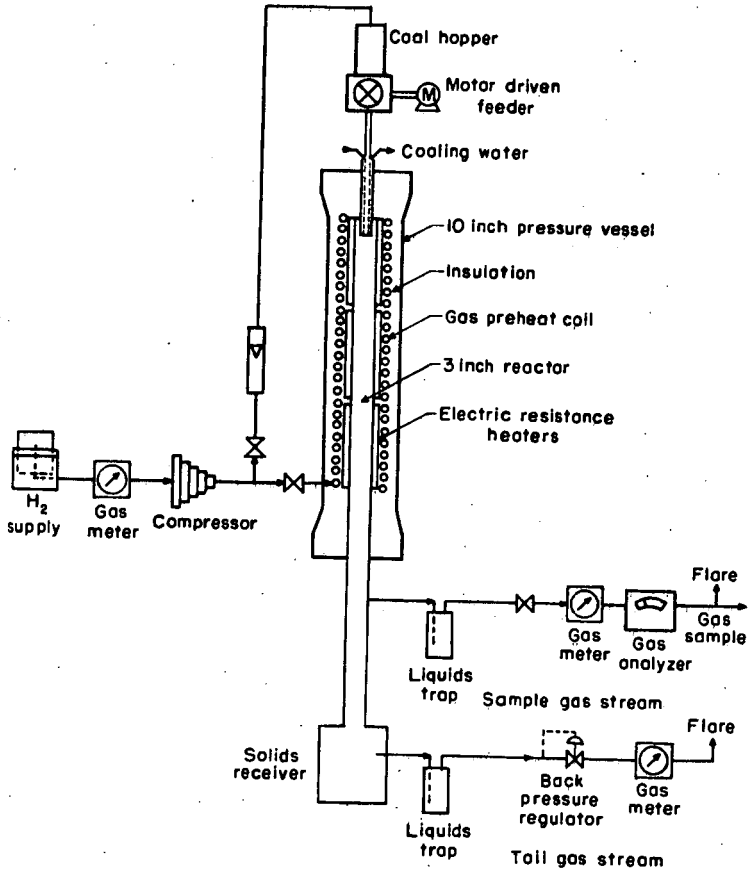


Figure 1—Schematic flowsheet for hydrogasification of coal in dilute phase.

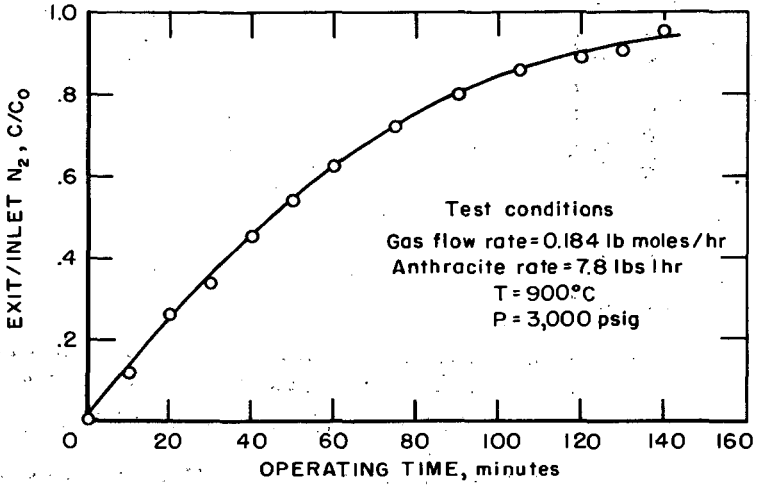


Figure 2-Behavior of the IHR reactor as a mixing vessel

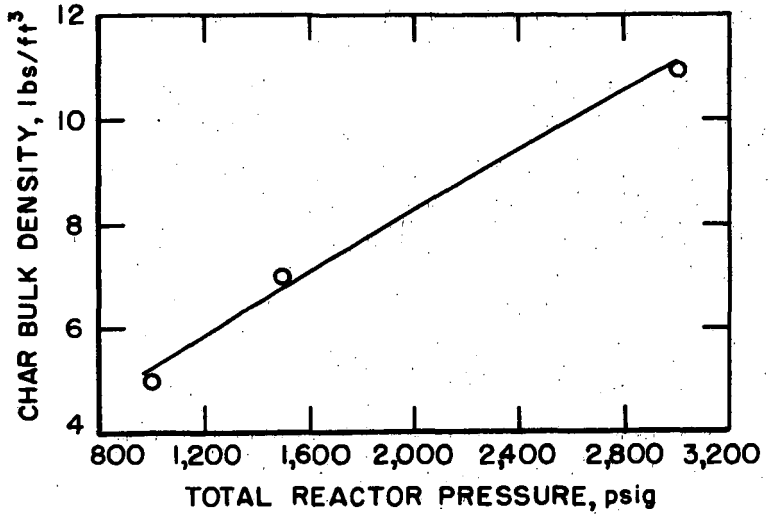


Figure 3-Effect of total reactor pressure on the bulk density of char produced by hydrogasification.

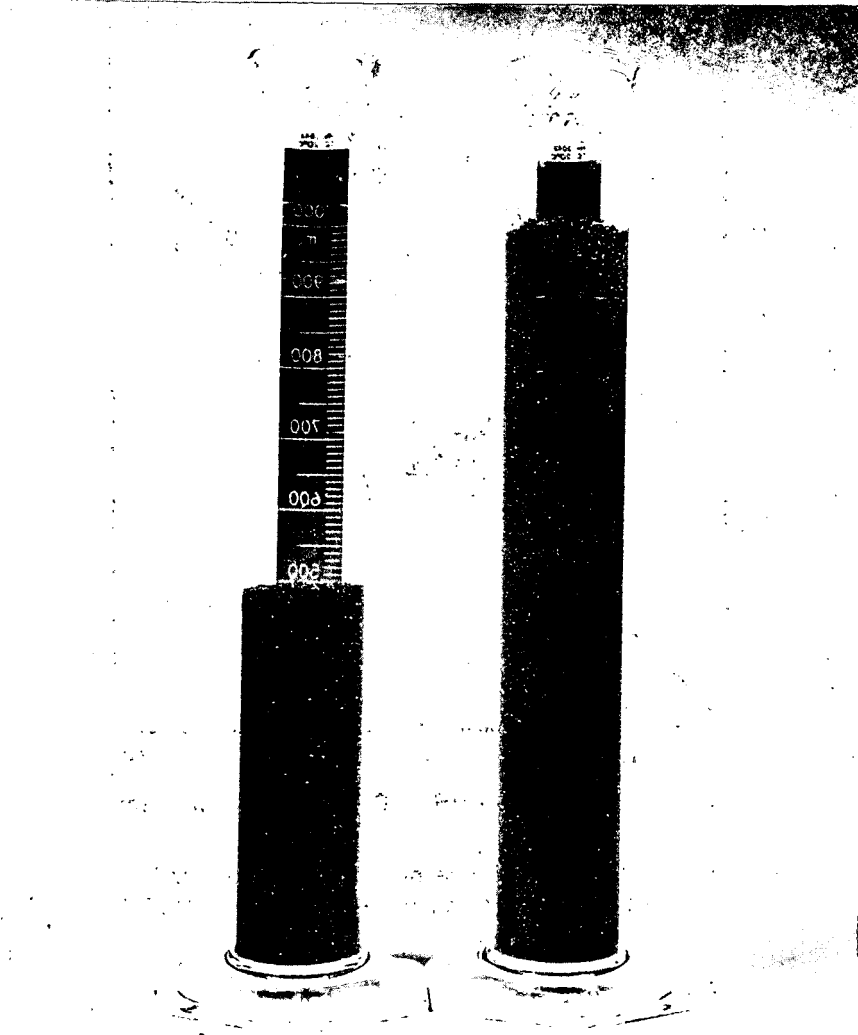


Figure 4 - Effect of pressure on bulk density of dilute-phase char.

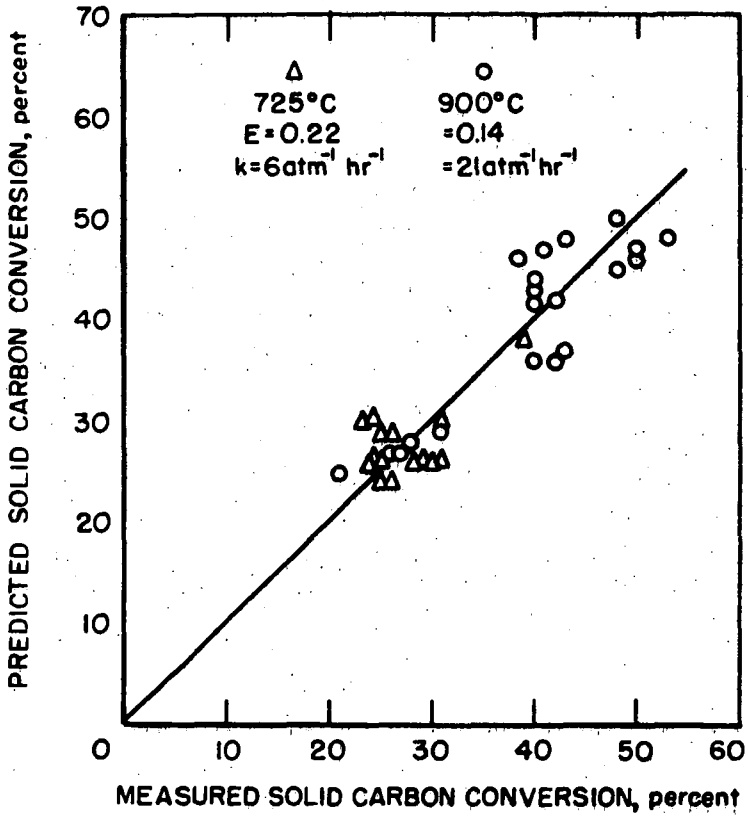


Figure 5-Prediction of average carbon conversion from reaction model at 725° and 900°C.

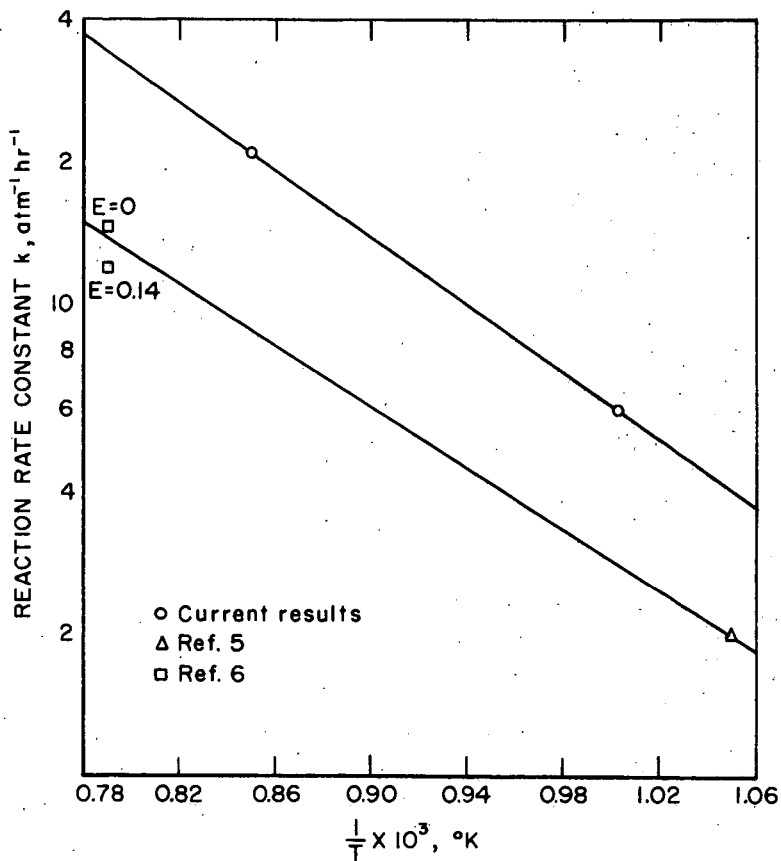


Figure 6—Effect of temperature on hydrogasification reaction rate constant.

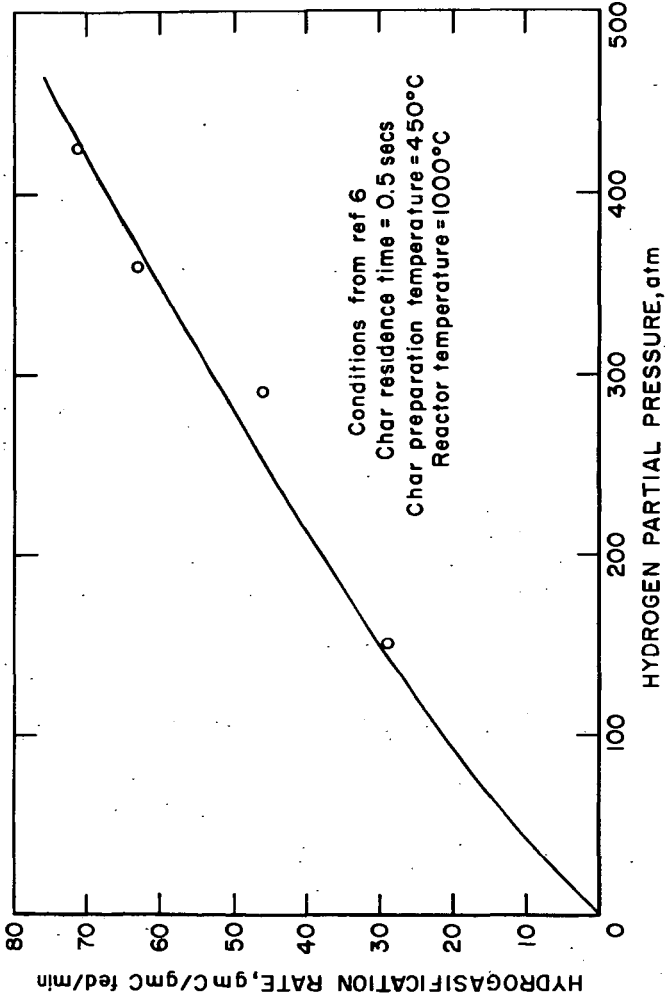


Figure 7 - Comparison of predicted char hydrogasification rate with that measured by Moseley and Paterson (6).

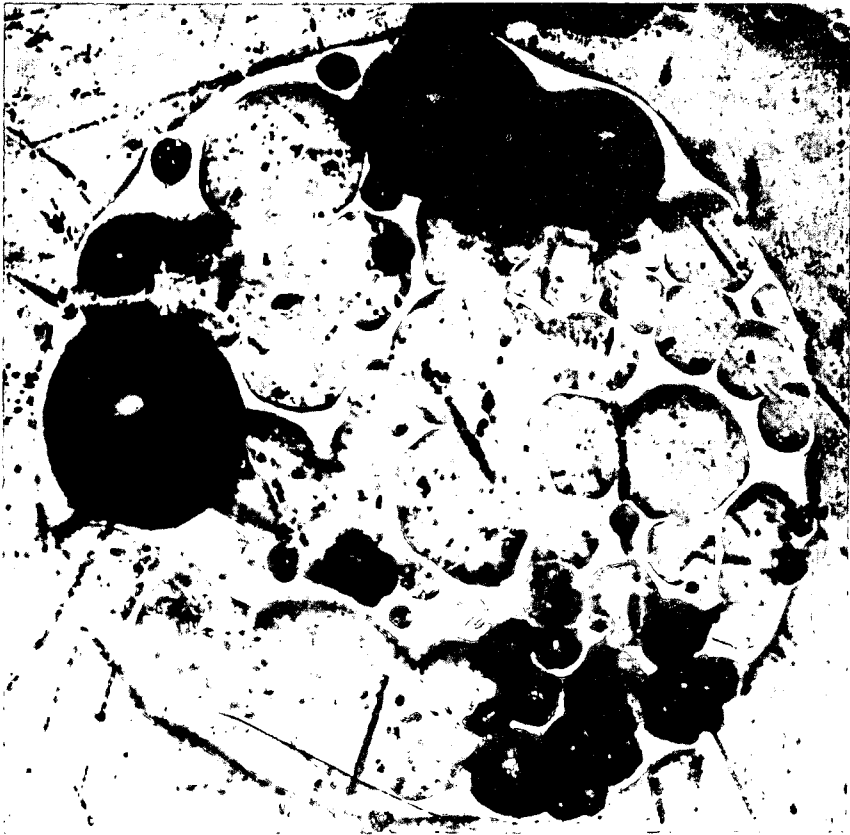


Figure 8-Cross section of char particle
at 220 magnification.

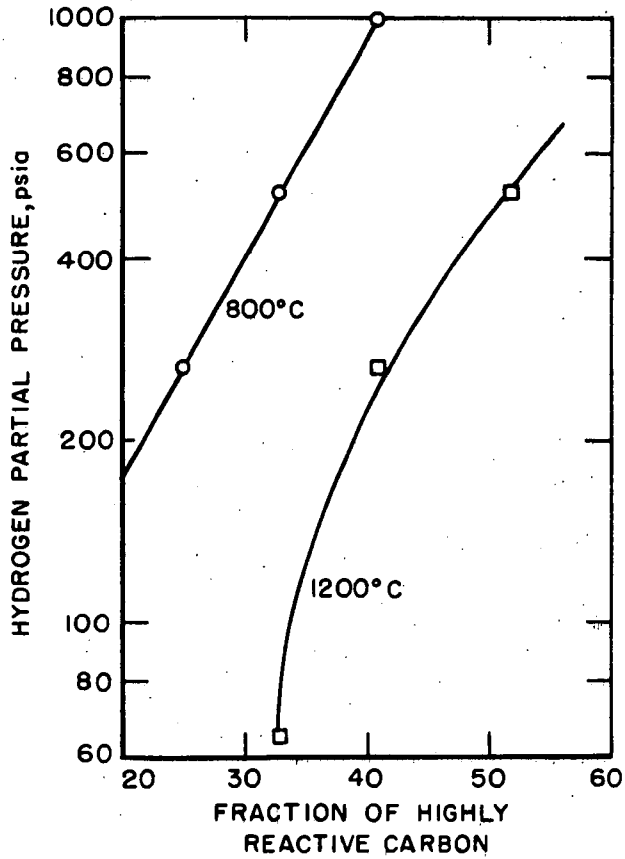


Figure 9 - Effect of hydrogen partial pressure and reaction temperature on carbon reactivity correlated from data presented by Hiteshue et al (8).

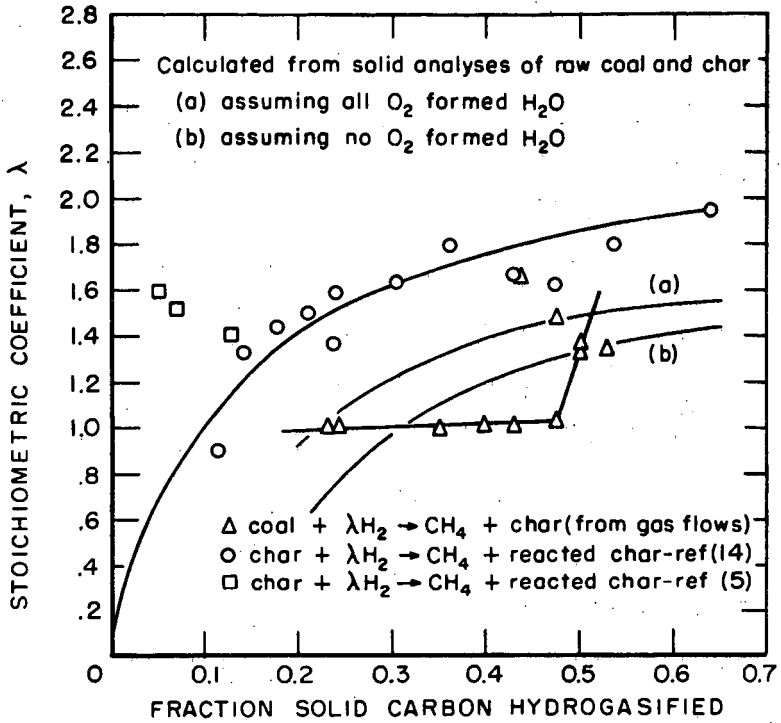


Figure 10-Dependence of the average stoichiometric coefficient for the hydrogasification of coal and char on carbon conversion level.

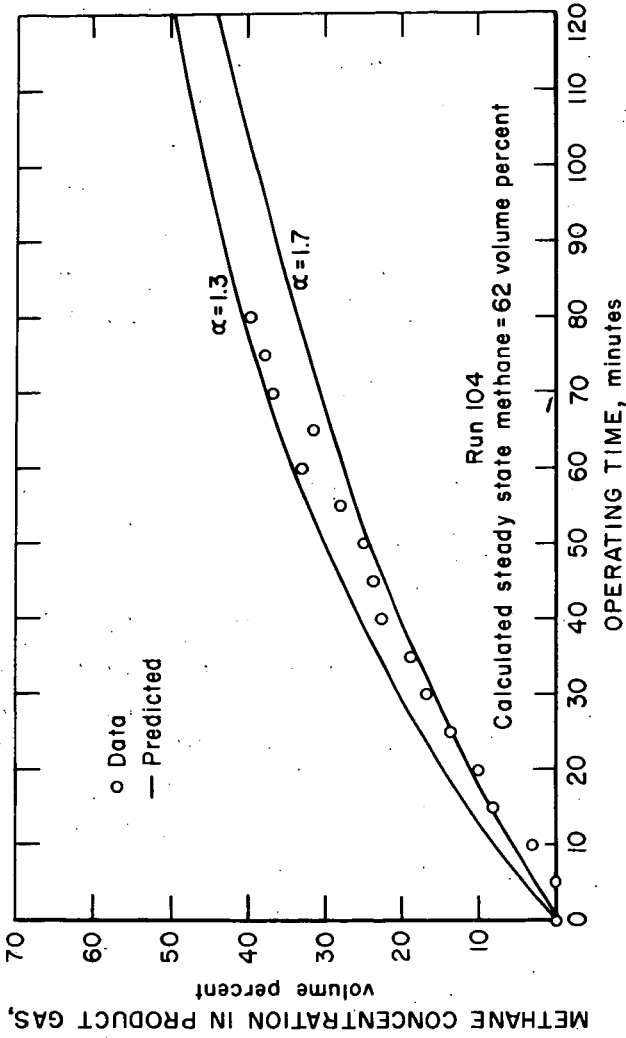


Figure 11- Transient hydrogasifier behavior with hydrogen feed gas at 900°C and 205 atm total pressure.

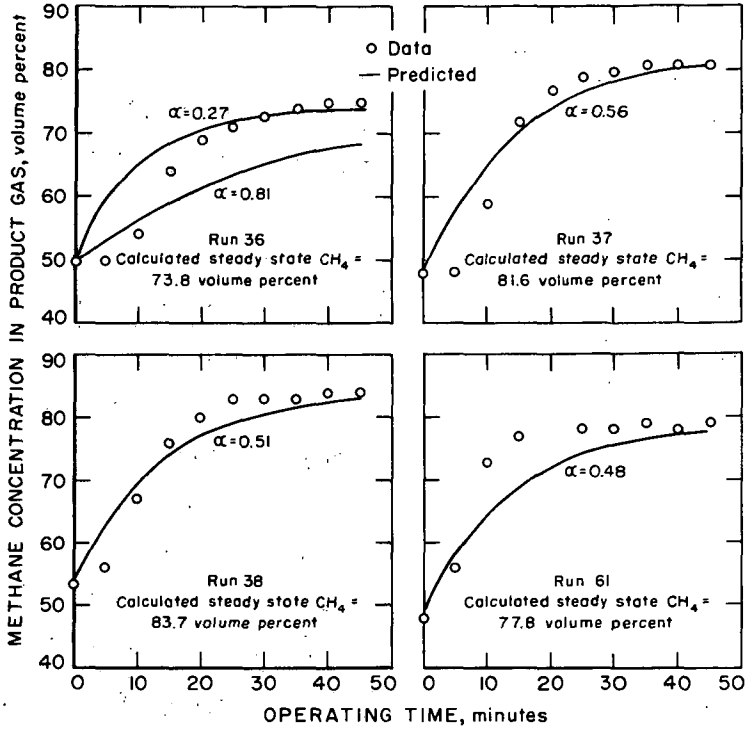


Figure 12- Transient hydrogasifier behavior with methane-hydrogen feed gas at 900°C and 205 atm total pressure.

OPERATION OF A SPRAYED RANEY NICKEL TUBE WALL REACTOR
FOR PRODUCTION OF A HIGH-BTU GAS

W. P. Haynes, J. J. Elliott, A. J. Youngblood, and A. J. Forney
Bureau of Mines, U.S. Department of the Interior
4800 Forbes Avenue, Pittsburgh, Pennsylvania 15213

INTRODUCTION

Almost all processes for the production of high-Btu gas from coal require a clean-up methanation step to upgrade the product gas to a heating value of at least 900 Btu/SCF. Such upgrading is needed both after steam-oxygen gasification of coal and after most processes for hydrogasification of coal. Methanation over a nickel catalyst is one of the most promising methods of achieving the required heating value. A major difficulty in the development of a suitable catalytic methanation reactor is in controlling the temperature of the highly exothermic reaction $3\text{H}_2 + \text{CO} \xrightarrow[400^\circ\text{C}]{\text{Ni}} \text{CH}_4 + \text{H}_2\text{O}$, where the heat of reaction is about 65 Btu/SCF of feed gas converted. Efficient heat removal is required to prevent excessive reaction temperatures and catalyst deterioration.

Catalytic synthesis of methane has been studied in various reactor configurations, such as :

- (a) Fixed-bed reactor, with cooling achieved through heat exchange surface; (1) (2)^{1/}

^{1/} Numbers in parentheses refer to references at end of paper.

(b) Fixed-bed reactor, cooled directly by gas recycle
(3) (4) (5);

(c) Fluidized-bed reactor, cooled indirectly by heat
exchange surface (6) (7); and

(d) Tube-wall reactor, where the catalyst is cooled
because of being integral with or bonded to heat-exchanger
tubes (8) (9).

The bench-scale developmental work performed at the Bureau of Mines on 1.2" and 1.3" outside-diameter single-tube tube-wall reactors has indicated that such reactors, with tubes coated with Raney nickel catalyst, provide excellent temperature control and result in high yields per weight of catalyst of up to 300,000 SCF of high-Btu gas per pound of catalyst (10). Development of the tube-wall reactor, therefore, is proceeding at the pilot-plant level in a multitube reactor unit. The initial experimental work performed in the pilot plant unit is reported in this paper.

Equipment

The tube-wall reactor used in this series of experiments was a multitube unit, as shown in figures 1 and 2. The shell of the reactor is 8-inch, schedule-40 stainless-steel pipe, with an overall length of 11 ft. The unit contains 7 catalyst tubes, each 2 inches in diameter by 7 ft long. The outer surface of each tube is thermally sprayed with Raney nickel over a length of 6 feet and to a depth of

0.020-0.030 inch. Each catalyst tube has a 1-inch diameter dip-tube down the center. Liquid Dowtherm* passes down the dip-tube and then boils as it passes upward through the annulus to remove the heat of reaction. The Dowtherm vapor enters the condenser above, is indirectly cooled and condensed with water, and then by gravity feeds back into the center tube. To achieve good contact between gas and catalyst, the coated lengths of the sprayed tubes are baffled so that the synthesis gas, as it passes upward through the reactor, is forced by the horizontal baffles to take a tortuous path across the tube surfaces.

Thermocouple wells were mounted along the length of the catalyst surface of four tubes. Three thermocouples were placed in each well and were spaced 2 feet apart. A calibrated and motorized drive moved these thermocouples a total of 2 feet to permit measurement of catalyst temperatures in 1-inch increments along the entire 6-foot length of each of the four tubes.

A schematic flowsheet of the reactor system is shown in figure 3, where it is shown that the feed gas to the reactor is preheated by a series of three heat exchangers. The first exchanger is steam-heated, the second exchanger recovers sensible heat from the hot product gas, and the third is heated by Dowtherm vapor. Product water is condensed from the product gas stream; then part of the dry product gas is returned to the feed gas stream. Recycle of dry product gas reduces

* Reference to trade names is made to facilitate understanding and does not imply endorsement by the Bureau of Mines.

the water vapor concentration of the reaction gas and thereby helps to maintain the activity of the catalysts as well as increase the yield of methane (10).

Fresh synthesis gas is made from natural gas in a Girdler plant and stored in 60,000 ft³ holders until needed. The gas then is compressed to 500 psi, passed through a silica gel trap for dehumidification, then through two charcoal traps in series to remove sulfur compounds. A continuous analyzer records the sulfur concentration in the feed gas which is maintained below 0.1 grain H₂S/1000 SCF. Analyses of fresh gas and product gas were performed by mass spectrometry and gas chromatography. Impurities O₂, N₂, and CO₂ were present in the fresh synthesis gas in the range of 0.1, 0.4, and 0 to 1 percent, respectively.

Operation

After the reactor system was assembled and leak-tested, the Raney nickel catalyst (42% Ni + 58% Al) was activated in place by treatment at 90° C temperature with 2 wt pct sodium hydroxide solution. After the aluminum was leached to the extent desired, as indicated by measurement of hydrogen evolution, the caustic solution was displaced with water, and the catalyst was washed with 20 gal per hr of cold tap water for about 24 hours. Distilled water was then used until a reasonably constant pH was attained in the wash water. In experiment TWR-1, a pH of 5.7 was reached after 48 hours washing; in experiment TWR-2, a pH of 9.0 was reached after 45 hours. These values were about 0.2 above pH of the fresh distilled water. After the water was drained, the activated catalyst was kept under a hydrogen

atmosphere until synthesis gas was fed to the reactor. The amount of aluminum digested was 85 percent in the first experiment and 50 percent in the second experiment. Catalyst in experiment TWR-2 was activated an additional 20 pct after 964 hours operation.

After activation of the catalyst, the unit was brought to operating pressure and temperature under an atmosphere of hot recycling hydrogen. Before the synthesis gas was admitted to the system, catalyst tube surface temperatures ranged from 325° to 339° C in experiment TWR-1 and from 369° to 387° C in experiment TWR-2.

Synthesis gas was fed into the system which was then brought to desired steady-state conditions by adjustment of gas flows, reactor pressure, and catalyst temperature. A minimum synthesis temperature of 390° C was reached within 5 hours in experiment TWR-1 and within 1 hour in experiment TWR-2.

Results

Most of the operating conditions over the length of experiments TWR-1 and TWR-2 are shown in figures 4 and 5. Heating values of the N₂-, O₂-free dry product gas are shown. Values of the H₂:CO ratio of the feed gas are not shown, but they ranged from 2.27 to 3.35.

Additional data, including H₂/CO ratios, conversions, product gas analysis, and yields, at selected times in experiments TWR-1 and -2 are presented in tables 1 and 2. The average temperatures shown

in tables 1 and 2 represent the average of temperatures of 4 tubes at some common distance from the gas inlet determined to be the hottest point in the reactor. The maximum temperatures are plotted in figures 4 and 5.

Discussion of Results

General Performance

The length of experiment TWR-1 was 338 hours. During the initial 100 hours of operation at a feed rate of 600 SCFH and maximum catalyst temperature of 398° to 401° C, the heating value of the product gas gradually decreased from 950 to 910 Btu/SCF^{2/}. This decrease indicated that the catalyst immediately began to lose activity. Overall loss of catalyst activity by the end of the experiment was so great that the heating value of the product gas fell to 720 Btu/SCF when the feed rate was 600 SCFH and maximum catalyst temperature was 403° C.

The length of experiment TWR-2 was 1055 hours, including the hours of synthesis after the second activation; this indicates that loss of catalyst activity was much slower than in the case of test TWR-1. After 675 hours of operation, product gas of 900 Btu per SCF heating value was being produced at 402° C maximum catalyst temperature, 300 psi, and 600 SCFH fresh feed rate. The increase in catalyst life in experiment TWR-2 is attributed to the repression of nickel carbide formation which is discussed later.

^{2/} Heating values are based on N₂-O₂-free gas with SCF taken at 60° F, 30 in. Hg. and dry.

The second activation of the catalyst in experiment TWR-2 improved the catalyst activity significantly, as is indicated by resultant increases in the heating value of the product gas. For example, as shown in figure 5, before the second activation at 964 hours, the product gas heating value was 690 Btu/SCF for a feed gas rate of 2400 SCFH; after the second activation and at 1055 hours, the heating value increased to 765 Btu/SCF for the same feed gas rate. The catalyst life in experiment TWR-2 might have been longer had the catalyst been activated to 70 pct initially rather than 50 pct. Dirksen and Linden (6) indicated that at activation of at least 65 pct of the catalyst is required for long catalyst life.

Although the system had charcoal traps to remove organic sulfur from the fresh synthesis gas, sulfur concentrations of up to 0.8 wt pct were determined on samples of the used catalyst in experiment TWR-2. This suggests that sulfur poisoning contributed to the decrease in catalyst activity.

Heat removal and control of catalyst temperature by means of the Dowtherm coolant was excellent. In both experiments, there were no runaway temperatures at any time.

Conversion and Gas-Feed Rate

As shown in tables 1 and 2, in the first part of experiment TWR-1, conversion of $\text{CO} + \text{H}_2$ was as high as 99 pct at a gas feed rate of approximately 600 SCFH; and 97.9 pct at approximately 1200 SCFH. In comparison, conversion of $\text{CO} + \text{H}_2$ during the early part

of experiment TWR-2 was lower; for example, at 71 hours conversion was 95.5 pct at about 1200 SCFH feed gas rate. This relatively lower conversion in experiment TWR-2 was caused by the excess of hydrogen in the feed gas, as shown by the $H_2:CO$ ratios greater than 3:1. Such hydrogen excess lowers the heating value of the product gas by acting as a diluent, but at the same time, favors CO usage.

The comparatively lower values of CO in the product gas of experiment TWR-2 are notable. Such high usage of CO is desired because it represses carbide formation, indicates good catalyst activity, and provides a pipeline gas of low toxicity.

As gas feed rates were increased to about 2400 SCFH or 106 SCFH per sq ft catalyst surface, CO + H_2 conversion decreased significantly. For example, in experiment TWR-2 at 71 hours and 267 hours, respectively, conversion dropped from 95.5 pct at 1216 SCFH feed rate to 89.4 pct at 2432 SCFH feed rate. This performance is considerably lower than that achieved in earlier bench-scale experiments (10) on a single-tube tube-wall reactor where conversions of greater than 98 pct were sustained for more than 1200 hours at gas feed rates of 105 SCFH per sq ft catalyst surface. Two other possible reasons (in addition to the presence of excess hydrogen) for the lower performance in the multitube reactor are that diffusional distances from the bulk gas to the catalyst surface for the multitube unit were several-fold greater than for the single tube unit and that turbulent mixing in the large multitube unit was poorer than in the

highly baffled bench-scale unit. Future modifications to the multi-tube reactor will improve these two factors.

Carbide Formation

In experiment TWR-1, formation of nickel carbide and flaking of the catalyst from the surface are suspected of contributing to the rapid decline in catalyst performance. Nickel carbide formation was verified by X-ray analyses of samples scraped from the surface of the spent catalyst tubes. The analyses showed in order of declining abundance: Ni_3C ; Ni; aluminum nickel catalyst (cubic F.C.); and Ni_xC ($x > 4$). Nickel carbide predominated at both the gas outlet and inlet ends of the catalyst tubes and in catalyst particles accumulated in the reactor bottom. Formation of nickel carbide was the result of too much exposure of the catalyst to CO at temperatures favoring carbide formation, less than 370° C.

Experiment TWR-2 was conducted with the aim of repressing carbide formation and achieving higher catalyst performance than was achieved in TWR-1. One step taken to minimize carbide formation was to get the catalyst temperature above the carbide formation region as soon as possible (within 1 hour) during start of synthesis and to maintain the catalyst temperature above 390° C throughout synthesis. The quick start-up was achieved by preheating the reactor and feed gas to higher temperatures than those used in experiment TWR-1. Another step

taken to inhibit carbide formation was to use a feed gas that contained excess hydrogen. These approaches proved effective, as shown by X-ray analyses of the catalyst surface at the conclusion of the experiment. Free nickel was the major constituent found on the catalyst surface, while nickel carbide (Ni_3C) was found to a lesser extent. No carbide was found at the gas outlet end of the catalyst tubes.

Catalyst Bonding

Inspection of the tube bundle at the conclusion of test TWR-1 showed that large segments of the catalyst had flaked from the tubes. Figure 6 is a photograph of a section where flaking occurred. Such flaking was not evident at the end of test TWR-2. A suggested explanation of the more stable bond in test TWR-2 is that the lower percent activation of the catalyst with caustic solution resulted in less initial disturbance of the bond between catalyst and tube than had occurred in test TWR-1.

Temperature Profile and Heat Removal

Temperature profiles measured along the catalyst tubes indicated that the amount of reaction occurring along the length of the catalyst tubes was dependent upon the following: velocity and direction of gas flow, distance from point of gas entry, and location of baffle plates.

Figure 7 shows a typical temperature profile of one of the catalyst tubes (tube F) in experiment TWR-1 after 50 hours of operation; feed gas rate is about 600 SCFH and recycle ratio is 1:1. The direction of gas flow was parallel, rather than normal, to the tube surface at the points of temperature measurement. On tube F, temperature peaks generally coincide with the location of a baffle plate. Temperature profiles of some of the other tubes showed peak temperatures at every other baffle plate. No satisfactory explanation of these patterns has been established. It has been noted that average tube temperatures may vary by up to 5° C from tube to tube.

Dowtherm temperatures remained relatively constant along the length of the catalyst tube. Typically, at 532 hours operation in experiment TWR-2, Dowtherm temperatures as measured in tube G were 386° C at the bottom, 386° C at the middle, and 387° C at the top. This indicates that Dowtherm circulation was good. Based on a heat release of 65 Btu per SCF synthesis gas converted during the 532-hour period and a difference of 18.2° F between the average tube surface temperature and the average Dowtherm temperature, the calculated overall heat transfer coefficient of the reactor is 182 Btu per hour per sq ft per ° F. This is of the same magnitude as the value of 275 Btu per hr per sq ft per ° F reported for a 3-ft single tube bench-scale unit (10).

Conclusion

A pilot-plant size tube-wall methanation reactor has been operated satisfactorily in two tests, providing excellent temperature control and needing a modicum of gas recycle. Catalyst life and yields of product gas were not as great as those achieved in previous bench-scale tests. However, use of higher temperatures and excess hydrogen in the second test inhibited carbide formation and increased catalyst life significantly over that of the first test. In future tests, a further increase in catalyst life should be achieved by a more rigorous removal of sulfur from the feed gas and a more complete activation of the catalyst. A satisfactory 900 Btu per SCF product gas was yielded at a specific feed rate of about 54 SCFH per sq ft catalyst. A reduction in excess hydrogen fed to the reactor and, possibly, an improvement in contacting of the gas and catalyst are needed to yield a satisfactory product gas at the higher gas feed rate of 105 SCFH per sq ft of catalyst surface, formerly achieved in the Bureau of Mines bench-scale units.

TABLE 1. - Selected operating results at various times in Experiment TWR-1

Synthesis, hours.....	22	48	145	192	312	336
System pressure, psig	300	300	300	300	400	400
Fresh gas rate, SCFH	677	607	1214	2383	1213	614
Fresh gas/catalyst area, SCFH/ft ²	30.1	27.0	54.6	106.2	54.0	27.3
Vol. recycle/vol. fresh gas,..	0.86	0.87	1.11	1.04	1.94	1.97
Vol. product gas/vol. fresh gas	0.27	0.267	0.276	0.406	0.406	0.343
H ₂ /CO in fresh gas.....	2.40	2.43	2.93	2.59	2.59	2.73
Catalyst temperature, ° C:						
Average	380	393	399	398	398	400
Conversion, pct:						
H ₂	99.0	98.8	97.0	76.5	77.8	86.2
CO	98.7	100.0	99.8	78.0	72.2	85.5
CO + H ₂	99.0	99.0	97.9	76.9	75.9	86.0
Product gas composition, vol. pct (N ₂ -free):						
H ₂	2.9	3.5	7.9	42.2	38.1	28.5
CO	1.3	0.0	0.2	14.2	21.2	12.4
CO ₂	3.6	4.8	3.8	3.0	2.4	1.3
CH ₄	92.2	91.7	88.1	40.2	38.2	57.7
C ₂ H ₆	--	--	--	0.4	0.1	0.1
Product gas heating value, Btu/SCF <u>1</u> /.....	948	941	919	598	581	720
Product water, lb/hr	4.17	3.91	14.5	13.3	11.4	5.45

1/ SCF based on 60° F and 30 in. Hg., dry

TABLE 2. - Selected operating results from Experiment TWR-2

Synthesis, hours.....	71	167	267	387	508	532	731	916	922
System pressure psig	300	300	300	300	300	300	300	400	400
Fresh gas rate, SCFH	1217	2388	2432	2419	604	1217	1222	1213	1218
Fresh gas/catalyst area, SCFH/ft ²	54.2	106.5	108.3	107.8	27.0	54.3	54.4	54.1	54.3
Vol. recycle/vol. fresh gas....	2.0	1.0	0.99	1.01	2.96	1.47	0	2.00	0
Vol. product gas/vol. fresh gas	0.251	.309	.341	0.345	.280	0.296	0.319	0.307	0.324
H ₂ /CO in fresh gas	3.18	3.02	3.34	3.35	3.09	3.09	2.93	3.16	2.93
Catalyst temperature, ° C: Average	406	407	408	411	405	408	405	406	408
Conversion, pct:									
H ₂	94.0	92.7	86.0	85.0	94.4	92.9	89.3	91.4	89.6
CO	100	99.3	100	99.4	100	100	100	96.4	100
CO + H ₂	95.5	95.4	89.4	88.6	95.7	94.6	88.1	92.7	92.3
Product gas composition, vol. pct. (N ₂ -free):									
H ₂	18.0	17.9	30.9	32.8	15.3	18.2	24.2	20.5	23.5
CO	---	0.5	---	0.4	---	---	---	3.1	---
CO ₂	0.2	1.2	0.8	0.9	.3	1.3	3.5	3.0	2.8
CH ₄	81.8	79.1	68.3	65.9	84.4	80.5	72.3	69.1	73.5
C ₂ H ₆	---	---	---	---	---	---	---	---	0.2
Product gas heating value, Btu/SCFH ₁	887	861	792	775	905	875	811.1	777	825
Product water, lb/hr	12.1	25.7	26.5	25.4	6.59	13.3	10.4	15.8	10.8

1/ SCF based on 60° F and 30 in. Hg. dry

LITERATURE CITED

1. Dent, F. J., and D. Hebden. The Catalytic Synthesis of Methane as a Method of Enrichment in Town Gas Manufacture. Gas Res. Board Comm. GRB 51, 1949, 41 pp.
2. Dirksen, H. A., and H. R. Linden. Pipeline Gas From Coal by Methanation of Synthesis Gas. Inst. Gas Technol. Res. Bull. No. 31, July 1963, 137 pp.
3. Dent, F. J., L. A. Moignard, A. H. Eastwood, W. H. Blackburn, and D. Hebden. An Investigation into the Catalytic Synthesis of Methane for Town Gas Manufacture. Gas Res. Board Comm. GRB 20/10, 1945, 103 pp.
4. Forney, A. J., R. J. Demski, D. Bienstock, and J. H. Field. Recent Catalyst Developments in the Hot-Gas Recycle Process. U.S. Bureau of Mines Rept. of Inv. 6609, 1965, 32 pp.
5. Wainwright, H. W., G. C. Egleson, and C. M. Brock. Laboratory-Scale Investigation of Catalytic Conversion of Synthesis Gas to Methane. U.S. Bureau of Mines Rept. of Inv. 5046, 1954, 10 pp.
6. Dirksen, H. A., and H. R. Linden. Pipeline Gas by Methanation of Synthesis Gas Over Raney Nickel Catalyst. Ind. Eng. Chem., vol. 52, No. 7, July 1960, pp. 584-589.
7. Schlesinger, M. D., J. J. Demeter, and M. Greyson. Catalyst for Producing Methane From Hydrogen and Carbon Monoxide. Ind. Eng. Chem., vol. 48, No. 1, January 1956, pp. 68-70.

8. Gilkeson, M. M., R. R. White, and C. M. Sliepcevich. Synthesis of Methane by Hydrogenation of Carbon Monoxide in a Tubular Reactor. Ind. Eng. Chem., vol. 45, No. 2, February 1953, pp. 460-467.
9. Field, J. H., and A. J. Forney. High-Btu Gas via Fluid-Bed Gasification of Caking Coal and Catalytic Methanation. A.G.A. Proc. of Synthetic Pipeline Gas Symposium, 1966, pp. 83-94.
10. Demeter, J. J., A. J. Youngblood, J. H. Field, and D. Bienstock. Synthesis of High-Btu Gas in a Raney Nickel Coated Tube-Wall Reactor. U.S. Bureau of Mines Rept. of Inv. 7033, 1967, 17 pp.



Figure 1. Catalyst Tubes and 8-inch Shell of Multitube Methanation Reactor

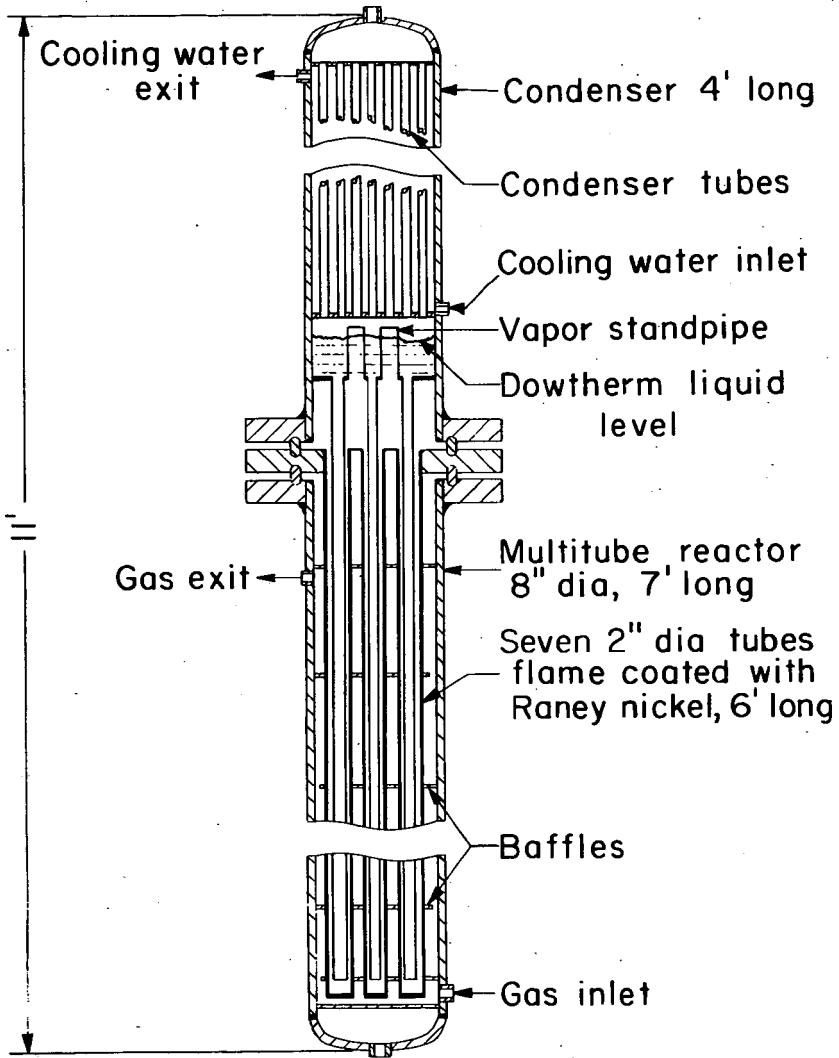


Figure 2. Multitube Reactor for Synthesis of High-Btu Gas

2-3-66

L-9196

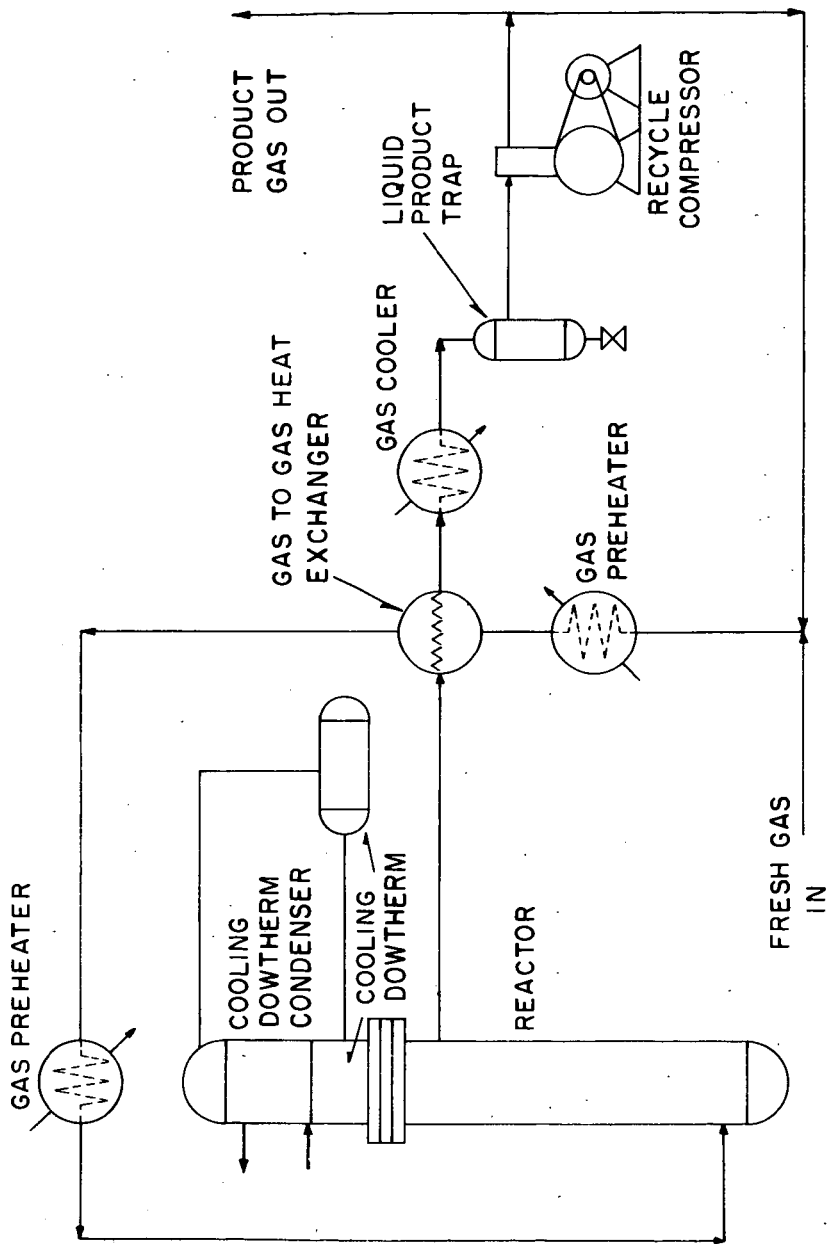


Figure 3. Schematic of Multitube Reactor Pilot Plant for Making High-Btu Gas

L-11288

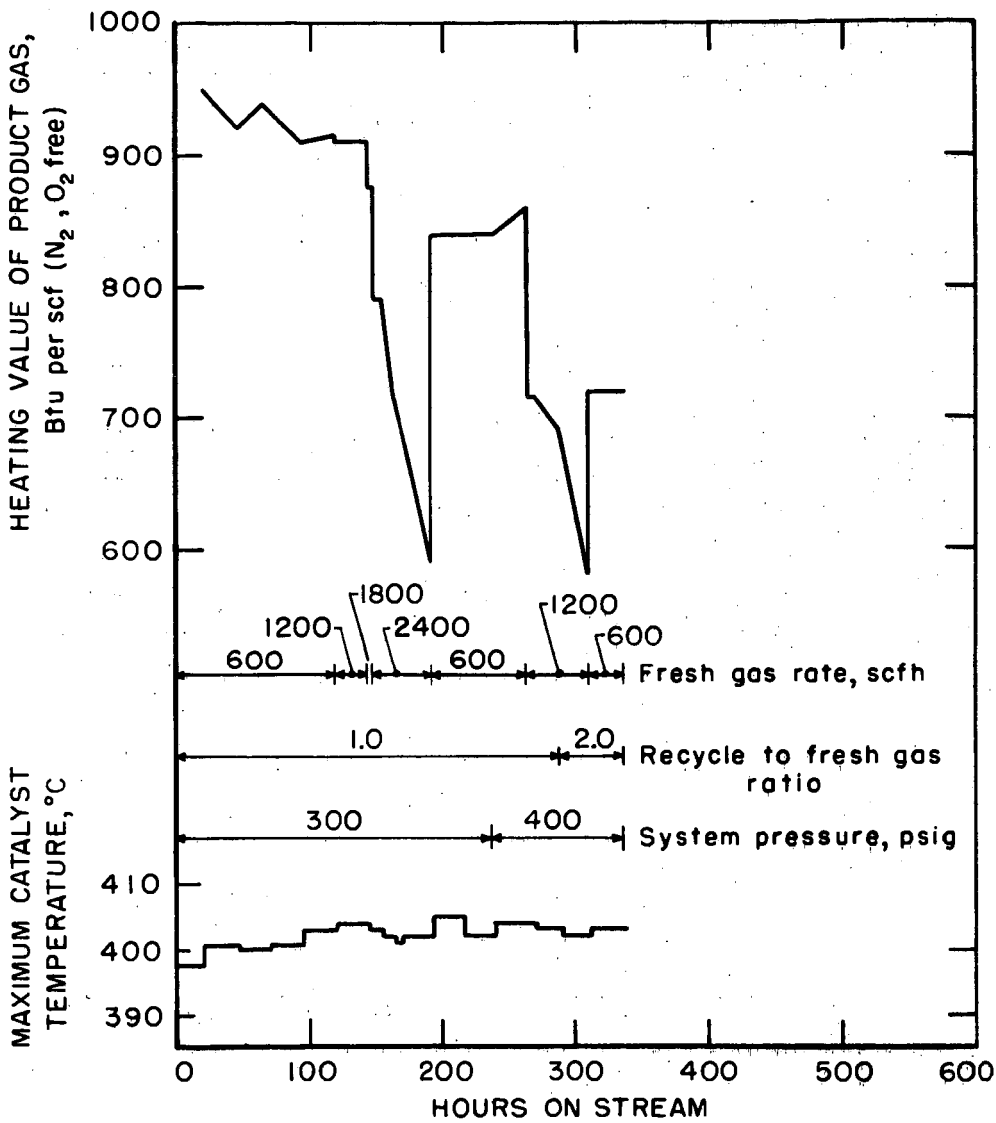


Figure 4. Operating Conditions - Experiment TWR-1

L-11554

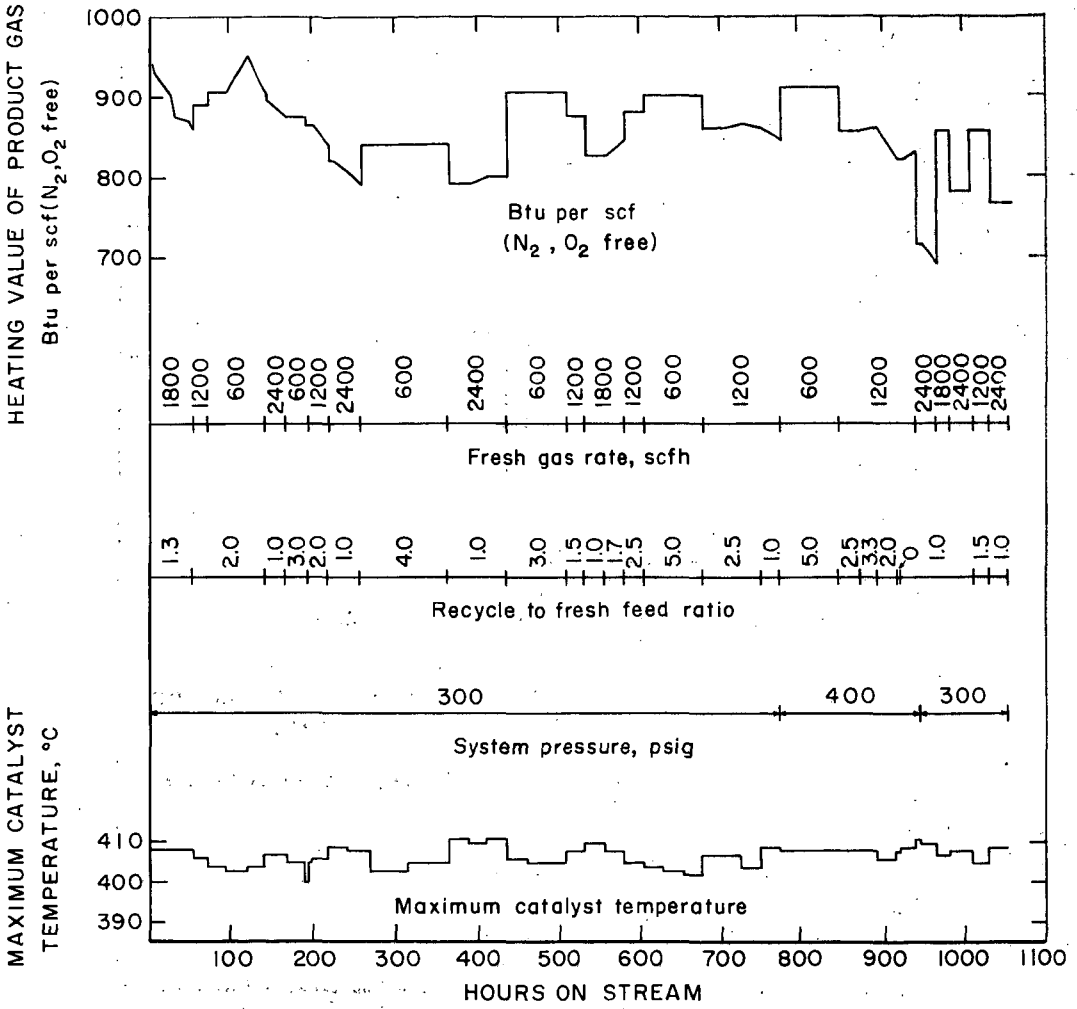


Figure 5. Operating Conditions - Experiment TWR-2



Figure 6. Section of Reactor Where Flaking Occurred

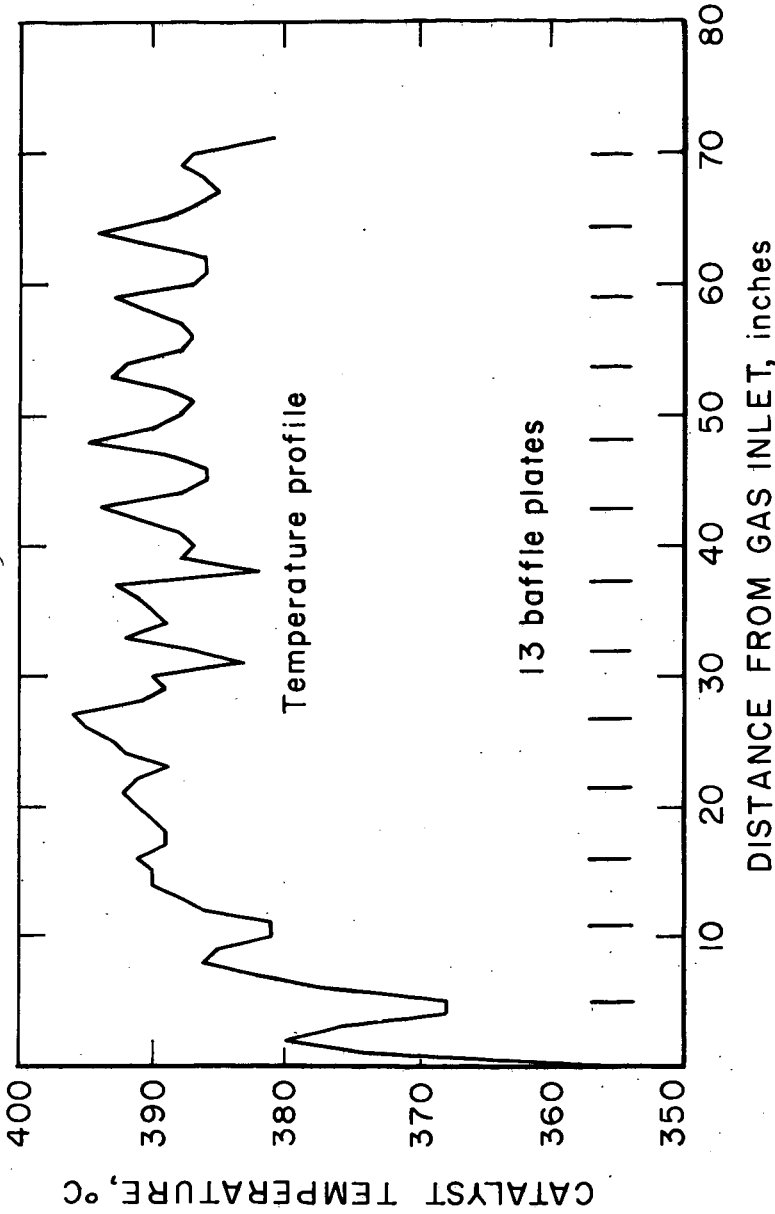


Figure 7. Temperature Profile of Tube F at 50 Hours Synthesis, Experiment TWR-1; and Location of Baffle Plates

L-11628

DESULFURIZATION OF RESIDS

H. D. Radford and R. G. Rigg

Research and Development Department, American Oil Company, Whiting, Indiana

INTRODUCTION

For the past several years there has been an increasing incentive to develop suitable technology for removing sulfur from petroleum residua(1,2,3,4,5). New York City now specifies a 1.0% maximum allowable sulfur concentration for its fuels(6), and similar restrictions have been, or soon will be, adopted in other metropolitan areas. However, typical sulfur concentrations in the residua from several important crude sources are:

<u>Crude Source</u>	<u>Characteristics of Resids</u>		
	<u>Type</u>	<u>Vol% on Crude</u>	<u>Wt% Sulfur</u>
Domestic	Vacuum	0 - 20	1.0 - 4.0
Caribbean	Atmospheric	56	2.6
Middle East	Atmospheric	50	2.5 - 5.0

Consequently, the need for desulfurized fuels is expected to increase rapidly in the near future.

Anticipating this need, American Oil Company has developed a fixed-bed catalytic hydrodesulfurization process that is now ready for commercialization. Among its unique features is a stable catalyst that resists poisoning by sulfur, nitrogen, metals, coke-forming materials, and other troublesome constituents of residua.

The process was developed in various bench-scale units, and then commercial feasibility was demonstrated in a fully integrated pilot plant having a maximum feed rate of 2 B/SD. Whenever possible, experimental runs were designed to simulate all operations required in a full-scale unit. As a result, the evaluations cover the effects of anticipated variations in catalyst performance and life, types of feedstocks, and desired desulfurization levels. Work has also been started on a process model for the prediction of plant size and process conditions for the most economical desulfurization of any given feed.

EXPERIMENTAL

Equipment

Figure 1 typifies the bench-scale units. The smaller ones have reactors varying in capacity from 20 to 250 cc of catalyst with allowable pressures up to 3500 psig. Operations were based on once-through gas and oil flow, batch-type product accumulation, and continuous gas release. Larger units capable of containing 1000 cc of catalyst and having gas scrubbing and recycle systems were also used.

The 2-B/SD pilot plant is shown schematically in Figure 2. The reactor section, which is 30 feet long and has an internal diameter of 2 inches, allows mass velocities about 50% as high as those anticipated for commercial design. Operation is adiabatic. Several separately controlled gas quenches are located along the reactor wall for the automatic injection of cooling gas to compensate

for the temperature rise in individual catalyst beds. A traveling thermocouple passes axially through the reactor to measure the complete temperature profile within the beds. A typical profile is shown in Figure 3.

The pilot plant also includes separators and fractionating towers. The only inputs are raw residual oil, hydrogen, and water for cooling and gas-scrubbing. Outputs are a desulfurized and stabilized residual oil, a naphtha fraction, and a gas stream which is continuously monitored by gas chromatography. In addition, the plant contains its own gas recycle and scrubbing facilities and is typically operated on pressure control. Only enough fresh hydrogen is added to compensate for hydrogen consumption and solubility losses.

Feedstocks

Table I lists the properties of typical resids and crudes used in the process evaluations. They cover a wide range of processing difficulty. The atmospheric resids from the Middle East are examples. Those designated B (Kuwait) and C are comparatively high-gravity, low-viscosity materials that are relatively easy to process. At the other extreme, Resid A is highly viscous, contains 5.2 wt% sulfur and 18-20 wt% asphaltenes (heptane insolubles), and has a 9.5°API gravity.

CATALYST EVALUATIONS

Over 140 possible catalysts were evaluated for the process. Criteria included:

1. low cost
2. high initial activity for removing sulfur
3. good activity maintenance
4. ability to resist poisoning by sulfur, nitrogen, metals, and other harmful constituents of petroleum resids.

The catalyst selected appears to have an optimum combination of the above attributes.

The deposition of metallic contaminants, especially vanadium and nickel, within the catalyst structure can be an especially severe problem in desulfurization processes. Hence, particle size is important; the most satisfactory catalysts have a high ratio of external surface area to total volume within the limitations of pressure drop considerations.

During some evaluation runs, the accumulation of vanadium and nickel in used catalyst particles was great enough to almost double the original weight of the fresh catalyst. However, the higher concentration of metals was always found near the outer surface, and considerable internal volume of the catalyst particle still had only a small concentration of metals. The distribution of metals longitudinally through the catalyst bed also showed a distinct pattern. Catalyst particles removed from the lower zone always contained considerably less vanadium and nickel than those taken from the top zone adjacent to the feed entrance.

Coke formation was never a problem when proper temperature profiles and hydrogen partial pressure were maintained in the reactor system. In

contrast to the deposition pattern of metals, carbon was fairly evenly distributed throughout the catalyst particle.

PROCESS PARAMETERS

Production of a material containing only 1 wt% sulfur from any given feedstock was the criterion for success in the application of the process. However, the feedstock itself strongly influences the process severity required to reach a given level of desulfurization.

With suitable variations in process conditions, all the feedstocks in Table I were desulfurized to the desired level. Table II shows typical data for Resids A and C, where the yields correspond to the production of a 1 wt% sulfur, 350+°F resid. There is very little conversion to materials that must be removed to permit the product to meet flash specifications for a residual fuel. As a result, hydrogen consumption is also low (shown as a negative yield in the table). For both resids, gravity increased, viscosity decreased, and sulfur, nitrogen, and metals contents were all reduced. In addition, carbon residue decreased by about 50%.

Effect of Reactor Volume on Desulfurization Level

Figure 4 shows the effect of reactor volume on the sulfur content of resids A and B at constant pressure, temperature, and catalyst activity. The relative reactor volume is, of course, proportional to the reciprocal of space velocity in volumes of oil per hour per volume of catalyst. Sulfur content of the product is intentionally plotted on a logarithmic scale to show that resid desulfurization deviates sharply from first-order kinetics, which would result in a straight line on such a plot.

A comparison of the points at which the curves pass through the 1 wt% sulfur level (dashed line) indicates that Resid A requires a reactor almost three times as large as the one required by Resid B to reach the 1 wt% sulfur level. Similar curves for various feedstocks can be developed and related qualitatively to the physical and chemical properties of individual resids.

Although such curves can be fitted by pseudo second-order kinetics, this approach is not considered appropriate because desulfurization of lighter individual molecules has been shown to be first order(7). Therefore, Figure 4 probably reflects a series of first-order desulfurization reactions with rate constants that depend on the chemical structure in which the sulfur atoms reside. This, in effect, explains the bending over or flattening of the curve as the sulfur level is reduced and more-difficult-to-remove sulfur atoms are encountered.

Effect of Desulfurization on Product Properties

As shown in Table II, hydrodesulfurization profoundly affects the viscosity of a residual fuel. Although only a small amount of atmospheric resid is converted to lower-boiling materials during desulfurization, the viscosity of the desulfurized resid is more readily correlated with the conversion to a particular boiling-range material than with the sulfur level of the product. This effect is illustrated in Figure 5 which shows the product viscosities of several typical desulfurized resids as functions of the amount of 650+°F resid converted to material boiling below 650°F. In some cases, such as Resids B, C, and D, it was possible to produce a low-sulfur material meeting No. 6 oil viscosity specifications. In other cases, such as Resids A and G, over-conversion of the resids would be required to meet specifications. This, of course, would

TABLE II

DESULFURIZATION DATA FOR RESIDS A AND C

	Properties of Feed and Product			
	Resid C		Resid A	
	Total		Total	
	Feed	Liquid Product	Feed	Liquid Product
Gravity, °API	17.2	23.7	9.5	19.5
Sulfur, Wt%	4.3	1.0	5.2	1.0
Nitrogen, ppm	1600	1300	4100	2600
Ramsbottom Carbon, Wt%	8	4	17	8
Pour Point, °F	65	55	85	20
Viscosity, SSF at 122°F	101	60	14000	90
Metals, ppm				
Nickel	9	4	58	22
Vanadium	32	9	167	50

	Desulfurization Yields					
	Resid C			Resid A		
	Wt%	Vol%	Sulfur, Wt%	Wt%	Vol%	Sulfur, Wt%
H ₂	-0.8	--	--	-1.2	--	--
H ₂ S + NH ₃	3.6	--	--	4.8	--	--
C ₁ -C ₄	0.8	--	--	1.2	--	--
C ₅ -350°F	1.7	2.1	0.05	1.0	1.3	0.01
350+°F	<u>94.7</u>	<u>98.5</u>	1.0	<u>94.2</u>	<u>101.3</u>	1.0
	100.0	100.6		100.0	102.6	

Hydrogen Consumption = 480 SCFB

Hydrogen Consumption = 760 SCFB

result in too high a hydrogen consumption and thus a higher processing cost. In these cases, dilution with cutter stock is usually a better way to meet viscosity specifications.

Metals removal is not particularly significant in the production of a residual fuel. However, it is important with respect to overall economics because deposited metals ultimately limit the useful life of the catalyst. Figure 6 shows the relationship between demetalation and desulfurization for several feedstocks. Although there is a distinct relationship for each feed, the overall pattern suggests that a generalized correlation is possible.

SUSTAINED OPERATION

The commercial feasibility of the resid desulfurization process depends principally on how well the catalyst performs in sustained operations over significant periods of time. Figure 7 shows the 350+°F product sulfur content plotted as a function of time-on-oil for the desulfurization of Resid C in a continuous operation in bench-scale equipment. Conditions were selected to yield a 350+°F product containing less than 1 wt% sulfur. Over a 60-day period, no problems were encountered in maintaining this sulfur level.

Figure 8 shows the results of a considerably more difficult continuous operation in which Resid A was desulfurized in the 2 B/SD integrated pilot plant. Over a period of about three months, the 350+°F product showed a level of no more than 1 to 1.2 wt% sulfur. Following this operation, samples of catalyst were removed from the reactor and used in subsequent bench-scale studies of catalyst life with a variety of resid feedstocks. Thus, total on-oil time for this catalyst was extended to over seven months.

Ultimately, sustained operation depends on how catalyst activity is affected by both the metals content of the feedstock and the severity of operation required to reach a particular sulfur level. As a result, general numbers for catalyst life cannot be quoted. However, the results in Figures 7 and 8 indicate that catalyst life will be in excess of one year for the desulfurization of a material like Resid C to the 1 wt% sulfur level, and at least six to eight months for a material like Resid A.

PROCESS MODEL

Work is now under way to develop a process model for predicting process requirements for the desulfurization of any given feed. The approach centers in first separating petroleum resids into oils, resins, and asphaltenes--the three fractions common to all resids. Next, reaction rates are determined for each fraction from various resids. Finally, a generalized process model is constructed on the basis of these rates.

Reaction rates for the same fractions from a variety of resids are proving to be remarkably similar. Typical curves of product composition versus overall conversion of the resid are given in Figure 9. These curves illustrate the behavior of the three fractions as well as the 650-1000°F gas oil during the hydroprocessing of Resid C. The resins, which are highly aromatic and contain significant quantities of sulfur, readily disappear; however, the oils, which are more paraffinic and contain less sulfur, disappear at a significantly lower rate. The curve for asphaltenes is similar to that for resins but has a flatter slope, indicating that asphaltenes are significantly less reactive. The curves being developed for other feedstocks will be incorporated in the process model for resid desulfurization.

ECONOMICS

The hydrodesulfurization process is still relatively expensive by petroleum processing standards. The capital investment for large reactors which operate at high pressures and high temperatures, the consumption of hydrogen during the processing, and the use of large volumes of a catalyst with a relatively short life all contribute to the costs. Moreover, processing costs also depend on the feedstock. As an example, Table III shows the difference in costs for desulfurizing Resid B and the more difficult-to-process Resid A to the same 1 wt% sulfur level. The comparison is based on Gulf Coast installation costs and fuel at 4¢ per FOE gallon, power at \$0.004 per KWH, and steam at \$0.45 per 1000 lb. These data show conclusively that even with feeds of similar sulfur contents which are desulfurized to similar levels, significant differences in processing costs exist. Capital charges and catalyst costs vary with the reactor size required. Utilities costs depend on hydrogen consumption and would be subject to further variability if a different fuel value were used. Consequently, specific cost estimates must be based on a specific feed, a specific desulfurization level, a specific place of investment, and a specific fuel value.

CONCLUSION

A process for the removal of sulfur from a wide variety of resid-containing materials has been developed. Sustained operation has been successfully demonstrated in pilot scale equipment using a proprietary catalyst. A process model which will allow the prediction of process performance for any feedstock under any set of processing conditions is now being developed. Where direct resid desulfurization is attractive for sulfur emissions control, use of this process and attendant model will allow design and operation of commercial units.

TABLE III

COMPARISON OF DESULFURIZATION COSTS
FOR 50,000 B/SD OF RESIDS A AND B

Basis: 1 Wt% sulfur in the 350+°F product

	<u>Economics</u> <u>Costs for Resid A minus B</u>
Costs, ¢/B of resid	
Utilities	3.7
Catalyst and Chemicals	4.3
All other direct and overhead	4.5
Capital charge	<u>12.4</u>
Total	24.9
Sulfur Credit	-3.2
Vanadium Credit	<u>-1.4</u>
Difference in upgrading costs, ¢/B of resid	20.3

REFERENCES

- (1) Blume, J. H., Miller, D. R. and Nicolai, L. A., Hydrocarbon Processing 48, No. 9, 131 (1969).
- (2) Steenberg, L. R., and Swanson, W. M., Paper presented at AIChE Meeting, New Orleans, Louisiana, March, 1969.
- (3) McFatter, W., Meaux, E., Mounce, W., and Van Driesen, R., "Advanced H-Oil Techniques," API Proceedings--Division of Refining, p. 489 (1969).
- (4) Frumkin, H. A., and Gould, G. D., Paper presented at AIChE Meeting, New Orleans, Louisiana, March, 1969.
- (5) Henke, A.M., Oil and Gas J. 68, No. 14, 97 (1970).
- (6) Rogers, L. C., and Stormont, D. H., Oil and Gas J. 67, No. 28, 29 (1969).
- (7) Frye, C. G., and Mosby, J. F., Chem. Eng. Prog., 63, No. 9, 66 (1967).

FIGURE 1
BENCH-SCALE UNITS FOR RESID
DESULFURIZATION

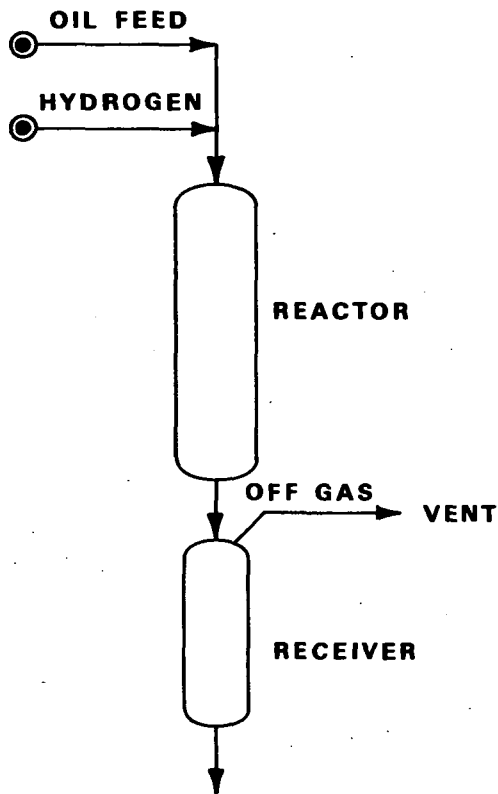


FIGURE 2
2 B/SD PILOT PLANT FOR RESID DESULFURIZATION

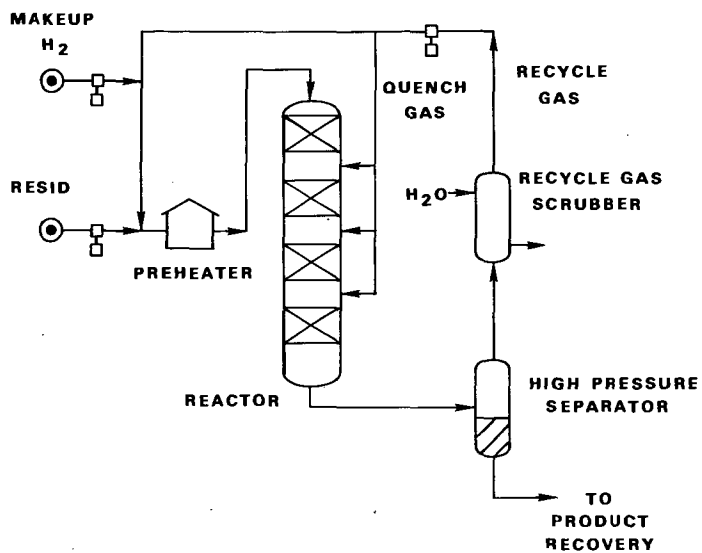


FIGURE 3

TYPICAL TEMPERATURE PROFILE IN 2 B/SD PILOT PLANT

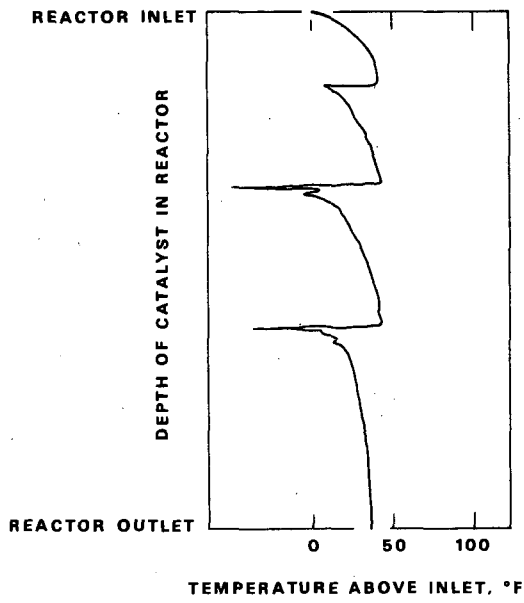


FIGURE 4
EFFECT OF REACTOR SIZE ON DESULFURIZATION LEVEL
OF RESIDS A AND B

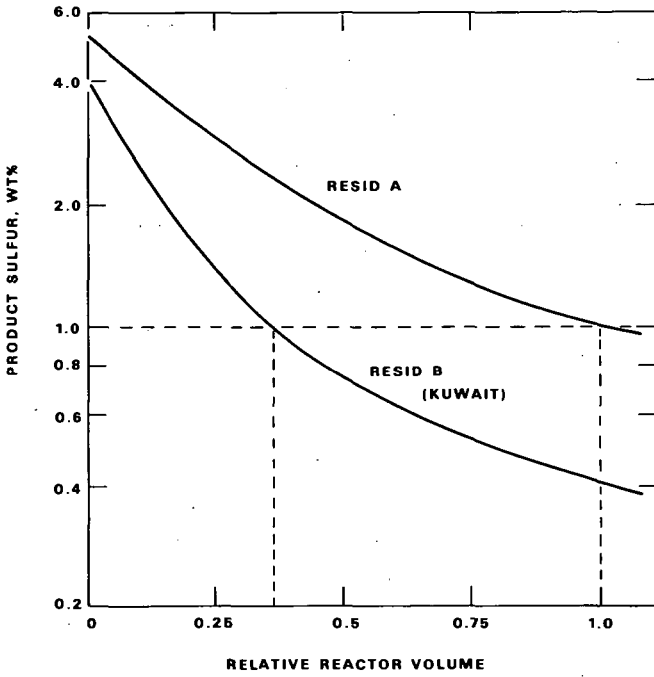


FIGURE 5
EFFECT OF PROCESS SEVERITY ON 350+°F PRODUCT VISCOSITY
OF VARIOUS RESIDS

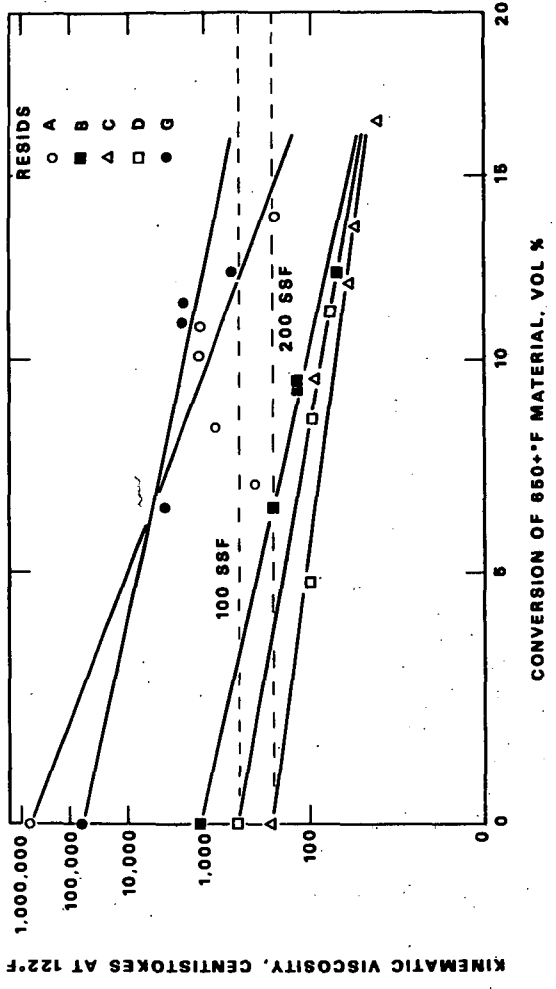
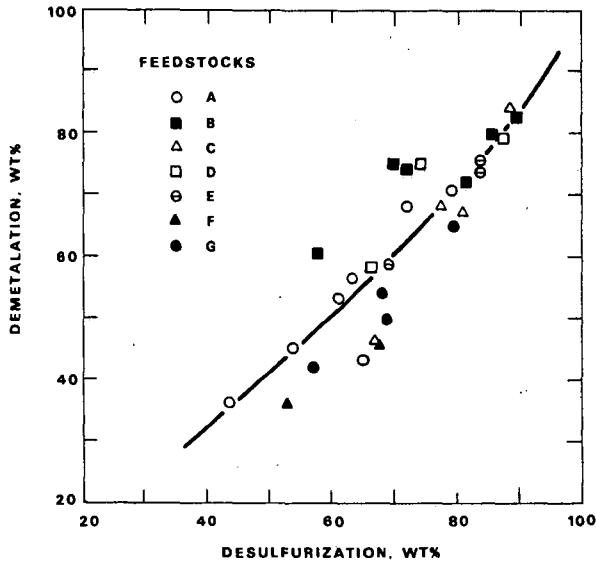


FIGURE 6
RELATIONSHIP BETWEEN DEMETALATION AND DESULFURIZATION
OF VARIOUS RESIDS



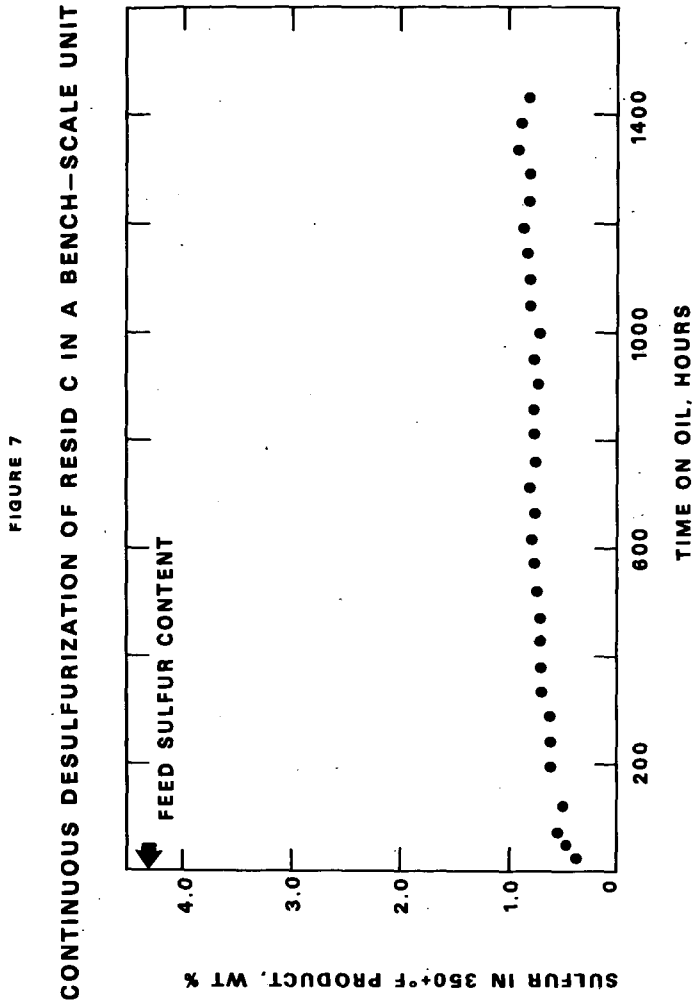


FIGURE 8
CONTINUOUS DESULFURIZATION OF RESID A IN THE 2 B/SD PILOT PLANT

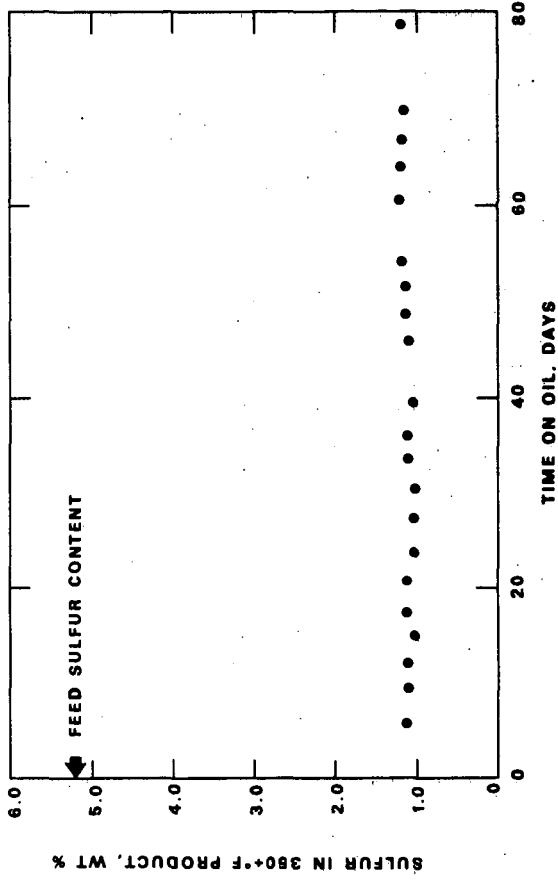
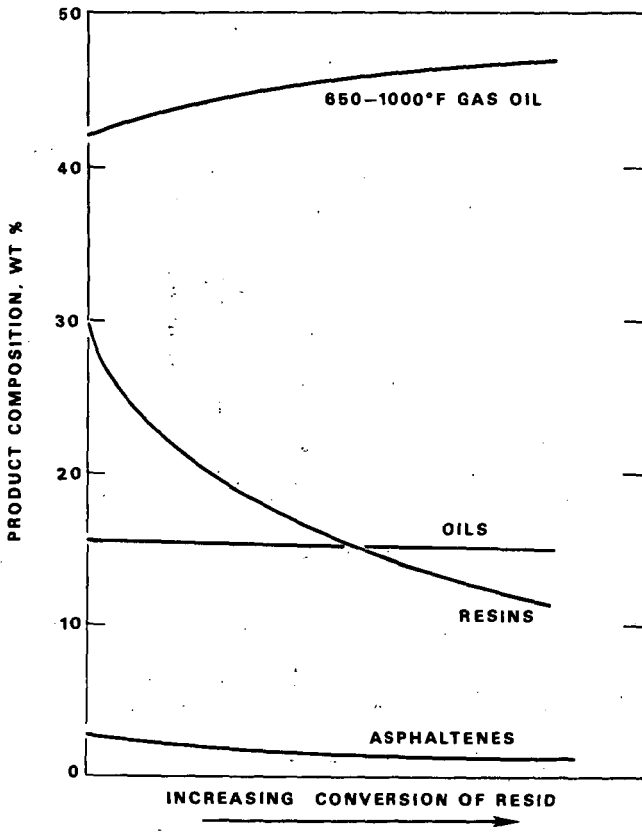


FIGURE 9
HYDROPROCESSING OF RESID C



DEMETALLATION, DEACTIVATION AND BEDPLUGGING
IN RESIDUUM HYDRODESULFURISATION

Esmond J. Newson

Technical University of Denmark
Institutttet for Kemiteknik
Bygning 229, 2800 Lyngby, Denmark

The reduction of sulfur oxide emissions resulting from the use of high-sulfur crudes has recently become of increasing importance. High sulfur petroleum fuel oils contribute to the problems of air pollution. The conversion of high sulfur crudes to synthetic crudes low in sulfur, would increase the supply of limited natural resources.

One method of reducing the sulfur content in crude oils and residua is residuum hydrodesulfurisation in trickle-bed reactors. Total operating costs for this process can be divided into three components i.e. catalyst costs, hydrogen consumption costs and utilities plus investment charges. Catalyst costs represent a significant fraction of the total operating costs and also control the hydrogen and investment costs.

The factors contributing to catalyst utilisation will be the subject of this paper. These factors are classified broadly into two categories. Intraparticle diffusion leading to pore plugging and rapid catalyst deactivation. Secondly, interparticle reaction leading to bed-plugging. The possibilities for increasing catalyst utilisation in these two respects will also be considered.

PORE DIFFUSION IN RESIDUUM DESULFURISATION-DEMETALLATION

From recent papers⁽¹⁻⁵⁾ on residuum hydrodesulfurisation, the major conclusion is that metals contents of the feeds essentially control catalyst utilisation. Analysis of pore diffusion problems will therefore be limited to a pore plugging deactivation mechanism which progressively retards mass transfer of the sulfur-containing molecules to the interior portion of the catalyst pellet. This mechanism has been recognised for some time⁽⁶⁻⁸⁾ but little quantitative information is available from journals or patent literature.

Effectiveness factors for demetallation of vanadium compounds are significantly less than 1.0.⁽³⁾ Assuming typical values of liquid hourly space velocity (1.0) and desulfurisation conversion (75%), a corresponding demetallation conversion results (75%).⁽¹⁾ Catalyst particle size can now be plotted against the effective diffusivity for demetallation with effectiveness factor as a parameter. In Figure 1, for an effectiveness factor of 0.75, with a catalyst particle size of 1/16 inch diameter, a minimum diffusivity of $5 \cdot 10^{-7}$ cm²/sec. is required. An effectiveness factor of 0.5 allows the minimum diffusivity to be as low as $2 \cdot 10^{-7}$ cm²/sec. A first order reaction has been assumed together with a spherical particle shape.

Figure 2 shows estimates for values of the effective diffusivity as a function of molecular weight. The Stokes-Einstein equation was used to estimate liquid diffusivities for large molecules⁽⁹⁾ together with a catalyst porosity of 0.5. The parameter in Figure 2 is the tortuosity factor with values of 2, 5, 10 and 20. The initial value is close to that for loosely packed beds and probably represents a minimum for a formed catalyst particle such as an extrudate. The final value of 20 may reflect the accumulation of metal sulfides and coke in pores of the catalyst particularly in an outer annulus of the pellet. From Figure 2, using a tortuosity factor of 5, an effective diffusivity of $3.5 \cdot 10^{-7}$ cm²/sec. is estimated for a compound of molecular weight 4000. The latter value is towards the lower end of the spectrum of asphaltene molecular weights for Arabian Heavy atmospheric residuum.^(1,3) A preliminary conclusion from figures 1 and 2 based on pore diffusion theory and an oversimplified molecular picture is that effectiveness factors of about 0.6 are probably attainable in demetallation of a feed such as Safaniya to 1 weight per cent product sulfur.

It can be estimated however that the effective diffusivity for demetallation is substantially lower than $3 \cdot 10^{-7}$ cm²/sec. for a Safaniya feed being reduced to 1% product sulfur. This may be the result of adsorption phenomena particularly for vanadium compounds.⁽⁶⁾ Other data for the desulfurisation reaction^(10,11) provide upper bounds to the estimates for effective diffusivity for metal containing compounds within the catalyst particle.

Effective Diffusivity for Desulfurisation

Kinetic data for the desulfurisation of Kuwait VGO is available at two different particle sizes of the same catalyst.⁽¹²⁾ An effective diffusivity of $8 \cdot 10^{-7}$ cm²/sec. was estimated. It is plotted on figure 1 and provides a useful upper limit for subsequent estimates. This value would probably be reduced at reaction rates more typical of current VGO practice. In the test data, the conversion (75%) and the liquid hourly space velocity (1.3) were modest by VGO standards. The above diffusivity means a tortuosity of 5.

Residuum desulfurisation data⁽¹⁰⁾ together with information from the patent literature⁽¹¹⁾ allows an estimate to be made for the effective diffusivity of a Safaniya feedstock. A value of about $2 \cdot 10^{-7}$ cm²/sec. was calculated for assumed process conditions of one liquid hourly space velocity and 60% desulfurisation conversion. This provides an upper limit to the value of the effective diffusivity for demetallation when desulfurising a Safaniya feed to 1% product sulfur. The precision of the estimates is contingent upon a number of assumptions so that only order of magnitude values are possible at this time.

The effective diffusivity for demetallation will be less than the corresponding value for desulfurisation since much of the desulfurisation takes place from that fraction of the feed boiling between 650-1000° F. Demetallation takes place from feed boiling above 1000° F.

Effective Diffusivity for Demetallation

Some data for demetallation⁽⁶⁾ in the form of concentration profiles in the pellet is available for an Iranian topped residuo, 21° API gravity. The vanadium concentration in the regenerated catalyst

pellet was extremely steep but the pellet diameter was 5 mm. An effective diffusivity for vanadium of $2 \cdot 10^{-7}$ cm²/sec. was estimated. This value is also plotted on Figure 1.

More recent data is available by means of electron micro-probe profiles in a spent catalyst pellet⁽³⁾. An effective diffusivity of $1 \cdot 10^{-7}$ cm²/sec. was estimated for vanadium during the desulfurisation of an Arabian Light feedstock, 17.5°API. Correlating the above estimates for effective diffusivity with feed gravity suggests an order of magnitude value of $3 \cdot 10^{-8}$ cm²/sec. for vanadium when desulfurising Safaniya to 75% conversion at a space velocity of 1.0. This value is indeed lower than the upper bound of $2 \cdot 10^{-7}$ cm²/sec. suggested from desulfurisation data.

Referring to the minimum diffusivity plot for demetallation, Figure 1, an effectiveness factor of about 0.1 is obtained for a Safaniya feed. In the same way, an effectiveness factor of 0.3 is obtained for an Arabian Light feed.

Catalyst Utilisation

The only aspect of catalyst life that is being considered is the ability of the catalyst to accept metals within its pores yet maintain desulfurisation conversions of approximately 75%. This degree of desulfurisation corresponds to approximately 75% demetallation⁽¹⁾.

The catalyst metals loading at end-of-run is determined by the effectiveness factor for demetallation associated with a particular feedstock. A pore plugging mechanism combined with effectiveness factors less than 1.0 means that the catalyst pore volume available for deposition of metal sulfides is reduced from the fresh catalyst value. For example, an effectiveness factor for demetallation of 0.1 means that a catalyst whose pore volume is 0.5 cc/gram will only provide 0.05 cc/gram of pore volume for deposition of metal sulfides and coke in the part of the catalyst where the pore-plugging mechanism is critical. Coke is considered to deposit uniformly throughout the particle but will play a minor role in the pore plugging mechanism. A value of 10 weight per cent coke has been assumed deposited on the spent catalyst together with a coke density of 1 gm/cc. This is about one-half the ideal value since the coke formed on a heterogeneous catalyst surface is unlikely to occur in its ideal state. Similar reasoning allows the use of 3 gm/cc as the nickel and vanadium sulfides density.

With these considerations, it becomes possible to estimate the catalyst life in residuum desulfurisation as a function of metals removed from the feed. The effectiveness factor (η) for demetallation is the important parameter. Figure (3) shows estimates for catalyst life as a function of feed metals deposited inside the catalyst pellet. These metals may well be derived from the asphaltene fraction of the crude oil and represent about 70% of the total metals in the residuum.⁽¹³⁾

Residua from Middle East crudes are in general predicted to have longer catalyst lives than Venezuelan stocks. Differences within Middle East stocks are also considerable. An Arabian Light feed for example with an effectiveness factor of 0.3 is predicted to have a catalyst life of about 7000 hours. A Safaniya feed was estimated to have an effectiveness factor of 0.1 so that the predicted catalyst life is about 1000 hours. This can be improved to 3000 hours by increasing the effective diffusivity threefold to about $9 \cdot 10^{-8}$ cm²/sec. The introduction of macropores could achieve this but the original activity and stability of the catalyst must be retained.

A similar comparison between Kuwait and Gach Saran residua gives a predicted life of about 3000 hours for Kuwait and 1000 hours for Gach Saran. This is not quite the factor of (x2) based on Gulf RDS life estimates⁽²⁾ but shows the correct trend.

The parameter that obviously must be checked by experimental observations with different feeds and catalyst is the effectiveness factor for demetallation at a given desulfurisation reaction rate. If product sulfurs less than 1 weight per cent are desired when processing Middle East residua such as Kuwait and Safaniya, then a 1/16 inch catalyst particle size imposes severe limitations on process conditions. Liquid hourly space velocities of about 0.5 and catalyst lives of about 6 months or less are envisaged.

Methods of increasing catalyst utilisation

Particle Shape

The effectiveness factor for demetallation essentially controls catalyst utilisation when the pore plugging model applies. With effectiveness factors for demetallation less than 0.5, the length dimension in the Thiele modulus is apparently the most important of the catalyst properties that constitute the modulus. The volume to surface ratio of the particles is the most general definition of the length dimension. For the same nominal particle size e.g. 1/16 inch diameter, the value of the length dimension is substantially influenced by the shape of the catalyst particle.

Figure (4) shows the influence of particle shape on effectiveness factor in the strongly diffusion influenced regime. The sphere was taken as a standard. Cylinders of length to diameter ratio equal to 3/1 and 10/1 were considered. Crushed particles were also included using volume and surface shape factors from a micromeritics text.⁽¹⁴⁾

It is interesting that cylinders are apparently the least desirable catalyst shape for a given nominal diameter. Particles in the form of "flakes" or "poker chips" are predicted to be the most effective. Ring-shaped catalysts are another alternative and have provided benefits in activity and stability for methanol oxidation.⁽¹⁶⁾ Decreased reactor pressure drop was an additional bonus.

A frequent counter-argument to the use of crushed catalyst particles is that an increased reactor pressure drop will result when using the catalyst in its crushed form as compared to cylindrical form. Using the Ergun equation⁽¹⁵⁾ for flow through packed beds, a decrease in the equivalent particle diameter of a factor of (x2) may be compensated by a 30% reduction in gas rate. This trade off may be attractive with a feed such as Safaniya when catalyst costs due to low effectiveness factors for demetallation, approach 20 c/Bbl.

Pore Structure

The effective diffusivity and hence the effectiveness factor for metals can be increased by increasing the pore diameter.⁽⁹⁾ The simplest expression relating the effective diffusivity to catalyst physical properties suggests that the diffusivity is directly proportional to pore diameter. At low effectiveness factors, the Weisz number criterion at constant observed reaction rate and particle size (1/16"), shows that the effectiveness factor for metals capacity is

directly proportional to pore diameter.

A pore plugging model would predict a greater dependence of effectiveness factor on pore diameter. The essential difference between the conventional pore mouth poisoning phenomena and pore-plugging is that the access of sulfur-bearing molecules to the interior of the catalyst particle is prevented when the diameter of the partially blocked pore approaches the size of the asphaltene and metal-containing molecules. This simple picture suggests that the effectiveness factor for demetallation is proportional to the square power on pore diameter based on estimates for the size of asphaltene molecules.⁽¹⁷⁾

Data is available⁽¹⁵⁾ to test this relationship but the method of preparation of the catalyst suggests that an increase in the macropore volume was probably the way the diffusivity was increased. This suggestion is consistent with the relatively large decrease in pellet density resulting from a modest increase in pore volume. When macropores (greater than 600Å diameter) are present in the pore structure, the concept of volume-average pore diameter is a better correlating parameter than surface average pore diameter.⁽¹⁸⁾ A relationship can be suggested between volume average pore diameter and fraction macropore volume. Desulfurisation effectiveness factors⁽¹⁰⁾ now correlate well with volume average pore diameter raised to the square power. This relationship would also hold approximately for demetallation and is close to the value required by a simple pore-plugging model. Obviously, more data needs to be considered for better evaluation of the effect of pore structure on the effectiveness factors for desulfurisation and demetallation.

Catalyst preparation techniques can be modified to significantly improve the micropore volume and pore diameter. Reduction of surface tension during drying is shown to increase the micropore volume of an extruded alumina.⁽¹⁹⁾ Calcination in wet air has a similar effect. For a given boehmite crystallite size, a compromise is necessary between pore volume and pore diameter of the extruded alumina.

BED-PLUGGING IN RESIDUUM DESULFURISATION

In addition to catalyst deactivation by the metals a second major problem in residuum processing is bed-plugging.^(1,3) Desalting alone is not enough to prevent the build-up of interstitial material. This material reduces bed voidage, especially at the top of a trickle-bed reactor, and causes a significant increase in overall reactor pressure drop. The interstitial deposits are composed mainly of the sulfides of iron, nickel and vanadium.⁽³⁾ They are contained in residuum stocks in organo-metallic compounds and in the case of iron, its feed concentration may obviously be supplemented by corrosion processes in lines ahead of the reactor. Nickel and vanadium sulfides depositing on the external surface of the catalyst pellet are probably held only weakly as nickel and vanadium in micelle-type structures. Their rate of reaction is probably greater than the nickel and vanadium deposited within the catalyst pellet. Coke deposits will also occur both inside the particle and interstitially.

Prediction of Bed-plugging

Estimation of plugging lives in trickle-bed-reactors can be made as a function of feed metals concentration reacting externally, with rate constant as a parameter. A first order reaction has been assumed. Interstitial deposits are considered to occur in the top 20% of the trickle-bed-reactor.⁽³⁾ Using the Ergun equation,⁽¹⁵⁾ pressure drop increase against decreasing bed voidage can be plotted in a dimensionless form Figure (5). Taking a factor of 5-10 increase in overall pressure drop as a criterion for the plugging life (θ_{PLUG}) the corresponding volume of interstitial deposits can then be calculated. This is translated to grams of interstitial metal sulfides per cc of reactor if a metal sulfide density of 3 gm/cc is assumed. This value is about one-half the ideal crystalline sulfide densities but in a trickle bed reactor metal sulfides formed are unlikely to occur in their well-ordered, ideal states. Assuming for example, first order rate constants from 1-10, plugging lives may be estimated, Figure 6.

Once again, the problems of processing Mid-East residua are

significantly less than Venezuelan residua due to the higher metal content of the latter. Within the crudes of the Mid-East, some distinctions may be drawn since demetallation rates decrease as molecular weight increases.⁽¹³⁾ This implies that interstitial rates of reaction for Arabian Heavy feeds are less than for Arabian Light Feedstocks. If it is considered that interstitially deposited metals are derived mainly from the maltene fraction of crude oils then about 30 % of the total nickel plus vanadium metals will be available for interstitial reaction requiring essentially little catalyst surface. In addition, the presence of 5-10 ppm of iron⁽³⁾ in the residuum will also be available for interstitial reaction and subsequent deposition as iron sulfides. For an Arabian Light feed, using a rate-constant between 5 and 10 hr⁻¹ and an entering feed metals concentration of 20 ppm, a plugging-life of about 7000 hours is predicted from Figure (5). With a Safaniya feed, a rate constant of about 2-5 hr⁻¹, an entering feed metals concentration of 40 ppm, a plugging life of about 6000 hours is predicted from Figure (5). Venezuelan residua would have very short plugging lives of about 1000 hours. In the comparison between Arabian Light and Safaniya feeds, the decreased rate of reaction has eased the plugging problem for the Safaniya feed.

The assumed value of the metal sulfides density would strongly affect the predictions in Figure 6 and the slope of the curves. The presence of salt and particulate iron has been found^(1,2) to substantially decrease plugging lives. For accurate predictions the interstitial rate constants and metal sulfides density should obviously be determined experimentally.

Methods of increasing plugging lives

The methods available depend on whether the fixed bed concept of operation is retained or the flexibility of an ebullating bed system is considered. The latter system will be considered first since one of the primary advantages of the ebullated bed is the lack of pressure drop buildup with time on-stream.⁽⁵⁾

Moving Beds: The advantages of the H-oid process have frequently been described and are generally associated with uniform distribu-

tion of reactants, isothermal operation, lack of bed plugging and continuous catalyst withdrawal and replacement. The formation of coke-catalyst agglomerates in the reactor is avoided if recycle of a gas-oil fraction is practised.⁽¹⁹⁾ However, there are disadvantages associated with the use of this reactor design if hydrodesulfurisation is of primary importance. Staging of the reactors becomes necessary to achieve the desired conversion levels.⁽²⁰⁾ This means that the flow through the reactor does not approach the plug flow of the trickle-bed operation. A completely mixed system probably defines the ebullating bed better and is consistent with the strong claims made for isothermal operation. This conclusion is also consistent with values for the height of a mixing unit (H.M.U.) obtained in three phase fluidisation studies.⁽²¹⁾ These studies showed that the H.M.U. for an air-water-ballotini system with 6 m.m. spheres was of the order of 4-10 cm i.e. approaches plug-flow. The column diameter was 9 inches, the bed height 14 feet. If the particle size was decreased to 1 m.m. (~ 1/32 inch) the value of the H.M.U. increased significantly to 40-100 cm. The change was attributed to bubble disintegration with the larger particles and bubble coalescence with the smaller particles. Using 0.1 m.m. particles (~ 200 mesh) it is thought that the value of the H.M.U. may increase by another order of magnitude to 10³ cm. The deviation from plug flow is considerable.

In summary, pore diffusion arguments dictate a small catalyst particle size of about 200 mesh, but mixing problems require a large particle size, about 6 mm., to approach plug flow. A compromise of 1/32 inch catalyst size seems to be suggested particularly if the problem of separating the fine catalyst from the oil is important. A completely mixed system would also result in higher hydrogen consumptions due to increased hydrocracking. The ebullated bed reactor volume must also be significantly greater than the plug-flow case. Bed expansions of the order of 50 %^(20, 21) are used and with a 75 % conversion, the volume of a completely mixed reactor system would be at least twice the volume of a plug flow reactor. Indeed, the bed-plugging problem is eliminated but deviation from plug flow and its associated disadvantages are to be expected.

Fixed Beds: If the fixed bed concept of operation is retained, then graded catalyst beds can be used to relieve the interstitial bed-plugging problem. Graded catalyst beds are already being used⁽³⁾ in deasphalted oil Isomax.

Graded catalyst beds incorporate the principles associated with the specific surface of variously sized particles and particle shapes with low pressure drop characteristics. Ringshaped catalysts have been used in methanol oxidation⁽¹⁶⁾ to decrease the pressure drop across the reactor. The presence of interstitial deposits reacting from the feed makes this approach particularly useful since the void volume per unit volume of reactor has been increased in comparison to cylindrical particles. The surface area of a catalyst particle per unit volume of reactor is inversely proportional to the diameter so that large particles at the top of a trickle-bed reactor will reduce the available surface for the interstitial reaction and spread the metals further down the bed.

CONCLUSIONS

Approximate methods have been outlined for the prediction of catalyst lives in fixed bed residuum desulfurisation. Predicted catalyst lives were consistent with trends in current RDS literature. A pore-plugging mechanism due to metals deposition was assumed to be the cause of catalyst deactivation for desulfurisation. Demetallation effectiveness factors less than 0.5 are considered typical for Middle East residua. Methods of decreasing the pore diffusion problem are related to special catalyst preparations and the use of unusual catalyst shapes.

Approximate methods have also been outlined for the prediction of fixed bed plugging in RDS. Plugging lives less than 8000 hours are considered likely for Middle East residua. For Venezuelan stocks 1000 hours may be typical. Novel catalyst shapes could again be useful. Deviation from plug-flow is expected with ebullating catalyst beds particularly with 200 mesh size particles.

More experimental data and more rigorous theoretical treatments are required to improve predictions.

REFERENCES

- 1) Moritz, K.H., et al., "Esso/Union Fuel Oil HDS Processes", Japan Pet. Inst., March 10, (1970), Tokyo.
- 2) Henke, A.M., "Gulf's Residual HDS Process", Japan Pet. Inst., March 10, (1970), Tokyo.
- 3) Scott, J.W. et al., "Chevron RDS Isomax Process", Japan Pet. Inst., March 10, (1970), Tokyo.
- 4) Sterba, M.J. et al., "HDS of Heavy Fuel Oils by the Isomax Process", Japan Pet. Inst., March 10, (1970), Tokyo.
- 5) Galbreath, F.B. et al., "H-Oil as a Tool for Low Sulfur Fuel Oil Production", Japan Pet. Inst., March 10, (1970) Tokyo.
- 6) Hiemenz, W, Sixth World Petroleum Congress, Frankfurt, June (1963), Section III, p. 307.
- 7) Arey, W.G. et al., Seventh World Petroleum Congress, Mexico City, April (1967), Elsevier, Vol. 4, p. 167.
- 8) Van Driesen, R.P., Rapp, L.M., Seventh World Petroleum Congress, Mexico City, April (1967), Elsevier, Vol. 1b, p. 261.
- 9) Satterfield, C.N., "Mass Transfer in Heterogeneous Catalysis", M.I.T. Press, Cambridge, Mass., (1970), Chapter 1, Chapter 3.
- 10) Cecil, R.R. et al., 61st. Annual A.I.Ch.E, Los Angeles, Calif., December 1968, Paper 12a.
- 11) Esso, Netherlands Patent Appl. 68/03924.
- 12) Ketjenfine 124-Series, Hydrotreating Catalysts, p. 10.
- 13) Larson O.A., Boucher, H., Div. Pet. Chem., ACS Preprints, March 23-26, (1966), B-95.
- 14) Dallavalle, J.M., "Technology of Fine Particles", Pitman, New York, (1943), p. 263.

- 15) Ergun, S., C.E.P. 42, No. 2, 39, (1952).
- 16) Oraina, J., Pernicone, N. La Chimica e L'Industria 52, No. 1, (1970); p. 1.
- 17) Dickie, J.P., Haller, M.N., Teh Fu Yen, J. of Colloid and Interface Science, 29, No. 3, (1969); p. 475.
- 18) Van Zoonen, D., Dantes, C.Th., J. Inst. Petrol. 49, No. 480, 383, (1963).
- 19) Johnson, M.F., Mool, J., J. of Catalysis 10, (1960), p. 342.
- 20) HRI, U.S. 3, 412, 210, November 1968.
- 21) HRI, U.S. 3, 418, 234, December 1968.
- 22) Michelson, M.L., Ostergaard, K., The Chemical Engineering Journal, I, No. 1 (1970), p. 37.

FIGURE 1: CATALYST PARTICLE SIZE vs. EFFECTIVE DIFFUSIVITY.

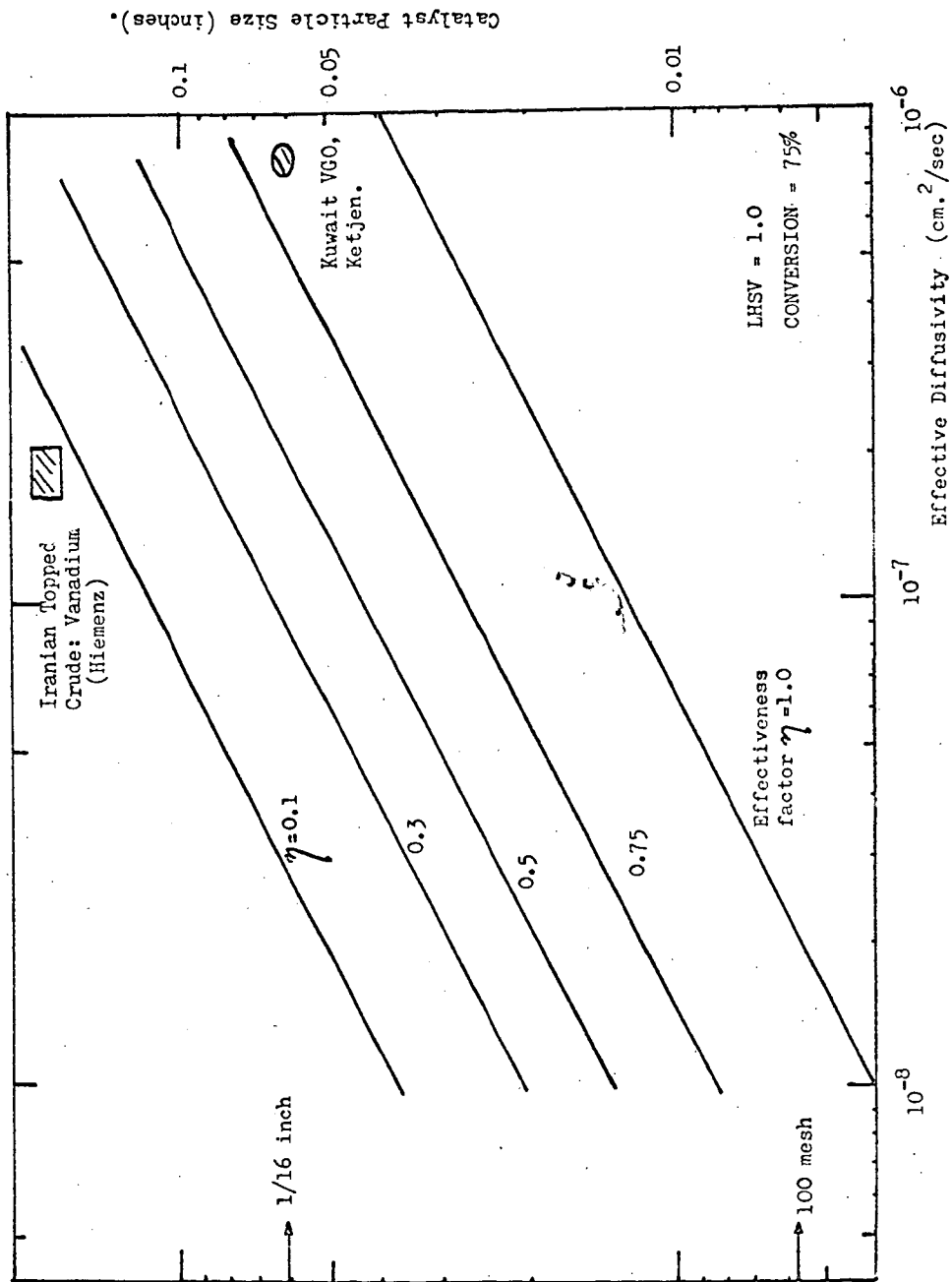


FIGURE 2 : EFFECTIVE DIFFUSIVITY vs. MOLECULAR WEIGHT.

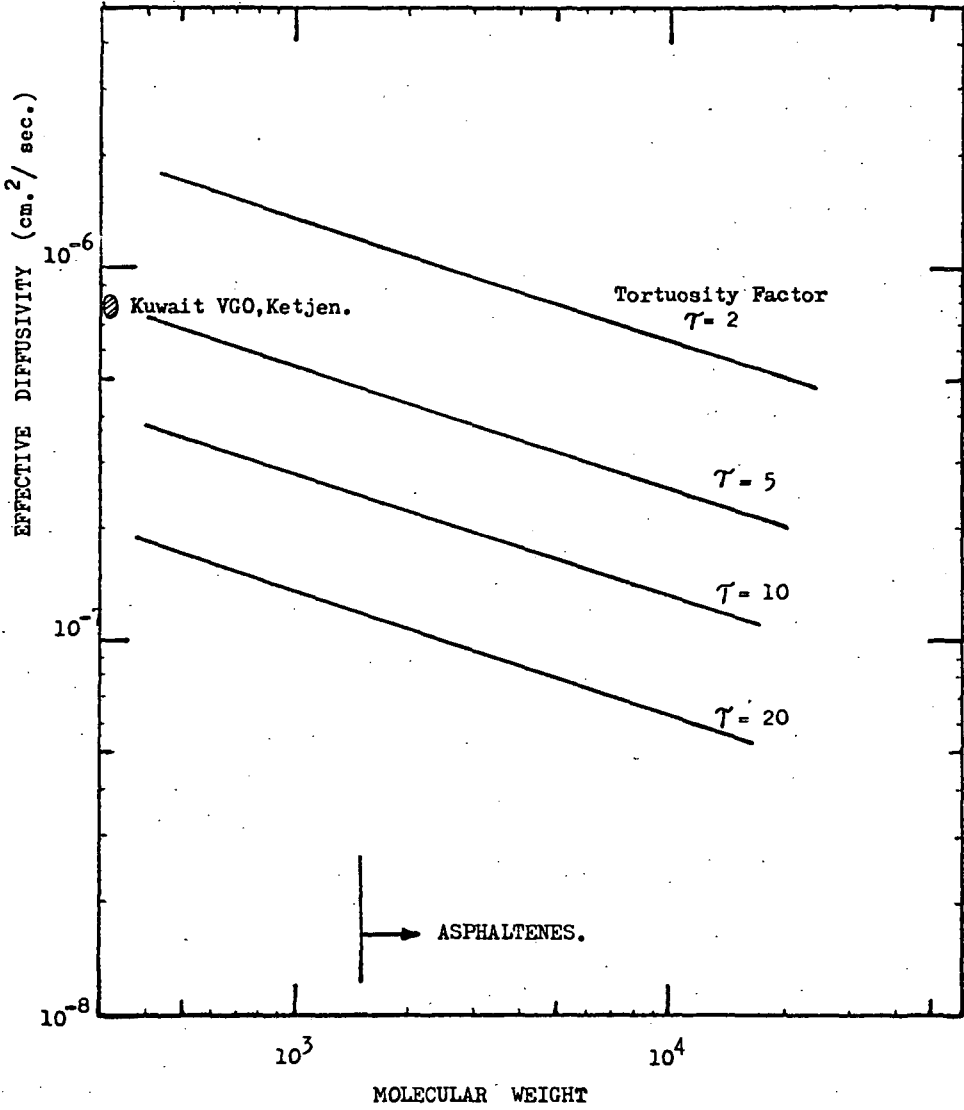


FIGURE 3 : CATALYST LIFE vs. METALS DEPOSITION IN RESIDUUM DESULFURISATION.

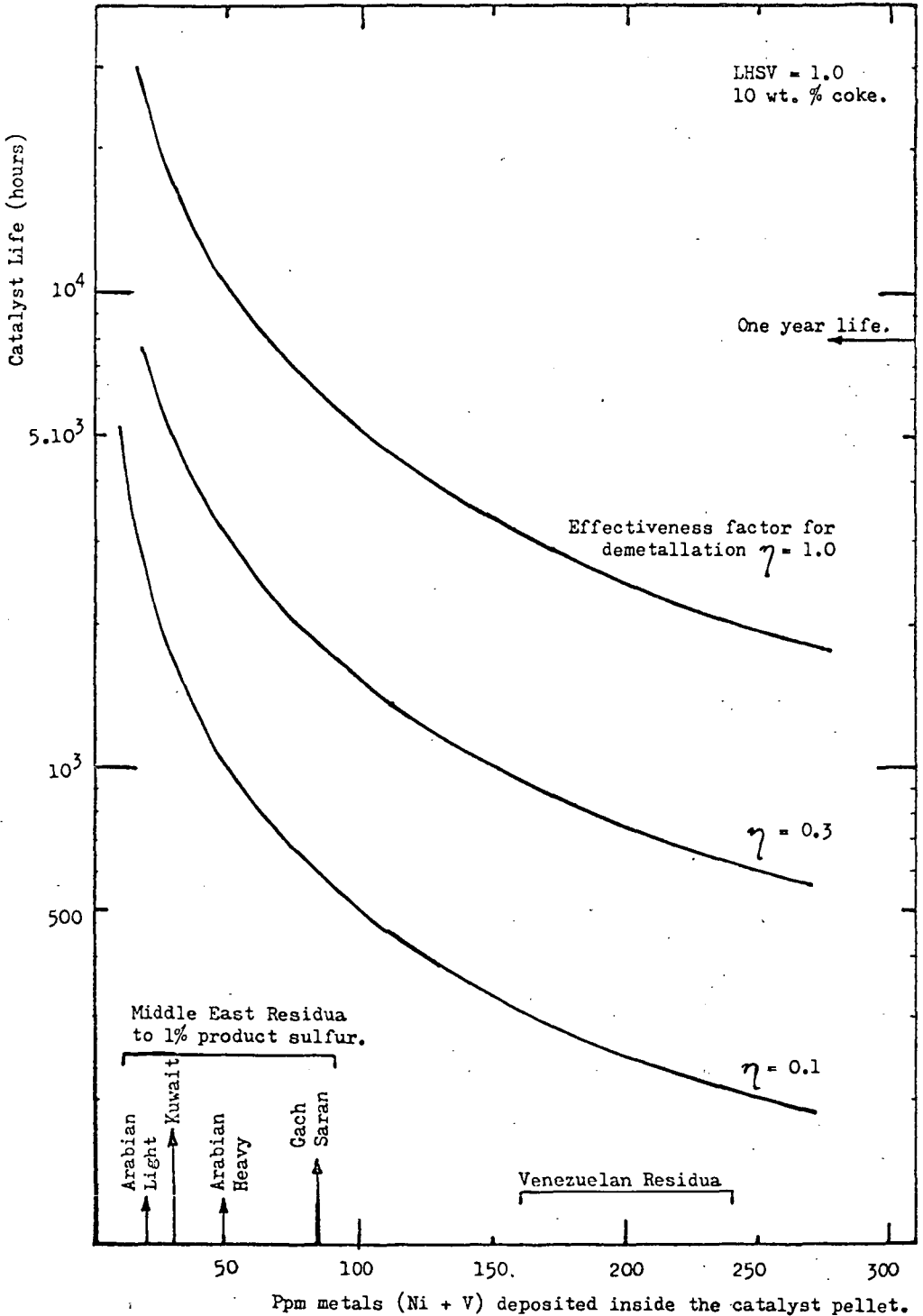


FIGURE 4 : EFFECT OF PARTICLE SHAPE ON EFFECTIVENESS FACTOR

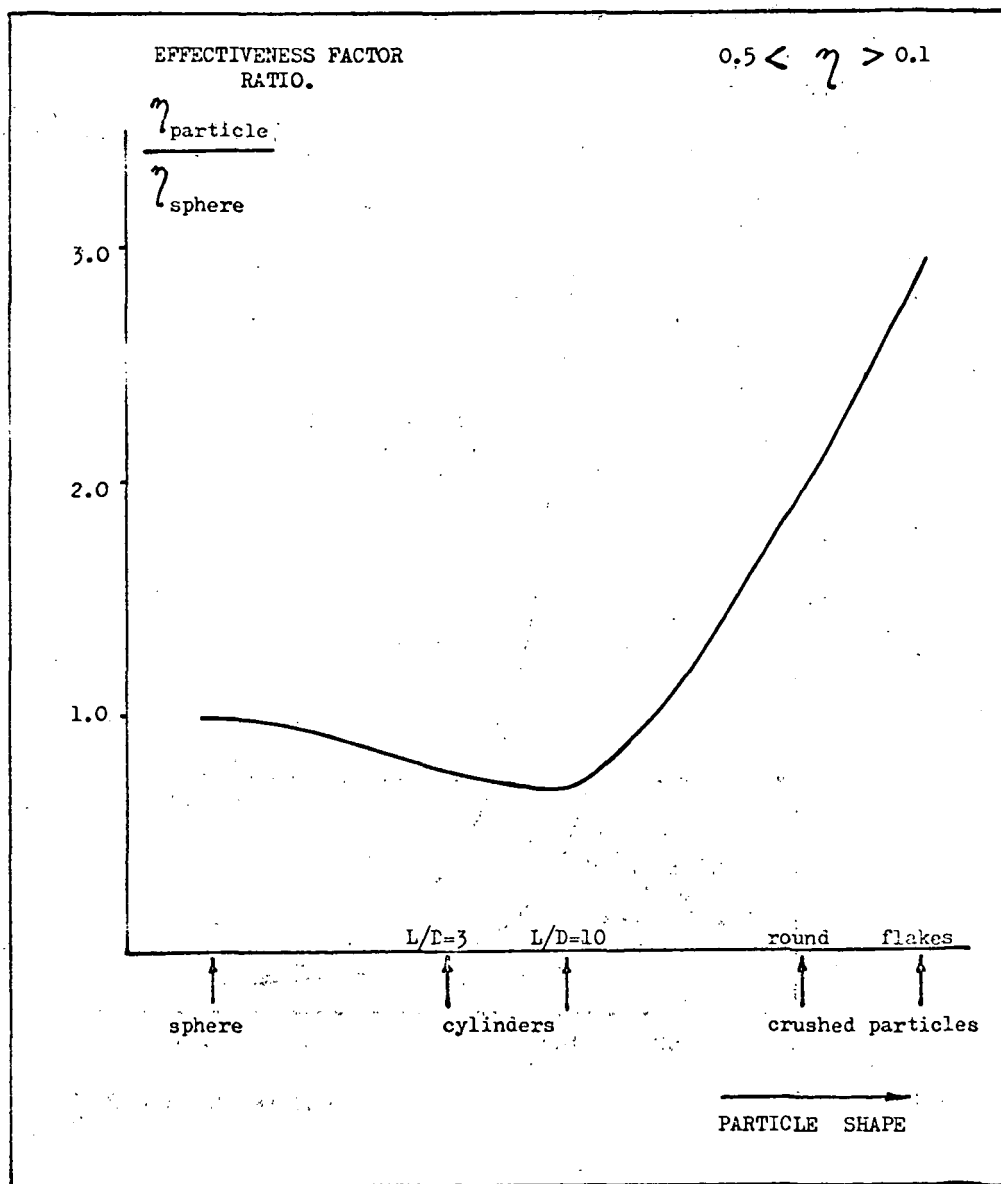


FIGURE 5 : EFFECT OF DECREASING BED VOIDAGE ON FIXED BED PRESSURE DROP.

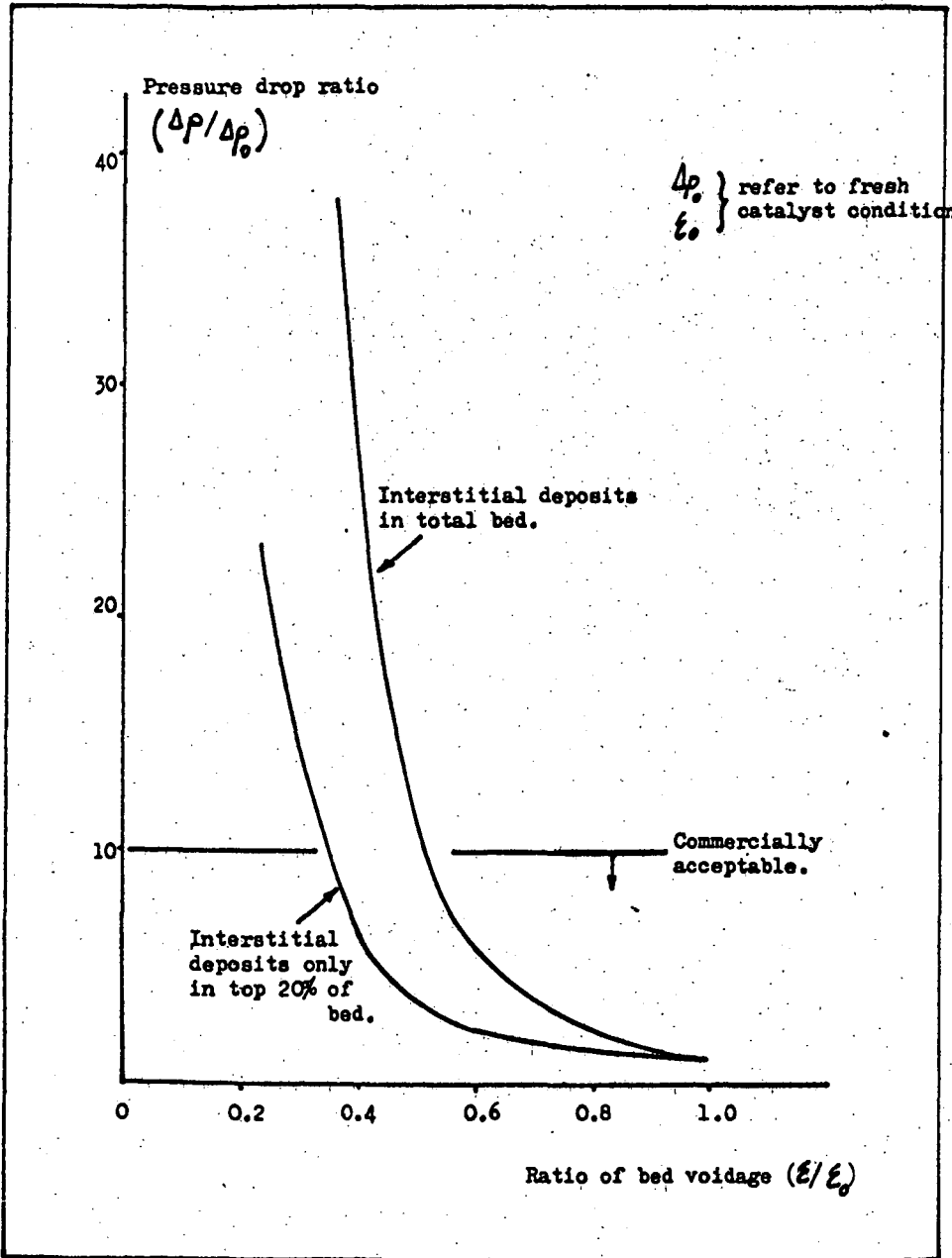
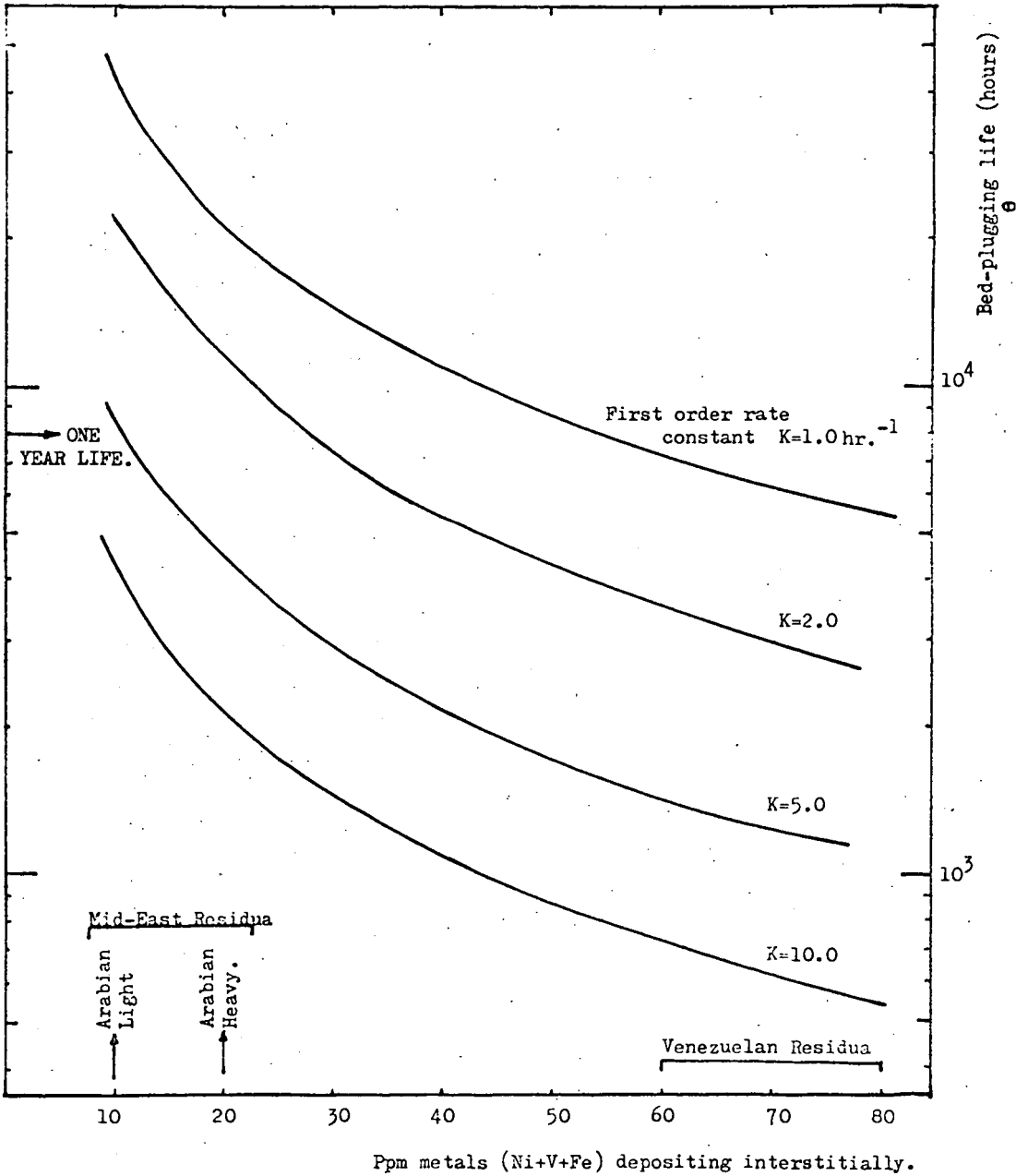


FIGURE 6 : BED-PLUGGING LIVES vs. INTERSTITIAL METALS DEPOSITION



HYDROGEN PROCESSING OF COAL AND THE KINETICS OF DESULFURIZATION

Marvin L. Vestal, Robert H. Essenhigh* and Wm. H. Johnston

Scientific Research Instruments Corporation
6707 Whitestone Road, Baltimore, Maryland

INTRODUCTION

The desulfurization of coal by hydrogen in the interests of abatement of air pollution, is a process with a potential for 90% sulfur removal or better, depending on the details of reactor design to cut down resorption back-reactions, and on other factors such as hydrogen concentration and reactor residence or contact time. The pollutant problem of course, is that of SO_2 and SO_3 formation during combustion of the coal - which is the dominant current use of coal - and there are in general two approaches to abatement. First, removal of the sulfur oxides from the combustion gases after formation. Second, the prevention of their formation by prior desulfurization of the coal. The first approach has the general drawback that even high S percentages in coal become very small percentages after dilution in air converted to combustion products. This means handling large volumes of gas containing small quantities of pollutant. Even on a weight basis the dilution is substantial: a given weight of S (say 0.05 lb) in one lb. of coal becomes about the same weight in about 12 lbs. of combustion products. Direct removal of the S from the coal by hydrogenation to form H_2S , therefore, has the appeal of handling substantially smaller quantities of material, either by weight or volume, together with the advantage that the component concentrations are also proportionately higher, thus improving chances of achieving a given target for efficiency of removal.

Desulfurization by hydrogen, however, is not a straightforward process since the H_2S formed in the first instance is very rapidly resorbed on carbon. Since the resorption is accentuated by higher temperatures and longer residence times, this generally means that net efficiencies of removal fall with increasing temperature and larger quantities of coal being processed. In considering reactor designs, which is the practical target of these desulfurization investigations, this chemical behavior means that an efficient reactor should operate at not too high a temperature, and that either the sweep gas should be at a very high velocity or else that a preferential absorber should be available in close proximity to the coal during hydrogenation. As a further consideration it is also evident that a suitable reactor design would either be a batch unit (such as a fluid bed), or a continuous counterflow, so that the terminal discharge of the almost cleaned coal should be in contact with a high hydrogen and low H_2S concentration.

The physical size of and retention time in any reactor are then determined by the desulfurization kinetics both in the presence and the absence of any preferential absorber. In a previous paper (1) we have already described most of

* Professor Robert H. Essenhigh is Director of the Combustion Laboratory at Pennsylvania State University, University Park, Pennsylvania.

what we now know of the chemistry and kinetics of the hydrodesulfurization of coal, obtained by adaptation of the Juntgen (2) "non-isothermal" method of experiment and analysis. This paper is concerned with discussing these and additional results of such experiments on S removal from coal, and H₂S capture by coal char, carbon, and CaO (as a possible preferential absorber) particularly as these relate to reactor design. This includes a brief outline of a possible reactor complex and a Sankey (Energy Flow) Diagram for such a system.

NON-ISOTHERMAL KINETICS

The non-isothermal method of Juntgen was extended theoretically and applied experimentally to the hydrodesulfurization of ten bituminous coals ranging from 1 to 5% (3). This powerful method overcomes the difficulties of partial achievement of equilibrium conditions of temperature, by treating temperature as a controlled variable. Essentially continuous measurements of reaction products in a flow system provide experimental functions whose theoretical interpretation identify sets of chemical reactions which are responsible for desulfurization. The kinetics of desulfurization of all ten coals are accounted for satisfactorily by five chemical reaction systems. This method gives activation energies and frequency factors for each chemical reaction.

We may summarize these chemical reactions and the rate data of coal desulfurization in hydrogen atmospheres by listing the measured kinetic parameters for the five major reactions and the two back reactions, as shown in Table I. Non-isothermal studies were also made of the removal of all H₂S by calcined dolomites and limestones and some regeneration kinetics of the resulting calcium sulfide as shown in Table II.

TABLE I

CHEMICAL REACTIONS AND RATE DATA OF COAL DESULFURIZATION IN HYDROGEN ATMOSPHERES

No.	Reaction	E ^{kcal} /mole	k ₀
1	(Org-S) _I + H ₂ → H ₂ S	34.5	3.1 × 10 ¹⁰ (atm H ₂) ⁻¹ min ⁻¹
2	(Org-S) _{II} + H ₂ → H ₂ S	41.5	2.8 × 10 ¹¹ " "
3	FeS ₂ + H ₂ → H ₂ S + FeS	47	2.8 × 10 ¹² " "
4	FeS + H ₂ → Fe + H ₂ S	55	2.1 × 10 ¹³ " "
5	(C-S) + H ₂ → H ₂ S	52	~ 2 × 10 ¹³ " "
6	Fe + H ₂ S → H ₂ + FeS	18	6.5 × 10 ⁶ (atm H ₂ S) ⁻¹ min ⁻¹
7	Coke + H ₂ S → (C-S) + H ₂	32	2.3 × 10 ⁸ " "

TABLE II

8	CaO + H ₂ S → CaS + H ₂ O	38	4.7 × 10 ¹³ (atm H ₂ S) ⁻¹ min ⁻¹
9	CaS + H ₂ O → CaO + H ₂ S	55	1.0 × 10 ¹⁴ (atm H ₂ O) ⁻¹ min ⁻¹
10	CaCO ₃ → CaO + CO ₂	58	3.0 × 10 ¹² min ⁻¹
11	CaO + CO ₂ → CaCO ₃	17	5.0 × 10 ⁴ (atm CO ₂) ⁻¹ min ⁻¹

The significance of these results to conditions of sulfur control can be seen by expressing them as rate constants versus temperature over the range of engineering interest. The rate constants for these reactions are shown from 400°C to 1000°C in Figure 1. There emerges a desulfurization band which encompasses the desulfurization reactions which account for the hydrodesulfurization of the ten bituminous coals studied.

REACTOR SELECTION FOR HYDRODESULFURIZATION

The requirement that back reaction of H₂S with carbon is to be suppressed by a combination of fast removal of product (H₂S), preferential absorber, and/or maintenance of high H₂ and low H₂S concentrations at termination of the reaction means that suitable reactors seem to be restricted to the fluid bed or some counterflow unit. In this paper we suggest that a continuous counterflow reactor is a better choice. There are, however, some simple general considerations on relative sizing that are pertinent and will be discussed first.

Relative Sizing of Reactors

Suppose any reactor has a true or effective capacity of C lb/hr. of material being treated. If the reactor volume is V cu. ft., the reaction time required is t (hours), and the average materials density is $\bar{\rho}$ (lb/cu. ft.) then these factors are related by

$$C = \bar{\rho}V/t \quad (1)$$

The specific capacity can then be defined as

$$C_v = (C/V) = \bar{\rho}/t \quad (2)$$

These two simple equations can now be used to provide estimates of the relative size of any pretreatment reactor for coal subsequently being burned in a boiler. If subscripts zero refer to the boiler, we first have the condition that the pretreatment and boiler capacities must be equal: so

$$C = \bar{\rho}V/t = \bar{\rho}_0 V_0/t_0 \quad (3)$$

or
$$V/V_0 = (\bar{\rho}_0/t_0) / (\bar{\rho}/t) = C_v^0/C_v \quad (4)$$

Consequently, if we want a pretreatment reactor say 10% of the boiler volume, the corresponding specific capacity must be ten times greater. Considering next that

$$C_v/C_v^0 = (\bar{\rho}/\bar{\rho}_0) (t_0/t) \quad (5)$$

then, for the same reaction times, the materials density must be ten times greater in the pretreatment reactor. In a boiler, C_v⁰ averages 2 lb/hr. cu. ft., t₀ is about 2 sec., and $\bar{\rho}_0$ is, therefore, about 0.02 oz/cu. ft. The pretreatment reactor density would then be about 0.2 oz/cu. ft. which corresponds to a fairly dense cloud. From our non-isothermal experiments (1, 3), it is clear that the reaction times are more likely to lie in the range from 20 to 200 sec., so that the pretreatment reactor densities must lie between 2 and 20 oz/cu. ft. (or g/litre). Since this latter figure is still below what is found in fluidized beds, such density loadings are possible, but these estimates also

illustrate the magnitude of the problem in terms of the solid loadings required. The fluid bed, however, has the disadvantage that it is a batch, not a continuous, process. On the other hand a continuous process that will provide the necessary particle loadings and still allow the potential for rapid exchange of gases with a preferential absorber would only seem to be provided by the cascade reactor (described below), unless the preferential absorber is mixed with coal which then creates problems of separation.

The Cascade Reactor

The cascade reactor is a vertical tube containing inclined shelves or plates to break the fall of particles cascading down from the top of the tube, against a rising current of reactive gas. It is based on the Cascade Heat Exchanger (4), which is a device intended to promote efficient heating of a gas by a solid (or vice versa) by counterflow, with advantage being taken of the relatively high heat exchange coefficient and large surface area of fine particles. One could, in principle, also obtain such exchange simply by pouring the particles into the top of a tube, but the nominal effectiveness of such a system is almost completely nullified by two factors. If the upward gas flow is slow, the particle shower can quite well create its own path by what is known as a "Chute-en-Masse" effect whereby the particles descend at very much higher velocities than in free fall of a single particle through a viscous fluid. Gas "contained" in the cloud is dragged with it, and incoming gas is likely to be short circuited through a more or less particle free region. Alternatively, if the gas velocity is quite high, the fastest velocities are at the center of the channel, which can pick up fines and carry them out of the system, while the velocity gradients throw the larger particles to the walls where they will fall at their greatest speed. If the particle concentration is also high at the walls the Chute-en-Masse effect may accelerate the rate of fall still further.

The purpose of the cascade plates can be described as a device for breaking the fall of the dust so that the retention time, and, therefore, the time available for heat exchange, is increased. The plates, therefore, prevent the dust plummeting down the center of the tube or the wall region.

The use of the cascade heat exchanger as a reactor is not known to have been proposed before. As a reactor it utilizes the counterflow operation of the cascade heat exchanger, with the possible gains to be achieved from breaking the fall of the dust to increase the retention time, but using the device for promoting reaction between a gas and a finely divided solid. The proposed reactor is intended to treat raw coal of appropriate fineness, with the objective of removing sulfur, delivering sulfur-free char and pyrolysis gas as primary output products, with H_2S as a potential source of sulfur as a by product (or co-product).

The basis of the method is low-temperature ($700^\circ C$) hydrogenation, using a recycled fraction of the pyrolysis gas, during which: (1) a sulfur-containing pyrolysis gas is evolved for cleaning in a later or parallel stage; and (2) the coke formed is also rendered sulfur-free by direct heterogenous reaction between hydrogen and the sulfur in the coke, generating H_2S .

To estimate the mean velocity of the particle stream through the reactor designated as v_m , will be crucial in all subsequent analyses of all purposes the reactor may be used for.

In such a system the chute-en-masse effect is likely to override all other factors, such as viscous drag through the gas. In fact, the viscous drag can be responsible for entrainment of gas in the same direction as the dust flow. This can be thought of as an ejector action helping to stimulate a cyclic flow. In the limit, therefore, the particles are most probably close to free fall under gravity without significant retarding forces.

The simplest condition, therefore, is for the particle stream to fall vertically from the tip of one plate to the tip of the next. It is assumed to accelerate at g from zero velocity to a maximum which is again reduced to zero on impact. In fact, of course, there will be a horizontal component after impact, but this will be considered later. Suppose, therefore, a cascade element has a depth d , so the free-fall-distance apart of the plate tips is $(d/2)$: then

$$(d/2) = (1/2) g t_{\text{imp}}^2 \quad (6)$$

where t_{imp} is the time to impact; or

$$t_{\text{imp}} = d/g \quad (7)$$

The mean velocity v_m is, therefore

$$v_m = (d/2) / t_{\text{imp}} \quad (8)$$

$$= (1/2) g d \quad (9)$$

The velocity varies only slowly with the cascade depth (d). If $d=1\text{ft.}$ (plate spacing 6 in.) $v_m = 2.8 \text{ ft./sec.}$ If $d=6 \text{ in.}$, $v_m=2 \text{ ft./sec.}$ If $d=1.5 \text{ in.}$, $v_m = 1 \text{ ft./sec.}$ This last is very narrow; the plate spacing is only 0.75 in. This would be adequate for many laboratory scale studies but handling 100 tons/hr. would be difficult.

It should, however, be emphasized that the calculations given above assume close to the worst conditions, and are, therefore, rather pessimistic. Average velocities of 1/2 to 1 ft/sec for plate spacings of 4 to 6 in. may be realistic with proper design. A 30 to 60 sec. retention time should, therefore, be possible with a unit 30 ft. high.

Cascade Reactor: Simple Analysis

The reactions involved in the cascade desulfurizer include the coal pyrolysis (initially assumed to be independent of the hydrogenation reactions).

For initial analysis purposes this can be treated as first order reaction using operational velocity constants. The rate of reaction can, therefore, be obtained directly as a function of time independent of the material location in the reactor. The location of the material in the reactor is then obtainable from the throughput velocity. This is valid for a plug flow system.

Assume that the rate of loss of pyrolysable material is proportional to the pyrolysable fraction. Let the pyrolysable fraction at any time t be V lb/lb of solid, then

$$dV/dt = -kV \quad (10)$$

where k , the velocity constant, may be the real velocity constant at a specified temperature, particle size, etc.; or it may be an "operational" velocity constant representing an effective or average constant that is valid to a specified margin of accuracy for a number of competing or consecutive reactions, possibly including changes in particle size and temperature. The variation of V with time (at constant temperature) is

$$V = V_0 \exp(-kt) \quad (11)$$

where V_0 is the maximum pyrolysable fraction. The relation to distance is then given by

$$z = v_m t \quad (12)$$

where z is the distance travelled through the reactor in a given time t , if v_m is constant, where v_m is the mean velocity. Equation (11) becomes

$$V = V_0 \exp[-(k/v_m)z] = V_0 e^{-kz} \quad (13)$$

showing that the slower the material travels through (small v_m), the larger the "distance constant, (k')" and the more complete the reaction. This is quite obvious but equation (13) makes the point explicitly. This re-emphasises that anything that can be done by way of reactor design to reduce v_m can provide more effective control of the completeness of reaction.

Consider now the throughput at two different planes. Take $z=0$ and $z=z$. At $z=0$, if the specific mass rate of input, lb. per hour per sq. ft. of reactor cross-section is M_0 , then the rate of input of pyrolysable solids is $(V_0 M)$; and the rate of input of non pyrolysable solids is $(1-V_0)M$. Similarly, at $z = z$, the mass rate of flow of non pyrolysable solids is $(1-V)M$. At steady state this quantity must be constant right through the reactor so

$$(1-V_0) M_0 = (1-V)M \quad (14)$$

$$\text{or } (M/M_0) = (1-V_0) / (1-V) = (1-V_0) / (1-V_0 e^{-kz}) \quad (15)$$

These equations can be rearranged in the form of a reactor efficiency.

Suppose M_c is the mass flow rate in an infinitely long reactor when pyrolysis is complete (i.e. the mass flow rate at any point of non-pyrolysable solids) then

$$M_c = M_0 (1-V_0) \quad (16)$$

Now suppose that for a finite length reactor the reaction is not complete, but the mass flow rate is M_{exit} . So

$$M_{\text{exit}} = M_o (1 - V_o) / (1 - V_{\text{exit}}) = M_c / (1 - V_{\text{exit}}) \quad (17)$$

Now defining reactor efficiency, n , as

$$n = \frac{V_o - V}{V_o} = 1 - V/V_o = 1 - e^{-kt} \quad (18)$$

In terms of the mass flow rates this can be written

$$n = (1 - M_c/M_o) / (1 - M_{\text{exit}}/M_o) \quad (19)$$

Since only mass flow ratios are involved the efficiency is independent of mass flow except to the extent that this might possibly affect the mean velocity through the reactor.

Reactor Efficiency Compatibilities

The information developed by the above analysis can now be combined with the kinetic data set out in Tables I and II and Figure 1 to estimate possible reactor efficiencies. The values obtained are essentially order of magnitude estimates but this is sufficient for our immediate purpose in demonstrating the reasonableness, or otherwise, of using the Cascade Reactor for at least some of the reactions involved in the desulfurization process. Primarily we are interested in estimating reactor temperatures at which reasonable reactor efficiency can be achieved; and to establish these (as estimates) let us assume 99% efficiency in each reaction. In Equation (18) we, therefore, have

$$\exp(-kt) \approx 10^{-2} \quad (20)$$

as the criterion for such efficiency. Since $\exp(-kt)$ can be written as $10^{-kt/2.3}$, and since the reactor retention time is estimated (above) to be 1/2 to 1 min., the values of the velocity constant, k , to meet the criterion of Equation (20) is that:

$$k \approx 5 \text{ to } 10 \text{ or greater (min)}^{-1} \quad (21)$$

Referring now to Figure 1 we find listed values of rate constants with dimensions $(\text{atm. min})^{-1}$ since all the reactions are all first order with respect to a reactive gas (H_2 , H_2S etc.). If the reactive gas concentrations are in large excess and in the region of 0.1 atm. then multiplying all the values of the rate constants given by 10^{-1} changes them in effect to pseudo first order constants for comparison with the criteria of Equations (20) and (21). For the values of k to lie between 5 and 10 the true rate constants must lie between 50 and 100. From Figure 1, this corresponds to temperatures in the desulfurization band of roughly 600 to 700°C. If the reactive gas concentrations are 0.01 atm., the rate constants then required (for 99% reaction efficiency) are raised to the range (roughly) of 700 to 900°C. With reactive gas concentrations of 0.001 atm. the required temperatures would be in the range 900 to 1200°C.

Summarizing, therefore, what we have estimated here: we have used the

cascade reactor retention times (estimated by the free fall assumptions) in combination with the reactor analysis for a first order reaction, to estimate the temperature ranges required for the reactor to be operated at, if reaction efficiency is to be 99%. To do this, the second order rate constants given in Figure 1 have been treated as pseudo first order constants by multiplying by 0.1, 0.01, and 0.001 atm. to represent average concentrations of the reactive gas involved; and for the desulfurization reactions the temperature range is found to be 700 to 800°C for an average reactive gas concentration of 0.01 atm.

This, it must be emphasized, is no more than a rough estimate to determine whether the cascade reactor may be a possible rational choice in any complete desulfurization scheme; and from the estimates obtained here it would seem that it probably is.

A REACTOR COMPLEX FOR HYDROGEN PROCESSING OF COAL

Although the prime purpose of this paper is to initiate analysis of suitable generalized reactors for desulfurization, by hydrogenation, of coal in terms of the kinetic behavior of known mechanisms (with particular attention, of course, to the cascade reactor), a brief look at a possible complete scheme for continuous hydrogen processing is not out of place. This brings into focus the inter-relationships that have to be developed quantitatively between component parts of any such scheme, particularly as this influences choice of any given type of reactor.

Schematic for Continuous Processing

As already mentioned above, one of the principal problems in desulfurization by hydrogenation is the speed of the back reaction as H_2S is resorbed on carbon (reaction 7 in Table I) as this then necessitates either the rapid physical removal of the H_2S (high throughput velocities) or the presence of a preferential absorber such as CaO (reaction 8 in Table II) for chemical removal. Unfortunately, mixing the absorber with the coal introduces subsequent problems of separation. The Cascade Reactor, however, would seem to permit an additional possibility that is something of a compromise between both alternatives: that the coal and absorbent streams can be kept separate while the gas streams are common. The method would be to operate two cascade reactors side by side with two sets of plates to separate the solid streams, but with arrangements to cross-mix the rising gas streams by suitable baffles.

The workability of such a proposal has yet to be demonstrated physically, but the advantages accruing from it, should it prove workable, are so substantial that it encouraged analysis to establish the energy requirements for a complete scheme based on this cross-mix reactor. The gross energy requirements have been examined by constructing a Sankey (Energy Flow) Diagram for the system (see below). The complete scheme is based, as explained, on the cross-mix reactor, but regeneration of the CaO with sulfur recovery is also included by incorporating two additional reactors: (1) for conversion of CaS to $CaCO_3$ and (2) for calcination to reform CaO .

The complete scheme is illustrated in the block diagram of Figure 2. This diagram shows a total of six chambers comprising one preparation unit

for drying and preoxidation, and four reactors. Their functions are as follows:

R0: Drying and Preoxidation (Preparation unit).

R1: Pyrolysis and Hydrogenation of sulfur-containing-coal, and including gas preheat of recycled fuel-gas by cooling char.

R2: Calcination of CaCO_3 to form CaO for H_2S absorption.

R3: Absorption of H_2S carried across from R1, by CaO . The concept requires a design such that the gases in R1 and R3 have equal access to both reactors while the coal and absorbent streams remain separate. CaS is formed by absorption.

R4: Regeneration of CaS formed by H_2S absorption in R3, utilizing reaction of steam and CO_2 to reform CaCO_3 , which is then cycled back to R2 after separation from reformed H_2S .

In selecting reactor types for all these operations, Reactors R1 and R3 are assumed to be Cascades. For the rest, however, the analysis leading to the Sankey Diagram is valid when any continuous counterflow reactor is used.

SANKEY DIAGRAM ASSUMPTIONS

In performing the Sankey Analysis a number of assumptions about the system and materials were made, as follows:

Sulfur Content and Removal

The coal to be treated is assumed to contain 5% sulfur by weight. This is assumed to be totally removed in Reactor R1 as H_2S by hydrogenation; absorbed in R3 as CaS , regenerated in R4 as H_2S , followed by recovery by the Claus Process.

Coal Pyrolysis

The maximum temperature of the coal is assumed to reach 700°C so pyrolysis corresponds to low temperature carbonization. For a 40% V.M. coal a 30% pyrolysis/hydrogenation, loss is assumed of which 5% is sulfur as H_2S . If the coal is such that the pyrolysis/hydrogenation loss is less than this the majority of the calculated energy flows in reactors R2, R3, and R4 are reduced approximately prorata. The balance of material (not pyrolyzed) is a semi-coke that can be assumed to be of higher reactivity than a full coke.

Temperature Profiles

In reactors R2, R3, and R4 the temperature profiles are simple, either rising or falling monotonically from one end to the other, with the counterflow material temperature falling or rising correspondingly. The reactor R1 presents a different problem. Its temperature is highest at the center, for both counterflowing materials, so an overall heat balance shows a relatively small net supply of heat, Q_{31} sufficient for the sensible heats of coal char and pyrolysis products and the heat of pyrolysis. This is the heat supply that has been calculated. It is assumed to be carried across from reactor R3 to R1 partly by hot gas transfer, and partly by conduction where the temperature differentials will allow this. In addition, there is a sizable quantity of heat, not included in the diagram, required for the initial sensible heat of the coal to heat

it from input temperature to reactor temperature (700°C). This is recovered in the hot-gas/pyrolysis-products transfer from R1 to R3, so it recycles continuously. It has to be assumed, however, that the appropriate heat transfer mechanisms will so operate that this necessary heat flow cycles properly. This is a substantial assumption.

REACTOR CONSIDERATIONS

Reactor Capacities and Reaction Times

These, of course, are not yet determined. The calculations are based on a coal supply of 100 lb. If the process capacity is to be 100 lb/hr. then the material and energy flows shown in the diagram become flow rates (lb/hr. of material CHU/hr. energy). The reactor duty is then specified, and the reactor capacity can be calculated from the reaction time so that the appropriate duty is attained. On the other hand, this may well affect the final choice of reactor. It seems probable that the reaction time for absorber regeneration in R4 at the temperature specified is too long for a cascade reactor to be feasible. However, the temperatures are such that a tunnel reactor, with a belt conveyor in counter-flow to the reactant gases, may be possible, or even an array of fluidized beds.

Losses and Source of Energy

Losses are initially neglected. The prime source of energy into the reactor set is by combustion of part of the cleaned pyrolysis products leaving reactor R3. This supplies some sensible and mainly potential heat to the reactor R2. On combustion most of this heat enters the CaO which carries it into R3. Some of this heat then exchanges with the cooler recycle gas and pyrolysis products. The balance (the majority) is assumed to be carried into reactor R1 as sensible heat where it is used for pyrolysis. Some of the heat of combustion in R2 leaves in the product gases which are cycled to R4, to provide the CO₂ and part of the H₂O required for reaction there. The rest is absorbed in the endothermic calcination in R2, but this is recovered again as heat of reaction, a little in R3 but most in R4. In addition, there is the internal cycling of sensible heat referred to in Temperature Profiles above. At present it seems necessary to assume that much of this is supplied by conduction through the construction materials of the dual R1 and R3 reactors, and is returned again to R3 by the pyrolysis products exchange.

Losses (wall; reactor exchange etc.) can then be included at any time by requiring an appropriate increase in the fraction of pyrolysis products burned in R2, with the heat thus generated assigned to losses.

Sankey Diagram Analysis

The Sankey Analysis is a heat and mass balance on each individual reactor. Based on the assumptions listed above, some of the inlet and exit temperatures could be preselected, as follows:

- R1: T_{\max} : (near center) not to exceed 700°C .
 T_{inlet} : assumed to be 50°C (following drying and light preoxidation).
 T_{outlet} : unspecified - to be determined (T_c).
- R2: T_{inlet} : selected as 500°C to match outlet temperature of R4 (see R4).
 T_{outlet} : specified as 1000°C to assure adequate calcination rate of CaCO_3 .
- R3: T_{inlet} : selected as 1000°C to match outlet temperature of R2.
 T_{outlet} : unspecified - to be determined (T_e).
- R4: T_{inlet} : Selected to match outlet temperature of R3 after this (R3) determination (T_e).
 T_{outlet} : because of the heat of reaction this exceeds T_{inlet} . Because of reaction requirements the peak temperature (which is T_{outlet}) must be lower than 600°C . A temperature of 500°C was selected for calculation to allow some margin for adjustment.

In then setting up the energy balances for the individual reactors there are four equations, one for each reactor, but with a total of five unknowns, only two of which are the unknown temperatures listed above.

1. T_c : the exit temperature of the semi-coke leaving R1.
2. Q_{31} : the heat transferred from reactor 3 to R1.
3. T_e : the exit temperature of the solids leaving R3 to enter R4, the solids being CaS , CaO , and inert.
4. M : the solids quantity cycling round reactors R2, R3, and R4, to temperate R4 and supply heat from R2 to R3.
5. P : the quantity of pyrolysis gas required to heat the CaCO_3 and inert in R2 to 1000°C .

The four reactors are treated separately. In all calculations input and output enthalpies are determined with respect to 0°C as zero. Atmospheric pressure is assumed so specific heats are all at constant pressure, where this is relevant.

Completing the heat and mass balances then led to sufficient information to complete the Sankey Diagram when a final item of information was included since the system was otherwise indeterminate with five unknowns but only four equations. The calculations showed that, if the physical mechanisms would allow it, heat could flow either from R1 to R3, or from R3 to R1. However, we know that the temperatures in R1 must always be less than those in R3 since otherwise net heat would not flow from R3 to R1, and the system would not work. If the mechanism of heat transfer is by conduction through the brickwork of the adjacent reactors, then a substantial temperature difference must be maintained between the two. This immediately limits the exit temperatures of R1 and R3 to 225°C or less (determined by the analysis); indeed it must be substantially less than 225°C if the temperature difference between the two reactors is also to be substantial. This restriction is less stringent, however, if the heat exchange between the two reactors is mainly convective. In the limit, in fact, if gaseous exchange between the two reactors is extremely fast - which is also highly desirable from the absorption point of view - the gas temperatures can be almost equal (the "stirred reactor" condition), and this is, in fact, the condition assumed. It is possible under good design conditions for this to be not unrealistic, at least for the lower half of each of the two reactors (R1 and R3), though it will not be true

at the top of each reactor. Here, the coal enters cold (50°C) and the CaCO_3 and inert enter hot (1000°C) and this is expected to provide sufficient temperature differential to generate the heat flow required to heat the incoming coal to 700°C .

Adopting the "stirred reactor" or equivalent temperatures condition for T_e and T_c , these have equal values at 225°C . The value of M required is then about 150 lb/100 lb. coal, and P is 3.8 lb. of volatiles/100 lb. coal. Finally, the net heat flow required for the coal pyrolysis at a coke exit temperature of 225°C is 32,500 CHU. In summary, therefore, the values adopted for the five unknowns are as follows:

1. and 2. $T_e = T_c = 225^{\circ}\text{C}$
3. $M = 150$ lb. inert/100 lb. coal.
4. $P = 3.8$ lb. volatiles/100 lb. coal.
5. $Q_{31} = 32,500$ CHU/100 lb. coal.

These are the values used for constructing the Sankey Diagram.

THE SANKEY DIAGRAM

The specific objectives in constructing the Sankey Diagram are restated below:

1. To determine the process feasibility in terms of the energy requirements.
2. To establish the expected reactor temperatures.
3. To establish the material flow requirements.

The prime conclusion drawn from the diagram is that the material and energy flows are acceptable and compatible with realistic reactor temperatures, so long as the simplifying assumptions are not too unrealistic. This is assessed to some extent in the following commentary.

1. Taken at its face value the Sankey Diagram summarizing the calculations supports the feasibility of the proposed process. Specifically, if the assumptions made are realistic, then the quantities of materials to be handled are not excessive, the temperatures involved are reasonable and well within limits of many current industrial processes. Perhaps most important of all, the energy self-consumption of the process is relatively small. As calculated it is under 13% of the energy of the cleaned pyrolysis products, and about 4% of the total potential thermal energy in the raw coal. This must, of course, be a somewhat optimistic estimate since the analysis excludes heat losses and power requirements for fans, pumps, transfer machines etc. Allowing for these by an increase of 50% in the self-consumption, then this becomes 6% of the potential energy.

2. This estimate of 6% self-consumption may at first sight seem a little high compared with the typical figure for a modern power station of 4 to 5%. This means that an additional 6% could be too high a penalty to pay; however, of the 6%, only 2 or 3% represents unrecoverable losses. This will be clear from examining the Sankey Diagram where the bulk of the 33,000 CHU supplied to the system by burning 3.8 lb. of pyrolysis products reappears in three ways:

(1) as sensible heat of the pyrolysis products, totalling 8,500 CHU; (2) as sensible heat of the char, totalling 6,300 CHU; and (3) as enthalpic heat of pyrolysis, totalling 20,000 CHU, but which reappears as slightly increased heat of combustion per pound of both char and pyrolysis products so it is recovered on combustion (These are the figures for Reactor R1 above: a further 2,300 CHU are supplied by the sensible heats of coal and hydrogen, and the H_2/S heat of reaction).

This means that about 2/3 of the energy supplied by combustion of the pyrolysis products is automatically recoverable on combustion of the cleaned output. Even more can be recovered if the char and pyrolysis products can be burned immediately without any wastage from cooling since this will recover most of the sensible heat in the output. The system is, therefore, potentially conservative from the energetics point of view.

3. There might still be problems in recovering the sensible heats in the two outputs. For the pyrolysis products this should be the simpler problem of the two since the gases only have to be mixed with air to provide a stable flame - at 1000°C flame holding is no problem - so these could be burned directly in a boiler. Problems would arise primarily as materials problems in confining the high temperature gases till they enter the boiler. Some degree of pre-cooling might, therefore, be required to a temperature where the gases can be handled in metal pipes. There might even be some reason to cool the gases completely and use them as a make-up source for pipeline gas (although the Btu/cu. ft. volume is a little low for this).

4. The problems in handling the char could be greater although the temperatures are initially very much lower. The char should be in much the same form that the coal is originally introduced. If the reactor is a cascade, the coal should be crushed. The char will, therefore, be relatively coarse and certainly unsuitable for immediate use in a conventional pulverized coal boiler: indeed, even if fine enough, conventional belief is that there would then be flame holding problems. The char would otherwise be nominally suitable for direct use in an axial-fired cyclone combustor, but this is only possible if the ash fusion characteristics are also appropriate.

This, unfortunately, indicates that some other combustor may have to be devised. One interesting possibility would be to construct another cascade unit, with water-cooled cascade plates, to burn the char in; however, this would require the development of an entirely new technology. The alternative is only a little better since it again requires a new technology. The char would be suitable for combustion in a fluid bed. Here the necessary technology is being developed. It is not yet commercial, but it is now in a usefully advanced research stage.

5. Development of new technology of a fairly complex character is also a factor militating somewhat against the proposed scheme. The problem that should be borne in mind is that current utility plants for the most part have a high reliability, and utility engineers for the most part are likely to expect additions to existing plants of similar reliability. This is also likely to be a serious matter in view of the current small margin of reserve generating capacity over increasing demand. Unscheduled outages at peak demand could result in brown-

outs or black-outs over appreciable regions. For these reasons it would obviously be desirable to develop the cleaning system in stages. This would mean completing reactors R1 and R2, using precalcined lime and not attempting sulfur recovery and regeneration in the first place. Recovery can then be developed on an open cycle basis, and if this proves successful, the closed cycle operation can be completed.

6. The success of the whole concept, however, is predicated upon certain key assumptions that are still somewhat marginal in our present state of information. The most important of these is the assumption that the gases will exchange with sufficient speed between reactors R1 and R3 that H_2S absorption by CaO will be reasonably rapid after the H_2S has been formed, and that resorption by coke will always be a minor process. If this is true then it is also likely to satisfy the second assumption that the temperatures in R1 and R3, at least in the lower sections of the two reactors, are much the same. A third critical assumption is that the reactors can be built tall enough, but without being excessively high, for the residence times to be long enough for both desulfurization and desorption. Finally, there are the closely related assumptions (1) that the heat exchange between R1 and R3 assumed to take place in the upper sections, that provides the sensible heat for the coal to reach $700^\circ C$, will take place; and likewise (2) that the heat recovery in the lower sections that will reduce the material temperatures to $225^\circ C$ will also be possible.

Definitive information on these assumptions is still lacking. This will require experiments on cascade operation. If, however, experiments should show them to be valid, then the cleaning process can be operated at least on an open cycle basis. Energetically this may be less satisfactory, but as mentioned above, the technological complexity will be reduced substantially.

7. There are, finally, two respects in which the Sankey Diagram is not quite complete:

(a) As already mentioned, sensible heat required to raise the incoming coal to $700^\circ C$ will be recovered from R1 and returned to R3 (if the assumed energy recovery in the lower sections occurs). Since this is continued exchange from R3 to R1 and back again, it should appear on the diagram as a closed loop of sensible heat. The actual quantity required for this is not very high: 16,250 CHU/100 lb. coal; and its omission is not mechanistically important if the system works as envisaged. For if it works, then this exchange occurs; if the exchange does not occur, then the system has failed as so far described. This, however, should only mean that alternative methods of injecting the necessary energy into R1 must be used. Appropriately modified for this, the scheme should still be operable although the overall energy balance may not look quite so good.

(b) The second omission is again a closed loop, this time of material. To make sure that sulfur is removed at an adequate rate the R1 reactor should contain as high a hydrogen concentration as possible, particularly in the lower sections for sulfur recovery from H_2S resorbed by the coke. Since most of the volatiles (containing the hydrogen) will be released near the center of the reactor, and will then rise, the lower section is likely to be deficient. An appropriate fraction of the cleaned pyrolysis products must, therefore, be

cooled (to allow handling) and injected into the bottom of reactor R1. Since this is a mass flow cycling internally there is no net decrease in the volatiles output; for complete representation, however, the diagram should include a closed loop to represent this recycle.

CONCLUSIONS

From the considerations discussed above, desulfurization of coal by hydrogenation before combustion appear to be feasible, energetically and materially. The kinetic data obtained by the non-isothermal method of Juntgen are quite adequate for making preliminary estimates of reactor size. From these it would appear that the reaction times for the desulfurization and for the H₂S absorption may be compatible with residence times in a reasonably sized cascade reactor. The regeneration and calcination on the other hand is problematical, but for these more conventional methods such as shaft reactors may be quite suitable. The possibility of making such judgments, therefore, illuminates the value and necessity of adequate kinetic data, such as were obtained by the non-isothermal method, to enable design of reactors in the rapid development of a new technology.

REFERENCES

1. a) Scientific Research Instruments Corporation Report SRIC 68-13 (1969).
b) M.L. Vestal and Wm. H. Johnston, "Chemistry and Kinetics of the Hydro-Desulfurization of Coal, "Chemical Institute of Canada and American Chemical Society Joint Conference, Toronto, May 25, 1970. In press.
2. a) Juntgen, Erdol and Kohle 17, 180 (1964).
b) Juntgen and Traenckner, Brennstoff-Chem. 45, 105 (1964).
c) See also Reference 3 - ref. 15-22.
3. Scientific Research Instruments Corporation Report No. SRIC 69-10 (1969).
4. N.J. Hassett, Industrial and Process Heating (November 1966).

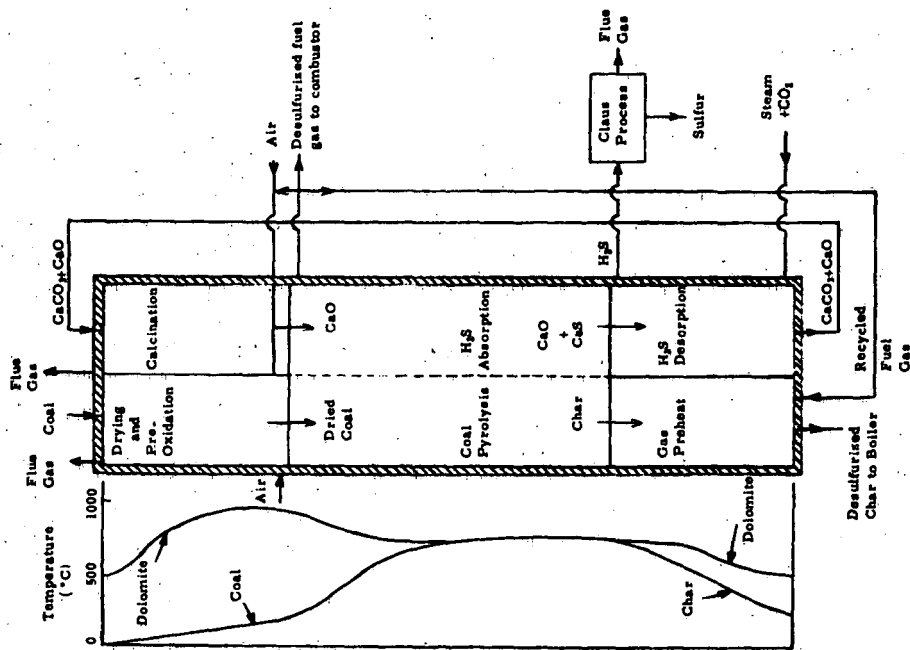


Figure 2. Simplified Block Diagram of Complete Conceptual Desulfurisation System

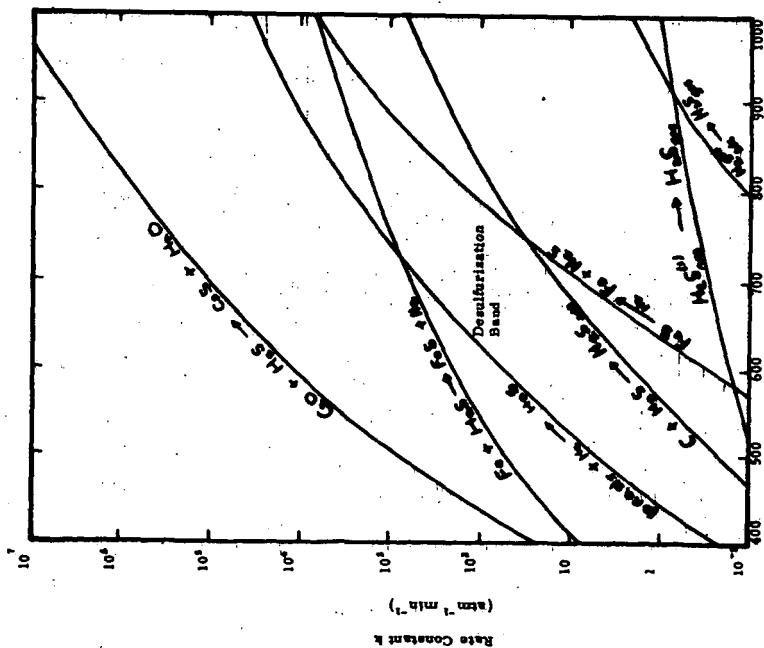


Figure 1. Rate constants for coal desulfurisation reactions and for important back reactions as functions of temperature.

PROCESS RESEARCH ON DESULFURIZATION OF PETROLEUM COKE

by

R. D. Ridley

Garrett Research and Development Company, Inc.
La Verne, California 91750

The individual and combined effects of sodium hydroxide, sodium carbonate, hydrogen, and hydrogen sulfide on desulfurization of petroleum coke have been reported on the literature many times (1-5). Hutchings (1) shows that essentially complete desulfurization is obtained using a high ratio of NaOH to coke, a temperature of 750-865°F, and a 7-1/2 hour residence time. Lukasiwicz and Johnson (2) desulfurized delayed petroleum coke with sodium carbonates and determined an optimum temperature of 1,400°F. They obtained up to 67 percent desulfurization using 0.28 gm Na₂CO₃/gm coke. Seventy percent of the sulfur removed was recovered as a sodium sulfide wash solution. The balance came off as H₂S. Mason (3) demonstrated that hydrogen was relatively ineffective for desulfurization of fluid coke. Almost 6 hours were required for a 50 percent sulfur reduction at 1,300°F. Mason also showed that the sulfur content of fluid coke could be increased by reaction with a H₂S-H₂ mixture. Gorin (4) and others (5) have also shown the deleterious effect of H₂S on char desulfurization. And finally Johnson (6) discovered the combined effect of sodium hydroxide and hydrogen for desulfurization of calcined coke.

This paper presents data on desulfurization of fluid petroleum coke with hydrogen, with sodium hydroxide and hydrogen and, as an outgrowth of this work, sodium sulfide and hydrogen. A screening study wherein over 80 potential sulfur acceptors were reacted with ground fluid coke at 1,400°F, identified NaOH and KOH as effective reagents and, in general, confirmed the conclusion of previous workers. The use of hydrogen and relatively small amounts of NaOH with fluid coke was found to be a highly efficient desulfurization route. As with all sodium hydroxide or carbonate systems, most of the sulfur was recovered as soluble sodium sulfur compounds, primarily Ha₂S. Some sulfur was also recovered from the off gases, both as H₂S and COS. Experiments wherein the sodium sulfide product was substituted for the sodium hydroxide reactant gave substantial desulfurization resulting in significant simplification of the commercial process concept as described in U. S. Patents 3472622 (7) and 3472624 (8) assigned to Tidewater Oil Co. (now Getty Oil Company).

Fluid coke is a petroleum coke produced as small, low surface, essentially spherical, dense particles. Ninety-five percent

falls in the particle size range of 14 to 200 mesh. Table I shows typical properties. The sulfur content is, of course, dependent upon the sulfur content of the residuum feed to the fluid coker. Coke used in this work varied from 3.7 to 7.2 percent sulfur. Oxygen content and surface area are functions of particle size as shown in Table II. One step in fluid coking is the reheating of coke to reaction temperatures by burning with air. This is accomplished in the coker burner; product coke is also withdrawn from this vessel. Thus the last reaction in fluid coking is an oxidation and it is not surprising to find oxygen in the product. Nor is it surprising to find more oxygen on the smaller particles which have more geometric surface area per unit weight. The measured surface area (BET) also increases with decreasing particle size. Figure 1 is a photomicrograph of two typical coke samples and shows the essentially spherical form of each particle. The basic structure is shown in Figures 2 and 3. Coke is laid down in thin layers or "onion skins" with burning occurring between laydown of layers. These onion skins are quite evident, and in Figure 3, a seed particle is also evident. This structure was described previously by Dunlop, Griffin, and Moser (9).

Desulfurization with hydrogen alone was found to be diffusion limited as indicated by a direct relationship with surface area as shown in Figure 4. Fluid coke was screened to obtain the different particle size fractions and reacted at 1,400°F for 1 hour with hydrogen gas flowing through the bed. Maximum sulfur removal was approximately 40 percent; desulfurization of unscreened coke under the same conditions is approximately 15 percent.

In another series of experiments, fluid coke was reacted with an equal weight of NaOH at 1,200°F for 1 hour and without a sweep gas. The product mix was cooled, extensively washed with water, and analyzed for sulfur. Essentially complete desulfurization was obtained. Figure 5 is a photomicrograph which shows that the coke particle is literally torn apart by these severe conditions. Unfortunately, surface area on this treated coke was not measured, but from other work, it is estimated to be close to 100 m²/gram. Thus, NaOH obviously either eliminated or dramatically reduced the diffusion barrier evident for desulfurization with hydrogen alone. If a reduced NaOH concentration would "open up" the coke surface, more efficient desulfurization with hydrogen would be anticipated.

Experiments with NaOH, H₂ and coke were made over the operating range of 800 to 1,600°F and 0.0 to 0.40 #NaOH/#coke. Aqueous NaOH (usually 50 percent solution) was sprayed onto coke particles in a liquids-solids blender. Thirty grams of the mix was placed in a quartz tube, hydrogen flow was started and the mix brought to reaction temperature. After a run, the samples were cooled, washed to remove sodium compounds - mostly sulfides - and the coke analyzed for sulfur. Figure 6 shows that

1,200°F to 1,400°F is the optimum temperature range; Figure 7 that 90 percent desulfurization can be obtained with 0.13 #NaOH/#coke at 1,220°F, with a 1 hour reaction time. The cokes from these runs were indistinguishable from raw coke under the same microscope used for the earlier photomicrographs. Data for these runs is shown in Table III. Residual sodium analyses were not made on these desulfurized cokes; however, later work showed that sodium on coke treated in this manner normally assayed 0.1 to 0.7 wt. percent.

Experiments with a 6.0 percent sulfur coke showed similar results although the percentage desulfurization was somewhat reduced. Figure 8 and Table IV shows data from two series of experiments; one run as indicated for the earlier experiments, the other using a larger reactor, a fluid bed, and a different system for addition of the hydroxide. Five hundred sixty grams of coke were loaded into the reactor, fluidized with nitrogen, and heated to 1,200°F. At this point, gas flow was switched to hydrogen and a 50 percent aqueous solution of NaOH admitted to the bed slowly through an atomizing nozzle. Addition of the desired quantity required 22 to 33 minutes after which the reaction was continued for one hour. Essentially the same results were obtained for the two systems.

At this point in this development it appeared that desulfurization was primarily due to the strong getter effect of sodium for sulfur and that hydrogen simply facilitated the transfer of sulfur from the coke to the sodium. It appeared that the getter was necessary to minimize the partial pressure of H₂S; without it, desulfurization would be severely restricted. Primarily to test this theory, several runs were made in which sodium sulfide was substituted for sodium hydroxide. These runs were mostly carried out in the larger reactor utilizing 560 grams of coke and varying amounts of sodium sulfide. The sodium sulfide came from two sources. Wash solutions from desulfurization runs with NaOH were spray dried to obtain an essentially anhydrous product having a sodium to sulfur mole ratio of 2.14 to 1. For other runs, vacuum dehydrated sodium sulfide trihydrate was used. The dehydration was accomplished in nickel crucibles at a pressure of 200 microns with a maximum temperature of 360°F reached in 6 to 8 hours. The trihydrate is theoretically 40.9 percent water; 37.7 percent was recovered, indicating that 3.2 percent water was not removed. When dried slowly the trihydrate remained as flakes which were easily ground to -40 mesh. If dehydration proceeded too rapidly the flakes would melt and form a fused mass unsuitable for further use. All dried Na₂S was stored in a dry, inert atmosphere.

Needless to say the desulfurization results were not what were expected. Sulfur reduction did drop, but less than anticipated. Table V shows comparisons between the NaOH and Na₂S systems for both cokes. For the higher sulfur coke desulfurization dropped from 76 to 45 percent. For the lower

sulfur coke, desulfurization dropped from 91 percent to 64 percent; however, additional residence time increased desulfurization with Na_2S as shown in Figure 9.

The significant point in this discovery is its effect on an overall process concept. All sulfur removal is as volatile sulfur compounds, i.e., H_2S and COS . These can be recovered easily from the gas stream. Sodium sulfide can be separated from the coke by washing, spray dried and recycled directly without conversion back to the hydroxide form. This is shown in Figure 10.

The wash step is still undesirable. For one thing it is costly, for another inefficient as it does not remove all the sodium added. Typical results show 0.1 to 0.7 wt. percent residual sodium. One more approach was attempted to substitute size classification for washing. Coke was screened to obtain two separate fractions: 60 to 80 mesh and 150 to 200 mesh. The 150 to 200 mesh sample was impregnated with NaOH and reacted to convert it to the sulfide form. The recovered particles were not washed. One hundred forty grams were mixed with 290 grams unreacted 60 to 80 mesh coke. This mix was reacted with hydrogen at $1,200^\circ\text{F}$ for two hours. After reaction, the 60 to 80 mesh coke was separated and analyzed. It was then washed and reanalyzed. Results are shown on Table VI. As can be seen some sodium was transferred to the larger particles, thus necessitating the wash. Thus this experiment failed to find a way to eliminate the washing step. However, the desulfurization results were considerable better than obtained with Na_2S and equally as good as with NaOH . Sixty nine percent desulfurization was obtained. This 69 percent compares to 66 percent obtained in one hour with NaOH and an estimated 50-55 percent that would have been obtained with the same quantity of Na_2S .

A clear picture of the reaction mechanism for coke desulfurization with sodium compounds and hydrogen has not really evolved although certain items are known. The getter effect of NaOH is helpful but unessential except where virtually complete desulfurization is required. It appears that the primary role of sodium is to eliminate or reduce the diffusion limitation which prevents effective desulfurization with hydrogen alone. Surface areas in desulfurized cokes were 30 to 60 m^2/gm compared to 10-12 m^2/gm on the raw coke. The partial pressure effect of H_2S , obvious in other work on coke and coal chars, is not limiting when sodium is present. Concentrations up to 5 percent H_2S plus COS had to occur in the initial stages of reaction. Some sodium either reacts with the coke particle or migrates into it to such a position that it cannot be removed by washing. However, no direct relationship was found between percent desulfurization and residual sodium. While not detailed in this report, there is evidence that the amount of sodium left on the coke is a function of the partial pressure of water vapor during the reaction.

In summary, the data obtained in this study is, consistent with that reported by other investigators of NaOH and CaOH-H_2 systems. Up to 97 percent desulfurization was obtained when processing with the NaOH- H_2 route. However, this data also shows up to 74 percent sulfur removal in a $\text{Na}_2\text{S-H}_2$ system. Eighty to 90 percent desulfurization is believed attainable by this route with further process optimization. The high partial pressure of H_2S that occurs in this $\text{Na}_2\text{S-H}_2$ system does not appear to significantly retard sulfur removal.

Acknowledgement:

The author wishes to thank Getty Oil Company, especially Mr. R. M. Hunt, Refinery Manager, for permission to present this paper. Too many persons to list assisted in this work and their help is sincerely acknowledged. The leadership exhibited by Dr. A. W. Lewis was particularly appreciated. The author also wishes to thank his present employer, Garrett Research and Development, for the time to prepare and present this paper.

REFERENCES

1. Hutchings, L.E., U.S. Patent 2,878,163, March 17, 1959.
2. Lukasiewicz, S.J., & Johnson, G.C. "Desulfurization of Petroleum Coke" *Industrial and Engineering Chemistry*, 52, No. 8 pp. 675-677, August 1960.
3. Mason, R.B., "Hydrodesulfurization of Coke" *Industrial and Engineering Chemistry* 51, No. 9, pp. 1,027-1,030, September 1959.
4. Gorin, E., Curran, G.P., and Batchelor, J.D., U.S. Patent 2,824,047 February 18, 1958.
5. Jones, J.F., Schmid, MR., Sacks, M.E., Chen, Y., Gray, C.A. and Eddinger, R.T., "Char Oil Energy Development" Report on Performance of OCR Contract 14-01-0001-235 for January-October 1966.
6. Johnson, U.S. Patent 3,009,781.
7. Ridley, R.D. U.S. Patent 3,472,622, October 14, 1969, assigned to Tidewater Oil Co. (now Getty Oil Co.)
8. Ridley, R.D. U.S. Patent 3,472,624, October 14, 1969, assigned to Tidewater Oil Co. (now Getty Oil Co.)
9. Dunlop, D.D., Griffin, L.I. Moser, J.F., "Particle Size Control in Fluid Coking" *Chemical Engineering Progress*, 54, No. 8, pp. 39-43, August 1958.

TABLE I

Typical Properties of Fluid Coke

Ultimate Analysis, wt.%

Carbon	87.83
Hydrogen	2.08
Nitrogen	1.34
Sulfur	(3.8-7.2)
Oxygen	1.33*
Ash	0.2

Physical Properties

Density, gm/cc	1.524
Surface Area, m ² /gm	10-12*

Screen Analysis

+14 Mesh	3.7
+60	26.4
+80	61.6
+100	75.7
+150	91.3
+200	98.5
-200	1.5

*Varies with particle size

TABLE II
Properties of Fluid Coke Size Fractions

<u>Tyler Mesh</u>	<u>Surface Area</u> <u>m²/gram</u>	<u>Oxygen, wt. %</u>
-35+60	8	1.19
-60+80	10	1.25
-80+100	16	1.33
-100+150	21	1.31
-150+200	38	1.48
-200		1.39

TABLE III
Desulfurization of Fluid Coke with NaOH and H₂

<u>Run No.</u>	<u>Temp.</u> <u>°F</u>	<u>NaOH/Coke</u> <u>wt./wt.</u>	<u>H₂</u> <u>V/V/hr.</u>	<u>Time, Min.</u>		<u>Sulfur</u> <u>wt.%</u>	<u>% Desul-</u> <u>furization</u>
				<u>Preheat</u>	<u>Reaction</u>		
Feed Coke	-			-	-	3.78	-
<u>Effect of Temperature</u>							
53D	1,200	0.10	530	8	60	0.51	86.5
63D	1,400	0.10	530	8	60	0.60	84.2
70A	1,600	0.10	530	8	60	2.14	43.7
<u>Effect of NaOH/Coke at 1,220°F</u>							
31B	1,220	0.25	530	90	60	0.10	97.4
44A	1,220	0.25	530	90	60	0.22	94.2
33B	1,245	0.15	530	90	60	0.32	91.5
34B	1,210	0.05	530	90	60	1.51	60.3
41A	1,220	0.05	530	90	60	1.37	63.9
40B	1,225	0.05	530	90	60	1.10	71.1
34A	1,210	0.00	530	90	60	3.01	20.8
<u>Effect of NaOH/Coke at 1,030°F</u>							
35A	1,030	0.40	530	90	60	0.16	95.8
35B	1,020	0.25	530	90	60	0.36	90.5
36A	1,040	0.15	530	90	60	0.67	82.4
36B	1,030	0.05	530	90	60	2.25	40.8
42A	1,030	0.05	530	90	60	2.38	37.4
42B	1,035	0.00	530	90	60	3.51	7.6

TABLE III (cont.)

Desulfurization of Fluid Coke with NaOH and H₂

<u>Run No.</u>	<u>Temp.</u> <u>°F</u>	<u>NaOH/Coke</u> <u>wt./wt.</u>	<u>H₂</u> <u>V/V/hr.</u>	<u>Time, Min.</u>		<u>Sulfur</u> <u>wt.%</u>	<u>% Desul-</u> <u>furization</u>
				<u>Preheat</u>	<u>Reaction</u>		
<u>Effect of NaOH/Coke at 820°F</u>							
37A	820	0.40	530	90	60	0.73	80.8
37B	830	0.25	530	90	60	0.94	75.3
38A	815	0.15	530	90	60	1.20	68.4
38B	830	0.05	530	90	60	2.84	25.3
43B	815	0.05	530	90	60	3.18	16.3
43A	820	0.00	530	90	60	3.78	0.1
<u>Effect of Time</u>							
53A	1,200	0.10	530	8	15	0.96	74.7
53B	1,200	0.10	530	8	30	0.87	77.1
53C	1,200	0.10	530	8	60	0.51	86.6
53D	1,200	0.10	530	8	120	0.47	87.6

TABLE IV
Desulfurization of Fluid Coke with NaOH and H₂

Run No.	<u>Quartz Tube</u>			<u>Pilot Plant</u>		
	<u>143</u>	<u>142</u>	<u>141</u>	<u>CD 12</u>	<u>CD 13</u>	<u>CD 16</u>
Reaction Temp., °F	1,200	1,190	1,200	1,200	1,200	1,200
Time, Minutes						
NaOH Addition	-	-	-	28	22	33
Reaction Time	<u>60</u>	<u>60</u>	<u>60</u>	<u>60</u>	<u>60</u>	<u>60</u>
Total Time	60	60	60	88	82	93
H ₂ Flow Rate V/V/Hr.	1,510	1,510	1,510	1,640	1,640	915
NaOH/Coke wt./wt.	0.05	0.10	0.15	0.065	0.078	0.147
Sulfur Analyses, wt.%						
Raw Coke	6.0	6.0	6.0	6.0	6.0	6.0
Desulfurized Coke						
Before Wash	*	*	*	4.0	5.0	*
After Wash	2.02	1.55	1.28	1.99	1.87	1.42
% Desulfurization	66	74	79	67	69	76
Residual Sodium, After Wash, wt.%	0.63	0.86	*	0.49	0.46	0.71

*Not determined

TABLE V
Desulfurization of Fluid Coke
Comparison of NaOH-H₂ and Na₂S-H₂ Systems

Run No.	Coke A		Coke B	
	CD-78	CD-16	CD-81	33B*
Reactant	Na ₂ S	NaOH	Na ₂ S	NaOH
Reactant/Coke, wt./wt.	0.135	0.147	0.15	0.15
Reaction Temp. °F	1,220	1,200	1,250	1,245
H ₂ Flow, V/V/Hr.	780	915	1,780	530
Sulfur Analyses, wt.%				
Raw Coke	6.0	6.0	3.8	3.8
Desulf Coke, Washed				
After 30 min.	4.25		1.75	
60	3.30	1.42	1.35	0.32
90	2.50		1.15	
120	-		1.00	
% Desulf @60 min.	45	76	64	91
% Desulf @90 min.	58	79**	70	94**
Residual Sodium, @ 60 min., After Wash	0.68	0.71	0.80	*
Na/S Mole Ratio in Wash	2.49	2.29***	2.39	*

* Not Determined

** Estimated

***Average 12 runs.

TABLE VI

Desulfurization of Fluid Coke
Use of Sodium Sulfide Carrier

Raw Coke, -60+80 Mesh, 6.0% S, grams	290
Reacted Coke with Na ₂ S, -150+200 Mesh, grams	140
Na ₂ S/Raw Coke, wt./wt.	0.056
Reaction Temperature, °F	1,200
Reaction Time, hrs.	2
Sulfur Analyses, -60+80 Mesh, wt.%	
Raw Coke	6.0
Before Wash	2.70
After Wash	1.86
% Desulfurization	69
Sodium Analyses, -150+200 Mesh, Recycle Coke, wt.%	
Start of Run	6.81
End of Run	1.40

PLATE 1

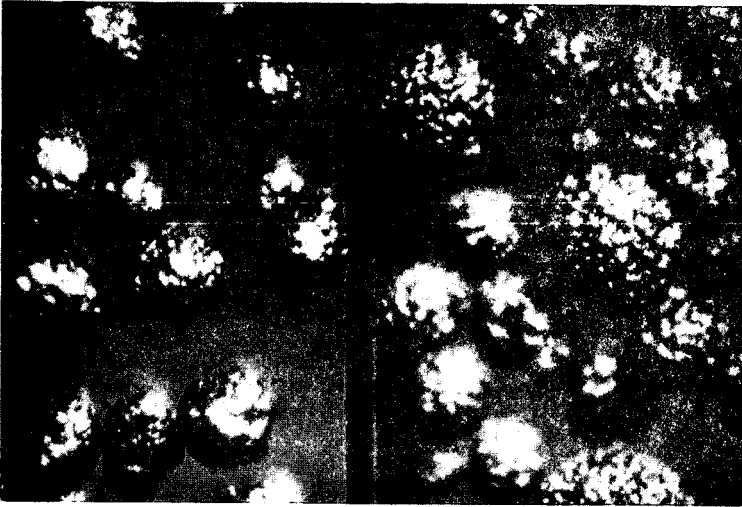


Figure 1. Fluid coke particles, untreated.



Figure 2. Fluid coke particle showing "onion skin" structure.

PLATE 2

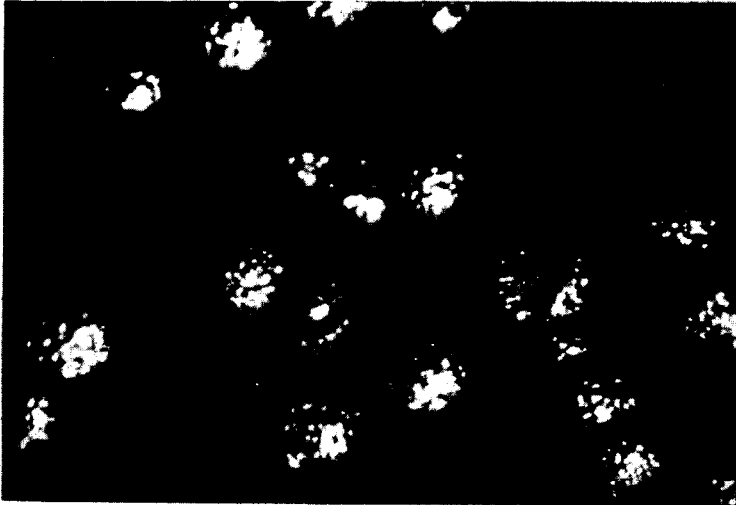


Figure 3. Fluid coke particle showing "onion skins" and seed particle.

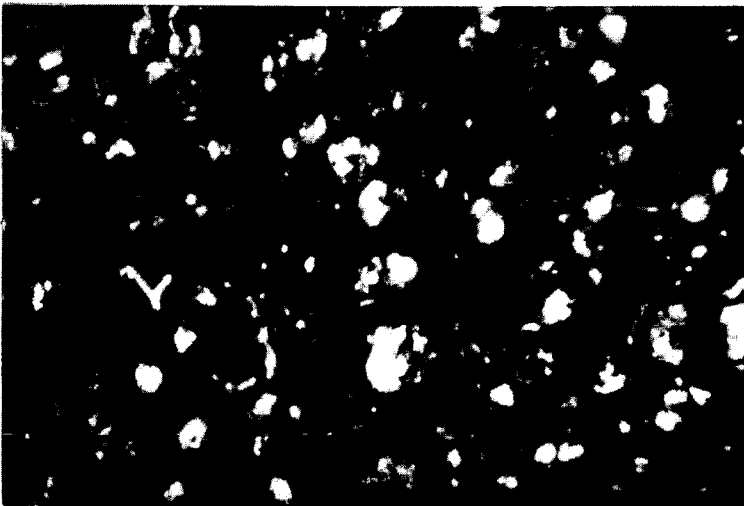
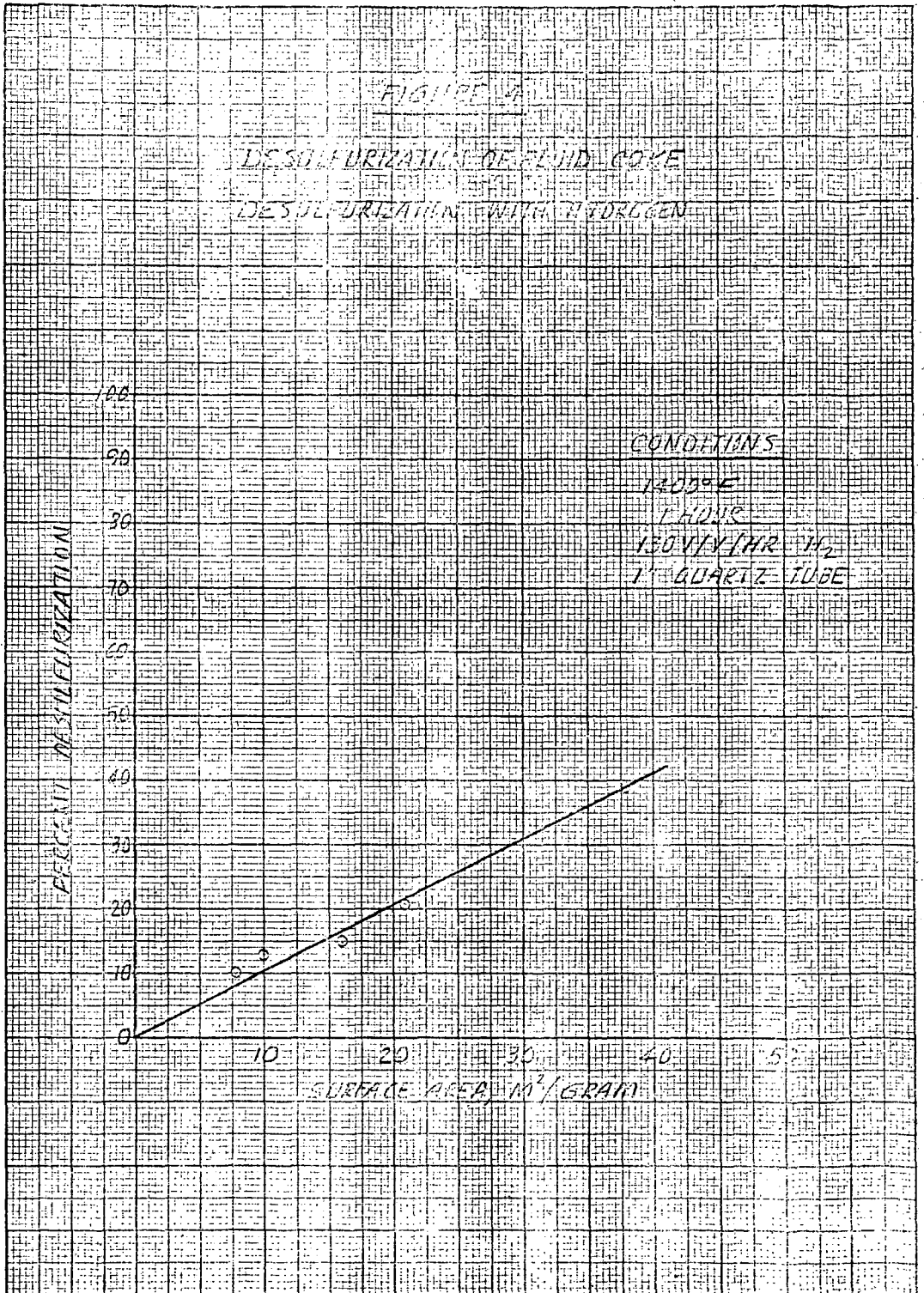


Figure 5. Fluid coke after reaction at 1,200°F, 1 hour, and with 1.0 gm NaOH/gm coke.



NOTES
DESULFURATION OF FLUID COKE
EFFECT OF TEMPERATURE
NaOH-H₂ SYSTEM

PERCENT DESULFURATION

100
90
80
70
60
50
40
30
20
10
0

1600 1500 1400 1300
TEMPERATURE, °F

RUN LENGTH - 1 HOUR
H₂ FLOW RATE - 530 V/V HR
NaOH/COKE - 0.10
PREHEAT TIME - 8 MINUTES

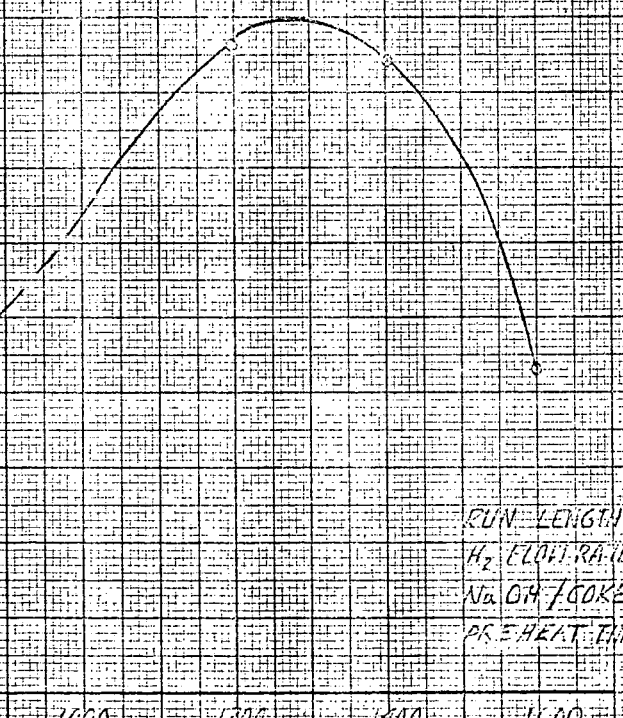


FIGURE 7
DESULFURIZATION OF FLUID COKE
EFFECT OF NaOH CONCENTRATION AND TEMPERATURE
NaOH-H₂ SYSTEM

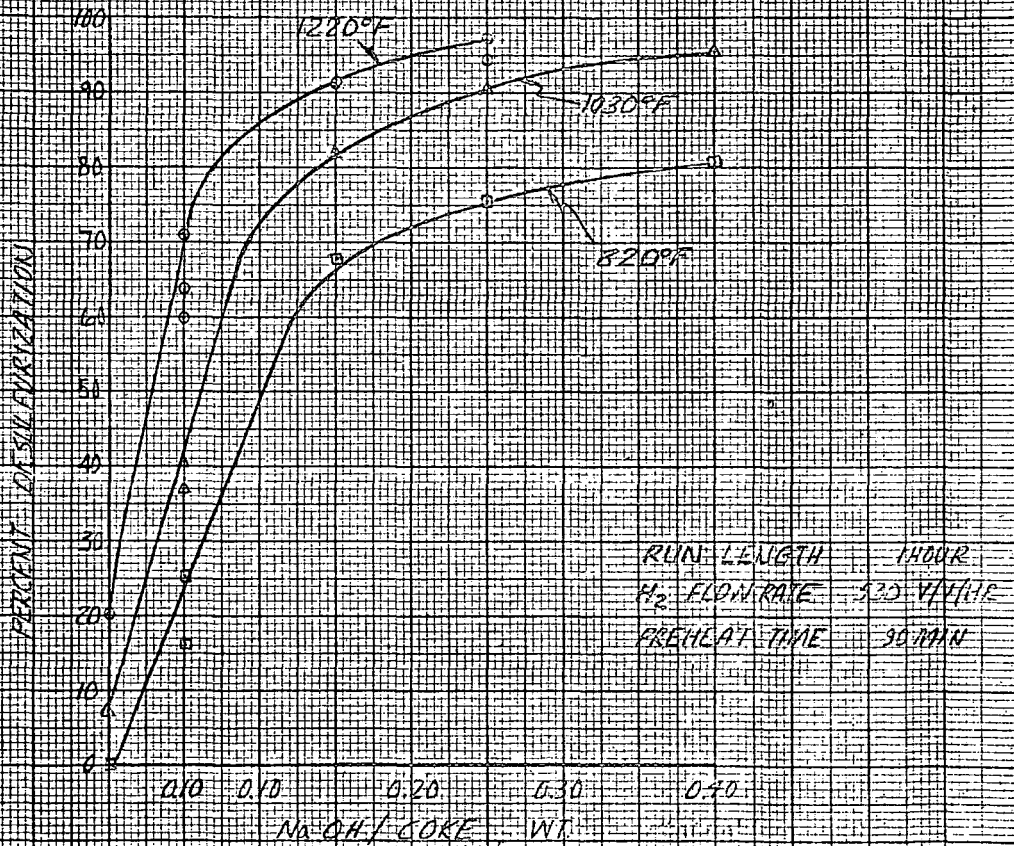


FIGURE 3

DESULFURIZATION OF FLUID COKE

EFFECT OF SCALE UP
NAOH-H₂ SYSTEM

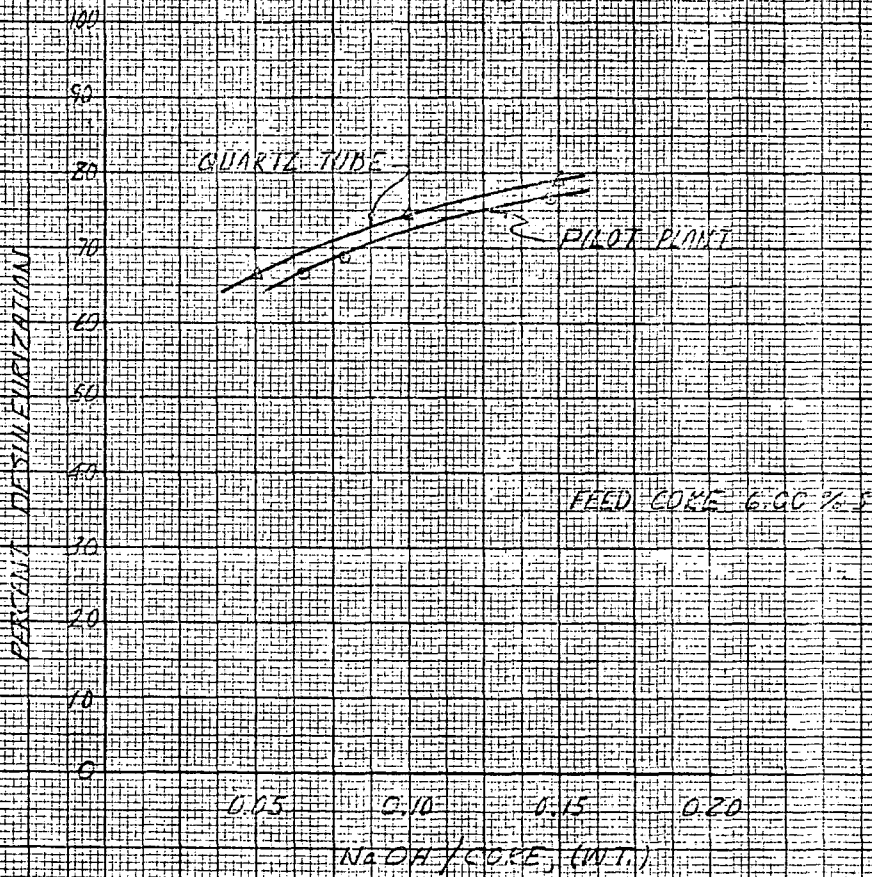


FIGURE 9
DESULFURIZATION OF FLUID CORE
COMPARISON OF $\text{Na}_2\text{S}-\text{H}_2$ AND $\text{NaOH}-\text{H}_2$ SYSTEMS

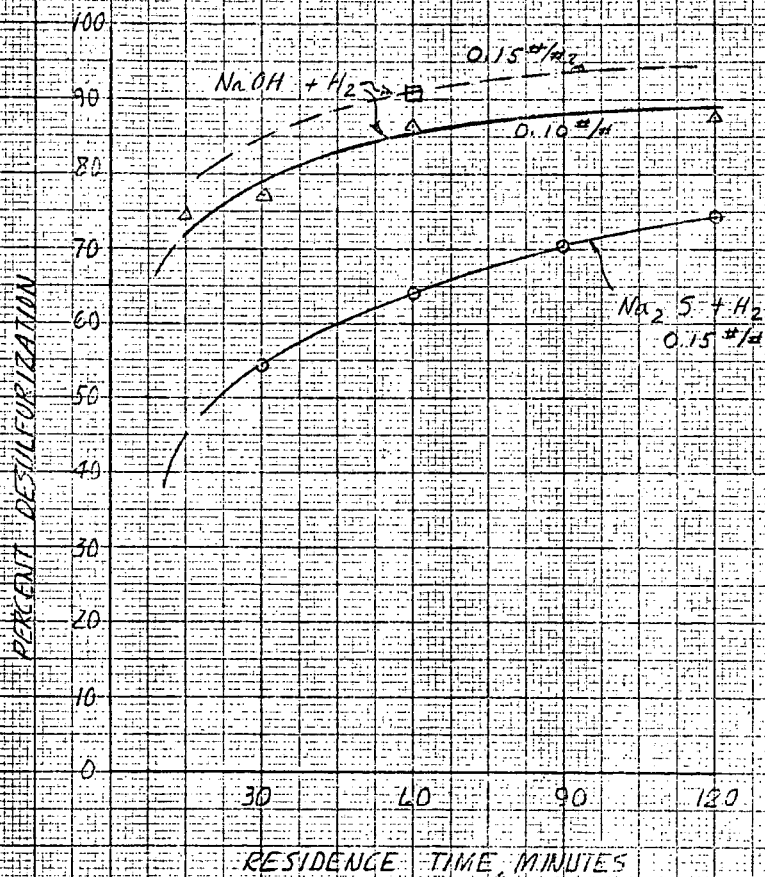


PLATE 3

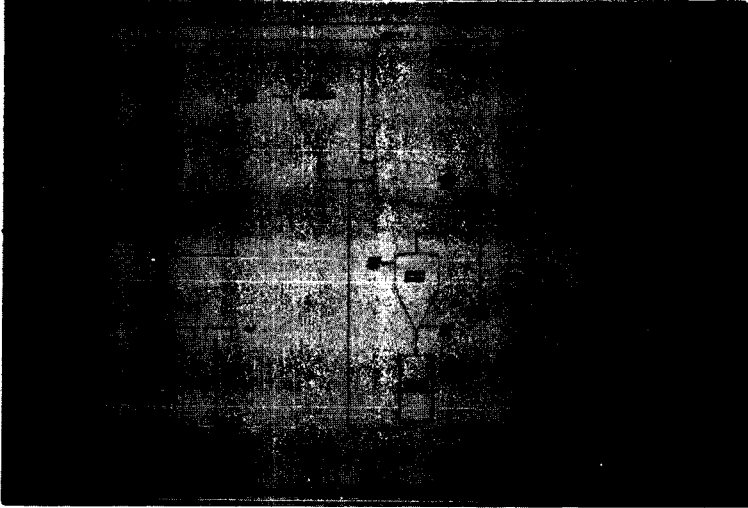


Figure 10. Flow diagram for fluid coke desulfurization with Na_2S and H_2 .

DESULFURIZING FUEL VIA METAL OXIDES

R. K. Bhada and W. L. Sage

The Babcock & Wilcox Co.
Research Center
Alliance, Ohio

INTRODUCTION

One concept for desulfurization of fuel involves conversion of the sulfur to hydrogen sulfide via partial oxidation with subsequent removal by reaction with a metal oxide to form a metal sulfide. The sulfide could then be regenerated with preheated air to produce a stream of concentrated sulfur dioxide. This scheme is illustrated in Figure 1. Such a scheme may be used in several processes. One such process for a two-stage combustion power cycle is illustrated in Figure 2.

While the concept appears attractive, very little is known about the reaction rates and limitations of desulfurization and regeneration. In order to obtain some preliminary data regarding these, bench-scale experiments were made using a synthetic gas. Temperature and gas flow velocity were varied. Based on results of these bench-scale experiments, a small pilot plant was built and tested employing coal gasification and a cyclic sulfur removal system. Iron oxide was selected because of its low cost and ease of availability. However, other oxides, such as zinc oxide, would probably be just as effective.

This paper describes our experiments and their results pointing to the utility of this desulfurizing concept.

APPARATUS AND PROCEDURE

Bench-Scale Experiments

A schematic diagram of the bench-scale experimental system is shown in Figure 3. Gas or air (depending on whether it is an absorption or regeneration cycle) flows at a controlled and measured rate through a quartz preheater into the reactant furnace. The furnace containing the reactant cell (details described later) is maintained so that the reactant surface temperature is constant at a predesigned value. The exit gases are cooled, analyzed, and vented through a stack.

High-temperature thermocouples are imbedded in the following five places to trace the temperature profile through the system: preheater, inlet to reactant furnace, surface of reactant, exit of reactant furnace, and exit of cooler (just prior to analysis). The flow rate is measured before preheating.

The hydrogen sulfide or sulfur dioxide is analyzed by a colorimetric method (modified Reich method) where the H_2S or SO_2 is reacted with a slightly acidic iodine solution. Additionally the other gaseous constituents of interest such as sulfur trioxide, carbon monoxide, carbon dioxide, and oxygen are periodically analyzed.

Two reactant materials were utilized: (1) sintered iron powder and (2) plain carbon steel. The sintered iron powder surface was fabricated in the form of cells of 0.25-inch inside diameter and reacting surface area of approximately 0.06 square foot. Each cell was formed by packing a tube with fine iron powder using a carbon rod to create the bore. The cells were then placed in a furnace at 70 F and raised to 1800 F at a rate of about 900 F per hour. The cells were held at 1800 F for 3 hours and then cooled gradually for 16 hours.

The plain carbon-steel surface was tested in two arrangements. The first arrangement was in the form of an annulus, and the second was in the form of a long single tube with three passes in the furnace. The first arrangement had a 3/8-inch diameter threaded rod in a 1/2-inch inside diameter pipe and was 21 inches long; the active surface was approximately 0.38 square foot. The second arrangement was 6.5 feet long, made of 0.269-inch inside diameter pipe; the reactant surface was thus approximately 0.45 square foot.

All tests were started with the oxidation cycle. Air at a controlled rate (set so that the velocity in the reactant cell was between 5 and 30 fps) was started through the system. The preheater temperature was then slowly raised, followed by raising the reactant furnace temperature. All thermocouples were continuously monitored. The cooling water was regulated to hold the stack gas temperature below about 150 F. After a sufficient oxidation period (greater than 1 hour), the air was turned off, and the gas was started. A synthetic gas, containing* approximately 1% H₂S, 12% CO, 8% CO₂, 1% CH₄, and the balance N₂, was started through the system at a controlled rate (set for a fixed velocity through the reactant cell). The exit gas was continuously analyzed for H₂S, and a record was also maintained of the temperature readings of the various thermocouples, the flow rate, and the CO and CO₂ contents of the exit gas. The synthetic gas flow was maintained until an appreciable breakthrough of H₂S was observed, usually about 1 hour, after which the gas was switched off and the air flow was started for regeneration. SO₂ was analyzed continuously, and temperatures, flows, and oxygen content were monitored intermittently.

After the regeneration, the absorption cycle could be started again. Several absorption and regeneration cycles were conducted in series to obtain some idea of the effect of cycling and continuous operation. At the end of the tests, the reaction cells were cut open and examined.

Pilot Plant Tests

The test equipment used is shown schematically in Figure 4, and a photograph is shown in Figure 5.

Coal is charged to a gasification chamber of 1-foot diameter and 10-foot length. This chamber is refractory lined to minimize heat losses. The make-gas from the gasifier passes through a one-stage cyclone chamber with an expected efficiency of 80 to 90% for particulate removal.

* Essentially the same composition as that of a synthetic gas from a gasifier.

The removal of hydrogen sulfide from products of combustion is accomplished by reaction on the iron oxide surface. The absorption cells were designed, employing a carbon-steel surface, to handle approximately 400 lb of gas flow per hour.

The arrangement of an absorbent cell is shown on Figure 6. The grid surface is made of 0.25-inch diameter carbon-steel rods. There are 1780 1-foot long rods in each cell providing 116 square feet of surface. The rods are staggered on 0.375-inch centers covering a 12-inch by 12-inch opening 18 inches deep. The cells are refractory lined with 2 inches of Kaocrete "D" to reduce heat loss.

A secondary furnace and combustor receives sufficient air to complete the combustion of make-gas, unreacted carbon, and auxiliary natural gas. The heat from the flue gas is absorbed by an air heater before the gases pass out the stack.

Air flow to the gasifier, secondary combustor, and cell regeneration is controlled by remote pneumatically operated dampers. Flow rates are determined by orifice meters, pressures by manometers or gages, and temperatures by well-type thermocouples. The fuel feeds are determined as follows: natural gas by orifice meter and coal from a calibration of feeder speed versus coal rate.

The method of gas analysis was the same as that in the bench-scale tests. Additionally the Barton Electrolytic Titrator was used for hydrogen sulfide detection at the exit, and a UV sulfur dioxide detector was used to closely follow the regeneration.

All shakedown and preliminary tests were started with the oxidation cycle. Combustion air to the primary combustor was set at a controlled rate to maintain a desired gas flow through two absorbent cells until steady-state conditions were established. The unit was heated up using natural gas by first placing the secondary combustor in service and then the primary. As the combustion air temperature was raised, the desired operating parameters were set in preparation for gasification and the absorption cycle. The combustion air temperature to the secondary and primary combustors was limited by the available air heater surface, resulting in a steady-state air temperature of 650 to 700 F during gasification. The pulverized coal was fed at approximately 50 pounds per hour for gasification. This gasification coal was transported by compressed air flowing at approximately 100 pounds per hour.

The gas leaving the absorption cells was continuously analyzed for H_2S , and the resulting data was recorded until significant breakthrough or saturation was apparent. After this occurred, regeneration was started, and the idle cell was placed in service on the absorption cycle. Normally, two of the cells were continuously on absorption while one of the three was on regeneration.

After the regeneration, the absorption cycle could be started again if desired. Absorption and regeneration cycles were conducted in parallel in order to obtain a better idea of the effect of cycling and continuous operation.

RESULTS

Bench-Scale Experiments

The following parameters were examined with the sintered iron oxide cells:

Cell dimensions: 0.25-inch inside diameter and 10.5 inches long
Cell surface temperature: 825 and 1200 F
Gas velocity: 7 to 18 fps

With the carbon-steel surface (annular and tubular arrangements), the following were the parameters:

Cell dimensions:

1. 3/8-inch threaded rod in 1/2-inch pipe, 21 inches long for the annular arrangement
2. 0.269-inch inside diameter and 6.5 feet long for the tubular arrangement

Cell surface temperature: 1200 and 1600 F
Absorption gas velocity: 7 to 20 fps

Time, temperature, and gas composition were obtained and are summarized in Tables 1 and 2.

The data in Tables 1 and 2 does not include intermediate sulfur concentrations during absorption and during regeneration.* For one set of parameters (1200 F cell temperature and 0.064 scfm flow during adsorption using the tubular heater of 0.45-square-foot surface) the concentration-time curves are shown in Figures 7 and 8; these are typical results and are similar to the behavior observed under other operating conditions.

A microscopic examination was also made of the specially-prepared tube, cut open after an absorption cycle. The main purpose was to determine whether iron sulfide was formed, and if so, whether the reaction was primarily at the surface or throughout the wall. The microscopic examination revealed that the reaction was primarily at the surface, as evidenced by Figure 9.

An odd phenomenon was observed at 1600 F cell temperature, both during absorption and during regeneration. It was found during absorption that more than 99% of the H₂S was absorbed with no breakthrough (or reactant saturation), even after 2 hours of absorption. However, regeneration with air was unsuccessful since surface deformation or deposition caused the flow passage to be blocked. An unusually large amount of internal heat caused the reaction tube to bend.

* Periodic Orsat gas analysis showed no change in composition of the other gas constituents during absorption, nor did it show any oxygen in the regenerated stream during the peak period of regeneration.

Pilot Plant Tests

A plot of pertinent data for a typical cycle employing cell No. 1 with a full grid and cell No. 2 with a half grid is shown on Figure 10. The free flow area through the grids was 0.33 square foot per grid. Make-gas flows were obtained by summing the air flow to the gasifier, the natural gas, and 50% of the coal. On this basis make-gas flows ranged from 350 to 500 lb/hr. An assumed make-gas temperature of 1000 F resulted in gas velocities of 5 to 8 fps using two grids or 10 to 16 fps using one grid, both ranges being well above the gas velocities employed for electrostatic precipitators. Inlet H₂S concentrations were varied from 1000 to 7500 ppm by volume using sulfur addition for the higher values. These concentrations would be obtained from 0.6 to 4.5% sulfur coal (based on 50% theoretical air).

The efficiency* of H₂S removal is plotted in Figure 11, which indicates that:

1. Removal efficiency is favored by operation at higher temperatures.
2. Removal increases with contact time. Contact times for the three curves are in the order of 0.25 sec for two cells, 0.12 sec for one cell, and 0.06 sec using half of the grids in one cell.

Note: Since total gas flow was constant the upper and center curves show a 2 to 1 velocity effect; however, the middle and lower curves have only retention time.

The cells were normally regenerated using preheated air (500 to 650 F) at flows ranging from 90 to 165 lb/hr. The grids appeared dark in color following the H₂S removal cycle and seemed to have some carbon deposition on the surface. Following regeneration the surface assumed a reddish, rust colored appearance. Using the last 120 minutes of data shown on Figure 10 and calculating on the basis of 6500 ppm removed from a gas throughput of 450 lb/hr, yields an hourly removal rate of 40 scf of H₂S. On the basis of the 90 lb/hr regeneration rate employed, an average 3.3% SO₂ content would provide a sulfur balance. This value appears to be a reasonable summation of the area under the SO₂ regeneration curves.

CONCLUSIONS

The following pertinent conclusions may be drawn from the results of the bench-scale and the larger-scale experiments:

1. The concept of absorption of H₂S by iron oxide and subsequent regeneration as a concentrated (12 to 15%) stream of SO₂ is technically feasible in the temperature range of 800 to 1200 F. The absorption does not decrease due to carbon particles in the gas. However, to avoid pluggage it is desirable to operate the absorption unit at 1100 to 1200 F.

* Efficiency is defined as H₂S removed/H₂S inlet x 100.

2. The overall desulfurizing reaction, $\text{H}_2\text{S} + \text{FeO} \rightarrow \text{FeS} + \text{H}_2\text{O}$, is extremely rapid and occurs at the iron oxide surface. The reaction appears limited only by surface saturation. This saturation limit lies above 25 scf of H_2S per 100 square feet of surface. Reaction rate and saturation limit are favored by the higher temperatures.
3. The overall regeneration reaction, $\text{FeS} + \text{O}_2(\text{in air}) \rightarrow \text{FeO} + \text{SO}_2(\text{in air})$ is also extremely rapid in the temperature range of 800 to 1200 F.

On the whole the preliminary experiments reported in this paper indicate that the absorption and regeneration reaction rates are rapid. Diffusion, rather than reaction, will control the design parameters. The surface saturation limit will determine the cycling period.

DISCUSSION

The initial intent of this work was to establish the technical feasibility of this concept of controlling sulfur emission from fossil fuel fired power plants. This feasibility has been established. The second objective was to obtain sufficient performance data to permit making a conceptual plant design and an economic evaluation. These are currently underway. No attempt was made to establish the precise reaction mechanism or the kinetics of the reactions.

TABLE 1. SUMMARY OF RESULTS WITH SPECIALLY-PREPARED SURFACE

Cycle	Diam, inches	Cell Wall Temp, F	Flow Rate, scfm	Velocity in Cell, fps	Length of Cycle, min	Exit Gas Sulfur Concentration**	
						At Start, ppm	At End, ppm
Absorption	0.25	1200	0.112	17.5	7	270 H ₂ S	1870 H ₂ S
Regeneration	0.25	1200	0.111	17.4	3	Large SO ₂ *	0 SO ₂
Absorption	0.25	1200	0.114	17.8	7	~200 H ₂ S	3300 H ₂ S
Regeneration	0.25	1200	0.117	18.3	2	Large SO ₂	0 SO ₂
Absorption	0.25	1200	0.114	17.8	7	~200 H ₂ S	5000 H ₂ S
Regeneration	0.25	1200	0.114	17.8	3	29000 SO ₂	0 SO ₂
Absorption	0.25	1200	0.064	10.0	10	~200 H ₂ S	3170 H ₂ S
Regeneration	0.25	1200	0.064	10.0	5	Large SO ₂	0 SO ₂
Absorption	0.25	1200	0.064	10.0	9	330 H ₂ S	1650 H ₂ S
Regeneration	0.25	1200	0.064	10.0	3	Large SO ₂	0 SO ₂
Absorption	0.25	825	0.064	7.75	9	220 H ₂ S	1700 H ₂ S
Regeneration	0.25	825	0.064	7.75	3	Large SO ₂	0 SO ₂
Absorption	0.25	825	0.064	7.75	9	220 H ₂ S	710 H ₂ S
Regeneration	0.25	825	0.064	7.75	2	Large SO ₂	0 SO ₂
Absorption	0.25	825	0.114	13.8	6	460 H ₂ S	1780 H ₂ S
Regeneration	0.25	825	0.114	13.8	2	Large SO ₂	0 SO ₂
Absorption	0.25	825	0.114	13.8	6	640 H ₂ S	1900 H ₂ S
Regeneration	0.25	825	0.114	13.8	2	Large SO ₂	0 SO ₂

* Due to rapid evolution of SO₂ it was not possible to measure exact amount.

** Inlet sulfur concentration was 10,000 ppm H₂S during absorption and approximately 0 ppm SO₂ during regeneration.
SO₂ exit concentration shown was after an initial transient period.

TABLE 2. SUMMARY OF BENCH-SCALE RESULTS WITH STEEL SURFACE

Cycle	Cell Type	Cell Wall Temp, F	Flow Rate, scfm	Velocity in Cell, fps	Length of Cycle, min	Exit Gas Sulfur Concentration*	
						At Start, ppm	At End, ppm
Absorption	Annular	1200	0.120	10.5	9	320 H ₂ S	2760 H ₂ S
Regeneration	"	1200	0.026	2.3	12	96500 SO ₂	0 SO ₂
Absorption	"	1200	0.060	7.0	33	120 H ₂ S	2740 H ₂ S
Regeneration	"	1200	0.026	2.3	17	151000 SO ₂	0 SO ₂
Absorption	"	1200	0.060	7.0	30	90 H ₂ S	2000 H ₂ S
Regeneration	"	1200	0.026	2.3	12	122000 SO ₂	0 SO ₂
Absorption	"	1200	0.120	10.5	8	110 H ₂ S	2660 H ₂ S
Regeneration	"	1200	0.027	2.4	7	96000 SO ₂	0 SO ₂
Absorption	"	1200	0.120	10.5	8	305 H ₂ S	2200 H ₂ S
Regeneration	"	1200	0.027	2.4	10	133000 SO ₂	0 SO ₂
Absorption	"	1615	0.060	8.8	128	<100 H ₂ S	No Breakthrough
Regeneration	"	1615	0.027	4.0	Large	0 SO ₂	0 SO ₂
Absorption	Tubular	1200	0.064	8.5	13	65 H ₂ S	3100 H ₂ S
Regeneration	"	1200	0.027	3.6	5	10100 SO ₂	0 SO ₂
Absorption	"	1200	0.064	8.5	17	50 H ₂ S	1210 H ₂ S
Regeneration	"	1200	0.031	4.1	5.2	13100 SO ₂	0 SO ₂
Absorption	"	1200	0.064	8.5	20	40 H ₂ S	1280 H ₂ S
Regeneration	"	1200	0.032	4.2	5.8	13100 SO ₂	0 SO ₂
Absorption	"	1200	0.062	8.2	24	45 H ₂ S	1400 H ₂ S
Regeneration	"	1200	0.028	3.7	8.3	12700 SO ₂	0 SO ₂
Absorption	"	1200	0.120	15.9	20	60 H ₂ S	1600 H ₂ S
Regeneration	"	1200	0.038	5.0	12	14300 SO ₂	0 SO ₂
Absorption	"	1200	0.120	15.9	24	90 H ₂ S	750 H ₂ S
Regeneration	"	1200	0.037	4.9	14	16000 SO ₂	0 SO ₂
Absorption	"	1600	0.120	19.7	80	50 H ₂ S	No Breakthrough
Regeneration	"	1600	0.027	4.4	Large	0 SO ₂	0 SO ₂

* Inlet sulfur concentration was 10,000 ppm H₂S during absorption and approximately 0 ppm SO₂ during regeneration.
SO₂ exit concentration shown was after an initial transient period.

FIGURE 1. HIGH TEMPERATURE SULFUR REMOVAL CONCEPT

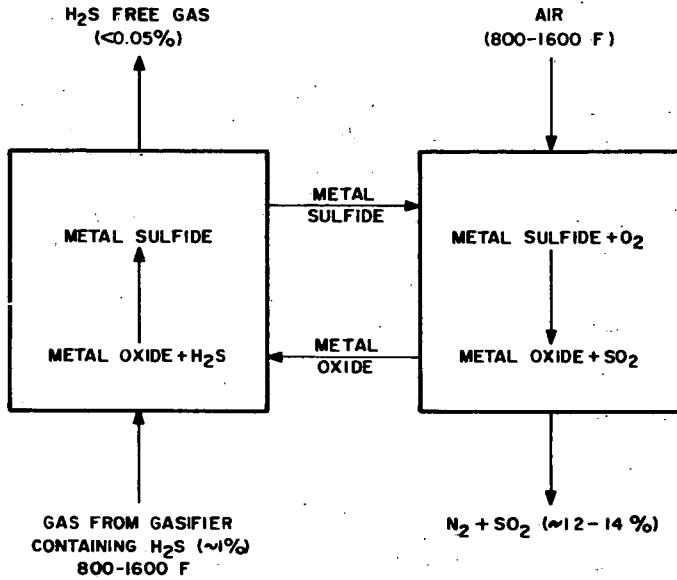


FIGURE 2. TWO-STAGE COMBUSTION POWER CYCLE

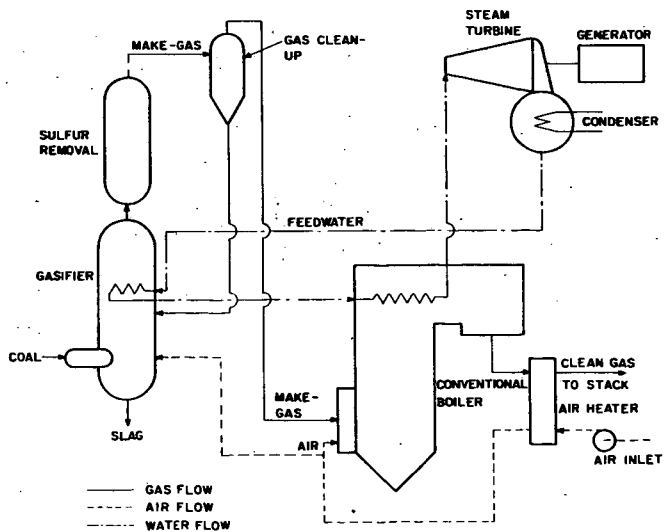


FIGURE 6. ARRANGEMENT OF ABSORPTION CELL FOR LARGE SCALE TESTS

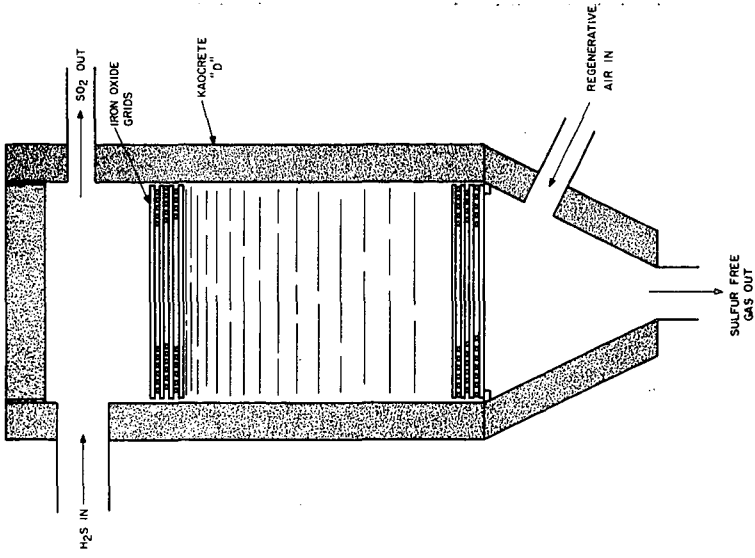


FIGURE 5. PHOTOGRAPH OF PILOT PLANT

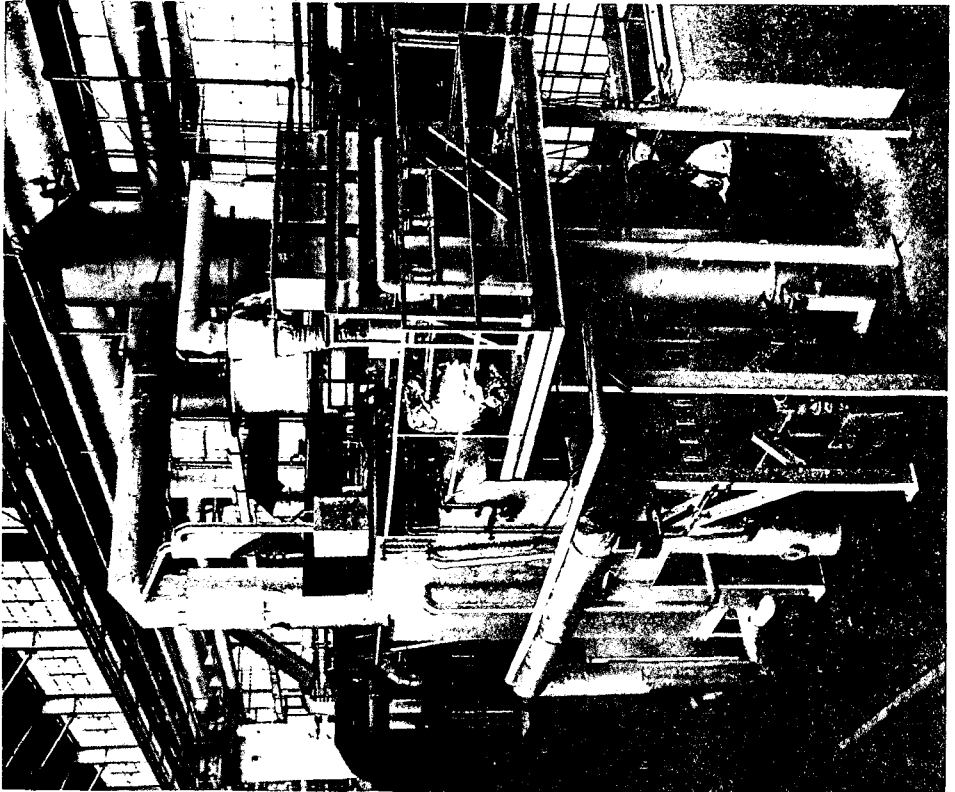


FIGURE 7. TYPICAL H₂S CONCENTRATION VS TIME CURVE DURING ABSORPTION FOR BENCH SCALE TESTS

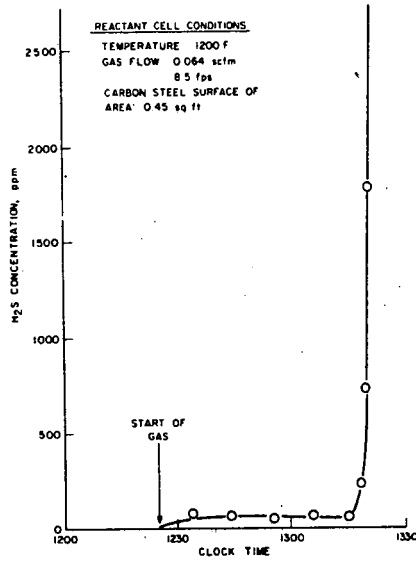


FIGURE 8. TYPICAL H₂S CONCENTRATION VS TIME CURVE DURING REGENERATION FOR BENCH SCALE TESTS

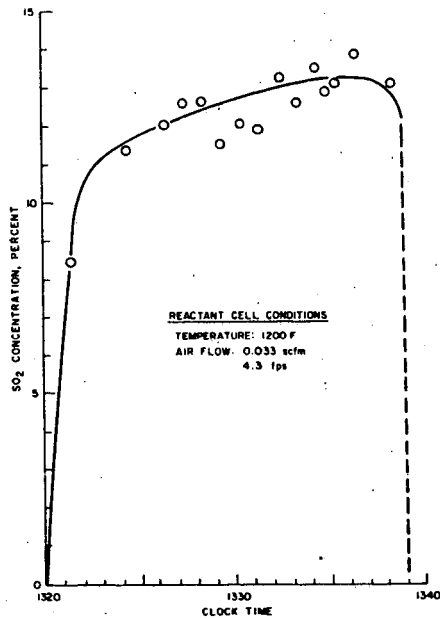
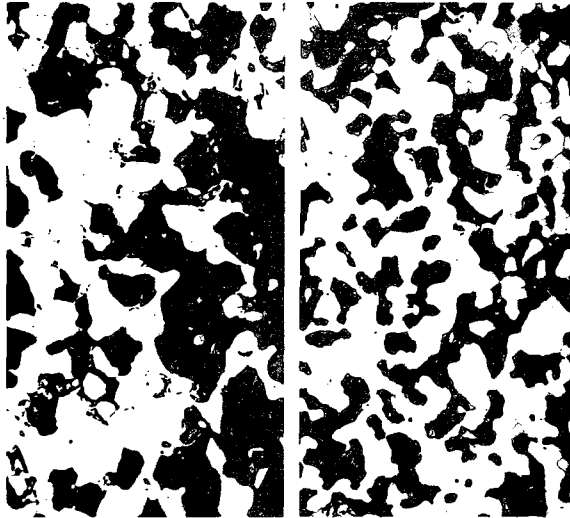


FIGURE 9. PHOTOMICROGRAPH OF REACTANT AFTER ABSORPTION CYCLE



Light network is FeS.
 Gray areas, high in FeO content, appear to contain FeS also.
 Near Surface

White areas are Fe.
 Gray areas are FeO, with little, if any, FeS.
 Interior of Wall

250X Magnification

FIGURE 10. PERFORMANCE OF CELLS NO. 1 (NORMAL GRID SURFACE) AND NO. 2 (ONE-HALF GRID SURFACE)

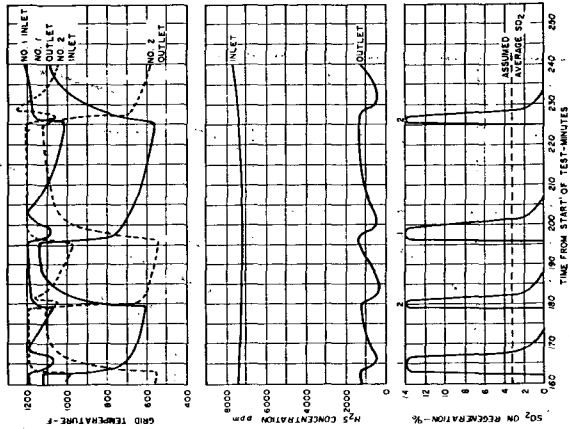
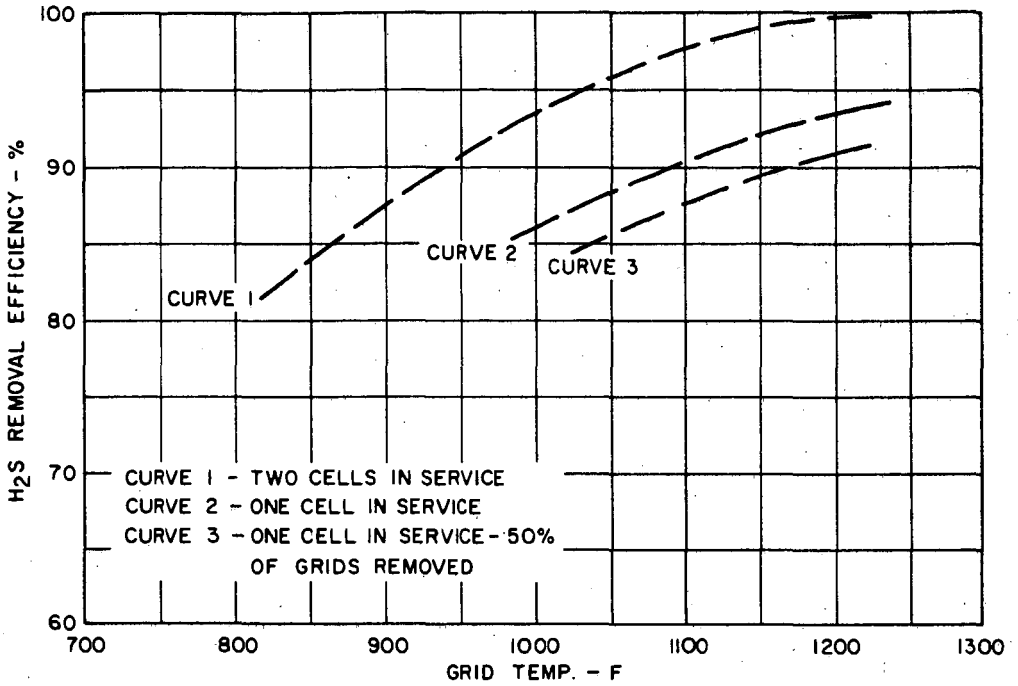


FIGURE 11. H₂S REMOVAL EFFICIENCY FOR LARGE SCALE TESTS



Hydrogenolysis of Benzo[b]thiophenes and
Related Intermediates over Cobalt Molybdena Catalyst

By

Edwin N. Givens and Paul B. Venuto

Mobil Research and Development Corporation
Research Department
Paulsboro, New Jersey 08066

INTRODUCTION

The chemistry of sulfur removal from high molecular weight heterocyclic sulfur compounds has become of increasing interest with the refining of high boiling and residual petroleum fractions. Benzothiophenes have long been recognized as major constituents of heavier fractions. The first isolated and identified member of this family was the parent compound, benzo[b]thiophene, I (1). Subsequently, 22 alkylbenzo[b]thiophenes have been identified in a 200-250°C distillate of Wason, Texas crude oil (2,3). Five compounds in this group, 2-methyl- (II), 3-methyl- (III), 2,3-dimethyl-, 2,4-dimethyl- and 2,7-dimethyl- benzo[b]thiophene, comprise over 80% of the benzothiophenes present in the 200-250°C distillate fraction.

Little quantitative information is available concerning the behavior of this type of fused 2-ring heterocyclic sulfur molecule under hydrogenative processing conditions (4). It has been reported that the hydrogenolysis of benzothiophene I with Raney nickel (2,5), palladium on alumina (6,7), molybdenum disulfide (8,9), and cobalt molybdena (10,11) gives ethylbenzene and ethylcyclohexane, or a mixture of these two compounds. Over molybdenum disulfide in the liquid phase, I is converted in 2 hours at 425°C

and 41 atmospheres to ethylbenzene in 90% yield (9) while at 340°C and 100 atmospheres, a lower temperature and higher pressure, I reacts just as easily (93% conversion) to give ethylbenzene in 80% yield and ethylcyclohexane in 8% yield (8). Cobalt molybdena is equally as effective, giving 91% sulfur free product in 8 hours at 400°C and 1 atmosphere (10,11). In contrast, almost no information is available on the hydrogenolysis of alkyl benzo[b]thiophenes. Likewise, little is known on the mechanism of this reaction. Cawley conjectured some years ago in comments to the work of Hoog, et. al. (11b) that 2,3-dihydrobenzo[b]thiophene(IV) is an intermediate in this reaction (12). There is as yet still no evidence regarding this supposition.

Evidence regarding the relative ease with which thiophene and benzo[b]thiophene desulfurize is contradictory. Landa and Mrnkova (8) found I was more easily desulfurized than thiophene. Yamada (9), on the other hand, found the opposite, while Papadopoulos and Wilson (10) found their reactivity nearly equivalent.

The lack of information on the chemical behavior of these important petroleum constituents has led us to an examination of the hydrogenolysis of benzo[b]thiophenes over a commercially available cobalt molybdena catalyst. The various benzothiophenes examined here are clearly representative of those found in petroleum since all were identified in Wasson, Texas, crude oil (2). In addition, various possible intermediates have been examined under the same conditions to further elucidate the sequence of steps involved in desulfurization.

EXPERIMENTAL

All melting points were obtained on a Fisher-Johns melting point block. The infrared spectra were determined with a Perkin-Elmer Model 337 grating spectrophotometer as either neat liquids or suspensions in potassium bromide pellets. The NMR spectra were determined on a Varian Model A-60 NMR spectrometer, using tetramethylsilane as the internal reference. The mass spectra were obtained with a CEC Model 21-103 mass spectrometer at an ionizing potential of 70 ev using an all glass inlet system. Gas-liquid partition chromatography was performed with an F&M Model 810 gas chromatograph using a 12 ft., 1/8 in. o.d. column packed with 20% Carbowax 20 M on Chromosorb W. Preparative separations were done either on this chromatograph or on a Hewlett Packard Model 775 preparative gas chromatograph.

A. Materials

Catalyst. The cobalt molybdena was Harshaw CoMo 0601 supported on an alumina surface (S. A. $160 \text{ m}^2/\text{g}$. CoO, 3%; MoO₃, 10.0%). The noble metal catalysts were 0.29% Pd, 0.32% Rh and 0.60% Pt on non-acidic alumina compositions (13). The catalysts were ground to 8/14 mesh particles and pretreated in hydrogen at 500-550°C for three hours immediately prior to use.

Benzo[b]thiophenes. 3-Methylbenzo[b]thiophene was prepared by the method of Werner (14) and Banfield (15). 1-Phenylmercapto-propanone-2 was prepared from thiophenol and 1-chloro-2-propanone and cyclized to 3-methylbenzo[b]thiophene; n_D^{20} 1.6237 [Lit. (16) n_D^{20} 1.6252]; Mw(MS) 148; sulfone, mp 140° [Lit. (14) 146-146.5°].

The following compounds were also prepared by the above method: 2,3-dimethylbenzo[b]thiophene, n_D^{20} 1.6071 (Lit. (14) n_D^{20} 1.6170) Mw(MS) 162; 2,3,7-trimethylbenzo[b]thiophene, mp 50 (Lit. (14) mp 51-2°) Mw(MS) 176: sulfone, mp 192° (Lit. (14) 190-191°); 3,7-dimethylbenzo[b]thiophene, $bp_{1.0}$ 92°, n_D^{20} 1.6069 (Lit. (15) bp_{12} 122-4, n_D^{15} 1.6090) Mw(MS) 162.

2-Methylbenzo[b]thiophene was produced from α (o-carboxyl-phenylmercapto) propionic acid [mp 196° (Lit. (17) mp 193-195°)] by the method of Hansch and Lindwall (18), mp 40° (Lit. (20), mp 51-52), Mw(MS) 148: sulfone, mp 107° (Lit. (20) 108.5-110°).

7-Methylbenzo[b]thiophene was synthesized by the method of Sunthankar and Tilak (21); $bp_{0.5}$ 56°, n_D^{20} 1.6110 (Lit. (21) bp_4 110-115°. 2,7-Dimethylbenzo[b]thiophene was prepared in a similar fashion $bp_{0.3}$ 66-67° (Lit. (20) bp_{11} 132-136°) n_D^{20} 1.6054, Mw(MS) 162.

2,3-Dihydrobenzo[b]thiophene. Oxidation of benzo[b]thiophene with hydrogen peroxide and acetic acid gave benzo[b]thiophene 1,1-dioxide, mp 139° (Lit. (22) 142-3°) that was hydrogenated over 10% Pd on carbon in ethanol to give 2,3-dihydrobenzo[b]thiophene 1,1-dioxide, mp 91° (Lit. (23) mp 91-92°). This was treated with lithium aluminum hydride in ether to give 2,3-dihydrobenzo[b]thiophene (24), bp_5 94-96°. (Lit. (25) bp_6 93°); n_D 1.6195 (Lit. (25) n_D^{25} 1.6195); infrared is identical with earlier data (25).

2,3-Dihydro-2,3,7-trimethylbenzo[b]thiophene

2,3,7-Trimethylbenzo[b]thiophene 1-dioxide in ethanol was reduced over 10% palladium on charcoal at 120°C and 750 psig hydrogen. The solvent was removed and the resulting material chromatographed over silica gel. Non-sulfone contaminants were removed with benzene and the product was then eluted with 50% benzene - 50% methanol.

This material was treated with lithium aluminum hydride in tetrahydrofuran for 1.5 hours. The deoxygenated product was separated by chromatography on silica gel. Two major products were isolated by preparative gas liquid chromatography consistent with threo- and erythro-2,3-dihydro-2,3,7-trimethylbenzo[b]thiophene.

First product: Mw(MS) 178; NMR δ 2-CH_3 & 3-CH_3 = 1.1-1.7 ppm (6), δ 7-CH_3 = 2.1-2.3 (3), δ 2-H = 3.2-3.8 (1), δ 3-H = 2.7-3.2 (1), δ H aromatic = 6.7-7.2 (3), $J_{\text{H}_2 \text{H}_3}$ = 8.0 Hz. Sulfone: mp 69-69.5°C. Integral ratios are shown in parentheses.

Second product: Mw(MS) 178; NMR δ 2-CH_3 and 3-CH_3 = 1.0-1.4 ppm (6), δ 7-CH_3 = 3.0-3.6 (3), δ 2-H = 3.2-3.8 (1), δ 3-H = 3.6-4.2 (1), δ H aromatic = 6.7-7.2 (3), $J_{\text{H}_2 \text{H}_3}$ = 6.8 Hz.

2-Ethylthiophenol. This compound was prepared by the method of Kwart and Evans (26). The oil product was dissolved in hexane and extracted with 10% sodium hydroxide. The base soluble material after acidification and distillation was found to be the desired product [bp 208° at 760 mm or 72° at 5 mm (Lit. (27) 208° at 1 atm.); n_D^{20} 1.5660].

The hexane soluble material proved to be 2-ethylphenyl methyl sulfide, bp₅ 87°; n_D 1.5700. Anal. Calcd. for C₉H₁₂S; C, 71.00; H, 7.94; S, 21.05. Found: C, 70.74; H, 8.03; S, 20.7.

Benzo[b]thiophene, β -phenylethyl mercaptan, and ethyl phenyl sulfide were obtained from commercial sources and required no further purification.

4,5,6,7-Tetrahydrobenzo[b]thiophene was prepared by the Clemmensen reduction of 4-keto-4,5,6,7-tetrahydrobenzo[b]thiophene; bp₅ 75° (Lit. (28) bp₃ 53-58°); n_D 1.5555 (Lit. (29) n_D^{20} 1.5572).

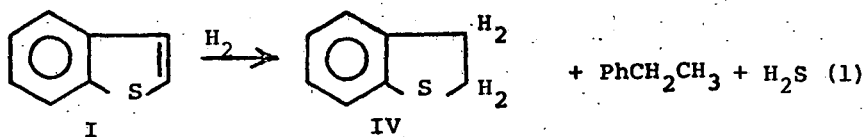
B. Apparatus, Procedure and Analysis

A continuous flow reactor system was employed. Reactants (diluted to 50% wt. in hexane) were flashed into the carrier gas and

passed through the catalyst bed. 100 mm of the tubular reactor length (140 mm x 22 mm) consisted of a quartz preheater maintained at the same temperature as the catalyst bed. The reactant flow was maintained by a syringe pump. The reactor effluent was passed through a water condenser and the liquid condensate analyzed. Product recoveries were excellent with little coke accumulation during the reaction. Analysis of the hydrocarbon and sulfur containing fractions was made by gas-liquid chromatography on a Carbowax 20M supported column. Positive identification of the products was accomplished by comparing retention times with authentic samples and by obtaining mass spectra of samples isolated by preparative chromatography and comparing them with known spectra. Conversions and product distributions are based on recovered condensate, where detector response is uncorrected except as determined by experimental means for I, IV and ethylbenzene where detector response is proportional to molar ratios.

RESULTS AND DISCUSSION

Both sulfur containing and sulfur free (hydrocarbon) products were formed in the gas phase hydrogenolysis of methyl and polymethyl substituted benzo[b]thiophenes at 1 atmosphere and 400°C over cobalt molybdena. Under these conditions benzo[b]thiophene (I) was converted to ethylbenzene and hydrogen sulfide (Table 1). Over alumina supported noble metal catalysts, 2,3-dihydrobenzo[b]thiophene (IV) was also a major product. No other species (other than those in equation 1) were observed in amounts greater than 1% of the product mixture.



The true catalytic nature of this reaction is obvious from two observations. First, the thermal stability of I, and presumably the other benzo[b]thiophenes, is evident from the absence of any reaction over nonacidic alumina under like conditions at 400°C. Secondly, the importance of hydrogen in this reaction is illustrated by the lack of any reaction of I over cobalt molybdena in nitrogen at 400°C.

Table 1

Hydrodesulfurization of Benzothiophene^a

Catalyst ^b	Conversion	Products		
		Ethylbenzene	IV	Other
Cobalt molybdena ^c	91-99	96	--	4
Cobalt molybdena ^d	none	--	--	--
Non-acidic alumina	none	--	--	--
Pt on non-acidic alumina	24	92	8	--
Rh on non-acidic alumina	14	84	16	--
Pd on non-acidic alumina	2	75	25	--

- a. Conditions: LHSV 0.30; $H_2/I = 3$; 400°C; samples taken after one hour on stream; Pretreat: H_2 , 3 Hrs. at 15 cc/min/8cc catalyst at 500°C; I charged as 50% by weight hexane.
- b. For catalyst descriptions see Experimental.
- c. In another run with H_2 - H_2S pretreat (25 cc/min. H_2 , 10cc/min. H_2S at 400°C) observed 99% conversion with same selectivity.
- d. Run made in N_2 ; sample taken at 0.5 hr. on stream.

All of the catalysts we tested were reduced in hydrogen for 3 hours at 500-550°C immediately before use. Since sulfiding had no effect on this reaction, the catalysts were used in the oxide state. A similar lack of any affect by sulfiding was observed by Lipsch and Schuit (30) on the thiophene desulfurization.

At a constant hydrogen-reactant ratio for cobalt molybdena the log conversion varies linearly with LHSV (Table 2). It appears that this reaction is not unduly complicated by diffusion problems at the conditions used here. No apparent aging was observed during these 4 hour runs over cobalt molybdena. This agrees with the results of Kolboe who found the same absence of aging for thiophene hydrogenolysis over cobalt molybdena (31). We also found that, with the noble metal catalysts, conversion of I dropped rapidly with time on stream.

Table 2

Effect of LHSV on Benzo[b]thiophene Conversion over Cobalt Molybdena

<u>LHSV</u>	<u>Flow Rate of I</u>	<u>H₂ Rate</u>	<u>Ethylbenzene</u>	<u>I</u>
0.3	1.2 cc/hr.	8 cc/min	83	13
1.0	4.0	25	63	34
2.0	8.0	50	44	54
4.0	16.0	100	18	82 ^b

a. Catalyst, 4cc (3.31 g); 400°C; yields in mole percent.

b. Contains 2% IV.

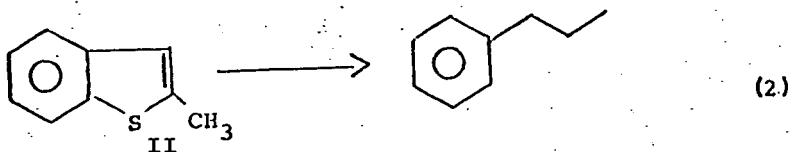
A. Product Characteristics

The product distributions from these reactants are dependent on the number and positions of methyl substituents, and

become increasingly complex as the number of methyl substituents increase in the reactant.

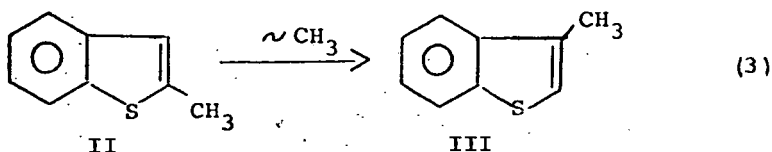
1. Primary Sulfur Extrusion

The main hydrocarbon products from this reaction arise from simple, direct sulfur extrusion. This is illustrated in equation 2 below with 2-methylbenzo[b]thiophene (II) which gave n-propylbenzene as the major hydrocarbon product (Table 3).



2. Alkyl Migration on Thiophene Ring

The major sulfur containing products arise from 1,2-methyl shifts on the thiophene ring. For example, the 3-methylbenzo[b]thiophene (III) produced from II arose by a simple methyl shift from the C-2 to the C-3 position as shown in equation 3.



3. Dealkylation From Thiophene Ring

Sulfur containing products also arise from loss of thiophene ring methyl substituents. For example, I was formed

- 144 -
Table 3

Product Distribution from Hydrogenolysis of Substituted Benzothiophenes^a

Product	R = H		R = CH ₃		R = CH ₃		R = CH ₃	
	-	2	.5	2	5	2	4	1
	-	4	.5	.5	.5	-	-	-
	96	86	6	7	10	10	3	1
	-	-	5	3	42 ^c	22 ^c	2	2
	-	-	75	54 ^b	18	10 ^c	8	4
	-	-	-	-	-	-	28 ^{c,d}	16 ^c
	-	-	-	-	-	-	8	(1)
other non-sulfur ^e	-	0.5(2)	1(2)	4(5)	1(3)	0.5(2)	5(2)	10(4) ^f
	Charge	-	1	8	2	11	-	2
	-	-	Charge	-	18 ^c	25	15	14
	-	-	9	14	Charge ^c	-	15	17
	-	-	-	-	-	-	Charge	-
other sulfur epds.	-	7(3)	2(1)	9(3)	3(1)	19(4)	12(3)	32(6) ^g

a. Conditions: CoMo O501 (Harshaw); 400°C; R₂/benzothiofene 3-5; pretreat, 3 hrs./550°C/H₂; yields are uncorrected vpc data taken after one hour on stream.

b. Max. of 0.5% 2-ethyltoluene, no 4-ethyltoluene as determined on a 5% Bentone 34-5% dinonyl phthalate on chromosorb W column.

c. Trapped from vpc and analyzed by MS.

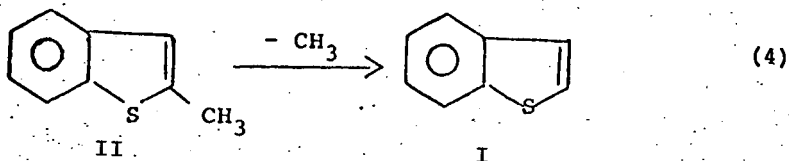
d. The small m/e 92 intensity (2% of m/e 91) excludes significant quantity of isobutylbenzene (m/e 92 is 07% of m/e 91) and n-butylbenzene (m/e 92 is ~65% of m/e 91).

e. Number of peaks shown in parentheses.

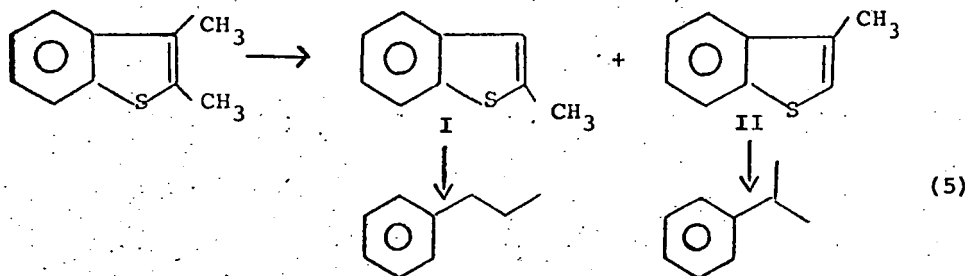
f. Two of these peaks were trapped by vpc. Molecular weights in one were 148 and 152 and in the other were 152 and 142 (possibly diethylindanes).

g. No 2,3-dihydro-2,3,7-trimethylbenzothiofenenes are present.

from II by simple dealkylation of the 2-methyl substituent as shown in equation 4.



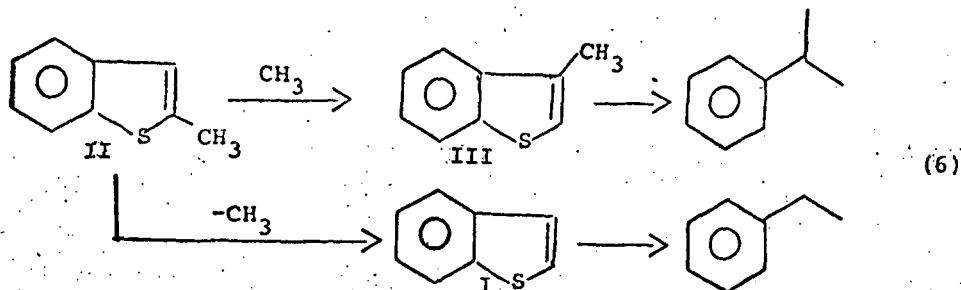
These dealkylation products were usually formed in smaller amounts than those produced via equation 3. This, of course, does not apply where both thiophene positions are occupied and the path in equation 3 is impossible. For example, II and III found in the product from 2,3-dimethylbenzo[b]thiophene, as shown in equation 5, resulted from monodemethylation reactions. These were the major sulfur products since simple 1,2-methyl shifts were not permitted in the reactant.



4. Secondary Sulfur Extrusion

Hydrocarbon products resulting from simple sulfur extrusion of rearranged and demethylated sulfur products are found in somewhat lesser amounts than the directly formed extrusion product in equation (3). This is illustrated by equation 6 where

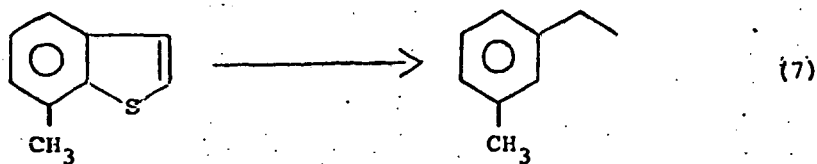
the cumene and ethylbenzene formed from II resulted from sulfur extrusion of the methyl rearranged and dealkylated products, III and I, respectively.



The same explanation is applied to the formation of *n*-propylbenzene and cumene from 2,3-dimethylbenzo[b]thiophene illustrated in equation 5.

5. Relative Inertness of Alkyl Substituents on Benzene Ring

Methyl substituents on the benzene ring of benzo[b]thiophene neither rearrange nor dealkylate under the conditions used in this study. The products are the same as those from non-six-ring substituted benzo[b]thiophenes except that each product bears an appropriately placed methyl substituent. For example, 7-methylbenzo[b]thiophene gave only 3-ethyltoluene (equation 7). Neither the ortho or para isomer was produced. The product distributions in Table 3, where the 7-methyl and the non-six-ring substituted benzo[b]thiophenes are compared, attest to this fact.



Applying these relationships permits us to predict with some certainty the products from hydrogenolysis of any other methyl- or polymethyl-benzo[b]thiophene. Using 3,7-dimethylbenzo[b]thiophene from Table 3 as an example, we found the predictions and results agree, namely:

1. 3-isopropyltoluene was the major hydrocarbon product (compare with equation 2);
2. 2,7-dimethylbenzo[b]thiophene and 7-methylbenzo[b]thiophene were the major sulfur containing products (compare with equations (3) and (4) respectively);
3. lesser amounts of 3-n-propyltoluene and 3-ethyltoluene than the major hydrocarbon product were formed (compare with equation (5));
4. no loss or migration of the methyl group originally attached to the benzene ring of the 3,7-dimethylbenzo[b]thiophene occurred.

The same applies to other examples chosen from Table 3.

B. Alternative Mechanisms

Although various alternative explanations may be applied to explain certain products, generally on close examination they are less tenable than those already postulated. For example, if ethylbenzene, formed from II, had arisen via cracking of n-propylbenzene, toluene should have been an even more abundant product than it was, since such a mechanism would have favored toluene over ethylbenzene. The concentration of ethylbenzene in the product was, in fact, 8 times greater than toluene. An equally unlikely

mechanism is the formation of ethylbenzene via cumene cracking since benzene would have been expected as the favored product. Again, the yield of ethylbenzene was some 8 times greater than that of benzene.

Cumene in the product may have formed from II through n-propylbenzene side chain isomerization, which is known to occur to a slight extent under these conditions. However, the presence of III in the product from the 2-isomer (II) and the observed similar relative hydrodesulfurization rates for these isomers (see conversion data in Table 4 below) require that at least some of the cumene comes via the hydrodesulfurization route in equation 5. It seems likely that these routes occur concurrently, with the sulfur extrusion route probably being favored.

C. Conversion - Hydrodesulfurization: Structure Effects

Although in these cases great similarity in product types and distributions exist, a wide range of conversions of the individual benzothiophenes was observed. Conversion, was not necessarily related to hydrodesulfurization. For example, of the 47% 2,3,7-trimethylbenzothiophene that reacted (Table 4), only 16% was converted to sulfur free products.

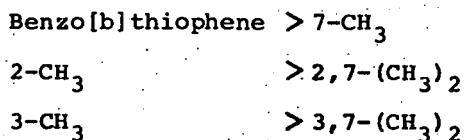
Table 4

Conversion and Hydrodesulfurization Selectivity of Methyl- and Polymethyl-benzo[b]thiophenes

Position (Me group)	none	7	2	2,7	3	3,7	2,3	2,3,7
Conversion ^{a-1}	91-99	60	74	54	43	47	39	47
Hydrodesulfurization ^{a-2}	91-99	57	66	43	32	24	15	16
Selectivity (%) ^b	100	95	89	80	75	51	38	34

a. Reported as percent reactant (1) converted and (2) desulfurized.
 b. Hydrodesulfurization/conversion x 100.

Several characteristics are readily apparent on examining these data. Generally an increase in the number of attached methyl groups decreased both conversion and hydrodesulfurization selectivity. Secondly, the presence of methyl substituents on the thiophene ring positions markedly lowered the hydrodesulfurization activity. Thirdly, a 3-methyl group caused a larger decrease in hydrodesulfurization selectivity than a 2-methyl substituent. An aromatic methyl substituent had a consistent but less pronounced effect. Therefore, the hydrodesulfurization selectivity sequence follows the order: $7\text{-CH}_3 > 2\text{-CH}_3 > 3\text{-CH}_3$. The consistent effect of an aromatic methyl group on the hydrodesulfurization selectivity is shown by comparing the following hydrodesulfurization yields:

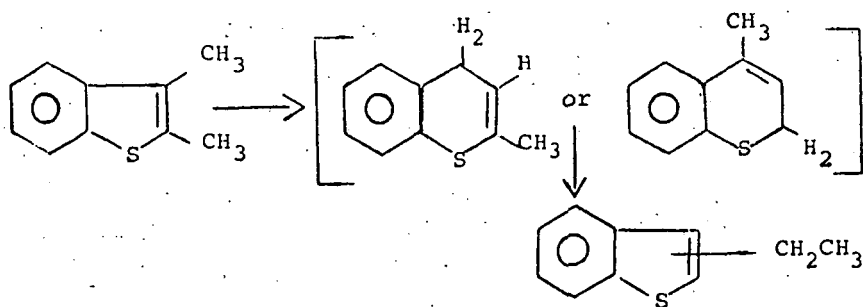


We found that the hydrodesulfurization selectivity of the 2,3,7-trimethyl derivative is about the same as that of 2,3-dimethylbenzo[b]thiophene.

D. Unidentified Products

The 2,3-dimethyl compounds yielded more hydrocarbon and sulfur containing products than any of the other reactants examined (see Table 3). They also gave more unidentified products than any of the other reactants. If simple 1,2-methyl shifts were the sole mechanism by which rearrangement products arose, then the abundance of other unidentified materials appears inconsistent with the rather limited number of conceivable products that could form. The

multiplicity of unidentified products may result from a ring expansion mechanism such as the one shown below involving thiachromene type intermediates. Products such as ethylbenzo[b]-thiophenes and thiachromenes could originate by this mechanism.



The multiplicity of unidentified hydrocarbon products from these 2,3-dimethyl substituted benzo[b]thiophenes appears to parallel the unidentified sulfur containing products in the same way that most of the hydrocarbon products are related to sulfur containing products for substrates having up to one thiophene methyl substituent.

E. Intermediates

1. Dihydrobenzo[b]thiophenes

Evidence of dihydrobenzo[b]thiophenes in these reactions at 400°C and one atmosphere pressure can be found both at low temperatures and at very high flow rates. At 400°C and 0.3 LHSV, the noble metal catalysts gave 2,3-dihydrobenzo[b]thiophene (IV) in rather low yield while cobalt molybdena gave none. Only at

higher space velocities (4 hr.⁻¹) did any IV appear, and then in only 2% yield (Table 2). At 300°C over cobalt molybdena the amount of IV in the product was equal to the ethylbenzene formed. No other products were present (Table 5). Therefore, the presence of IV in the product mixtures is consistent with it being an intermediate in this reaction.

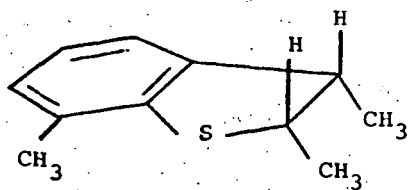
Table 5

Hydrodesulfurization at Lower Temperature over Cobalt Molybdena^a

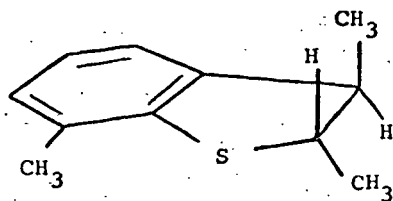
Reactant ^b	Temp.	PhCH ₂ CH ₃	V	IV	I	PhCH ₂ CH ₂ SH
I	300	10	--	9	80	--
IV	290	8	--	74	18	--
2-CH ₃ CH ₂ PhSH (V)	290	94	5	0.1	1	--
PhCH ₂ CH ₂ SH (VI)	300	91 ^c	--	--	--	9

- a. H₂/HC = 3-5/1; LHSV = 2.4.
- b. Reactants charged as 25% by weight in hexane.
- c. Includes 6% styrene in the product.

We also observed the dihydro intermediate from the trimethyl substrate. When 2,3,7-trimethylbenzo[b]thiophene was passed over cobalt molybdena at 290°C only about 1% conversion was observed. In addition to 3-sec-butyltoluene, two other peaks identical with the retention times of erythro- and threo-2,3-dihydro-2,3,7-trimethylbenzo[b]thiophene were found. These two isomers shown below were prepared separately by the method described



erythro



threo

in the experimental section and are, at present, indistinguishable as to stereochemistry.

When 1% of 2,3-dimethylbenzo[b]thiophene was converted in the same way as noted above, sec-butylbenzene was found along with two peaks in the chromatograph not detected in the 400°C run. The retention times of these 2 peaks were similar to those observed above for the 2,3-dihydro-2,3,7-trimethylbenzo[b]thiophenes, which suggests the presence of erythro- and threo-2,3-dihydro-2,3-dimethylbenzo[b]thiophene. We have not, however, compared these retention times with authentic samples.

When IV was passed over cobalt molybdena under the conditions of this reaction, I and ethylbenzene were the only main products. The product distributions from I (Table 1) and IV (Table 6) were almost identical at 400°C and 0.3 LHSV. Even at

Table 6

Hydrodesulfurization of 2,3-Dihydrobenzo[b]thiophene (IV)^a

<u>Catalyst</u>	<u>Product Distribution</u>			
	<u>IV</u>	<u>I</u>	<u>Ethylbenzene</u>	<u>Other</u>
Cobalt molybdate	2	1	95	2
Cobalt molybdate ^b	1	8	89	2
Cobalt molybdate ^c	2	68	30	--
Non-acidic Alumina ^c	95	5	--	--
Pt on non-acidic alumina ^c	27	61	12	--
Rh on non-acidic alumina ^c	24	66	10	--
Chromia-alumina ^c	32	58	10	--

a. Conditions: 400°C; LHSV 0.30; H₂/II = 4; samples taken after one hour on stream; IV is charged as a 50% (by weight) mixture in hexane.

b. 350°C.

c. No carrier gas.

~300°C the conversions of I and IV and the yield of desulfurized product were about the same (Table 5). We did observe some departure from apparent equilibrium at 400°C and 4 LHSV where the distributions from reactions of I and IV differed somewhat (Table 7). Since IV is itself a source of hydrogen the different partial pressures of hydrogen in these two reactions could affect the product distribution, although such a large increase in desulfurized product (18 to 40%) would not be expected. Without a large excess of hydrogen a constant ratio of I and IV cannot be anticipated.

Table 7

Comparison of the Hydrodesulfurization of
I and IV over Cobalt Molybdena^a

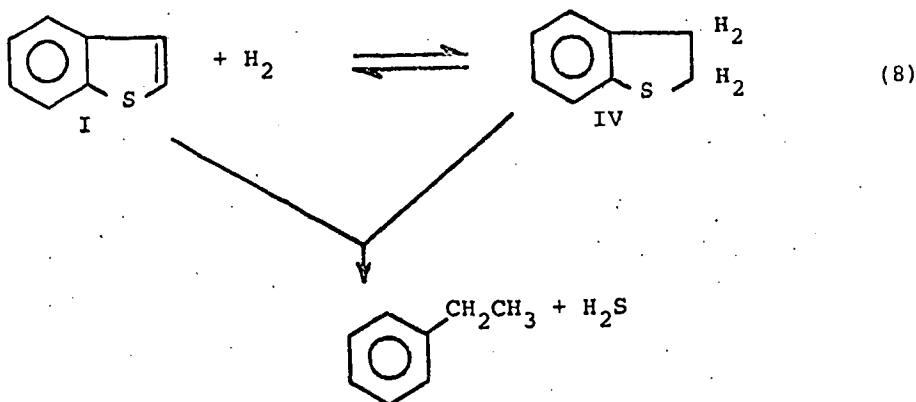
<u>Charge (% wt) 50% in Hexane</u>		<u>Reactant Composition</u>		
I	IV	<u>PhCH₂CH₃</u>	I	IV
100	--	18	80	2
50	50	22	70	8
---	100	40	56	3

a. Liquid flow rate: 4 cc/hr., H₂, 25 cc/min; 400°C; LHSV 4.

At 400°C IV will dehydrogenate to the extent of 5% over alumina. Addition of Pt or Rh increases the reaction of IV to 73 and 76%, respectively (Table 6). Although desulfurization was small it was similar to that observed for I over these same catalysts.

Therefore, it appears that equilibrium occurs rapidly between I and IV (as depicted in eq. 8). The desulfurization reaction that gives ethylbenzene is a slow step that drains this

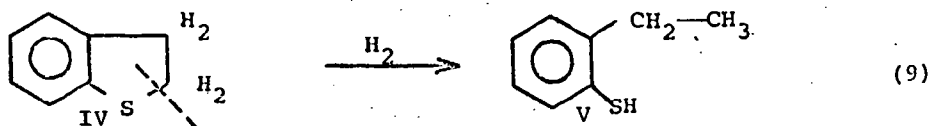
equilibrium state in a non-reversible manner. Since both I and IV form ethylbenzene at comparable rates, to exclude either as a



source of desulfurized product is not possible by our data. If we assume for the present that IV is the source of ethylbenzene, desulfurization may be a multistep process involving first a cleavage of one carbon-sulfur bond to give a discrete mercaptan intermediate followed by a second carbon-sulfur bond cleavage to give hydrocarbon product and H_2S . Alternatively, sulfur may be lost in a one step process involving a synchronous breaking of two carbon-sulfur bonds giving rise to hydrocarbon product directly without involving mercaptan intermediates.

2. 2-Ethylthiophenol

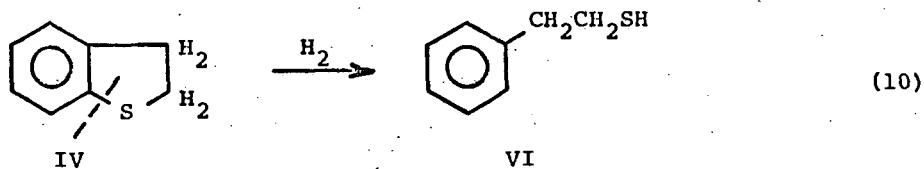
A stepwise carbon-sulfur bond cleavage in IV could result in 2-ethylthiophenol (V) (eq. 3) if the bond between C_2 and S were broken as shown in eq. 9.



Such an intermediate has never been detected in our product mixtures. When V was passed over cobalt molybdena in hydrogen at 290°C, 94% was converted to ethylbenzene and 1% to I (Table 5). Since under similar conditions thiophenol is also completely converted to benzene, it appears that the rate of desulfurization of aryl mercaptans, in particular V, is about 30 times faster than that of I * excludes any likely possibility of finding them in the product mixture. The presence of 1% of I in the product can be explained by the reversibility of eq. 9 as is well known (27,32). The reverse reaction in hydrogen apparently is not favored at 400°C.

3. β -Phenylethyl mercaptan

Cleavage of the other carbon-sulfur bond is also possible (eq. 10). β -Phenylethyl mercaptan (VI) might be a likely intermediate although, again, it could not be detected. At 300°C in



hydrogen it forms ethylbenzene and styrene in greater than 90% yield without any trace of I or IV. VI appears to react at about the same rate as V which is 30 times faster than either that of I or IV.* Since alkyl mercaptans are so easily desulfurized, even

*This can be deduced from the data in Table 5.

in the absence of hydrogen, it is highly unlikely that VI can be found. Indeed, it must be at most only a very short-lived intermediate.

The reversibility of this reaction (eq. 10) at either 300° or 400°C is not likely, although under suitable conditions (600°C) I can be formed (33,34). On examining the reaction somewhat further, it appears that even alumina will catalyze its decomposition, giving styrene primarily. In the presence of a hydrogenation function, however, ethylbenzene is the main product (Table 8). A solid (mp 133-135°C) was observed from the reaction

Table 8

β -Phenylethyl Mercaptan (VI) Hydrogenolysis^a

<u>Catalyst</u>	<u>Gas</u>	<u>Styrene</u>	<u>Ethylbenzene</u>
Al ₂ O ₃	H ₂	84	14
Pt/Al ₂ O ₃	H ₂	1	96
Pt/Al ₂ O ₃	N ₂	22	74
CoMo	H ₂	--	100

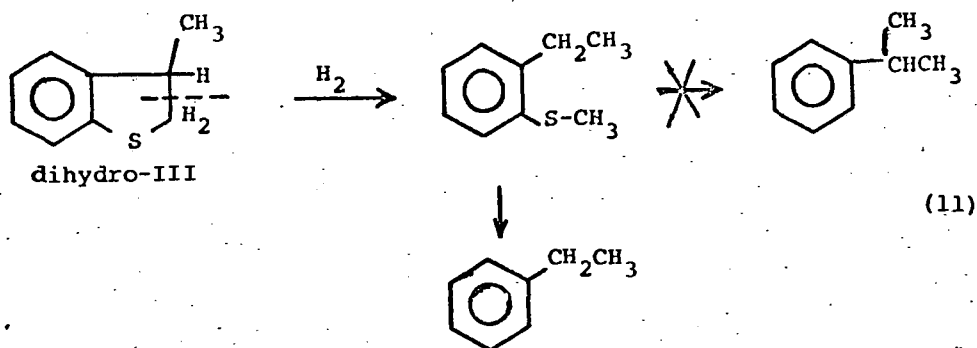
a. 400°C; LHSV 0.30; Conversion 100%; non-acidic alumina(13) was used.

in hydrogen over alumina. Its mass spectrum had a parent ion that was also the base peak at m/e 236. This is suggestive of diphenylthiophene isolated previously in similar systems (33).

OTHER INTERMEDIATES

There are other alternative routes besides those that arise by initial carbon-sulfur bond cleavage. We have examined the possibility of an initial C-C cleavage. If dihydro III were

fragmented as shown here, methyl 2-ethylphenyl sulfide would be formed (eq. 11). In order for this sulfide to fit the product



distribution, it must desulfurize to give cumene. Under these conditions 2-ethylphenyl methyl sulfide gave no cumene. The only products found were a small amount of I and ethylbenzene (Table 9). Over Pt/Al₂O₃ somewhat more I was formed, but no cumene. This rules out the possibility of an important C₂-C₃ bond-breaking sequence.

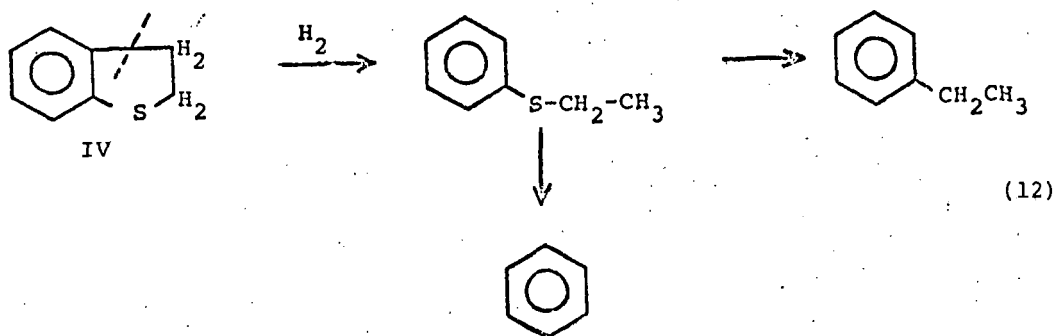
Table 9

Hydrogenation of Alkyl Aryl Sulfides at 400°C

R	R'	Catalyst	Gas	Conv.	Products		
					Benzene	PhCH ₂ CH ₃	I
H	C ₂ H ₅	Pt/Al ₂ O ₃	H ₂	99	99	--	--
H	C ₂ H ₅	Al ₂ O ₃	N ₂	41 ^a	--	--	--
C ₂ H ₅	CH ₃	CoMo	H ₂	100 ^b	--	99	--
C ₂ H ₅	CH ₃	Pt/Al ₂ O ₃	H ₂	99 ^b	--	89	8

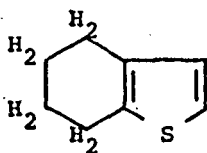
- a. Thiophenol was the only product.
- b. No 2-ethylthiophenol, cumene or III was detected.

The possibility of cleavage of the $C_{\text{aryl}} - C_{\text{alkyl}}$ bond (eq. 12) was also eliminated since ethyl phenyl sulfide



reacts in hydrogen over Pt/Al_2O_3 (Table 9) to give benzene in 99% yield. No ethylbenzene was detected, nor were I and IV found. Presumably cobalt molybdena would act similarly. Since neither ethyl phenyl sulfide or 2-ethylphenyl methyl sulfide gives products consistent with those observed from the respective benzothio-phenes, C-C bond cleavage is apparently unimportant in these reactions.

Other partially hydrogenated structures besides IV are also possible intermediates. Complete or partial hydrogenation of the aromatic ring system to destroy the resonance stabilization of the ring system has been proposed before desulfurization reactions (11). Hydrodenitrogenation reactions are also thought to proceed by this route (35,36). Therefore, 4,5,6,7-tetrahydrobenzothiophene (VII), a partially hydrogenated benzothiophene and thus a possible intermediate, was examined under these conditions at 400°C over



VII

cobalt molybdena. It reacted almost completely, giving I, IV and ethylbenzene (Table 8) which is consistent with the products from I. However, even in the absence of hydrogen, VII was converted easily, although not without a hydrogenation function present. At

Table 10
Reaction of 4,5,6,7-Tetrahydrobenzothiophene (VII)

<u>Catalyst</u>	<u>Temp. °C</u>	<u>Conv.</u>	<u>PhCH₂CH₃</u>	<u>I</u>	<u>IV</u>	<u>Other</u>
Cobalt molybdena ^a	400°	92	36	58	3	
Cobalt molybdena ^b	290°	12	22	3	9	(63% other hydrogenated material)
non-acidic alumina ^c	400°	0				
Cobalt molybdena ^d	400°	100	30	67	--	

a. LHSV 4.0; H₂/HC = 4; 50% VII in hexane

b. LHSV 2.4; H₂/HC = 4; 25% VII in hexane

c. LHSV 0.30; N₂ as carrier gas; 50% VII in hexane

d. LHSV 0.30; N₂ as carrier gas N₂/HC = 4, toluene and IV less than 1%. 50% VII in hexane

290°C, however, VII was only 12% converted, 63% being hydrogenated materials not previously observed from I or IV. The behavior at low temperature precludes any possibility of VII being an intermediate in this reaction.

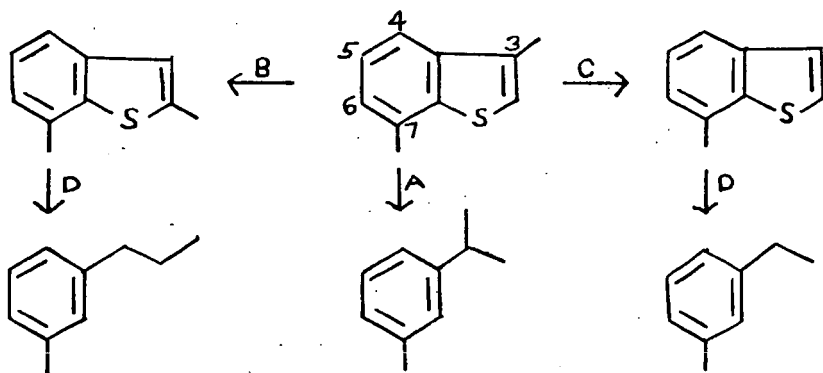
Therefore, in summary our results show that desulfurization may occur by a sequence involving cleavage of one C-S bond to give a mercaptan, followed by cleavage of the second bond to give ethylbenzene. The relative ease of hydrogenolysis of the C-S bonds of either the aryl mercaptans or alkyl mercaptans appears to be about the same under these conditions. In the absence of hydrogen,

however, the alkyl carbon-sulfur bond is broken preferentially since ethyl phenyl sulfide over alumina in N_2 gives phenyl mercaptan in 40% yield as the only product (Table 9). Our data can only conclude that if a stepwise process does occur, then carbon-sulfur bond cleavage would not be selective.

CONCLUSIONS

1. The products from hydrodesulfurization of methyl-substituted benzo[b]thiophenes at atmospheric pressure and $400^\circ C$ stem from certain common paths, as pointed out and schematically illustrated for 3,7-dimethylbenzo[b]thiophene below.

- A. Direct sulfur extrusion from the primary reactant.
- B. Alkyl group migration on the thiophene ring.
- C. Dealkylation from the thiophene ring.
- D. Sulfur extrusion from rearranged or demethylated secondary products.
- E. Relative inertness of benzene ring methyl groups to dealkylation or migration.



2. Conversions, product distribution and hydrodesulfurization selectivities were highly dependent upon the number and positions of the methyl groups. The greater the number of methyl groups, the lower the conversion. Thiophene methyl groups lower the conversion and hydrodesulfurization selectivities more than a methyl substituent on the benzene ring.

3. Dihydrobenzo[b]thiophenes appear to be intermediates in these reactions. Their detection under certain reaction conditions and their behavior under similar reaction conditions supports this conclusion.

4. The desulfurization step involves C-S bond breaking. No evidence was found for C-C bond breaking.

5. Aromatic ring saturation is not necessary before C_{aryl}-S bond breaking occurs.

ACKNOWLEDGEMENT

We would like to express our gratitude to Mr. Frank Harvey for his outstanding laboratory assistance and to Dr. Burtron H. Davis for fruitful and stimulating discussions relative to these studies.

REFERENCES

1. F. P. Richter, A. L. Williams and S. L. Meisel, J. Am. Chem. Soc., 78, 2166 (1956).
2. R. L. Hopkins, H. J. Coleman, C. J. Thompson and H. T. Rall, Anal. Chem., 41, 14 (1969).
3. H. J. Coleman, C. J. Thompson, R. L. Hopkins, N. G. Foster, M. L. Whisman and D. M. Richardson, J. Chem. Eng. Data, 6, 464 (1961).
4. J. B. McKinley, The Hydrodesulfurization of Liquid Petroleum Fractions, in Catalysis, Vol. V, ed., P. H. Emmett, Reinhold, New York, Chapter 6.
5. For review see discussion and references:
H. Hauptmann and W. F. Walter, Chem. Rev., 62, 347 (1962).
G. R. Pettit and E. E. van Tamelen, Organic Reactions, 12, 356 (1962).
6. C. J. Thompson, H. J. Coleman, C. C. Ward and H. T. Rall, Anal. Chem., 32, 424 (1960).
7. C. J. Thompson, H. J. Coleman, R. L. Hopkins and H. T. Rall, J. Gas Chromatography, 1 (1967).
8. S. Landa and A. Mrnkova, Coll. Czech. Chem. Comm., 31, 2202 (1966).
9. M. Yamada, Koru Taru, 12, 8 (1960); Chem. Abstracts, 60, 11978 g (1964).
10. R. Papadopoulos and M. J. G. Wilson, Chem. and Ind., 427 (1965).
11. (a) H. Hoog, Recueil, 69, 1289 (1950);
(b) H. Hoog, G. H. Reman and W. C. Smithuysen, 3rd. World Pet. Cong. Sect. IV, p. 282 (1951).

REFERENCES (Cont'd)

12. See comments by C. M. Cawley in Ref. 11b.
13. We are grateful to Dr. Burton H. Davis of Mobil Research and Development Corporation for supplying these catalysts.
14. E. G. G. Werner, Rec. Trav. Chim., 68, 509 (1949).
15. J. E. Banfield, W. Davies, N. W. Gamble and S. Middleton, J. Chem. Soc., 1956, 4791.
16. W. E. Haines, R. B. Helm, and J. L. Stephens, "Physical Properties of Sulfur Compounds," API RP 48, July 24, 1961.
17. B. R. Muth and A. I. Kiss, J. Org. Chem., 21, 576 (1956).
18. C. Hansch and H. G. Lindwall, J. Org. Chem., 10, 383 (1945);
See Ref. 19.
19. D. A. Shirley, "Prep. of Organic Intermediates," John Wiley, New York (1951) p 275.
20. M. Pailer and E. Romberger, Monatshefte Fur Chemie, 91, 1070 (1960).
21. A. V. Sunthankar and B. D. Tilak, Proc. Indian Acad. Sci., 32A, 396 (1950).
22. F. G. Bordwell, B. B. Lampert and W. H. McKellin, J. Am. Chem. Soc., 71, 1702 (1949).
23. F. G. Bordwell, J. Am. Chem. Soc., 72, 1986 (1950).
24. F. G. Bordwell, J. Am. Chem. Soc., 73, 2253 (1951).
25. S. F. Birch, R. A. Dean and E. V. Whitehead, J. Inst. Petroleum, 40, 76 (1954).
26. H. Kwart and E. R. Evans, J. Org. Chem., 31, 410 (1966).
27. C. Hansch and W. A. Blondon, J. Am. Chem. Soc., 70, 1561 (1948).

28. M. C. Kloetzel, J. E. Little, and D. M. Fisch, J. Org. Chem., 18, 1511 (1953).
29. P. Cagniant, Compt. Rend., 230, 100 (1950).
30. J. M. J. G. Lipsch and G. C. A. Schuit, J. Catalysis, 15, 179 (1969).
31. S. Kolboe, Can J. Chem., 47, 352 (1969).
32. C. Hansch, B. Schmidhalter, F. Reiter and W. Saltonstall, J. Org. Chem., 21 265 (1956).
33. P. B. Venuto, P. S. Landis and D. E. Boswell, Ind. Eng. Chem. Prod., Research and Development, 7, 44 (1968).
34. C. Hansch and F. Hawthorne, J. Am. Chem. Soc., 70, 2495 (1948).
35. O. A. Larson, Div. of Petrol. Preprints, 12 (4), B-123 (1967).
36. R. A. Flinn, O. A. Larson, and H. Beuther, Hydrocarbon Processing and Petroleum Refiner, 42 (9), 129 (1963).